Technische Universität Kaiserslautern
Fachbereich Chemie

Photochromic Switches on Polyolefin Catalysts

Dem Fachbereich Chemie
der Technischen Universität Kaiserslautern
zur Erlangung des akademischen Grades
„Doktor der Naturwissenschaften“
eingereichte Dissertation
(D 386)

vorgelegt von
Robert Lawrence Jones Jr.,
M.Sc. Chem/ M.Sc. Bio.
aus (Houston, Texas USA)

Betreuer der Arbeit: Prof. Dr. H. Sitzmann
Tag der wissenschaftlichen Aussprache: (Oktober 7, 2005)

Kaiserslautern 2005

Dem Fachbereich Chemie der Technischen Universität Kaiserslautern am 14. September 2005 als Dissertation eingereicht.

Dekan:	Prof. Dr. Hans-Jörg Krüger, Ph.D.

Prüfungskommission:

Vorsitzender:	Prof. Dr.-Ing. Stefan Ernst
1. Berichterstatter:	Prof. Dr. Helmut Sitzmann
2. Berichterstatter:	Prof. Dr. Werner Thiel

Die vorliegende Arbeit entstand in der Zeit von Februar 2004 bis September 2005 im Forschungslaboratorium der Basell Polyolefin GmbH.

Photochromic Switches on Polyolefin Catalysts

Robert L. Jones Jr.
September 2005

Zusammenfassung

Metallocene mit photochromen Gruppen des Diarylethen Typs wurden synthetisiert, charakterisiert und als Katalysatoren für die Olefinpolymerisation getestet.

Die Polymerisation von Propen mit unverbrücktem Bis(2,3-dibenzo[b]thiophen-3-yl)cyclopenta[b]thien-3-yl)zirkoniumdichlorid/ MAO (**80**) führt durch Bestrahlung bei 254 nm laut GPC zu einer bimodalen Polymerverteilung. Dies liegt an dem Anstieg des Polymeranteils mit niedrigem Molekulargewicht, wenn die geschlossene Form des Katalysators/Photoschalters gebildet wird. Ähnliche Katalysatorstrukturen ohne photoschaltbare Gruppen liefern dagegen unter gleichen Bedingungen kein bimodales Polymer.

Die Polymerisation von Propen mit Dimethylsilyl[(1,5-dimethyl-3-phenylcyclopenta[b]thien-6-yl)][(2,3-dibenzothien-3-yl)cyclopenta[b]thien-6-yl)]zirkoniumdichlorid/ MAO (**86**) bei Bestrahlung mit 254 nm führt zu einem dreifachen Anstieg des Molekulargewichts des Polymers.

Die bei den Polymerisationen von Ethen und Ethen/Hexen mit (**80**) hergestellten Polymere zeigten nach der Bestrahlung im UV keine Unterschiede in den gemessenen Polymereigenschaften. Die Polymerisationen von Ethen/Hexen-Mischungen mit (**86**) zeigten eine erhöhte Aktivität und einen erhöhten Einbau des Co-Monomers (Hexen) bei UV-Bestrahlung.

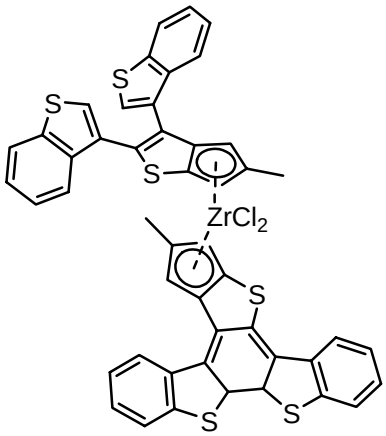

(**80**)

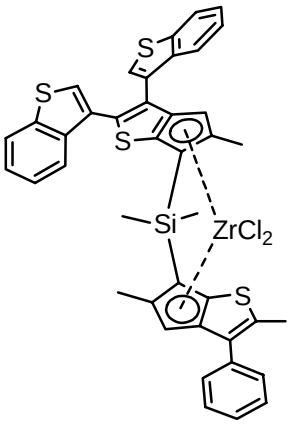

(**86**)

Abstract

Metallocenes containing diarylethene type photochromic switches are synthesized, characterized and tested in polyolefin catalysts.

Propylene polymerizations using unbridged bis(2,3-dibenzo[b]thiophen-3-yl)cyclopenta[b]thien-3-yl)zirconium dichloride/MAO (**80**) treated with 254nm UV irradiation produced bimodal polymer distributions by GPC. This was due to an increase in the low molecular weight fractions when the closed form of the catalyst/photoswitch was made. Comparison with similarly structured catalyst without photoisomerization properties did not produce bimodal polymer under identical conditions.

Propylene polymerizations made with dimethylsilyl[(1,5-dimethyl-3-phenylcyclopenta[b]thien-6-yl)][(2,3-dibenzothien-3-yl)cyclopenta[b]thien-6-yl)]zirconium dichloride/MAO (**86**) with 254nm UV irradiation caused a 3 fold increase in the polymer molecular weight.

Polymers made with ethylene and ethylene/hexene using (**80**) after UV irradiation did not show differences in measured polymer properties. Polymerizations with ethylene/ hexene mixtures using (**86**) had increased activity and co-monomer (hexene) incorporation with UV irradiation.

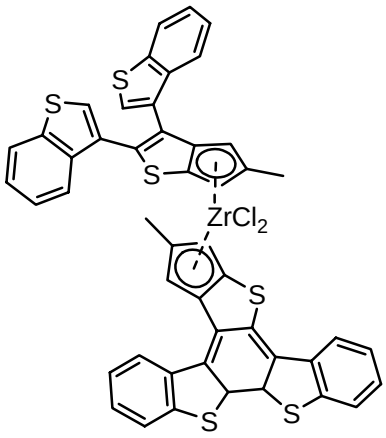

(**80**)

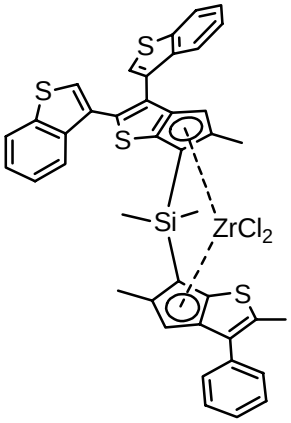

(**86**)

Table of Contents

List of Figures

Index of Tables

Hypothesis

It should be possible to control the structure, properties, and products of a polyolefin catalyst by changing the ligand shape during a reaction through incorporation of a photo-molecular switch. Changing the ligand during a reaction cycle could affect properties of a catalytic system resulting in modification of the catalyst product. The effect could be demonstrated using a photoswitch integrated into a zirconocene and operated during a catalytic olefin polymerization to create changes in polymer properties (stereo- and regio-chemical monomer insertions, co-monomer insertion orientation and rate, reactor blends, or controlled insertion of co-monomers).

1.0 Introduction

The ligand component of a catalyst with its geometric and electronic properties contains information that directly influences the outcome of a reaction. Ligand interactions direct the orientation of a substrate, influence binding and help lower activation energies allowing the reaction to proceed towards a certain outcome. Contribution from ligand association can define the reaction product.

In metallocene poly-α-olefin catalysis the ligand plays a fundamental role in defining the polymer product. The ligand directs monomer insertion, orients the growing polymer chain, and directly orchestrates the product properties[1]. Every metallocene catalyst with a unique structure produces a unique polymer and has unique reactivity towards monomer and co-monomers. Changing the ligand shape or arrangement during the polymerization leads to altered polymers and broadens the scope of products from any single catalyst component.

Catalysts having micro-motor like ligand components that oscillate[2] or substituents which can rotate in and out of the reaction center during a polymerization[3] are changes in ligand geometry that dynamically effect monomer or co- monomer insertion and polymer stereo- and regio- specificity. Control over change in these ligand systems are influenced by physical environment under which the catalyst is operated. In these catalytic systems, factors such as ligand substitution, solvent, and co-catalyst /counter-ion selection all effect switching/ rotational changes. The oscillation and gyration conformations in the population of catalyst molecules are a distribution under control by the system[4]. These changes are manifested in the polymer properties produced by the catalyst ligand complex.

In the last several years, molecules addressable through distinct photochemical quanta have been discovered and studied. Most recently, photoswitching in catalytic reactions to

---

[1] John A. Ewen, M. J. Elder. R. L Jones, Luc Haspeslagh, Jerry L Atwood, Simon G. Bott, Kerry Robinson, "Metallocene/polypropylene structural relationships: Implications on Polymerization and Stereochemical Control Mechanisms", *Eur. Polym. Fed. Symp. Polym. Mater., 3rd*, (**1990**), 48-49, *Makromolekulare Chemie, Macromolecular Symposia* (**1991**) 253-95.

2 a) G.M. Wilmes, M.B. France, S.R. Lynch, R.M. Waymouth, "Effects of ligand substitutions on the rotation rate of indenyl ligands in bis(2-arylindenyl)zirconocenes by NMR line-shape analysis and relaxation in the rotating frame", *Organometallics* (**2004**), *23*(10), 2405-2411. b) Shirley Lin and Robert M. Waymouth, "2-Arylindene Metallocenes: Conformationally Dynamic Catalysts To Control the Structure and Properties of Polypropylenes", *Acc. Chem. Res*., (**2002**) *35* (9), 765 -773.

[3] a) Stephen A. Miller and John E. Bercaw, "Isotactic-Hemiisotactic Polypropylene from C-Symmetric, ansa-Metallocene Catalysts: A New Strategy for the Synthesis of Elastomeric Polypropylene", *Organometallics*, **2002**, *21,* 934-945 b) Miller, S. A.; Bercaw, J.E., "Catalyst System for the Polymerization of Alkenes to Polyolefins", U.S. Patent 6,469,188, 2002, U.S. Patent 6,693,153, 2002, c) J. A. Ewen, R. L. Jones, M. J. Elder, I. Camurati, and H. Pritzkow, "Stereoblock Isotactic-Hemiisotactic Polypropylenes and Ethylene/Propylene Copolymers Obtained with ansa-Cyclopenta[1,2-b;4,3-b']dithiophene Catalysts", *Macromolecular Chemistry and Physics* (**2004**) *205*, 302-307.

[4] for example, Maxwell-Boltzmann distribution.

direct stereoselectivity has been explored using molecular photoswitches[5]. Photo-switching molecules change shape and physical property depending on the type and amount of radiation received. Although current developments have been concentrated in photo-display and memory devices, use as an accessible modulator in catalytic ligand field technology is on the application horizon.

Changing ligand configuration with a switch activated by irradiation provides additional control by which ligands in a catalytic reaction could be modified. In reactions where the ligand orientation is critical to the product outcome or produce product modifications such as in a metallocene catalyzed olefin polymerization, such control could be useful in tailoring the final polymer properties.

In order to reduce the catalytic photoswitching hypothesis to practice in polyolefin catalysis selection of target molecules and reaction conditions leading to clear measurable results is necessary. Applications of the control over a catalytic process, once demonstrated, could be expanded industrially to any number of catalytic processes involving variable ligand fields.

1.1 Review of the literature on olefin polymerization

There are many catalytic systems available for demonstrating photo-control over a ligand influenced reaction event. In some instances, the changing shape of the ligand system could be useful in alternating the reactive site of a catalyst for coupling reactions. Living systems are no stranger to the influence of irradiation in changing ligand orientations in biochemical reactions (mammalian visual pigments for example).[6]

The sensitive changes in the ligand geometry of a single site polyolefin catalyst can result in large differences in the polymer produced in the reaction. The non-bonded interactions that result in changes in the low energy conformation of monomer, especially for propylene, can be measured and are specific for each catalytic system producing a polymer chain. Multiple catalysts used in a single reaction soup create broadened molecular weight distributed polymer products: the bimodal distribution of the product is made from the two catalytic systems producing different polymers. Using this to an advantage, the influence of changing the ligand geometry and the analysis of the properties of the polymer provide a direct result from the changing ligand conformations of the catalytic system.

Olefin polymerization catalysis has origins in the 1950s and single site polyolefin catalysts have more recently developed into commercial applications. A general review of the polyolefin catalytic system follows.

---

[5] David Sud, Tyler B. Norsten, and Neil R. Branda, “Photoswitching of Stereoselectivity in Catalysis Using a Copper Dithienylethene Complex”, *Angew. Chemie. Int. Ed.*, (**2005**), *44*, 2019-2021.

[6] see for example: Steven W. Lin, Gerd G. Kochendoerfer, Kate S. Carroll, Dorothy Wang, Richard A. Mathies, and Thomas P. Sakmar, " Mechanisms of Spectral Tuning in Blue Cone Visual Pigments", *J. Biological Chem.* (**1998**) *273*(38) 24583–24591.

1.1 Historical aspects: Ziegler-Natta catalysis

Controlled addition of clear colourless liquid titanium tetrachloride to a hydrocarbon solution containing aluminium alkyl reduces the titanium(IV) to the trichloride and forms brown sand like particles. The crystalline form of titanium trichloride so formed is called the beta form, β-$TiCl_3$[7]. When β-$TiCl_3$ is again treated with aluminium alkyl, active polymerization sites are formed on the surface. In the presence of olefin such as ethylene or propylene, polymer is formed at these cationic sites. The crystalline form of the catalyst can be modified with heat treatment (the β-form converts to the purple gamma form) and if the olefin is propylene, a more stereospecific crystalline isotactic polymer is formed.

The catalyst particle prepared in the fashion described above is a conglomerate of $TiCl_3$ crystallites having different sites at faces, edges and corners. The position of each Ti reactive center and the relation to adjacent atoms determines the type of polymer that will be produced by a cationic site. The ligand geometry which determines the product of the catalytic reaction is a rigid framework consisting of surrounding adjacent atoms in the crystal.

First generation Ziegler Natta (Z/N) catalysts contained the inside, middle, and outside of the catalyst particle being $TiCl_3$. The monomer is polymerized on the outer surface of the crystallites whereas the inner parts of the $TiCl_3$ particles are not accessible to the monomer. At the end of the polymerization process, the interior and middle of the catalyst particle remain active and upon exposure to air (moisture), the active $TiCl_3$ residues in the polymer particle decompose producing TiO_2 and HCl. In addition, in these early 1st generations of Ziegler-Natta (Z/N) catalysts, the quantity of $TiCl_3$ remaining in the catalyst particle was enough to discolour the polymer particle and was a residue that needed to be minimized. In later and current commercial modifications to the Z/N catalysts the interior of the catalyst particle was replaced with a like crystalline structure, $MgCl_2$.

On the surface of the catalyst particle, many different faces of the $TiCl_3$ crystallite are active polymerization centers. Not all sites produce the same type polymer. To mask sites that give rise to polymers that are unwanted, the Z/N catalyst is treated with an electron donor compound (hence the term "donor"), which reacts effectively with sites producing unwanted polymer products (such as atactic polymer)[8]. Internal and external donors can be used, and the sites in the crystalline matrix are readily modified.[9]

---

[7] Boor, J. *Ziegler-Natta Catalysts and Polymerization*; Academic Press: New York, 1979.

[8] Donor shape and selectivity are critical aspect of controlling or blocking reactive sites and also a potential for photochemical control, a topic dealt with later in this paper.

[9] It may be possible to modify the donor molecule in the same fashion as with the single site catalyst center, affecting the Z/N reactive site with a photoswitch (further described in the outlook section, *vide infra*).

Early Z/N workers searched for a single catalytic site "model" system that was capable of demonstrating the mechanism of polymerization taking place at a metal center[10]. As a result, a single titanium atom (then later zirconium and hafnium) was fashioned into a molecule capable of being the active polymerization center and were used to elucidate the olefin polymerization mechanism. Hypotheses were devised and tested and learning based on the modifications and changes in the ligand structure surrounding the metal center helped to develop currently accepted polymerization mechanisms.

Single site catalysts for polymerization of olefins have become one of the most commercially investigated metal complexes having a ligand component. In particular, propylene polymerizations have been studied due to polymer stereochemistry which effect physical properties of the polymer. Hence we distinguish between the classic multi-site Ziegler/Natta Ti/$MgCl_2$ supported catalysts *and* single site Group IV metallocenes *and* single sided cyclopentadienyl MX_3 type complexes, constrained geometry Dow catalysts (CGD), Dow/Symyx nitrogen containing Hf-pyridyl-imine complexes, Mitsui FI catalysts, and late transition metal (DuPont/ Brookhart/ Gibson type) single site catalysts: there are recent, comprehensive reviews[11].

[10] a) D. Breslow and N.R. Newberg, *J. Am. Chem. Soc.*, (**1957**) *79*, 5072, b) G. Natta, P. Pino, G. Mozzanti, U. Giannini, *J. Am. Chem. Soc.* (**1957**) *79*, 2975.
[11] Abhimanyu O. Patil and Gregory G. Hlatky (eds.), "Beyond Metallocenes: Next-Generation Polymerization Catalysts" The American Chemical Society, Washington DC (**2003**) 249 pages.

Figure 1. Single site olefin polymerization catalyst examples.

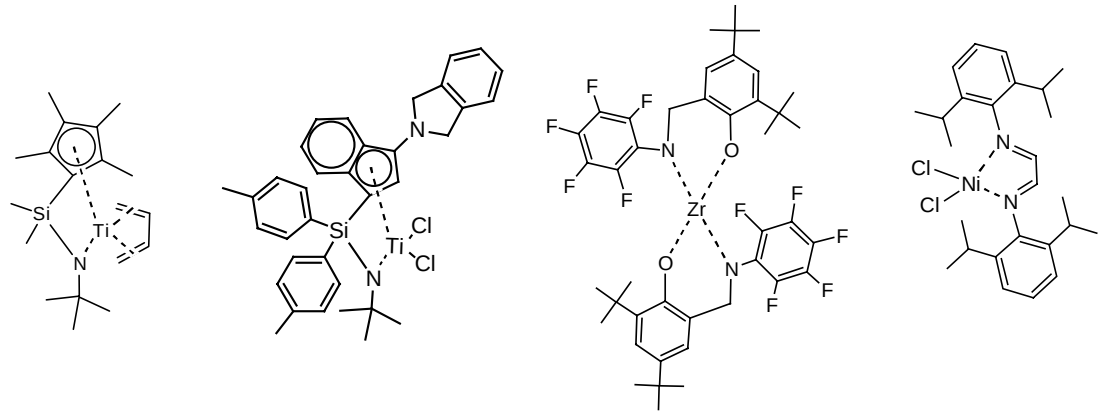

(**1**) (**2**) (**3**) (**4**)

examples of Dow's constrained geometry catalysts

Mitsui/ Coates FI catalysts

Brookhart/Gibson diimine

1.2 Polyolefins

Polypropylene (PP) and ethylene-propylene co-polymers (EP) are a large market segment of commodity materials[12]. Derived from petroleum resources, the polymerization of ethylene and propylene into oils, waxes, and polymers using classic Ziegler Natta catalysts is a mature field. Commercially, over 40 million tons of PP will be produced in 2005[13], and positive growth rate of the market is predicted in the coming years (*vide infra*).

Commercially marketed highly crystalline polypropylene has a melting temperature of ~163°C[14]. This allows the material to fit into a number of applications not suitable for polyethylene (m.pt. ~135°C). The glass transition temperature of PP is 0°C however, and this limits PP to non-freezer applications. This drawback is overcome by decreasing the polymer glass transition temperature by making an ethylene-propylene (EP) copolymer. The lowering of the glass transition temperature is dependent on the amount of co-

---

[12] *Irvin I. Rubin* **"**Handbook of Plastics Materials and Technology, (**1990**): John Wiley & Sons, 1792 Pages ISBN: 0471096342.

[13] John. R. Severn, John C. Chadwick, Robert Duchateau, Nic Friederichs "Bound but not Gagged: Immobilizing Single-Site α-Olefin Polymerization Catalysts", *Chem Review* (**2005**) *in press*.

[14] For an excellent review, see: Edward P. Moore Jr. (editor) "Polypropylene Handbook, Polymerization, Characterization, Properties, Processing, Applications", Hanser Publishers, Munich, Vienna, New York, **1996**, 419 p. ISBN 1-56990-208-9.

monomer added into the polymer. The trade off in this scenario is stiffness/crystallinity. As the polymer becomes more ethylene rich, the flexibility of the polymer increases and applications change.

There are many applications and processes where the flexibility and behaviour of EP co-polymers are well suited[15]. In applications where glass transition temperatures are not critical, homopolymers having flexibility rather than rigidity may become influential (for example: drinking cups that do not stress crack). In cases such as films for food wrapper/storage applications, flexibility is desired. Sterilizable blood bags and medical tubing and syringes are another application where high stiffness/crystallinity could become a drawback. The hot tack sealing temperature of films is a further example.

Different types of EP copolymers are possible: random and block copolymers are commercially produced. The random copolymers (raco's) are flexible materials and are produced in gas phase reactors or in bulk with ethylene added in the matrix. Block copolymers are produced by sequentially treating the active catalyst/polymer chain with ethylene, essentially changing monomer post-process streams (heterophasic copolymer: heco's). As in the case of homo-PP, the molecular weight of the polymer chains (M_w), the molecular weight distribution ($M_w/M_n = Q$), the distribution of the co-monomer in the individual chains or in the distribution all play an integral role in the final properties of the polymer.
Particularly interesting for this work is that controlled errors in the polypropylene backbone would disrupt crystallinity and find applications because such polymers are less rigid (i.e., plastomers).

Since their invention there has been increasing demand for metallocene polyolefins. Although less commercially accepted than originally predicted (to capture a 10% portion of the market segment), in the field of polyethylene and elastomers, production capacity as a result of demand has grown substantially. In fact,

"*Demand for metallocene and single-site polymers is projected to advance more than 20% per year to 5.1 billion lbs in 2009, valued at $5.3 billion. Opportunities will result from the considerable processing and performance advantages these materials hold over other materials. ….. LLDPE will remain the dominant polymer, although more rapid growth is expected for much smaller polypropylene and high density polyethylene plastics, as well as elastomers such as thermoplastic olefins (TPO's). Film and sheet will remain the leading application……"*[16]

Of these substantial commercial materials it is "tailored material properties" that can be obtained that are most important. What are specifically being marketed are polymer

---

[15] See, for example: Stefan Mansei, Ernesto Perez, Rosario Benavente, Jose M. Perena, Antiono Bello, Werner Roll, Robin Kirsten, Stefan Beck, and Han Herbert Brintzinger, " Synthesis and Properties of Elastomeric Polypropylene", *Macromol. Chem. Phys*. (**1999**) *200*, 1292-1297.
[16] "Metallocene & Single Site Polymers", The Freedonia Group Inc. (**2005**):, 767 Beta Drive Cleveland, OH 44143-2326 USA website: www.freedoniagroup.co phone: 800-927-5900 (US) see www.freedoniagroup.com/pdf/1913embro.pdf.

properties. The control over polymer properties are directly related to the polymer microstructures: the molecular weight and molecular weight distribution of polymer chain lengths, the stereo and regio-control of tactic placements, and the placement and content of co-monomer: these are critical aspects of making marketable tailored polymer.

1.3 Metallocene Polyolefin Catalysts

John A. Ewen[17] first taught us that isotactic polypropylene could be made using metallocenes.[18] In an elegant first principles application of ^{13}C-NMR, Ewen showed single molecular species with a chiral ligand producing isotactic polymer through either a chain end or site control mechanism. Using Brintzinger's -*rac*/-*meso* EBITiCl$_2$[19] and Kaminski's MAO[20], and by fractionating and analyzing the polymer, the microstructure was elaborated. From these simple and profound beginnings, the stereo- and regio-chemical control over monomer insertion into a growing polyolefin chain achieved a penultimate success through Group IV metallocenes. These early studies led to the understanding of the mechanism of polymerization and provided insight into the rational design of catalyst systems[1]. Many modifications to the basic indene ligand structure followed, including changes to the bridging atoms and modifications to the indene structure with alkyl and aryl substituents. Within the decade following Ewen's first report, Spaleck and co-workers modified the bridged indenyl ligand framework to include 2-methyl-4-phenylindenyl[21]. Finally the heterocenes included modifications to the ligand geometry that dramatically improved catalyst reactivity and tacticity control[22]. The major contributions in this area are shown in Figure 2.

---

[17] http://www.johnaewen.com/medal2.html

[18] a) John A. Ewen, "Mechanisms of Stereochemical Control in Propylene Polymerizations with Soluble Group 4b Metallocene/Methylalumoxane Catalysts", *J. Am. Chem. Soc.*, (**1984**) *106*, 6355-6364, b) "Process and catalyst for polyolefin density and molecular weight control." Welborn, Jr.; Howard C.; Ewen; John A. (Exxon Chemical Patents Inc.) US 5,324,800 (**1994**).

[19] Wild, F. R. W. P.; Zsolnai, L.; Huttner, G.; Brintzinger, H. H. J.*Organomet. Chem*., (**1982**) *232*, 233.

[20] A. Andersen, H.-G. Cordes, J. Herwig, W. Kaminski. A. Merck, R. Motweiler,J. Pein, H. Sinn, H. –J. Vollmer, Angew. Chem., (**1976**) *88*, 688-689.

[21] W. Spaleck, F, Kuber, A. Winter, J. Rohrmann, B. Bachmann, M. Antberg, V. Dolle, E.F., Paulus, *Organometallics* (**1994**) *13*, 954-963.

[22] (a) John A. Ewen, Michael J. Elder Robert L. Jones, Arnold L. Rheingold, Louise M. Liable-Sands, Roger D. Sommer, *J. Am. Chem. Soc.* (**2001**) *123* (20), 4763-4773, (b) J.A. Ewen, R.L. Jones, M.J. Elder, A.L. Rheingold, and L.M. Liable-Sands, *J. Am. Chem. Soc.* (**1998**) *120*, 10786-10787.

Figure 2. Historical Developments in Metallocene Polyolefin Catalysis 1: Ligand Effects on C_2 - Symmetric Zirconium Indenocene Catalysts in Bulk at 70°C.[23]

Entry	Zirconocene	Activity Kg PP/(mmol cat*h)	mmmm (%)	m.pt. (°C)	M_w (g/mol)
(**5**) 1985	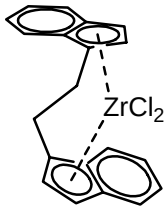	188	78	135	24,000
(**6**) 1988	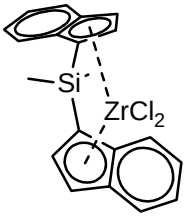	190	82	137	36,000
(**7**) 1992	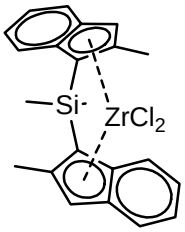	99	88	145	195,000
(**8**) 1994	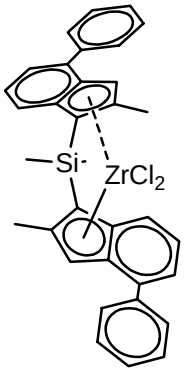	755	85	156	1,287,000

Isotactic polymers from un-substituted bridged indene metallocenes such as (**5**) had low melting points and low molecular weight.[24]. The synthesis of these complexes was facilitated by changing the bridging atom to silicon[25] (**6**), which makes the catalyst more

[23] J.A. Ewen, M.J. Elder and R.L. Jones "The Evolution of Metallocenes for Polypropylene: Stereochemistry and Molecular Weight Control through Catalyst Design." in "*Polypropylene. Past Present and Future: The Challenge Continues.*" (**1998**), Conference Proceedings Published by Montell Polyolefins, Distributed by Tecnimont, Viale Monte Grappa 3, 20124 Milano, p. 191.

[24] W**.** Kaminsky, K. Killper, H.H. Brintzinger, F. R. W. P. Wild, *Angew. Chem., Int. Ed. Engl.* (**1985**) *24*, 507.

[25] a) J.A.Ewen, " Alpha olefin polymer products and catalyst systems", United States Patent 6,872,790 March 29, **2005,** b) J. A. Ewen,. L. Haspeslagh, M. J. Elder, J. L.Atwood, H. Zhang,; H. N.Cheng, In

rigid and increases catalyst activity[26]. Dramatic improvements on the stereospecificity and molecular weight of the polymers were made by substituting a methyl group in the 2-position adjacent to the bridging carbon on the cyclopentadienyl ring (**7**)[27]. In a final improvement on the indene series, the substitution of a phenyl group in the 4- position on the annulated 6-membered (indenyl) ring (**8**) produced high activity catalyst and a high melting point polymer.[28]

Group 4 metallocenes containing heterocyclic ring(s) fused to the metal bonded cyclopentadienyl ring were invented as a step beyond the indene structures described above[29]. Bridged thiophene or pyrrole pentalenes with substitution patterns similar to those taught by the carbocene metal complexes with homo-cyclic ligand structures were found to have higher activities as well as high stereo and regio control over monomer insertion[30]. Furthermore, by extending control over the orientation of the substituted groups, it was possible to gain additional control over regio- and stereo-chemical placements in the polymer[31]. The orientation of the pendant phenyl group(s) controlled by adjacent substitution (methyl, phenyl, isopropyl, etc) influenced the orientation of the pendant phenyl, tolyl, or xylyl substituents, which influenced the growing polymer chain.

For polypropylene, isotactic, syndiotactic[32], hemi-isotactic[33], and atactic[34] polymer have been achieved in high yields[35]. These unique polymer structures come from substitution

---

"Transition Metals and Organometallics as Catalysts for Olefin Polymerization", Kaminsky W., Sinn, H., Eds.; Springer-Verlag: New York, **1988**; p 281.

[26] W. A. Hermann, .J.Rhormann, E. Herdtweck, W. Spaleck, A. Winter, *Angew. Chem.*(**1989**) *28*, 1511.

[27] W. Spaleck, M. Antberg, J. Rohrmann, A. Winter, B. Bachmann, P.Kiprof, J. Behm, W. A. Herrmann, *Angew. Chem*. (**1992)** *104*, 1373**;** *Angew. Chem., Int. Ed. Eng.* .(**1992**) *31*, 1347**.**

[28] Walter Spaleck, Frank Kuber, Andreas Winter, Jurgen Rohrmann, Bernd Bachmann, Martin Antberg, Volker Dolle, and Erich F. Paulus, " The Influence of Aromatic Substituents on the Polymerization Behavior of Bridged Zirconocene Catalysts", *Organometallics* (**1994**) *13*(3), 954-963.

[29] "Metallocene compounds, process for their preparation and their use in catalytic systems for the polymerization of olefins." John A. Ewen, Michael J. Elder, Robert L. Jones, (Basell Technology Company) US 6,635,779 (**2003**); US 6,444,833 (**2002**).

[30] a) "Expanding the Scope of Metallocene Catalysts: Beyond Indenyl and Fluorenyl Derivatives." John A. Ewen, Robert L. Jones, Michael J. Elder, pp.150-169 in *Metalorg. Catal. for Synth. and Polym.* (**1999**), Ed. W. Kaminsky, Pub. Springer, Berlin, Germany. b) "Metallocene Polymerization Catalysts: Past, Present, and Future." J.A. Ewen, in *Metallocene-Based Polyolefins* (**2000**), *1*, pp. 3-31, Eds. John Sheirs, W. Kaminsky. John Wiley and Sons Ltd., Chichester.

[31] Gaetano Guerra, Paolo Corradini, and Luigi Cavello, "Molecular Modeling of Stereo and Regioselectivity of Group 4 Heterocenes in the Polymerization of Propene", *Macromolecules* (**2005**), *38*(9) 3973-3976.

[32] a) J. A. Ewen, R. L. Jones, A. Razavi, J. D. Ferrara, "Syndiospecific Propylene Polymerizations with Group 4 Metallocenes." *J. Am. Chem. Soc.* (**1988**) *110*, 6255-6256, b) J. A. Ewen, M. J. Elder, R. L Jones, S. Curtis, H. N. Cheng, "Syndiospecific Propylene Polymerizations with iPr[CpFlu]$ZrCl_2$." *Stud. Sur. Sci. Catal.,* (**1990**) *56*, 439-482.

[33] J. A. Ewen, M. J. Elder, C. J .Harlan, R. L. Jones, J. L. Atwood, S.G. Bott, K. Robinson; "π-Face Selectivity in Syndiospecific Propylene Polymerizations with Zr(IV) Monoalkyl Cations." *ACS Polymer Preprints* (**1991**) *32*(1), 469.

[34] a) L. Resconi, R.L. Jones, A. Rheingold, and G. Yap, "High -Molecular-Weight Atactic Polypropylene from Metallocene Catalysts. 1. $Me_2Si(\eta^5\text{-9-Flu})_2ZrX_2$ (X=Cl,Me)." *Organometallics* (**1996**) *15*, 998 – 1005, b) Luigi Resconi, R.L. Jones, E. Albizzati, I. Camurati, F. Piemontesi, F. Guglielmi, and G.

patterns on metallocene cyclopentadienyl catalysts that tailor the control over making the polymer chains in a precise fashion. Each change in the catalyst architecture created new polymer properties and demonstrated control over the microstructure and polymer properties that was specific to the substitution patterns like those described above.

In extending control over monomer insertion to create elastomeric type of polypropylene co- and homo-polymer, Waymouth et. al. used an unbridged oscillating aryl substituted indene to produce isotactic-atactic blocks (see Figure 3)[36]. Although there has been debate over the ultimate structure of the polymer and the mechanism by which it is formed[37], the polymer properties are interesting[38].

Figure 3. Waymouth's oscillating catalyst

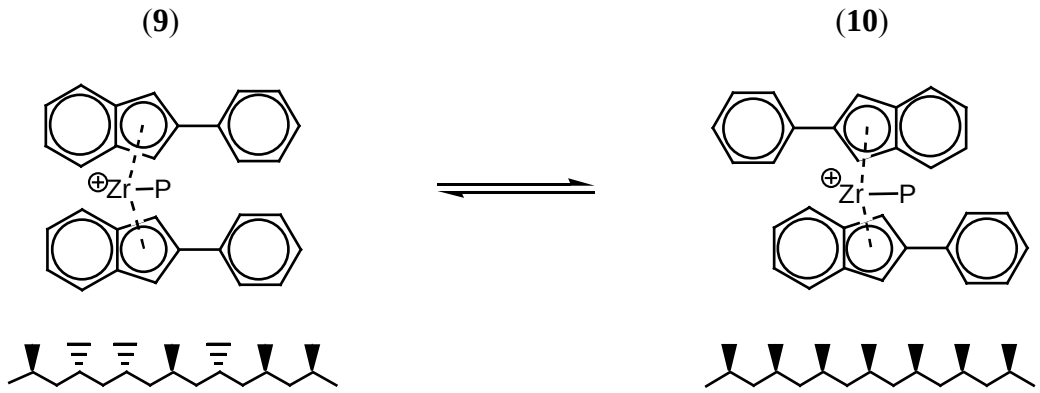

Alternative methods for producing elastomeric propylene have been made with un-symmetric ligands (C_1) as described by J.C.W. Chien, Collins[39], Rieger[40], and more recently Kaminsky[41]. Equally interesting, Miller and Bercaw have made hemi-isotactic syndiotactic block polypropylene (hit-PP-sPP) by substituting a rotating adamantyl group into the ligand framework of an otherwise syndiospecific catalyst.

Balbontin, "High Molecular Weight Amorphous Polypropylene from Metallocene / MAO Catalysts", *Polymer Preprints* (**1994)** *35*, 1, 663-4.

[35] For recent reviews and leading references, see: a) Brintzinger, H. H.; Fischer, D.; Muelhaupt, R.; Rieger, B.; Waymouth, R. M. *Angew. Chem., Int. Ed. Engl.* (**1995**) *34*, 1143. b) *Ziegler Catalysts, Recent Scientific Innovations and Technological Improvements*; Fink, G., Muelhaupt, R., Brintzinger, H. H., Eds.; Springer: Berlin, 1995, c) Kaminsky, W.; Arndt, M. *Adv. Polym. Sci.* (**1997)** *127*, 143-187, d) Alt, H. G.; Koeppl, A. *Chem. Rev.* (**2000**) *100*, 1205-1221, e) Coates, G. W. *Chem. Rev.*(**2000**) *100*, 1223-1252. (f) Resconi, L.; Cavallo, L.; Fait, A.; Piemontesi, F. *Chem. Rev.* (**2000**) *100*, 1253-1345.

[36] Coates, G. W.; Waymouth, R. M. *Science* (**1995**), *267*, 217-219.

[37] Vincenzo Busico, Valeria Van Axel Castelli, Paola Aprea, Roberta Cipullo, Annalaura Segre, Giovanni Talarico, and Michele Vacatello, *J. Am. Chem. Soc.* (**2003**), *125*, 5451-5460.

[38] Lin, S.; Waymouth, R. M. *Acc. Chem. Res.* (**2002**) *35*, 765-773.

[39] William J. Gauthier and Scott Collins, *Macromolecules* (**1995**) *28*, 3779-3786.

[40]Sandra Deisenhofer, Tanja Feifel, Jurgen Kukral, Martti Klinga, Markku Leskela , Bernhard Rieger, "Asymmetric Metallocene Catalysts Based on Dibenzothiophene: A New Approach to High Molecular Weight Polypropylene Plastomers" *Organometallics* (**2003**) *22,* 3495-3501.

[41] Bjorn Heuer and Walter Kaminsky, "Alternating Ethene/Propene Copolymers by C_1-Symmetric Metallocene/MAO Catalysts" *Macromolecules* (**2005**) *38*, 3054-3059.

Figure 4. Rotating Adamantyl catalyst.[3]

(**11**)

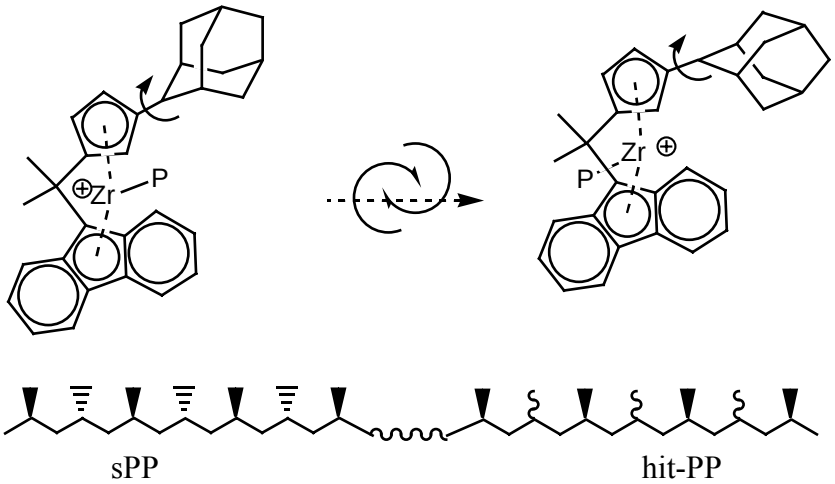

In the above catalytic systems, control over orientation of monomer insertion depends on the geometry of the ligand. Non-bonding interactions allow for selected conformations influencing monomer orientation at the metal center. The catalyst molecules present in the reaction mixture randomly adapt one of these selected conformations and occasionally switch to another possible confirmation according to laws of probability. Although normal physical parameters of the system can play a part (such as reaction temperature for molecular weight control, hydrogen addition for chain termination, etc.), the final outcome of the monomer insertion is under the control of the single site catalyst molecule and the ligand confirmation at the time of insertion.

In an effort to modify this control, ligands that could be influenced by external parameters rather than random changing conformations were considered.

One potential source of control are switches: molecules whose geometry is altered by external stimuli such as electric potential (molecular transistors) or light energy (photomolecular photoswitches). Molecular transistors are a developmental field, whereas molecular photoswitches are becoming increasingly studied.

In my initial studies, two types of photoswitches were considered: the substituted dihydropyrenes recently reviewed by Mitchell, and the dithienylethenes[42]. Both of these photoswitches exhibit gross and significant changes in structure upon treatment with light or UV (depending on the nature of the reacting group). The proper placement of these components of the ligand framework of a metallocene catalyst was part of the challenge and subject of this work.

[42] Masahiro Irie, *Chem. Rev.,* (**2000**) *100*, 1685-1716.

As alternative, non-metallocene polypropylene catalysts under development are of interest. Dow/Symx reports on propylene polymerizations with non-Cp containing complexes appear promising, although less control over monomer insertion is indicated[43]. Syndiotactic polymerizations of propylene using Mitsui's FI[44] catalyst have been improved by Coates[45]. These molecular structures are also candidates for making "photochromic ligand" controlled types of polymers, especially because of their potentially "living" catalytic centers[46].

1.4. Photoswitches and Metallocenes

Photochromic photosensitive molecules are well studied and have been reviewed[47]. Aside from the fulgides, the more immediately applicable molecules suited as attachments to olefin polymerization catalysts are diarylethenes (DAE) and possibly dihydropyrenes (DHP) (see Figure 5). These observations are based on prior experiences in synthesizing a metallocene ligand molecule whose reactivity can produce unwanted side products. In addition to presenting synthetic challenges, certain types of photo-reactive groups could possibly poison the polymerization reaction. The economy of synthesis is a key factor in the ligand design.

---

[43] James C. Stevens and Daniel D. Vanderlende, "Isotactic Polypropylene Copolymers, Their Preparation and Use", WO 03/040201 A1 International Publication Date 15 May (**2003**): Assignee The Dow Chemical Co. b) Thomas R. Boussie, Gary M. Diamond, Christopher Goh, Keith A. Hall, Anne Pointe, Margarete K. Leclerc, Cheryl Lund, Vince Murphy, "Methods of Copolymerizing Ethylene and Isobutylene and Polymers Made Thereby ", International Publication date: 13 June (**2002**), Symyx Technologies Inc.

[44] Makoto Mitani, Rieko Furuyama, Jun-ichi Mohri, Junji Saito, Seiichi Ishii, Hiroshi Terao, Takashi Nakano, Hidetsugu Tanaka, and Terunori Fujita, "Syndiospecific Living Propylene Polymerization Catalyzed by Titanium Complexes Having Fluorine-Containing Phenoxy-Imine Chelate Ligands", *J. Am. Chem. Soc*. (**2003**) *125*, 4293-4305, b) for a review, see: Haruyuki Makio, Norio Kashiwa, Terunori Fujita "FI Catalysts: A New Family of High Performance Catalysts for Olefin Polymerization" *Adv. Synth. Catal.* (**2002**) *344*(5), 477-493.

[45] a) P. D. Hustad, J. Tian, G. W. Coates, "Mechanism of Propylene Insertion Using Bis(phenoxyimine)-Based Titanium Catalysts: An Unusual Secondary Insertion of Propylene in a Group IV Catalyst System" *J. Am. Chem. Soc.* (**2002**) *124*, 3614-3621, b) J. Tian,; P. D. Hustad,; G. W. Coates, "A New Catalyst for Highly Syndiospecific Living Olefin Polymerization: Homopolymers and Block Copolymers from Ethylene and Propylene" *J. Am. Chem. Soc.* (**2001**) *123*, 5134-5135.

[46] a) Mitani M, Nakano T, Fujita T, " Unprecedented living olefin polymerization derived from an attractive interaction between a ligand and a growing polymer chain", *Chemistry* (**2003**) *9*(11), 2396-403; see also: b) Abhimanyu O. Patil and Gregory G. Hlatky (eds.), "FI Catalysts for Highly Controlled Living Polymerization of Ethylene and Propylene: Creation of Precisely Controlled Polymers" in "Beyond Metallocenes: Next-Generation Polymerization Catalysts" (**2003**) 249 pages.

[47] A) Photochemistry reviews, see for example: *Journal of Photochemistry and Photobiology C: Photochemistry Reviews.* b) Tian H, Yang S. Recent progresses on diarylethene based photochromic switches", *Chem Soc Rev.,* (**2004)** *33*(2):85-97.

Figure 5. Examples of the diarylethene (DAE) and dihydropyrenes (DHP) photoswitches (open and closed conformations).

Diarylethene type photoswitch:

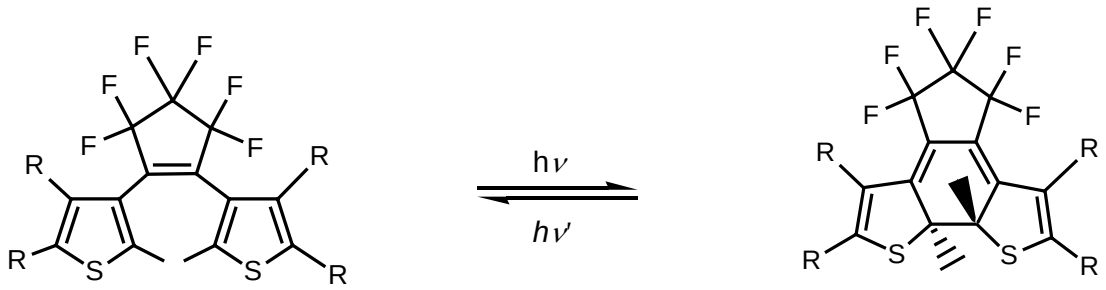

(**12**) (**13**)

colorless, open form colored, closed form

Dihydropyrene type photoswitch:

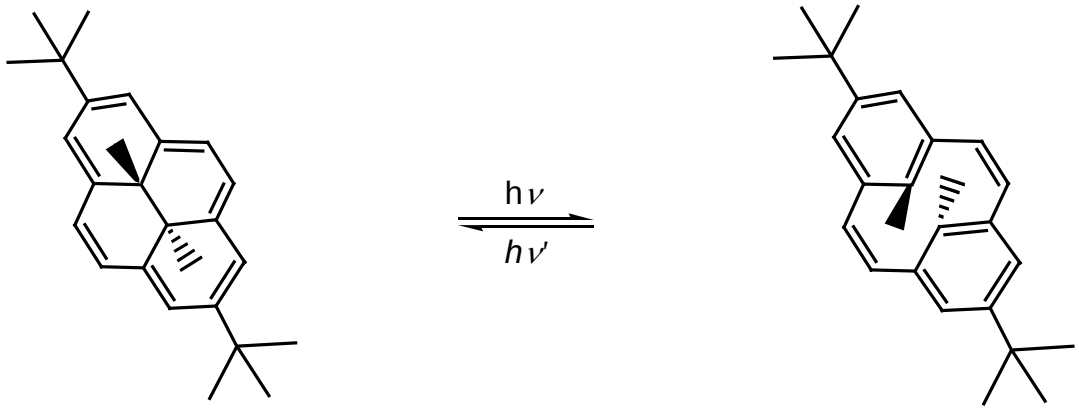

(**14**) (**15**)

green, closed form colourless, open form

From a synthetic point of view, the diarylethene (DAE) photoswitches (PS) are well studied molecules. Many examples exist and substitutions of many different types have been described. In addition, polymeric DAE photoswitches have been made and characterized.

The amount and type of radiation necessary to open (or close) a photoswitch is the (coloration) quantum requirement. The number of molecules responding to the photo-irradiation event is the quantum yield. DAE photoswitches have good coloration quantum

yields and thermal stability[48]. Thermal stability is an important factor in selecting a candidate for polyolefin catalytic ligand development, as temperature is an important means for controlling the molecular weight in polymerization reactions.

The two photo-reactive DAE groups placed on a ring system adjacent (*–cis*) to each other can become oriented in either of 2 conformations: parallel or anti-parallel (see Figure 6)**.** Electrocyclic reactions forming the closed form of the photoswitching molecule can take place only from the anti-parallel conformer in accordance with Woodward-Hoffman rule based on comparable orbital symmetries of 1,3,5-hexatriene. The conrotatory cyclization reaction has been modelled and is proposed to involve π-conjugation pathways involving electron tunnelling[49].

Figure 6. Parallel and anti-parallel conformers of a DAE photoswitch (**16**, **17**):

(parallel conformer) (anti-parallel conformer)

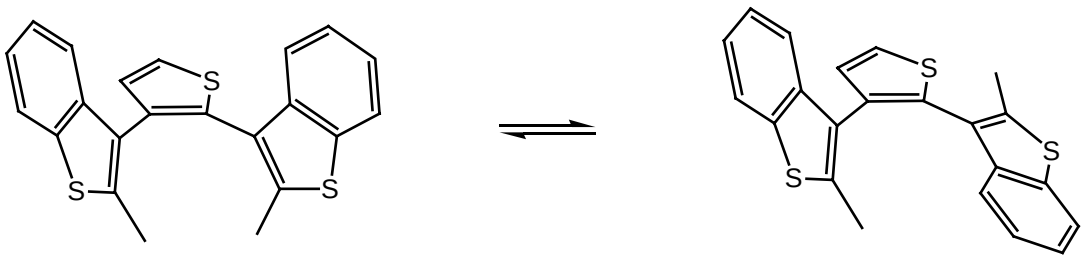

(**16**) (**17**)

The *cis-trans* photo-isomerization found in the stilbenes is avoided by attaching the diarylethene components to a cyclic molecule such as cyclopentene, hexaflurocyclopentene, etc. While a limited number of cyclic rings have been studied as part of the parent ring, many different substitutions on thiophene rings have been reported. Each particular substitution has a unique gated response and provides a handle on photo- accessibility. Careful selection and placement of substitutions in the molecule chosen for the photoswitch is necessary for reason previously described (poisoning with the polymerization reaction, etc). The selection of substituents that are known to have positive outcomes in similar polyolefin catalysis ligands is preferred. A napthyl substitution on indene has been shown to have a very positive effect on the outcome of

[48] a) Kingo Uchida, Eriko Tsuchida, Yoshifumi Aoi, Shinichiro Nakamura, and Masahiro Irie, "Substitution Effect on the Coloration Quantum Yield of a Photochromic Bisbenzothienylethyene", *Chemistry Letters,* (**1999**), 63 -64, b) Yasushi Yokoyama, Hidenori Shiraishi, Yutaka Tani, Yayoi Yokoyama, and Yoshitaka Yamaguchi, "Diastereoselective Photochromism of a Bisbenzothienylethene Governed by Steric as Well as Electronic Interactions", *J. Am. Chem. Soc.* (**2003**), *125,* 7194-7195.

[49] Jun T. Li, Gil Speyer, and Otto F, Sankey, "Theoretical modeling of conduction switching in photochromic molecules", American Physical Society, March Meeting 2004, March 22-26, (**2004**), Palais des Congres de Montreal, Montreal, Quebec, Canada, MEETING ID: MAR04, abstract #N37.003, b) Jun T. Li, Gil Speyer, and Otto F, Sankey "Conduction switching in photochromic molecules" *Phys. Rev. Lett.* (**2004**) *93*, 248 - 302.

dimethylsilyl bridged zirconocene polymerizations, increasing the molecular weight and polymer melting point. A similar substitution in this position, but heterocyclic, would look like benzothiophene. Photoswitches having components such as 2-methyl-benzo[b]thiophene have been described[50].

Substitution studies have also addressed the possibility of controlling the parallel- anti-parallel conformations, the stability of such systems[51], and the effect on energy transfer and modulation.[52] Substituting larger substituents such as isopropyl instead of methyl in the 2-position of benzothiophene has increased the quantum yield through steric hindrance in forming the parallel conformer. The availability of the synthetic methods for such analogs is a resource for future investigations.

The heterocenes are a class of polyolefin complexes that have been shown to be one of the most active and stereospecific class of metallocenes invented to date (*vide supra*). The fusion of a thiophene ring onto a Cp ring, with the proper substituents creates very accessible and long lived polymerization active centers. Substitution of photoswitching components directly onto the Cp however, could create fluctuations in the metal bonding properties and influence molecular stability. This could create undesirable polymerization products or poisons during a polymerization reaction.

---

[50] Masahiro Irie and Kingo Uchida, "Synthesis and Properties of Photochromic Diarylethenes with Heterocyclic Aryl Groups", *Bull. Chem. Soc. Jpn.,* (**1988**), *71*, 985-996, see also reference 122.
[51] Mahmut Kose, Miyuki Shinoura, Yayoi Yokoyama, and Yasushi Yokoyama, "Diastereoselective Photochromism of Bisbenzothienylethenes with an Oxycarbonyl-Related Functional Group on the Side Chain", *J. Org. Chem*., (**2004**) *69*, 8403-8406.
[52] Franc¸isco M. Raymo and Massimiliano Tomasulo, "Electron and energy transfer modulation with photochromic switches", *Chem. Soc. Rev*., (**2005**), *34*, 327-336.

Figure 7. Possible changes in the bonding patterns of metallocene rings during photoswitching in substituents directly attached to the Cp ring.

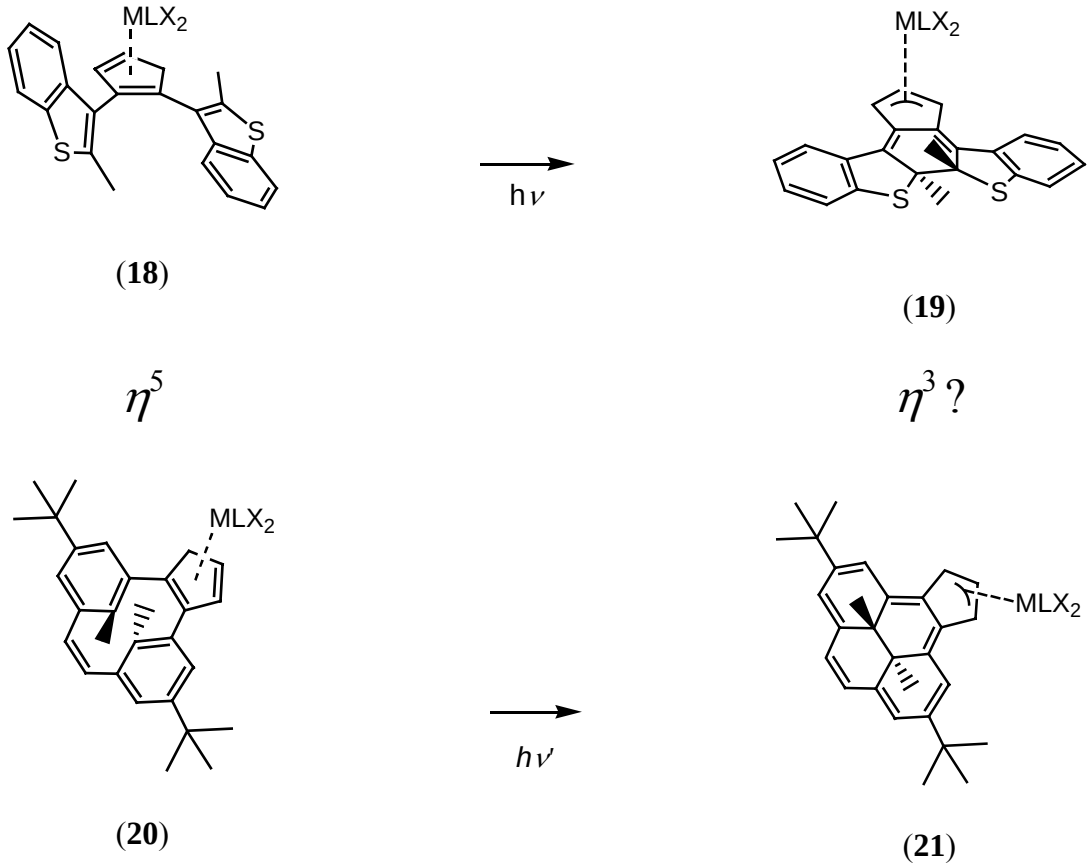

I hypothesized that by substituting the photoactive components onto the 2 and 3 positions of the thiophene fused ring (see Figure 8 for thiopentalene numbering scheme), changing electronic effects at the Cp-ring metal bonding during a polymerization would be remote and the diarylethene photoswitch would be positioned more effectively. The ligand geometry could be influenced and controlled through the opening and closing of the components of the switch in a portion of the molecule away from the metal bonded Cp ring, but at positions known to haven dramatic influence on polymer properties. The opportunity to include photochromic switching of hapticity at the metal center is an opportunity which could be further explored, but is beyond the scope of this dissertation.

Figure 8. Numbering scheme for thiopentalene.

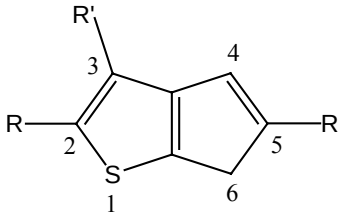

As part of an on going development program for heterocene polyolefin catalysis, a number of potentially available photochromic thiopentalene complexes containing diarylethene substitutions have been made (see Figure 9). These complexes were made chiefly to study the effectiveness of controlling the orientation of the -3' substituted aryl group and the effectiveness of stereo-control the -2 position has on polymerization behaviour. These compounds have adjacent aryl substitution in the 2 and 3 positions on the thiophene ring of the *ansa*-heterocene (zirconocene complex). These examples are less optimized switches and were evaluated for their response in open and closed form in polymerizations (see results/ experimental sections).

Figure 9. Selected phenyl substituted heterocenes without (controls) and with adjacent -aryl substitutions.

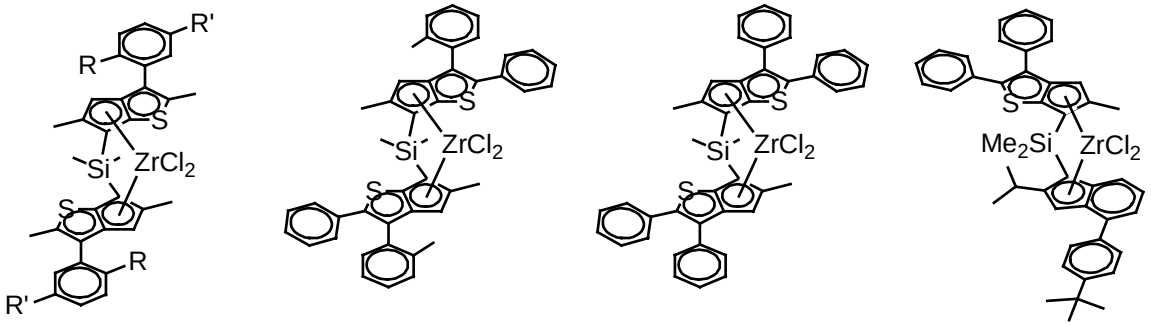

(**22**) R, R' = H
$Me_2Si(2,5Me_2\text{-}3\text{-}PhTp)_2ZrCl_2$
(**23**) R =Me, R' = H
(**24**) R, R' = Me

(25)
$Me_2Si(2\text{-}Ph\text{-}3\text{-}TolylTp)_2ZrCl_2$

(**26**)
$Me_2Si(2,3\text{-}Ph_2Tp)_2ZrCl_2$

(**27**)
$Me_2Si(2,3\text{-}Ph_2Tp)(2iPr4tBuPhInd)ZrCl_2$

The diaryl heterocene complexes shown in Figure 9 have the disadvantage that having phenyl (or tolyl) substituent would be subject to limitations of related photochromatic molecules: they are (typically) thermally unstable and irreversibly cyclize.

Reacting metallocenes photochemically to modify the structure is not a new concept. Bridged metallocenes are typically produced in either a –*rac* or –*meso* orientation and the result can be modified photochemically. Photoisomerization of zirconocene complexes

from -*rac* to -*meso* form (or vice versa, depending on conditions) under irradiation is well know (*vide infra*) however, wavelengths required for photoisomerization of these aryl-thiopentalene metallocene complexes may interfere (i.e., overlap *rac* – *meso* conversion).

Kaminsky studied the photoisomerization of polymerization active metallocenes[53] and detailed photochemical experiments on *ansa*-EBI metallocenes (example: (**5**)) have been described[54]. Upon irradiation, photogenerated ligand and metal centered radicals are formed which are the first steps in *rac*- *meso* isomerization. The treatment of catalytically active *ansa*-metallocenes with radiation is known to affect the photoisomerization from -*rac* complex into -*meso*. This result was also described by Brintzinger[55], where the irradiated metallocene complexes were reacted with 1 equiv of a di-lithium salt of a racemic binaphthol. Upon treatment with intense light (125 W Hg lamp) for 1-2 h in benzene or toluene solutions, the metallocene complex was quantitatively converted to -*rac* binaphtholate complex.

Photoreactivity and –*rac/-meso* conversion rate of metallocenes also depends on the central metal and the substitution pattern. Collins and co-workers reported that the substitution pattern on the Cp ring affects final –*rac/-meso* ratios[56].

Brintzinger has recently studied the more general topic of spectral characterizations of the activated metallocene–MAO complexes with varying wavelengths of visible and UV radiation. These studies provided information about the activated polymerization catalyst and indicate that the wavelengths used to characterize these complexes are not photoisomerizing them[57].

More recently, Erker has studied the synthesis of bridged group 4 metallocenes with bis(alkenylcyclopentadienyl)[58]. Intramolecular photochemical [2+2] cycloaddition of

---

[53] Kaminsky, Walter; Schauwienold, Anne-Meike; Freidanck, Frank. " Photoinduced rac/meso interconversions of bridged bis(indenyl) zirconium dichlorides", *Journal of Molecular Catalysis A: Chemical* (**1996**), *112*(1), 37-42.

[54] Andrea Barbieri, Anna Droghetti, Silvana Sostero, and Oraqzio Traverso, " Photochemistry of *ansa*-zirconocenes: ethylene-bis(1-indenyl)- and ethylene-bis(4,7-dimethyl-1-indenyl)zirconium dichlorides", *J. Photochem. Phorobiol. A: Chem*., (**1999**) *129*, 137-142.

[55] a) H.H. Brintzinger, "Process for converting the achiral meso form of an ansa-metallocene complex into the chiral racemic form" United States Patent 5912373, Issued June 15 (**1999**), b) Katrin Schmidt, Annette Reinmuth, Ursula Rief, Josef Diebold, and Hans H. Brintzinger, "Photochemical Isomerization of Me_2Si-Bridged Zirconocene Complexes. Application to Stereoselective Syntheses of ansa-Zirconocene Binaphtholate Stereoisomers", *Organometallics* (**1997**) *16*, 1724-1728.

[56] a) Collins, S.; Hong, Y.; Taylor, N. J. *Organometallics* (**1990**) *9*, 2695. b) Collins, S.; Hong, Y.; Ramachandran, R.; Taylor, N. J. *Organometallics* (**1991**) *10*, 2349.

[57] U. Wieser, H.H. Brintzinger, "UV/VIS Studies on the activation of zirconocene-based olefin-polymerization catalysts". in Organometallic Catalysts and Olefin Polymerization, R. Blom, F. Arild, E. Rytter, M. Tilset, M. Ystenes, Eds.; Springer: Heidelberg, 2001; p 3. b) U. Wieser, F. Schaper, H.H. Brintzinger, N.I. Mäkelä, H.R. Knuuttila, M. Leskelä, "Effects of an interannular bridge on spectral and electronic properties of bis(cyclopentadienyl) and bis(indenyl) zirconium(IV) complexes" *Organometallics*, (**2002**) *21*, 541.

[58] G. Erker, S. Wilker, C. Krüger, R. Goddard, "Intramolecular [2 + 2] Cycloaddition of Bis(alkenylcyclopentadienyl)zirconium Dihalides: A Novel Way of Synthesizing ansa-Metallocene Complexes", *J. Am. Chem. Soc*. (**1992**) *114*, 10983-10984.

these substituents on the cyclopentadienyl portion of the molecule form a bridge similar to ethylene type 2 carbon ansa metallocenes. These molecules have been studied in comparison with other synthetic pathways leading to complexes with bridging ligands and also in polymerizations.[59]

The photo-association of the cyclopentadienyl ring binding to the metal center and the ring slippage reactions have been studied[60], and have been identified in changing the type of polymer produced.

For the diarylethenes, cyclo-alkenes substituted with heterocyclics such as thiophenes (instead of aryls) have been shown to be thermally stable, have high quantum yield, and are potentially stable to isomerization. Isomerization (cis- trans-) or rearrangement of the thiophene substituents (dancing) of photoswitching components in the thiopentalene olefin system was not probable: 2,3-disubstituted thiopentalenes would not be likely to rearrange. Diarylethenes having thiophenes with -2 positions substitutions including hydrogen, methyl, or halogen substitutions are most common and are stable, well characterized compounds. Methyl substituted thiophenes are simple and accessible; the benzothiophene component has also been investigated and is available in a variety of examples (see below).

In addition, the closed form of the 2,3-benzothiophene thiopentalene substitution (**29**) would be similar in structure to previously studied indenes[61] and heterocenes which have been shown to be active in polymerizations with propene. Dimethylsilyl bis(4-phenyl-thianaptha[b]cyclopentyl)zirconium dichloride (olefin (**28**) drawn in Figure 10) is structurally similar to the closed form of olefin (**29**); the open form (**30**) would be similar to a napthalenic type of substitution (*vide supra*).

---

[59] W.-L. Nie, G. Erker, G. Kehr, R. Fröhlich, "Formation of a Unique ansa-Metallocene Framework by Intramolecular Photochemical [2+2] Cycloaddition of Bis(2-alkenylindenyl)zirconium Complexes", *Angew. Chem. Int. Ed. Engl.* (**2004**) *43*, 310-313. alternatively: "Bildung eines neuartigen ansa-Metallocen-Gerüsts durch intramolekulare photochemische [2+2]-Cycloaddition von Bis(2-alkenylindenyl)zirconium Komplexen", *Angew. Chem.* (**2004**) *116*, 313-317.

[60] Bernd Klingert , Achim Roloff[1], Bernhard Urwyler, Jakob Wirz, " Photochemical Ring Slippage of Bis(pentafluorophenyl)titanocene: Reaction kinetics and matrix isolation of the primary photoproduct", *Helvetica Chimica Acta* (**2004**) *71*(8) 1858 – 1867.

[61] Nicole Schneider, Monika E. Huttenloch, Udo Stehling, Robin Kirsted, Frank Schaper, and Hans H. Brintzinger, "ansa-Zirconocene Complexes with Modified Benzindenyl Ligands: Syntheses, Crystal Structure, and Properties as Propene Polymerization Catalysts", *Organometallics* (**1997**) *16*, 3413-3420.

Figure 10. Similarities heterocene olefin (**28**) and diarylethenes photoswitch olefins in closed (**29**) and open (**30**) conformations.

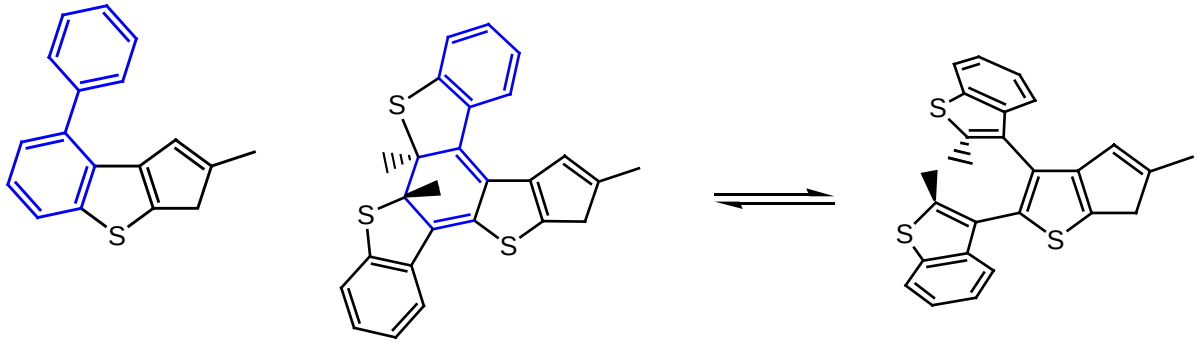

(**28**) (**29**) (**30**)

Polyaromatic types of complexes containing benzoindene ligands have been made and studied in propene polymerizations.[61] The metallocene complex made from (**28**) type of catalytic system is a comparable heterocene.[62]

Substitution of thiopentalene with substituted thiophenes as photoswitching components in the 2,3- position would create similarities between structure (**31**) and (**33**), with the exception that the thiophene rings would be smaller than the 2,4 substituted benzene substitution previously reported. Ewen et al. previously reported the silyl-bridged complex (**24**) as being highly stereospecific making few regio-errors and producing a high molecular weight polymer.

The expected polymer from an *ansa*- metallocene catalyst having a benzothiophene substitution in the 3-position would be predicted to have a similar properties. The open form of the 3- substituted thiopentalene as a photoswitch component would also be expected to behave in the same way.

[62] M.J. Elder and R.L. Jones, J.A. Ewen, "Organometallic transition metal compound, bis-cyclopentadienyl ligand system and process for preparing polyolefins" 19 May **2005**. PTC Int. Appl. WO 2005 44,870.

Figure 11. Comparative diarylethene systems and conventional thiopentalene ligand olefin components.

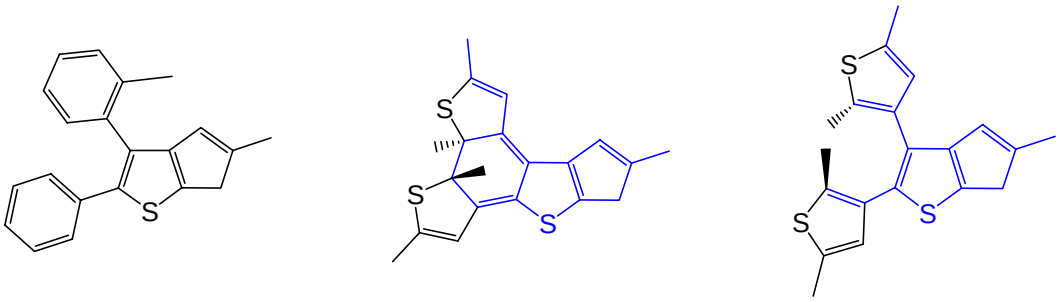

(**31**) (**32**) (**33**)

From the heterocene ligand (**28**) was fashioned a bridged metallocene catalyst with high activity making high molecular weight polymer. The structure of this olefin ligand component resembles (**29**) in the closed form of the diarylethene (DAE) 2,3-(2-methylbenzo[b]thiophene)thiopentalene photoswitch (Figure 10). The flat geometry that was first suggested by Ewen[63] as an experimental control and basis for influencing the stereo-tactic and regio-tactic monomer placements in (**22**), (**23**) and (**24**), and could possible be further explored. We note here that the decreasing –stereo and –regio errors for (**22**), (**23**) and (**24**) coincided with the orientation of the plane of the phenyl substitution in the thiopentalene ligand component: the greater the angle of the plane of the phenyl group with the plane of the thiopentalene ligand component, the higher the melting point was of the polymer produced (see Figure 14).

1.4.1 The Diarylethene Photoswitch

In recent years, excellent reviews of the literature have been made concerning diarylethenes (DAE) photoswitches[64] . In addition, studies on diarylethene switches have been the subject of dissertations[65].

[63] J. A. Ewen, personal Communication, **1986**.
[64] a) Masahiro Irie, "Diarylethenes for Memories and Switches", *Chem. Rev.* (**2000**) *100,* 1685-1716, b) He Tian* and Songjie Yang, "Recent progresses on diarylethene based photochromic switches", Chem. Soc. Rev., (**2004**) *33*, 85-97.
[65] Modified graphic from: Linda Nienke Lucas, "Dithienylcyclopentene optical switches: towards photoresponsive supramolecular materials" Groningen : University Library Groningen, (**2001)**.

Figure 12. Stilbene photocyclization reactions to produce dihydrophenanthrene

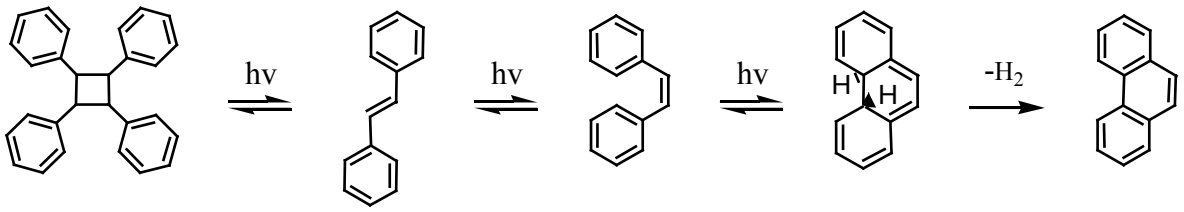

(**34**) (**35**) (**36**) (**37**) (**38**)

In the opening of his DAE review, Irie points out that for stilbene, *"When the 2- and 6-positions of the … phenyl rings were substituted with methyl groups, the elimination reaction was suppressed and the compound underwent a reversible photocyclization reaction, that is, a photochromic reaction, even in the presence of oxygen. The lifetime of the colored dihydro- type isomer of 2,3-dimesityl-2-butene was, however, very short (t1/2) 1.5 min at 20 °C)…… Such a thermally unstable photochromic system is not useful for optical memories and switches."* [64]

The fact that most photochromic compounds are thermally sensitive and revert to their open form when heated may not be a disadvantage when considering an application in catalytic systems. Control over the population of molecules having any given state could be better met if opening of a photochromic molecule is aided by a thermally activating event.

Clearly, for the photo-active portions of a molecule to react, these must be maintained in the proper orientation. Rings adjacent to each other in proximity are a steric requirement for the diarylethenes. Ring systems were introduced into switches to prevent the -*cis* to -*trans* photoisomerization which can compete with the photo-cyclization process. In addition Woodward Hoffman rule must be satisfied for a cyclization reaction to occur.

Diarylethene photoswitches are thermally stable and have tuneable photochromic properties based on their substitution pattern. The most cited examples have substituted thiophenes on fluorinated cyclopentene. Substituted thiophenes have been successfully substituted onto perfluorocyclopentene[66], 1,2-bisaryl-substituted maleic anhydride[67], maleimide[68], quinine[69], 2,5-dihydrothiophene and cyclopentene[70].

---

[66] M. Hanazawa, R. Sumiya, Y. Horikawa and M. Irie, *J. Chem. Soc.*, *Chem. Commun.*, (**1992**) 206.
[67] M. Irie and M. Mohri,, *J. Org. Chem.*, (**1988**) *53*, 803.
[68] T. Yamaguchi, K. Uchida and M. Irie, *J. Am. Chem. Soc.*, (**1997**) *119*, 6066.
[69] X. Deng and L. S. Liebeskind, *J. Am. Chem. Soc.*, (**2001**) *123*, 7703.
[70] a) Linda N. Lucas, Jan van Esch, Richard M. Kellogg and Ben L. Feringa, "A new class of photochromic 1,2-diarylethenes; synthesis and switching properties of bis(3-thienyl)cyclopentenes", *Chem. Commun.*, (**1998)**, 2313–2314. b) Zhen-Nian Huang, Bao-An-Xu, Sheng Jin, and Mei-Gong Fan, " Facile Synthesis of Novel Photochromic 1,2-Diheteroaryl-Substituted Cycloalkenes by Titanium-Induced Intramolecular Coupling Reaction", *Synthesis* (**1998**) 1092.

Wynberg[71] showed that the "…irradiation of 2,3-diphenylthiophene" (**39**) "in dilute ether solution gave a single product …isolated in high yield which was identified as phenanthro[9,10-b]thiophene" (**40**) (see Figure 13). The reaction is very similar to the conversion of cis-stilbene (**36**) to phenanthrene (**38**)[72]. This reaction provided a model for the anticipated conversion by irradiation of the diaryl thiopentalenes into the closed forms of the photoswitches that we tested and report.

Figure 13. Irridation of 2,3-diphenylthiophene to phenanthro[9,10-b]thiophene.[73]

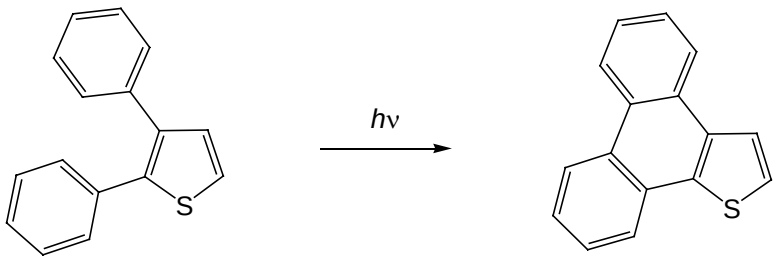

(**39**) (**40**)

In our early studies with thiopentalenes in polyolefin catalysis, the influence of the pendant phenyl group in the 3 position on the thiophene ring was proposed and studied[74]. It was found that when going from a methyl substitution in the -3 position to a phenyl group in the -3 position, the melting point of the polymer made from the catalyst produced increased. This was as expected, based on the carbocene teachings from earlier studies. What was not known, (but predicted by Ewen[75]) was that the orientation of this ring could be influenced by the number and types of substituents on either the pendant phenyl group or by substituents in the neighbouring -2 position on the thiophene ring. Subsequent studies have indicated that changes in the orientation of the 3- ring from planar to 90° have a measurable effect of the regio-chemical errors made by the

---

[71] Hans Wynberg, H. van Driel, Richard M. Kellogg, and J. Buter, J. *Am. Chem. Soc*., (**1967**) *89*, 3487 – 3494.

[72] (a) Yusheng Dou and Roland E. Allen, "Dynamics of the photocyclization of cis-stilbene to dihydrophenanthrene", *Journal of Modern Optics*, (**2004**) *51*(15-18) 2485 - 2491 (b) R. Srinivasan and John C. Powers, Jr., " Photochemical Formation of Phenanthrene from *cis*-Stilbene in the Vapor Phase", *The Journal of Chemical Physics* (**1963**) *39*(3), 580-584, (c) see also L. G. Samsonova, T. N. Kopylova, N. N. Svetlichnaya, O. S. Andrienko, "The Phototransformations of trans-Stilbene and Its Derivatives on Laser Excitation", *High Energy Chemistry* (**2002**) *36*(4) 276 – 279.

[73] Hans Wynberg, H. van Driel,' Richard M. Kellogg, and J. Buter, "The Photochemistry of Thiophenes. IV. Observations on theScope of Arylthiophene Rearrangements, *Journal of the American Chemical Society* (**1967**) *89*(14), 3487-3494.

[74] (a) J.A. Ewen, "Zirconium Catalysts with Cp Ring-fused to Pyrroles and Thiophenes" presentation at ACS National Meeting in New Orleans, Aug. **1999**.

[75] John A. Ewen, *ibid*.

catalysts[76]. The melting point of the polymer increases with increasing torsion angle of the 3' substituted ring (see Figure 14).

Substitution of varying sizes in the -2 position adjacent to the aryl group in the -3 position on thiophene have been made and tested. Molecular modelling studies have also confirmed this effect.[31]

Figure 14. Varying substitution on the -3 position of thiophene[31].

torsion angle of the -aryl substitution[(a)]: 0° (flat) | 54° | 80° | 90°

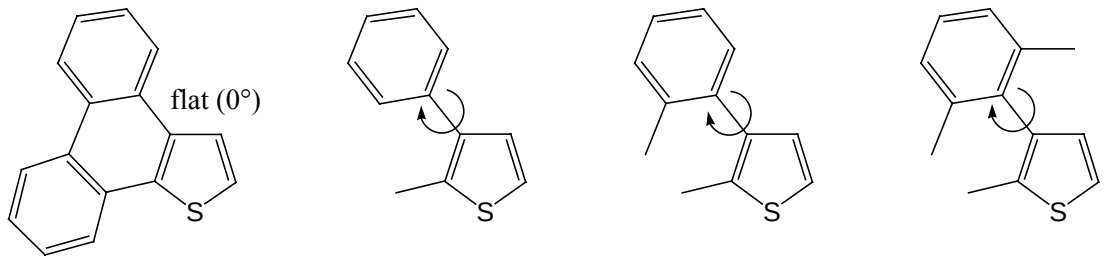

T_m2 = 156°C [(b)] | T_m2 = 162°C [(b)]

(41) **(42)** **(43)** **(44)**

a) Calculated torsion angles for the preferred conformations of the phenyl and tolyl substituted zirconocene were calculated by J.A. Ewen, personal communication.
b) Conditions for the polymerizations using the zirconocenes made from these ligand precursors: 4L stainless steel autoclave, 2.2 L propylene, 5 ml 10% MAO in toluene, 70°, 1 h.

1.4.2 The Dihydropyrene Photoswitch

As an alternative to the diarylethene photoswitch, dihydropyrene (DHP) (**14**, **15**) is available and studied extensively by Mitchell[77]. The chemistry of these molecules has been reviewed[78], and the evolution of the structures which are being developed today in this area are interesting.

The basic DHP photoswitch (see Figure 5) has methyl groups in the interior positions to prevent irreversible ring closure. The *tert*-butyl groups have been added to increase solubility. Additional modifications included polycyclic structures and multiply connected switching molecules, some of which can be addressed independently.

---

[76] see for example Exxon-Mobil Patent application WO 03/050131A1, filed Dec. **2001**.
[77] Reginald H. Mitchell is one of the leading workers in this field and has numerous contributions: see http://www.chemistry.uvic.ca/mitchell/mitchell.htm for information on his groups work at the University of Victoria.
[78] Reginald H. Mitchell, "The Metacyclophanediene-Dihydropyrene Photochromic Switch", *Eur. J. Org. Chem.* (**1999**), 2695-2703.

DHP is a negative photochrome: it is coloured in the thermally stable form and becomes colour-less upon irradiation[79], and undergoes dramatic changes in electronics and geometry upon photochemical activation.

Following the synthetic protocol described by Mitchell, the DHP photoswitch can be synthesized in good yield and reasonable purity (see experimental section). The molecule seen in Figure 5 (**14**, **15**), has been synthesized on a large scale and modified with a large number of substituents for a variety of applications.

The addition of the Cp ring on DHP has been demonstrated and has been shown to be photochemically active as a anion complexed with a metal[80]. In addition, metallation of a DHP-arene complex with ruthenium and chromium has been reported[81]. As pointed out earlier, the disruption in bonding at the active metal center during a polymerization reaction could be a problem, so alternatives to the use of the dihydropyrene-photoswitch (DHP-PS) needed to be developed.

A disadvantage of the DHP-PS is thermal sensitivity. At higher temperatures, these photoswitches revert to the closed form. For most current polymerization reactions, especially solution processes involving low monomer concentrations, higher temperatures may be required (above 100°C).

In order to simply gain a handle to do chemistry and make constructions onto the DHP photoswitch, a reactive group such as a halogen was preferred. Bromination of the DHP system is known[82]. This method, as an alternative to the previously described work by Mitchell's group constructing a Cp directly on the DHP photoswitch, would provide some distance between the penta-hapto bonding in the Cp ring system and the changing aromaticity in the photoactive centers on the switch (a situation described earlier for the diarylethene cyclopentadienyl photoswitch).

---

[79] Reginald H. Mitchell, Timothy R. Ward, Yongsheng Chen, Yunxia Wang, S. Ananda Weerawarna, Peter W. Dibble, Michael J. Marsella, Adah Almutairi, and Zhi-Qiang Wang, "Synthesis and Photochromic Properties of Molecules Containing [e]-Annelated Dihydropyrenes. Two and Three Way ð-Switches Based on the Dimethyldihydropyrene-Metacyclophanediene Valence Isomerization", *J. Am. Chem. Soc*., (**2003**), *125*, 2974-2988.

[80] Reginald H. Mitchell, Wei Fan, Danny Y.K. Lau, and David Berg, "An Annulene-Fused Cyclopentadienide. A Photochromic Cyclopentadienodimethyldihydropyrene Where the Fused Cyclopentadienide Group Resembles Benzene in Its Effect on the Dihydropyrene-Metalocyclophane Valence Isomerization", *J. Org. Chem.,* (**2004**) *69*, 549-554.

[81] Reginald H. Mitchell, Zinka Brkic, Vittorio A. Sauro, and David J. Berg, "A Photochromic, Electrochromic, Thermochromic Ru Complexed Benzannulene: an Organometallic Example of the Dimethyldihydropyrene-Metacyclophanediene Valence Isomerization*", J. Am. Chem. Soc.,* (**2003**), *125*, 7581-7585.

[82] a) Masashi Tashiro and Takehiko Yamato, "Metacyclophanes and Related Compounds. 4. Halogenations of 8,16-Dialkyl-anti-5,13-di-tert-butyl[2.21-metacyclophan-1-enes and 2,7-Di-tert-butyltrans-10b, 10c-dialkyl- 10b, 10c-dihydropyrenes", *J. Am. Chem. Soc.,* (**1982**) *104*, 3701-3707 b) Reginald H. Mitchell, Yongsheng Chen and Ji Zhang, "N-Bromosuccinimide-Chloroform, A more Convenient Method to Nuclear Brominate Reactive Aromatic Hydrocarbons", *OPPI Briefs*, (**1997**) *29*(6), 715-719.

Applications of the DHP photoswitch in polyolefin catalysis not involving direct switch-Cp coupled complexes or non-metallocenes were considered. In recent presentations, publications and patents by Dow and others, non-metallocene catalysts containing pyridyl-amine-Hf complexes with sigma bonded ancillary ligands were described[83]. In evaluating these materials the opportunity to explore the possibility of the placement of a DHP photoswitch in such a molecule was considered: It could be possible to mount the DHP photoswitch onto a pyridyl-amine-Hf catalyst and effect a change in the properties of the polymer made by a α-olefin polymerization.

The pyridyl-amine-Hf complex is made with aromatic substituents in a position on the molecule that are potentially sensitive to changing ligand geometries. These catalysts were discovered using the combinatorial methods developed by Symyx[84], and combinatorial methods have been applied in making libraries for evaluation. In a related patent[85] Symyx has provided a number of examples for the synthesis of these types of complexes.

Differences in the polymer made between phenyl and phenanthrene substitutions at the bridging carbon between the bonding N and the pyridyl group were observed, and the substitution of a tolyl group was reported in the patent literature.

---

[83] a) James C. Stevens, H. Boone, T. Boussie, G.M. Diamond, C. Goh, K. Hall, A.M. LaPointe, M.K. Leclerk, J. Longmire, V. Murphy, R. Rosen, J. Shoemaker, H. Turner, V. Busico, R. Cipullo, and G. Talarico, " New Highly Active Group 4 C_1-Symmetric Catalysts for Isotactic-Selective High Temperature Solution Polymerization of Propene, and Copolymerization of Propene With Ethene. 1 – Synthesis, Process and Products", *European Polymer Conference on Stereospecific Polymerization and Stereoregular Polymers, Proceedings*, Milano, Italy (**2003)** June 8 – 12, b) V. Busico, R. Cipullo, G. Talarico, and J.C. Stevens, ibid.

[84] Boussie, T.R. et.al. Journal of American Chemical Society, 125, **2003,** 4306-4317.

[85] Symyx Patent, WO 02/46249

Figure 15. Selected examples of the pyridyl-amine-Hf complex from WO 03/040201.

Example G: Example H: Example J:

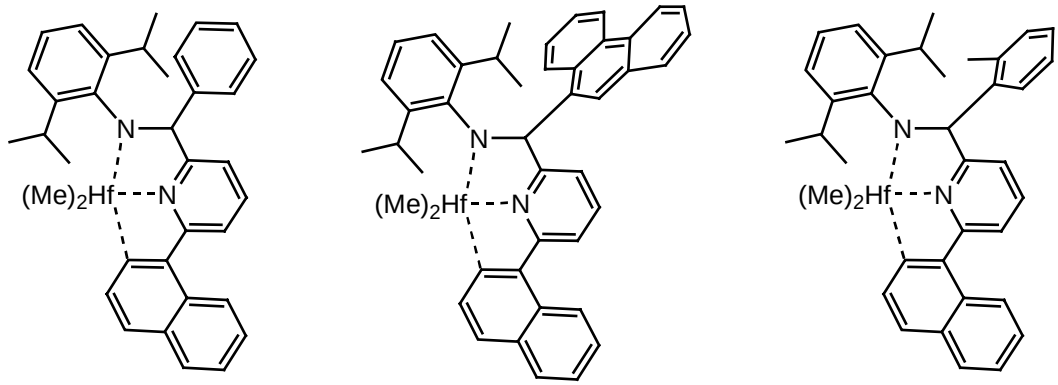

(**45**) (**46**) (**47**)

1.5 Selection of targets:

Synthesis of a commercially viable catalyst containing a photoswitch must be simple and economic. The methods used must be synthetically accessible if these molecules are to become more than academic curiosities, especially in the field of polyolefin catalysis.

Two types of reported photoswitches, dihydropyrene photoswitch (DHP-PS1) and diarylethene-PS (DAE-PS) were candidates for development into polyolefin catalyst examples. Based on the above, the DHP photoswitch could be cobbled onto a pyridyl-amine-Hf type system and make new polymers. The DAE photoswitching components could also be fashioned onto a metallocene catalyst with the possibility of influencing ligand geometries that could control monomer insertions.

1.5.1 Synthetic Strategies and Methods for the DHP model:

In consideration of the above, the addition of a DHP photoswitch at the bridging carbon between the bonding N and the pyridyl group could be effective in changing polymerization dynamics (see Figure 16). For this study, earlier work on the Cp-fused DHP ligand was considered useful but controlling the changing hapticity of the Cp-metal bond is currently left for future development.

One major advantage in the DHP systems is that almost quantitative conversion of the forms is achieved. Moreover, the drastic change in the geometry between the open and closed form is potentially very directing. Synthetic methods needed to effect this combination were in existence based on the reported methods for placing different substituents at critical positions.

Figure 16. Candidate for DAE photoswitch polyolefin catalysis model: the DHP- pyridyl-amine-Hf complex:

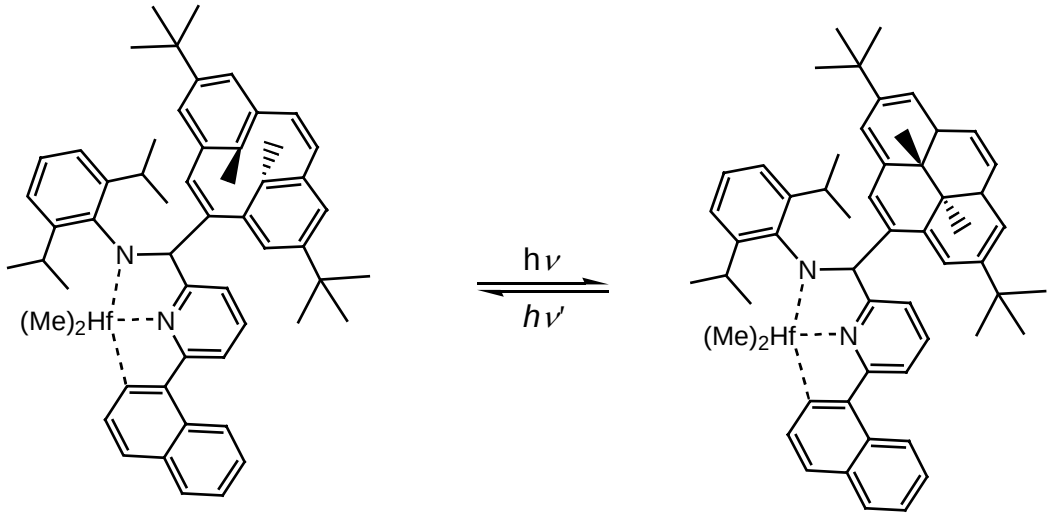

(**48**) (**49**)

1.5.2 Synthetic Strategies and Methods for the DAE model:

Synthetic strategies that have been developed for the current literature examples of DAE photoswitches are not directly applicable to making metallocenes. Firstly, most of the known DAE photoswitches are constructed onto 5 membered saturated rings that do not have available bonding sites for a catalytic metal. Literature examples in which the parent ring systems onto which photoreactive hetero-diaryl groups have been attached have predominately included hexafluorocyclopentane, cyclopentane[86], or dihydrothiophene[87]. Secondly, substitutions of reactive groups (such as fluorescence or electrochemically active groups) have been reported[88], most of which could interfere with the polymerization reaction. Thirdly, the methods for constructing the DAE photoswitches although simple and straightforward (involving coupling and cyclization steps/ ring closure) are in general, low yielding.

The DAE photoswitch having benzothiophene substitutions were targeted based on the following observations:

---

[86] Linda N. Lucas, Jan van Esch, Richard M. Kellogg and Ben L. Feringa, "A new class of photochromic 1,2-diarylethenes; synthesis and switching properties of bis(3-thienyl)cyclopentenes", *Chem. Commun.* (**1998**) 2313–2314.

[87] Zhen-Nian Huang, Bao-Au Xu, Sheng Jin, Mei-Gong Fan, "Fascile Synthesis of Novel Photochromic 1,2-Diheteroaryl-SSubstituted Cycloalkanes by Titanium Induced Intramolecular Coupling Reaction", *Synthesis* (**1998**) 1092-1094.

[88] Francisco M. Raymo and Massimiliano Tomasulo, "Electron and energy transfer modulation with photochromic switches" *Chem. Soc, Rev.* (**2005**) *34*, 327-336.

The 2-methylbenzothiophene when attached to hexafluoro-cyclopentane provides reasonable opening/closure reaction kinetics at reasonable irradiation intensities. In addition, from a synthetic standpoint, when incorporating 2-methylbenzothiophenes as photochemical reacting substitutions, the benzo- substitution limits side reaction that could have taken place on a thiophene nucleus. An un-substituted thiophene as a photoswitching substitution would provide available reaction sites for the construction of the Cp ring onto thiophene (for example, the Friedel-Crafts/ Nazarov cyclization to build a Cp-ring would not be regioselective and cyclize on the photoswitching side of the molecule: a target for later study), and the 3 position, although less reactive, could also be susceptible. In addition, diarylethenes having benzo-thiophene as a substitution have shown excellent fatigue resistance and thermal stability.

Thiophene substitutions on a thiopentalene which have ketones or amino-imino substituents could also be problematic, creating sites for by-product reactions, but if protected could become useful as monomers.

In beginning this project some of the scouting experiments and synthetic methods produced marginal results. The methods developed for synthesis of components not used in the final DAE-ligand-catalyst photoswitches are included for selected examples. Some of the intermediates are novel compounds that may be useful for making other photo-switching compounds and may find alternative application. For example, no diarylethene photoswitches reported in the literature are linked to cyclopentadienyl or unsaturated heterocyclic ring systems such as thiophene. In addition, no example of a heteropentalene type photoswitch has been reported to date. These selected compounds made in the evolution of a successful synthetic strategy and are included.

1.6 Discussion of Synthetic Methods:

The synthesis of metallocenes having heteroatoms ring-fused to cyclopentadiene has been discussed in several patents[89] and publications [90]. The synthesis of the thiopentalenes and the methods that have evolved in making them into commercially viable metallocene catalyst components can be gleaned from patent literature.

---

[89] John A. Ewen, Michael J. Elder, Robert L. Jones, "Heterocyclic ring-fused metallocene catalysts for olefin polymerization" (**2003**) 29 pp, US 6635779 B1 20031021, b) John A. Ewen, Michael J. Elder, Robert L. Jones, "Metallocene compounds, their preparation, and use in catalytic systems for the polymerization of olefins" (Basell Technology Company B.V., Neth.). PCT Int. Appl. (**2001**), 78 pp. WO 2001044318 A1 20010621 Priority: US 99-461858 19991215.

[90] see especially the supplemental materials section in: a) John A. Ewen, Robert L. Jones, Michael J. Elder, Arnold L. Rheingold and Louise M. Liable-Sands' " Polymerization Catalysts with Cyclopentadienyl Ligands Ring-Fused to Pyrrole and Thiophene Heterocycles", *J. Am. Chem. Soc.* (**1998**), *120*, 10786-10787, b) John A. Ewen, Michael J. Elder, Robert L. Jones, Arnold L. Rheingold, Louise M. Liable-Sands, and Roger D. Sommer, " Chiral Ansa Metallocenes with Cp Ring-Fused to Thiophenes and Pyrroles: Syntheses, Crystal Structures, and Isotactic Polypropylene Catalysts*", J. Am. Chem. Soc.* (**2001**) *123*, 4763-4773.

1.6.1 Bromination of Thiophenes

Bromination of thiophene or substituted thiophenes was an integral part of the synthetic protocol. In orienting experiments successful mono-bromination followed by lithiation was strategic in developing coupling reactions involving either nickel or palladium. Electrophilic bromination of thiophene, thiopentalene, and selenophenes is well known, and for example takes place using bromine in aqueous sodium acetate[91]. This method can, however, lead to varying amounts of di-brominated products. The method was not selective.

In an unrelated synthesis, Mitchell has shown that electrophilic bromination of dihydropyrene can take place using NBS under mild conditions[92]. The conditions are similar to those used in free radical bromination, but are more selective towards unsaturated bonds rather than aliphatics.

Using a modification of the Mitchell protocol, treatment of 2-methylbenzo[b]thiophene resulted in the selective bromination at the -3 position, with a small amount of di-brominated product (the second bromine substitution taking place on the fused ring and not on the 2-methyl position). Similarly, treatment of 2,5-dimethylthiophene under identical conditions selectively mono-brominated in the -3 position in high yield. Finally, treatment of 5-methylcyclopenta[b]thiophen-6-one with two equivalents of NBS did not yield the desired product, 2,3-dibromocyclopenta[b]thiophene-6-one, and electrophilic bromination using 2.5 equivalents of molecular bromine with sodium acetate was required. In this experiment only traces of tri-brominated product were formed.

---

[91] Olle Karlsson, "Bromination of some Heteroaromatic Acyl Compounds with Aqueous Bromine/Sodium Acetate", *Synthetic Communication*, (**1981**), *11*(1), 29-34.
[92] R.H. Hitchell. Y. Chen, J. Zahng, "N-Bromosuccinamide-Chloroform, A more convenient method to nuclear brominate aromatic hydrocarbons", *OPPI Briefs*, (**1997**) *29*(6), 715-719.

1.6.2 Lithiation of Thiophenes

Lithium halogen exchange reactions are important for preparing Grignards and/or boronic acids used in the synthetic procedures described. Treatment of thiophenes and benzothiophenes with nBuLi is convenient and well studied[93]. 3-lithiothiophene has been shown to be stable even at room temperature when prepared in hydrocarbon (hexane) solvents using small amounts of THF[94]. 3-Lithiothiophenes prepared in cold ethereal solutions are unstable at ambient temperature towards ring opening to provide phenylacetylene when treated with an electrophile such as dimethylsulfate[95].

Thiophen-yl Gringard reagents have been prepared by sonic irradiation of metal/ bromothiophene mixtures: coupling reactions proceeded in high yields.[96] In some of our experiments 3-benzothienylmagnesium bromide in diethyl ether was synthesized by the entrainment method with 1,2-dibromomethane[97] in analogy with a reported procedure[98].

1.6.3 Kumada Coupling (Ni) / Suzuki Coupling (Pd)

Coupling (aryl)halides with Grignard reagents using 1,3-bis(diphenylphosphinopropane nickel (II) chloride (NiDPPP) (**50**) and other Ni reagents has been reviewed[99]. Recent reviews on the method and application of Pd sources have been published[100].

1.6.3.1 Arylboronic Acids

One of the best methods for coupling heteroaryl groups is the Suzuki coupling reaction[101]. A number of methods exist for preparation of boronic acids from thiophenes[102].

---

[93] R.P. Dickinson, B. Iddon, "Synthesis and Reactions of 3-Benzo[b]thienyl-lithium", *J. Chem. Soc. (C),* (**1968**), 2733 – 2737.

[94] Xiaoming Wu, Tian-an Chen, Lishan Zhu, and Ruben D. Rieke, "Room Temperature Stable 3-Lithiothiophene: a Fascile Synthesis of 3-Functionalized Thiophenes", *Tetrahedron Letters* (**1994**), *35*(22), 3673-3674.

[95] R.P. Dickinson and B. Iddon, "On the Stability of 3-benzo[b]thienyl-lithium", *Tetrahedron Letters,* (**1970**), *17,* 975-978.

[96] A. Amer, A. Burkhardt, A. Nkansah, R. Shambana, A. Galal, H.B. Mark Jr., and Hans Zimmer, " Studies of Some Hindered 2,2'-Bithienyls and 3,3' –Bridged 2,2 –Bithienyls with Special Reference to their UV Spectra and Oxidation Potentials", *Phosphorus, Sulfur, and Silicon*, (**1989**) *42*, 63-71.

[97] D.E. Pearson, D. Cowan, and J.D. Becker, *J. Org. Chem*., (**1959**) *24*, 504-509.

[98] S. Gronowitz, K. Pettersson, *J. Heterocyclic Chem.*, (**1976**) 1099-1100.

[99]a) Kohei Tamao, Koji Sumitani, Yoshihisa Kiso, Michio Zembayashi, Akira Fujioka, Shun-ichi Kodama, Isao Nakajima, Akio Minato, and Makoto Kumada, "Nickel-Phosphine Complex-Catalyzed Grignard Coupling. I. Cross-Coupling of Alkyl, Aryl, and Alkenyl Grignard Reagents with Aryl and Alkenyl Halides: General Scope and Limitations", *Bull. Chem. Soc. Japan* (**1976**) *49*(7), 1958-1969, b) K. Tamo, S. Kodama, I. Nakajima, and M. Kumada, "Nickel-Phosphine Complex-catalyzed Grignard Coupling-II, Grignard COupling of Heterocyclic Compounds", *Tetrahedron* (**1982**) *38*(22) 3347-3354.

[100] Sambasivarao Kotha, Kakali Lahiri, and Dhurke Kashinath, "Recent applications of the Suzuki-Miyaura cross-coupling reaction in organic synthesis", *Tetrahedron* (2**002**) *58*, 9633-9695.

[101] A. Suzuki "Recent advances in the cross-coupling reactions of organoboron derivatives with organic electrophiles, 1995-1998", *J. Organomet. Chem*., 576 (**1999**), *1* (22), 147-168, b) Adam F. Littke, Chaoyang Dai, and Gregory C. Fu, "Versatile Catalysts for the Suzuki Cross-Coupling of Arylboronic

High yields have been reported for preparing boronic thiophenes. 2-thiophene boronic acid, 3-thiophene boronic acid, and 2-benzo[b]thiophene boronic acid are commercially available (Aldrich). Improved methods for preparation are available[103]. Di-substituted thienylboronic acids are also reported[104].

In our experimental protocol, a di-coupling Suzuki reaction was preferred. Reaction for di-substituted 1,1-alanines have been reported[105]. This study couples two benzothiophene-2-boronic acid or benzothiophene-3-boronic onto a substituted di-halogen in one pot, simultaneously, using 5 equivalents (EQ) of the boronic acid, 20 mol% $PdCl_2(PPh_3)_2$, 4 EQ Na_2CO_3, in 10% water in DME. Yields ranged from 40 to 90%. This was the protocol we eventually modified and developed as an integral part of our systems.

Acids with Aryl and Vinyl Halides and Triflates under Mild Conditions", *J. Am. Chem. Soc.* (**2000**) *122*, 4020-4028.

[102] a) Salo Gronowitz and Dan Peters, "Convient Synthesis of Various Terheterocyclic Compounds by Pd(0)-Catalyzed Coupling Reactions", *Heterocycles* (**1990**) *1*, 30, 645-658. b) Salo Gronowitz and Karolina Peters, Palladium Catalyzed Coupling of 3-Thiopheneboronic acid with Halothiophenes", *Chemica Scripta* (**1983**) *22*, 265-266, c) Salo Gronowitz, Vladimir Bobsik, and Karolina Lawitz, Palladium Catalyzed Synthesis of Unsymmetrical Bithienyls from Thiopheneboronic Acids and Halothiophenes" *Chemica Scripta* (**1984**) *23*, 120-122 d) Claus Christophersen, Mikael Begtrup, Søren Ebdrup, Henning Petersen, and Per Vedsø, " Synthesis of 2,3-Substituted Thienylboronic Acids and Esters", *J. Org. Chem* (**2003)**, *68*, 9513-9516.

[103] Elizabeth Tyrrell and Philips Brookes, "The Synthesis and Application of Heterocyclic Boronic Acids", *Synthesis*, (**2004**) *4*, 469-483.

[104] Claus Christophersen, Mikael Begtrup, Soren Ebdrup, Henning Petersen, and Per Vedso, "Synthesis of 2,3-Substituted Thienylboronic Acids and Esters", *J. Org. Chem*. (**2003**) *68*, 9513-9516.

[105] Ana S. Abreu, Nata´lia O. Silva, Paula M. T. Ferreira, Maria-Joaõ R. P. Queiroz, and Mariano Venanzi, "New β,β-Bis(benzo[*b*]thienyl)dehydroalanine Derivatives: Synthesis and Cyclization", *Eur. J. Org. Chem.*, (**2003**), 4792-4796.

2.0 Results

Polyolefin catalyst intermediates and organometallic complexes made containing a photoswitch are summarized below. Details of the synthetic methods and analytical results characterizing the compounds are included in the experimental section.

Two types of metallocene complexes having a diarylethene component were made and tested: un-bridged and bridged. The most direct route demonstrating the effectiveness of a DAE photoswitch was to first make an olefin component, then make the bis-ligand zirconium complex from it. The unbridged bis DAE-olefin-PS containing two photo-switchable components was less preferred in initial testing scenarios than a single photoswitch component system. It was the simplest and most direct to make.

In addition, the ketone intermediate (**77**) having a photoswitch was metallated with one equivalent of nBuLi, dehydrated to olefin, made into an anion, and then reacted with commercially available $nBuCpZrCl_3$ (**51**) (Figure 22). The intermediates were well characterized, although the final zirconocene complex contained a mixture of inseparable material (see Figure 77).

A C_1 symmetric bridged photoswitch was made as an additional example. The known 2,5-dimethyl-3-phenylthiopentalene –anion was reacted with chlorodimethylsilane to produce a chlorosilane intermediate that was reacted with a DAE-PS thiopentalene anion component to make a Me_2Si- bridged ligand. The zirconocene was made from this following standard methods and the results are described below.

2.1 Synthetic Results

2.1.1 Intermediates and Organometallic Complexes

Initially, the possibility of substituting di-heteroaryl photoswitch components directly onto a cyclopentadiene molecule was investigated and synthesis of substituted Cp molecules was initiated. The synthetic strategy is outlined in Figure 18**:** As a starting material, 3-methylcyclopent-2-enone (**56**) was reacted with the Grignard prepared from 2-methyl-3-bromobenzothiophene (**55**).

Figure 17. DAE_PS Initial Synthetic Strategy involving 3-methyl-cyclopenta-2-one as starting material (scouting reactions):

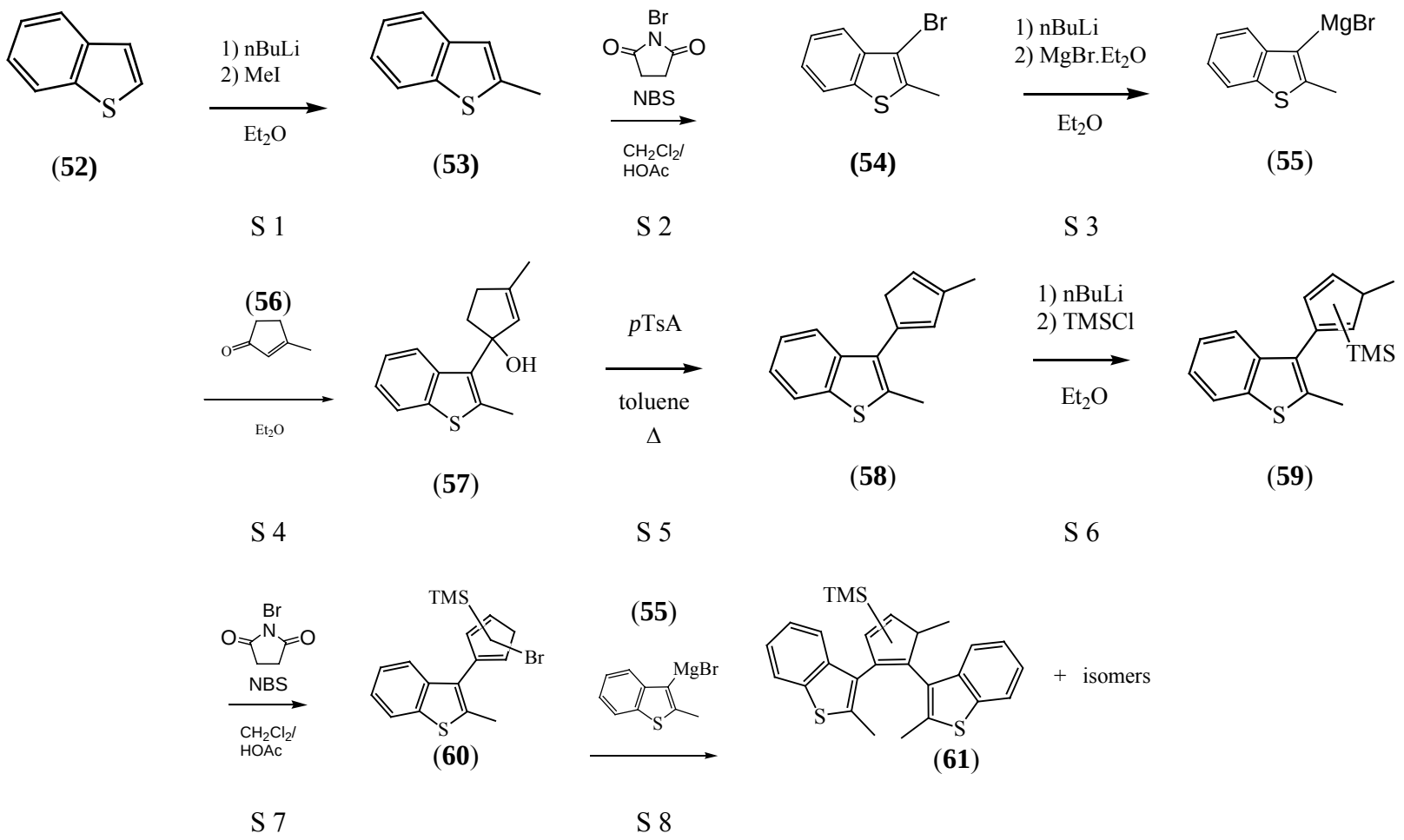

Starting from commercially available benzo[b]thiophene[106] (**52**), the addition of butyllithium was followed by quenching with iodomethane producing 2-methylbenzo[b]thiophene (**53**) in almost quantative yield. Bromination of (**53**) using NBS in a mixture of acetic acid and methylene chloride produced mono-brominated 3-bromo-2-methylbenzo[b]thiophene (**54**). A small amount of di-brominated product was detected. Interestingly, the 2nd bromine atom added onto the molecule was aromatic and did not halogenate the methyl group.

In this synthesis, the 2-methyl-3-bromobenzo[b] thiophene (**54**) is a common intermediate and was used to prepare the Grignard reagent (**55**) via magnesium bromide etherate entrainment (*vide supra*). A cold ethereal solution of (**54**) was treated with n-butyllithium (nBuLi), and then added to a cold ethereal slurry containing magnesium bromide etherate. Alternative methods of Grignard preparation tested including direct reaction with activated Mg, or reaction with ethylmagnesium bromide, but did not provide satisfactory results.

After dehydration of the alcohol (**57**) to the olefin (**58**), the cyclopentadiene was aromatized then quenched with trimethylsilylchloride (TMSCl) for the purpose of restricting access to the sites on the Cp ring that were not targeted for substitution. Double bond isomers were not a problem (other than difficulty in interpretation of the analytical results) as subsequent synthetic steps which formed the metallocene complex anion would equalize the double bond mixture. The initial steps in this synthesis however, were low yielding: only a small amount of product was recovered. After reduction to the olefin, subsequent experiments included deprotonation of the substituted cyclopentadienyl ring followed by quenching with TMSCl. These steps produced multiple-TMS isomers at (S6) which were inseparable. No attempt to react the TMS-Cp-2-MeBzTp was undertaken: this route was abandoned.

Alternatively, a diacetylene route was initiated, where di-substituted acetylene was to be followed with cyclization using titanocene, ethylene, and CO. The preparation 2-methyl-3-lithio-benzothiophene was straightforward (sampling and iodine quenching of the intermediate produced the iodine substituted benzothiophene) however, no reaction from quenching with lithium-TMS-acetylide was detected.

In our first successful attempts at making a photoswitch ligand component, thiophene was substituted with two adjacent groups containing 2-methylbenzothiophene (Figure 18).

[106] Also identified as thianaphalene

Figure 18: Synthesis of 2,3-di(2-methylbenzothiophen-3-yl)thiophene (**65**):

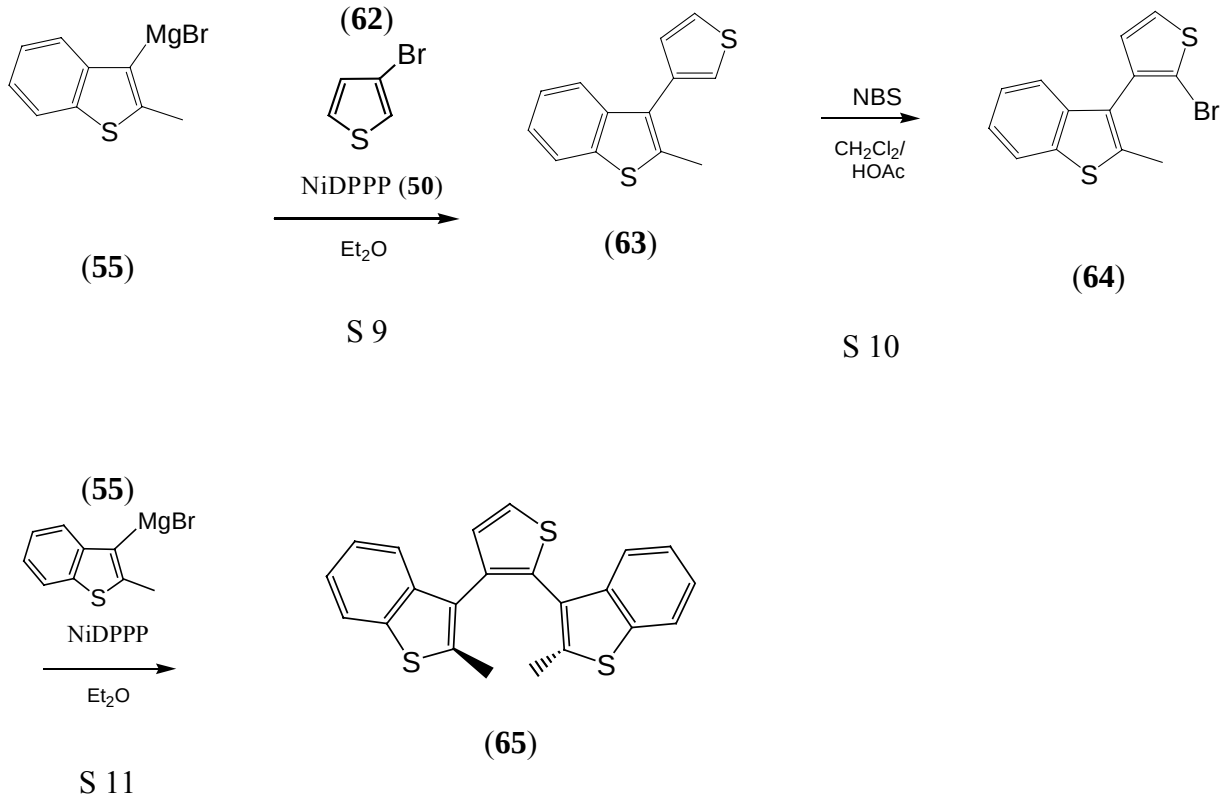

The 2-methylbenzothiophene-3-yl magnesium bromide Grignard reagent (preparation described in Figure 17) was coupled to 3-bromothiophene (**62**) (step S9), in diethyl ether using NiDPPP (**50**) as coupling catalyst. In our experiments the Ni coupling steps gave low yield and was kinetically slow. Our initial forays into these syntheses were done in diethyl ether rather than a higher boiling solvent (such as THF) due to the unfavourable experiences with THF.

Bromination with NBS in step S10 was regio-selective: the bromine added in the 2-position between the sulfur and the coupled 2-methylbenzothiophene forming (**64**). The yield for this step is high and goes to completion in reasonable time.

In step (S11), 2-methyl-3-magnesiumbromobenzo[b]thiophene (**55**) was coupled using Ni-DPPP (**50**) in the same fashion as before. Again, the yield for this step was low and the reaction was run for several days before being worked up. The product from this reaction, 2,3-(3'-2-methyl benzo[b]thiophenyl)thiophene (**65**), was photochromic (see Figure 57). Characterization of the complex included GCMS, ^{1}H-NMR, UV-Vis, and X-ray crystallography (for the parallel conformer: see experimental section).

The next step in this reaction sequence would be to cobble a Cp ring on the free side of the thiophene ring. Unexpectedly, our conventional technique (Eaton's reagent at 70°-80°C for 20 min) failed repeatedly. Whereas the coupled Friedel-Crafts-Nazarov-cyclization [107] of phenyl or tolyl substitutions in the 2,3- positions on thiophene produce excellent results with Eaton's Reagent catalyzed cyclization of methacrylic acid, the synthon (**65**) produced only trace amounts of product (as detected by GCMS in two attempts at the cyclized target). Alternative methods which are used to produce pentalene ring structures such as super polyphosphoric acid (sPPA) or more conventional longer routes were not attempted.

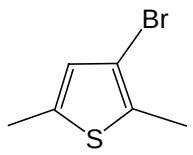

(**66**)

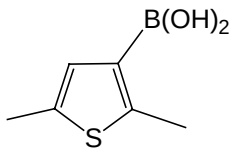

(**67**)

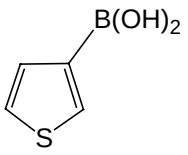

(**68**)

Following the procedure described above could be used to make switching components having dissimilar heteroaryl substituted groups. The use of 2,5-dimethyl-3-bromothiophene (**66**) instead of 3-bromo-2-methylbenzo[b]thiophene (**54**) would produce 2,3-di-substituted thiophenes having differing substitutions. Once one hetero-aryl group is coupled in the 3- position and the thiophene ring brominated, a second similar or different heteroaryl group could be coupled in this fashion. This method could be useful for other systems (such as photochromic polymers, etc.), changing the wavelength addressability of these compounds.

For improving this result, alternative higher boiling solvents (such as isopropyl or t-butyl-alcohol) could increase the Kumada-coupling reaction rate. In addition, alternative Ni-coupling ligands might also improve the yield of the second coupling reaction. Finally, optimization of the cyclization reaction with methacrylic acid producing the heteropentalene product could be further explored. The use of sPPA instead of Eaton's reagent for making the heteropentalene could be optimized.

Benzothienyl substitutions in the 2 and 3 positions on thiophene as photoswitching components have **not** been previously reported and were of interest for a number of reasons. The ability to create a -cyclohexene (PS-closed) fused ring system adjacent to and from a thiophene or a thiopentalene with irradiation was not obvious. In addition, the reversible isomerization of these photoswitches in the literature have "fatigue resistance" depending on the substitution type and position in relation to the parent (substituted)-cyclopentene ring. For our thiophene system (**65**), photo-reversibility was observed, first

---

[107] for a review of Nazarov cyclization reactions with conditions see S. E. Denmark, *Comp. Org. Syn.* (**1991**) 5**,** 751-784 .

on a thin layer chromatographic plate, then in GC vials prepared for analysis. The NMR tube sample of (**65**) was repeatedly coloured with 254 nm UV and decoloured with visible light. Photo-switching in this system was observed from the visible range (purple) to colourless. Photodecomposition was not measured however, when comparing the structure of isolated photo-decomposition product reported for similar DAE switches (see Figure 19)[108], the decomposition pathway for thiophenes could be less available.

Figure 19. Photodecomposition product reported for hexafluorCp-DAE photoswitches (see reference 108 and text for explanation):

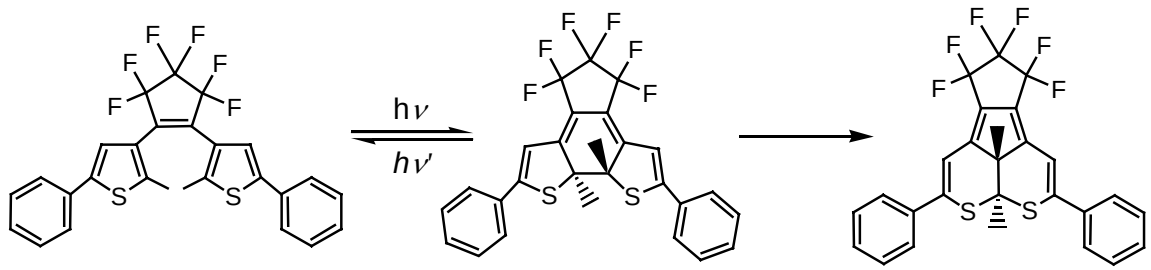

(**69**) (**70**) (**71**)

The ^{1}H-NMR of (**65**) is presented in Figure 56. The presence of isomers in the aromatic region is indicated, probably due to the presence of parallel and anti-parallel conformers. Typical signals for the methyl groups on the benzothiophene are measured in the region typical for these aliphatic protons.

The UV-vis absorption spectrum of (**65**) was measured (see Figure 57) and was comparable to published spectra of known photochromic molecular switches. In addition, the solution of (**65**) prepared for NMR slowly evaporated and yielded crystals for which the x-ray structure was determined (see Figure 58). The crystals were determined to be the parallel conformer of (**65**) rather that the photochromic anti-parallel conformer. Since the solution prepared for NMR was photochromic, the result indicated that some portion of the sample was photoactive and some was not. In any case, the structural characterization further confirmed the synthetic result and indicated that making photochromic thiophenes was possible and that thiopentalenes could support a photochromic system.

The presence of this parallel conformer in the X-ray analysis brings forward one of the challenges facing DAE photoswitches in general. The presence of the parallel conformer lowers the overall quantum yield and efficiency of the system. This problem of parallel and anti-parallel conformers has however been addressed and progress made towards solution[109].

---

[108] Masahiro Irie, Thorsten Lifka, Kingo Uchida, Seiya Kobatake, and Yuriko Shindo, "Fatigue resistant properties of photochromic dithienylethyenes: by product formation", *Chem. Commun.,* (**1999**) 747-750.
[109] a)Yasushi Yokoyama, Hidenori Shiraishi, Yutaka Tani, Yayoi Yokoyama, and

Our initial success for (**65**) relied on Ni- type Kumada coupling of the 3-thienylmagnesium-bromide with 2-methyl-3-bromobenzothiophene (**54**). The failure of the Nazarov cyclization in subsequent steps led to a shift in the direction and targets for the first example of a polyolefin catalytic photoswitch component. Alternative routes to the di-substituted thiopentalenes were considered. Rather than sequentially coupling one heteroaryl group at a time, a di-coupling reaction was imagined. Using 2,3-dibromothiophene and 2-methyl-3-magnesiumbromobenzo[b]thiophene, the Ni-dppp coupling failed. At this point, the uses of alternative coupling reactions were considered.

Suzuki coupling methods (described above) are available for heterocenes and show good functional group tolerance, proceeding often in higher yields than the Ni coupling, however, the preparation of a boronic acid becomes necessary. 2-thiophene boronic acid and 3-thiophene boronic acid are commercially available and were tested for reactivity against 3-bromo-2-methylthiophene. Under the experimental protocol the (commercially available) 3-thiophene boronic acid reacted in reasonable yields to give the expected Suzuki coupled product.

The reaction scheme for the synthesis of the first diarylethene photoswitch polyolefin metallocene complex is presented in Figure 21. The reaction between thiophene and methacrylic acid (step 1) to produce the ketone has been well documented[98]. The starting material for this synthesis is the di-bromo-thiapentalene ketone (**75**) prepared from the electrophilic bromination thiapentalene ketone (**74**). When this di-bromide is reacted with 5 equivalents of benzothiophene-3-boronic acid (**76**), using bis(triphenylphosphine) palladium chloride as a catalyst and potassium carbonate in refluxing dimethoxyethane/ water, the di-coupled reaction product is formed in 2 h.in almost 90% yield.

The ketone formed in this reaction is then reduced to the alcohol with lithium aluminium hydride in an ethereal solution. Further dehydration to the olefin is accomplished using para-toluenesulfonic acid monohydrate (*p*TsA) in refluxing toluene.

Yoshitaka Yamaguchi, " Diastereoselective Photochromism of a Bisbenzothienylethene Governed by Steric as Well as Electronic Interactions", J. Am. Chem. Soc. (**2003**) *125*(24), 7194-7195, b) "Diastereoselective Photochromism of Bisbenzothienylethenes with an Oxycarbonyl-Related Functional Group on the Side Chain", *J. Org. Chem.* (**2004**), *69*, 8403-8406.

Disadvantages in the use of commercially available 3-benzothiophene boronic acid (**76**) are that in the final complex, the acidic proton on the benzothiophene ring is an available reactive site. In the final steps of metal complexation where base is used to de-protonate the cyclopentadienyl ring, it is possible to instead de-protonate either the 2- or the 3- substituted benzothiophenes (see Figure 20). This was the expected situation; since the pKa of a cyclopentadiene ring proton is lower than 2-(substitution) thiophene protons. In getting around this situation, an application of the switching mechanism was used: the deprotonation was carried out in the presence of UV light, closing the photoswitch and (probably) changing the availability of the benzothiapentalene proton to deprotonation. Bridgehead reactivity in bicyclic molecules is well studied. In this case, the 2-benzothiophene protons become bridgehead protons and less acidic than the Cp protons.

Figure 20. Protons available for deprotonation in the DAE (**79**) photoswitch.

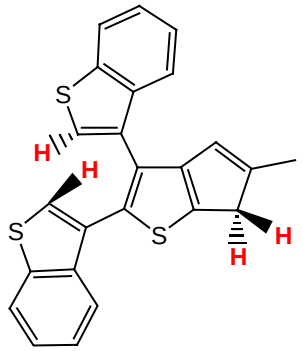

(**79**)

By producing the anion in the presence of UV, the closed form of the photoswitch is processed and the protons that are available for making an anion are limited: anions are less likely to be formed at a bridgehead carbon. This is one of the reasons the methyl substitution in the 2- position on the benzothiophene ring is preferred (the molecule becomes synthetically more accessible).

Addition of the metal to the anionic complex takes place in diethyl ether under standard conditions. Isolation of the complex from dichloromethane filtration produced an orange free flowing powder having a mass in agreement with the desired complex.

Figure 21: Synthesis of (**80**).

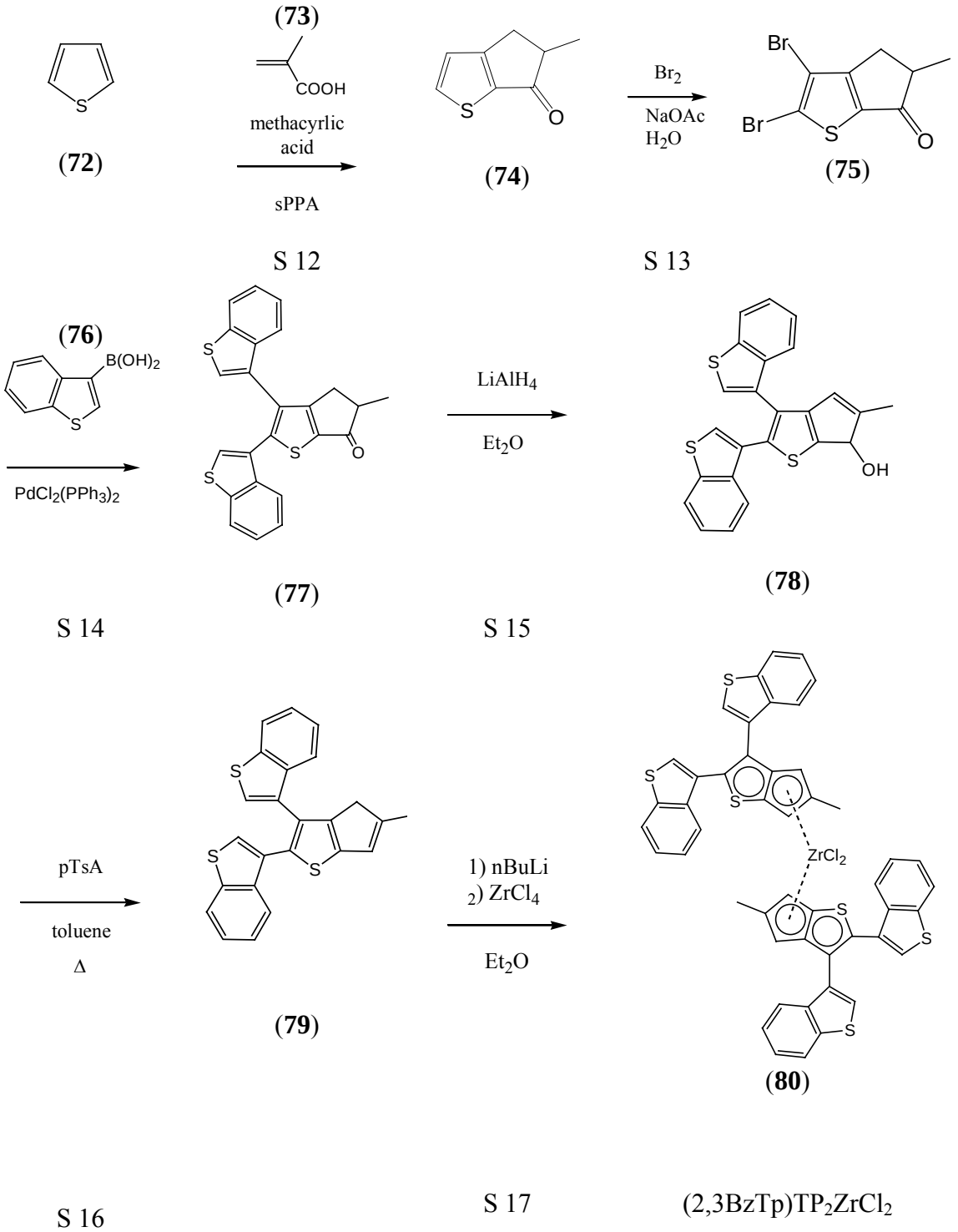

The olefin (**79)** in Figure 21 was one of the first heterodiaryl-thiopentalenes made and will be interchangeably abbreviated **PS1** thought out the remainder of the text. Thiopentalenes are abbreviated **TP**.

2.1.2 Synthesis of additional Complexes.

The simplest complex to make, and one that demonstrated the ability of the photoswitch to meet criteria for polymerization catalysis was the unbridged species made above. By making an anion from the olefin and reacting this with one half of a molar equivalent of zirconium tetrachloride, a catalytically active zirconocene complex was made and tested (see below).

In addition, by treating the ketone (**81**) with n-butyllithium and reducing the alcohol made from this complex, a more soluble type of precursor for making a metallocene was derived.

Figure 22. Synthesis of 2,3-di(benzo[b]thiophen-3-yl)-5-methyl-6-n-butyl cyclopenta[b]thiophene (**83**).

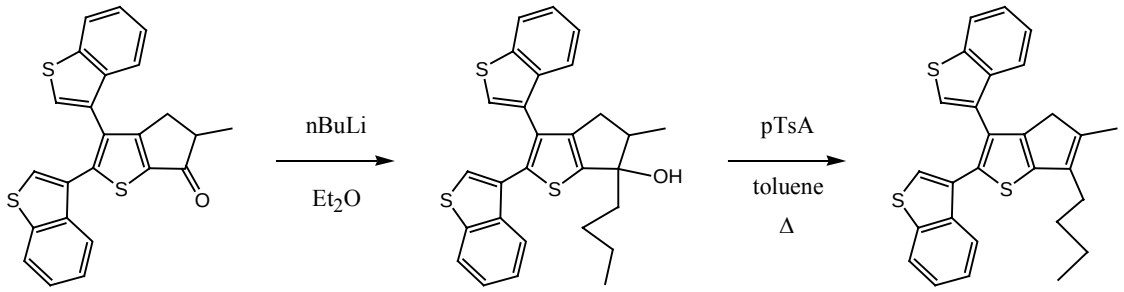

(**81**) (**82**) (**83**)

In addition, the cyclopentadienide generated by metallation of (**79**) was reacted with one equivalent of chlorodimethyl(2,5-dimethyl-4-phenylcyclopenta[b]thiophen-6-yl)silane to form the bridged ligand shown in Figure 23. This ligand was then treated with 2 equivalents of n-butyllithium, then 0.5 equivalents of zirconium tetrachloride was added, The zirconocene was isolated and characterized, and included in polymerization testing (*vida infra*).

Figure 23. Synthesis of dimethylsilyl(2,3-dibenzo[b]thiophen-3-yl)-5-methylcyclopenta[b]thiophen-6-yl)(2,5-dimethyl-4-phenylcyclopenta[b]thiophen-6-yl)]zirconium dichloride (**86**).

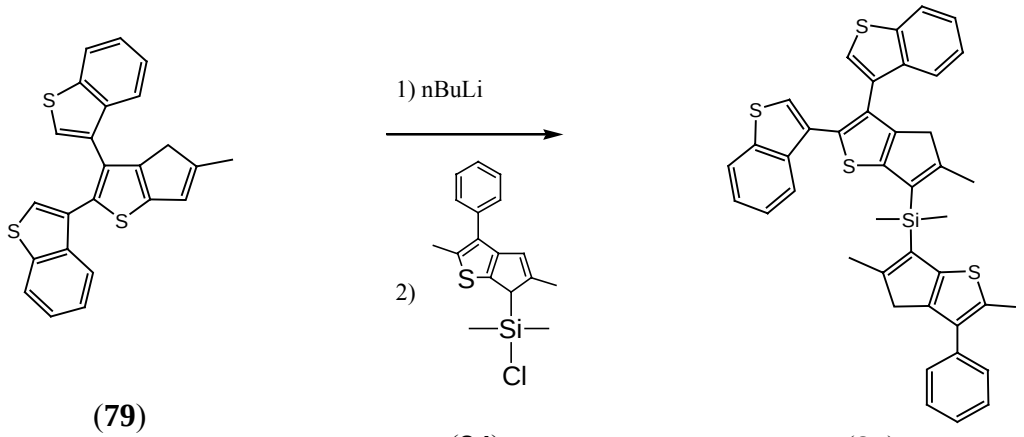

(**79**) (**84**) (**85**)

S 18

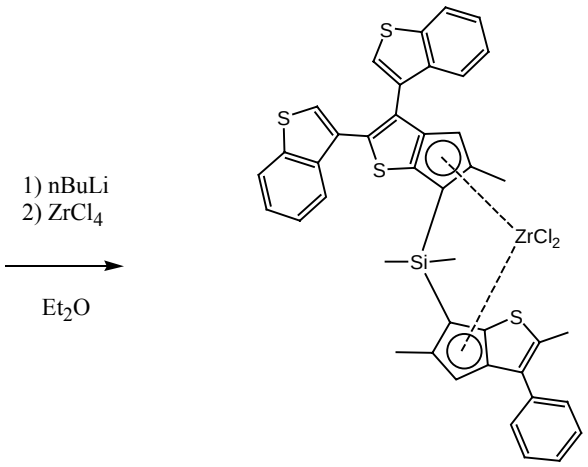

(**86**)

Preparation of a thiophene type (heteroaryl-) boronic acid necessary for optimization of the catalytic photoswitch would contain a methyl, ethyl or isopropyl group in the 2-position, be coupled to the thiopentalene in the 3-position, have optional substitution in the 4- position, and have substitution in the 5-position. I prepared the 2-

methylbenzo[b]thiophen-3-boronic acid following the method of "in situ quench" method described by Li, et. al[110], where a hexane/THF solution containing triisopropyl borate (**88**), 2-methyl-3-bromobenzothiophene (**54**) at -78°C are treated with n-butyllithium and slowly warmed before quenching with dilute HCl. This method worked for (**54**) although results varied and the amount of material obtained from these trials did not provide enough material for subsequent studies. This method required further optimization.

Figure 24. Synthesis of 2-methylbenzo[b]thiophen-3-boronic acid (**88**).

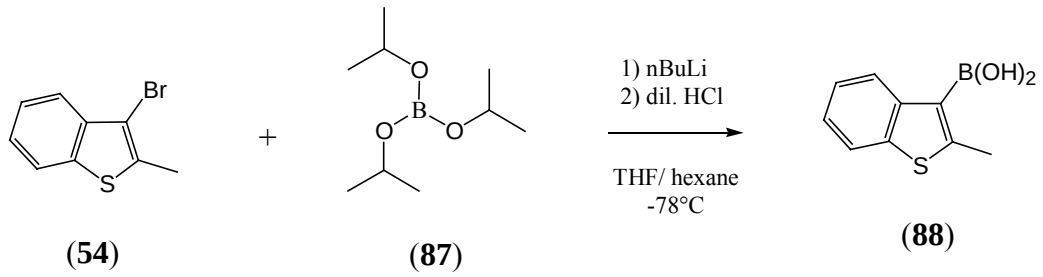

S 19

2.1.3 Synthesis of mono-Cp complexes:

Two thiopentalene-zirconium tri-bromide catalysts were prepared: one without and one with photoswitching components following a method described for making mixed ligand metallocenes as catalysts for elastomeric polypropylenes[111]. A toluene solution of the photochromic ligand (**79**) was reacted with zirconium tetrakisdimethylamide to give the heteropentalene-zirconium-tris(dimethylamide), which is further reacted with 3 equivalents of trimethylsilylbromide to give the mono-pentahapto heteropentalene, either of which is shown in Figure 25 below.

As reported for the aryl-zirconocene-trisamide complexes, the impurities contained in these complexes were not easily removed by recrystallization[111], and interference with the polymerization testing in ethylene and ethylene/hexene (below) was considered.

---

[110] Wenjie Li,* Dorian P. Nelson,* Mark S. Jensen, R. Scott Hoerrner, Dongwei Cai, Robert D. Larsen, and Paul J. Reider, "An Improved Protocol for the Preparation of 3-Pyridyl- and Some Arylboronic Acids", *J. Org. Chem.* (**2002**), *67*, 5394-5397.

[111] Christopher D. Tagge, Raisa L. Kravchenko, Tappan K. Lal, and Robert M. Waymouth, "Mixed Ligand Metallocenes as Catalysts for Elastomeric Polypropylenes", *Organometallics,* (**1999**), *18*, 380-388.

Figure 25. Synthesis of mono-Cp-zirconocene complexes (**90**) and (**93**).

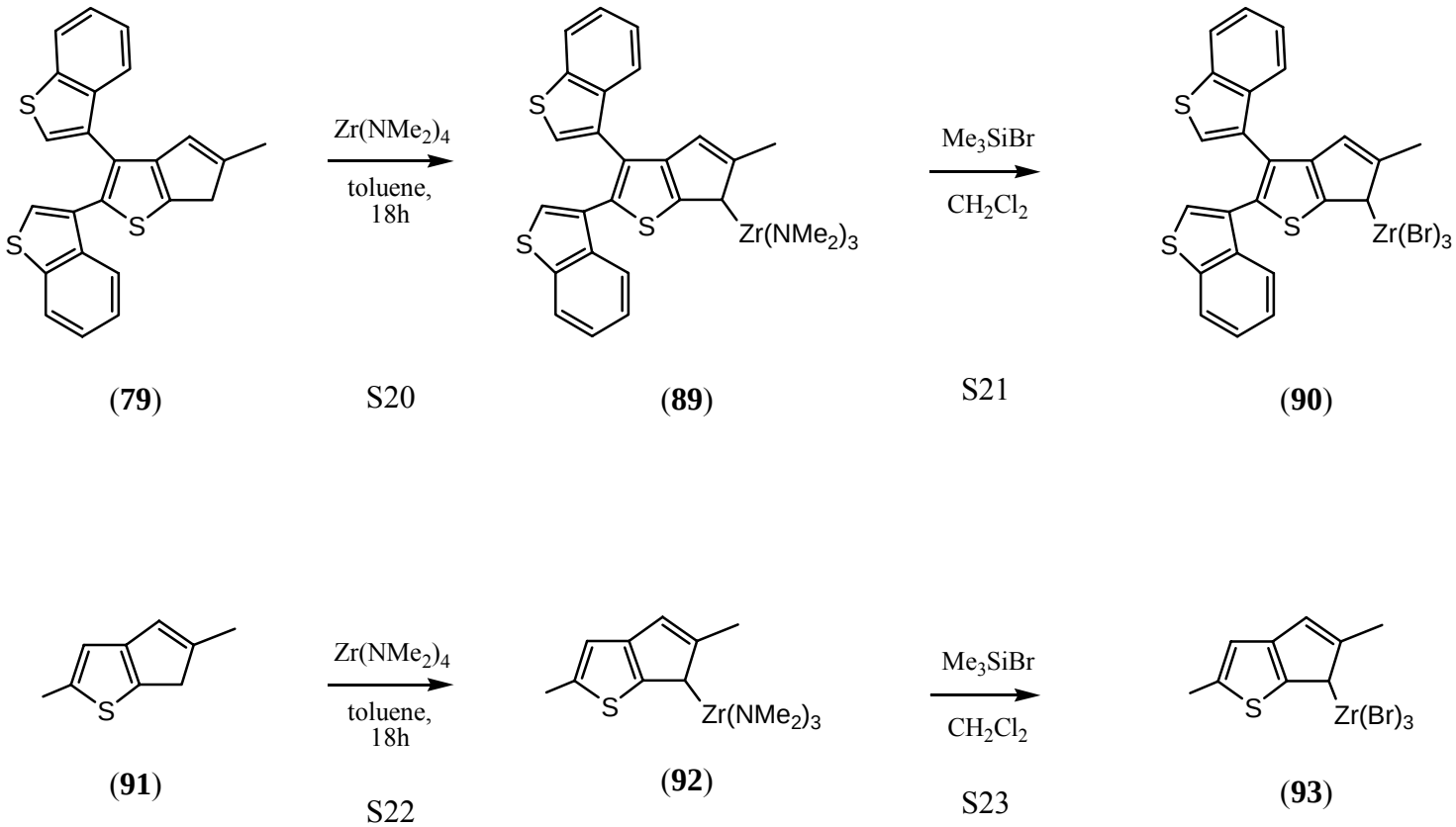

2.1.4 Synthesis of Te ligands

It has been previously shown that selenium and tellurium can be cobbled into heterocene catalysts with differing effectiveness in the polymerization reaction[112]. The use of chalcogen heterocycles in photochromic ring forming reactions has not been explored and could find further application. The chemistry developed for the synthesis of chalcogen containing pentalenes could be applied to photoswitches (although no direct examples currently exist in the literature).

A logical synthetic scheme for the synthesis of complexes similar to these proposed for the sulfur containing hetero-photoswitches presented could follow this likely path:

Figure 26. Synthesis of 3-bromotellurophene (from reference 113).

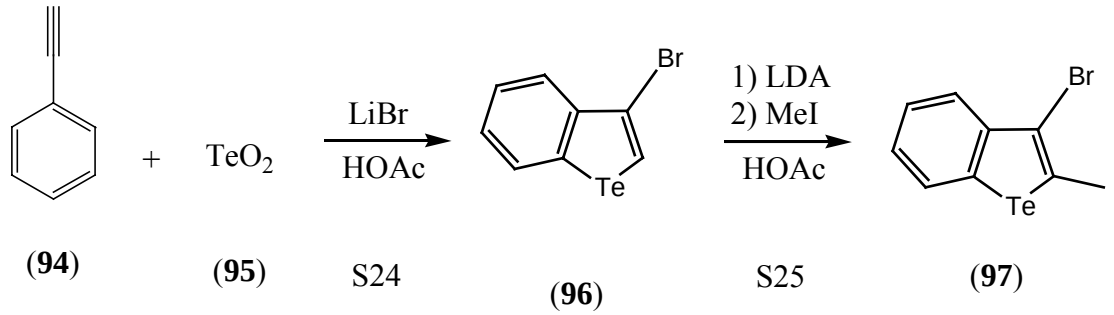

Synthesis of 3-bromotellurophene[113] proceeded as described in Figure 26. The product from the reaction between phenyl-acetylene, tellurium dioxide, and lithium bromide in acetic acid was treated with Cl_2 gas and solids were collected and washed with $Na_2S_2O_5$. The yield was 57% based on TeO_2. The target could possibly be selectively methylated in the 2- position by treatment with LDA, followed with iodomethane.

Although it has been reported that the tellurium ring system is not stable to 3- position reactions such as lithium or Grignard formation[113], an exchange reaction could be possible. In this vein, the synthesis of the 3-tellurophene boronic acid via the low temperature simultaneous lithium debromination-hydroboration reaction described above for making 2-methyl-benzothiophen-3-boronic acid (described above for (**88**), was performed. In my hands only traces of the BzTe-boronic acid were formed, with one of the major products from the reaction having a mass corresponding to the boroxine (**99)** in Figure 27.

---

[112] R. L. Jones, M. J. Elder, J. A. Ewen, "Metallocenes with Cp Ring-Fused to Chalcogen Heterocycles: Synthesis and Polymerization Results", Phosphorus, Sulfur, and Silicon and the Related Elements, (**2005**) *180*(3-4) 827 – 843.
[113] Bergman, et. Al., *J. Organomet. Chem.*, (**1980**) *199*, 377 – 387.

Figure 27. Synthesis of tris(benzo[b]tellurium-3-yl)-boroxide (**99**).

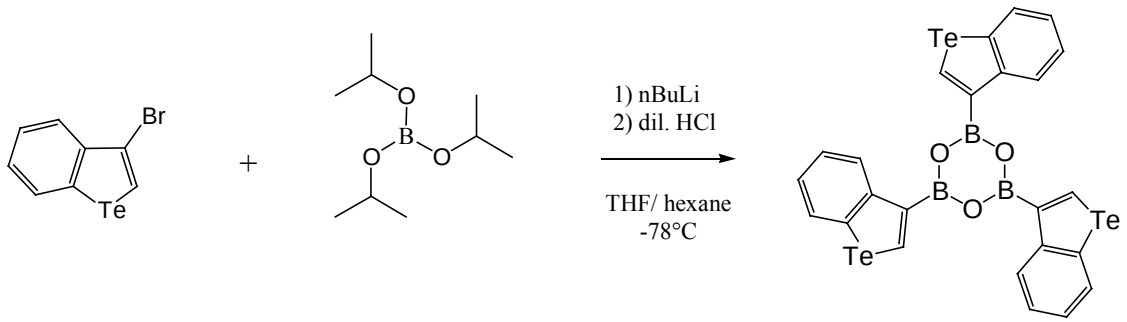

(**98**) (**87**) S 26 (**99**)

Upon standing, the boroxine decomposes from a red crystalline substance to dark brown/black oil (indicating extraction of tellurium). The method used for the synthesis was repeated and the boroxine used directly in a palladium catalyzed Suzuki coupling reaction with a synthon prepared having one benzothiophene attached to thiopentalene in the 2- position and bromine in the -3 position (**100**).

Figure 28. Suzuki coupling using the in situ prepared Te-boroxane:

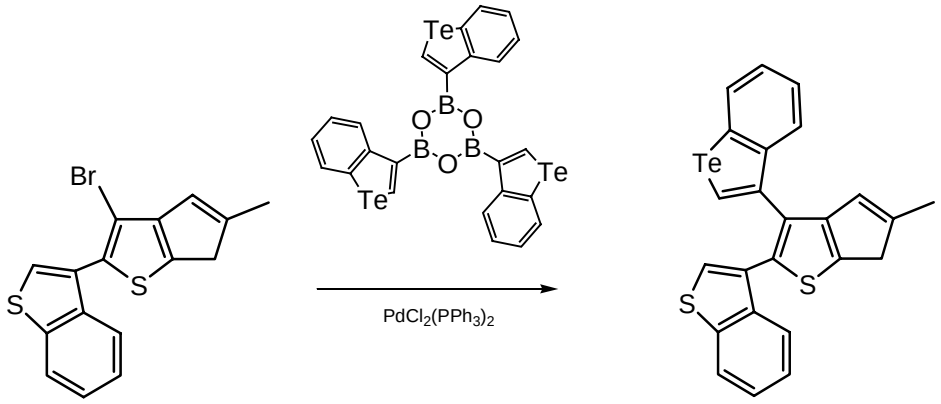

(**100**) S27 (**101**)

The product from the reaction produce clean signals in the ^{1}H-NMR, but the mass from MALDI and LCMS-MALDI did not correspond to the target. Further optimization of this method is required.

2.2 Polymerization Results

Polymerization testing with selected catalysts was done in propylene liquid (bulk), in toluene solutions with a steady stream of propylene gas at atmospheric pressure, with ethylene in toluene solutions, and ethylene/hexene co-polymerizations in dilute solution. In some cases, multiple polymerizations were needed to determine optimum conditions for the experiment (catalyst loading vs activity, slurry density of the final polymer in solution or bulk, etc). In selected cases, the experimental data is included from these runs.

Catalysts were activated with methyl-aluminoxane (MAO) prior to the start of polymerization testing. Although activators such as MAO, modified MAO (MMAO), trityl tetrakis(pentafluorophenylborate) (BArF), etc. as well as scavengers such as triisobutylaluminum (TiBAl), have been shown to directly effect the polymerization behaviour of conformationally dynamic unbridged metallocenes[114], these components were not chosen as a starting point for our studies.

The effect of irradiation on polymerization catalysis has not been reported (other than the *rac-, meso-* isomerization discussed earlier), neither has the effect of irradiation on polyolefin catalysts with or without photochromic substitutions. Where appropriate, catalysts containing a photoswitch were run against a control having similar geometries (see Figure 29). For example, the catalyst containing the 2-methyl-6-phenyl indene ligand (**28**) was made and polymerized in identical procedure as unbridged photoswitch organometallic complex (**102**). Similarly, the bridged photoswitching molecule (**86**) was compared against the known heterocene (**8**) in identical procedures; the results are reported in the following tables.

[114] Robert M. Waymouth, Gregg M. Wilmes, Maik Finze, Sarah E. Reybuck, and Shirley Lin, "Conformationally-dynamic Metallocenes: Hypersensitive Systems for Modulating Stereochemistry", *Polymeric Materials: Science and Enineering* (**2002**) *87*, 48.

Figure 29. Unbridged complexes compared in polymerization experiments:

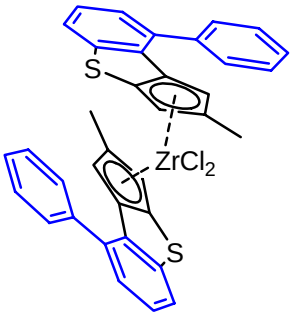

(**102**)

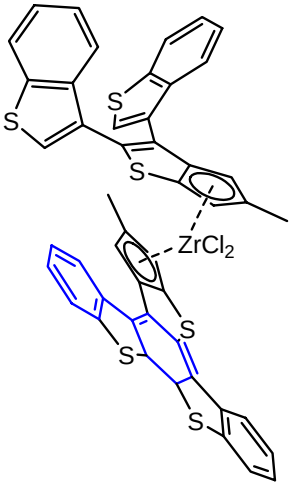

(**80**)

Figure 30. Bridged complexes compared in polymerization experiments:

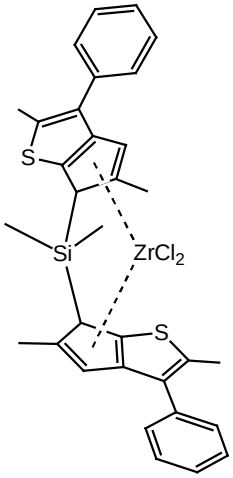

$C_{32}H_{32}Cl_2S_2SiZr$
Mol. Wt.: 670.94

(**22**)

$Me_2Si(2,5\text{-}Me_2\text{-}3\text{-}PhTP)_2ZrCl_2$

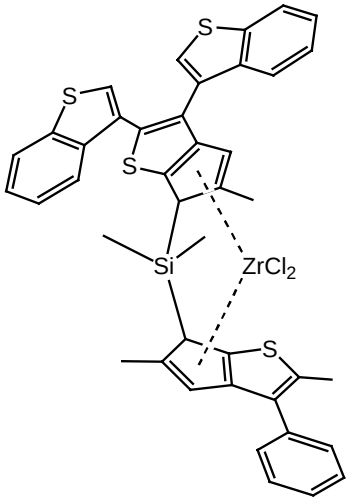

$C_{41}H_{32}Cl_2S_4SiZr$
Mol. Wt.: 843.17

(**86**)

$Me_2Si(2,3\text{-}BzTp\text{-}5\text{-}MeTP)(2,5\text{-}Me_2\text{-}3\text{-}Ph_2)ZrCl_2$

2.2.1 Solution Propylene Polymerization results with bis[(2,3-benzo[b]thiophen-3-yl)cyclopenta[b]thiophen-yl]zirconium dichloride (**80**)/ MAO.

A dried borosilicate glass Schlenk tube containing toluene and half the amount of MAO used in polymerizations was charged with a solution containing the catalyst and the remainder of the MAO. Irradiated polymerizations were done with two 6 watt 254 nm UV lamps placed on either side and adjacent to the glass tube surface. The temperature was recorded and propylene was bubbled through the catalyst solutions at a constant rate (~15 to 20 l/h) for the duration of the experiment. The experiment was ended by pouring the contents into acidic methanol and collecting the solids by filtration. Results are included in Table 1.

Table 1. Propylene solution polymerizations comparing (**102**) and (**80**) without and with 254 nm UV irradiation during polymerization [(a)].

Run ID	Cat Load [mg]	Al/Zr	Time [min]	Mass /g PP	Activity [g PP/mmol cat/h]	GPC M_w [g/mol]	GPC M_n [g/mol]	Q [M_w/M_n]
120 (**102**)	10	498	90	1.02	47	6770	1984	3.4
121 (+UV) (**102**)	10	498	90	0.71	32	8092	2659	3.0
112 (**80**)	6	427	60	0.12	18	29015	8984	3.3
113 (+UV) (**80**)	5	570	60	0.09	18	21427	4148	5.2
117 (**80**)	10	532	90	0.38	24	14311	4169	3.4
118 (+UV) (**80**)	10	532	90	0.04	3	7293	1696	4.3

(a): see text for explanation of results

Catalyst (**102**) was almost twice as active a catalyst than (**80**) under non-irradiated conditions. For (**102**) under normal or irradiated conditions, activity, M_w, M_n, and Q (M_w/M_n) are similar.

For (**80**) at low catalyst to reactor loading (entries -117 and -118) the activity of the catalyst is about half that of (**102**), but the values for M_w are doubled. In addition, the UV treated polymerization Q value is higher than expected for a single site catalyst, normally indicating alternative catalyst species are active.

The last 2 entries are polymerizations made with (**80**) at higher catalyst loadings and comparable with those conditions run with (**102**). The catalyst (**80**) makes a broader M_w when done under the influence of UV than the untreated sample. The GPC curves for the polymers made with (**102**) are compared in figure 2:

The lower activity irradiated (**80**) (entry 118) may been due to loss of polymer in the liquid phase after filtration, (the soluble polymer was not recorded as part of the product in these initial experiments). Irradiation of (**80**) causes the molecular weight distribution of the crystalline polymer (Q value) to increase.

Figure 31: GPC trace from run ID -120 and -121: (**102**) with (magenta) or without (grey, dashed) 254 nm UV:

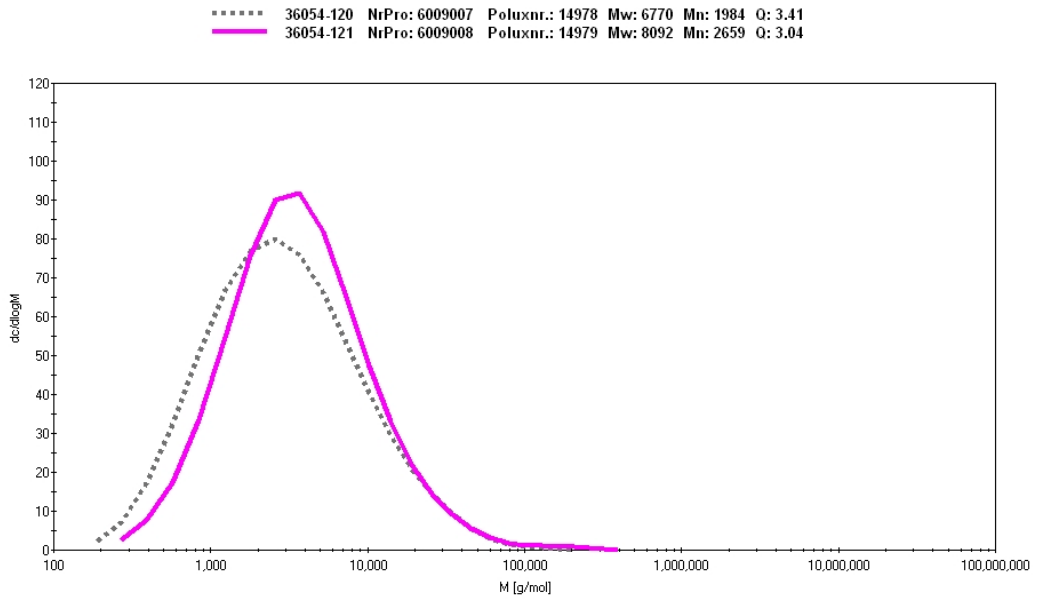

Although broad, the 2 GPC curves for (**102**) in Figure 2 are similar in molecular weight and molecular weight distribution. There is a slight decrease in Q for polymer made from the irradiated polymerization.

The GPC curves for the polymerization experiments using (**80**) are compared in Figure 32 and Figure 33. In either polymerization campaign, there is an increase in the molecular weight distribution caused by increasing amount of low molecular weight polymer in the irradiated samples. The GPC trace indicates a bimodal polymer distribution. For entry -112 and -113, the high M_w fraction remains the same molecular weight, while in addition there is a shift to bimodal lower M_w polymer. For entry 117 and 118 at the higher catalyst concentration, there is a slightly lower M_w but more pronounced bimodal polymer distribution showing as a lower molecular weight shoulder.

Figure 32 : GPC trace from entry -112 and -113: (**80**) with (magenta line) and without (grey line) 254 nm UV irradiation:

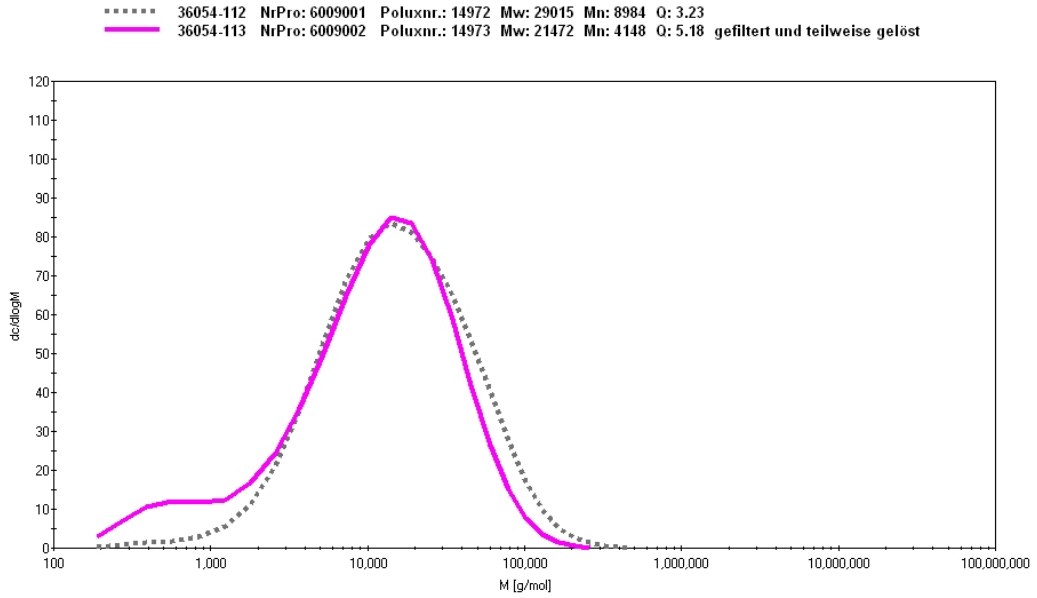

The GPC trace made from the irradiation polymerization experiment is bimodal with a low molecular weight distribution shoulder. Repeating this experiment with more catalyst and longer polymerization time produced a similar, more dramatic result (see Figure 33):

Figure 33. GPC trace from entry 117 and 118: (**80**) without (grey dashed line) and with (magenta line) 254 UV:

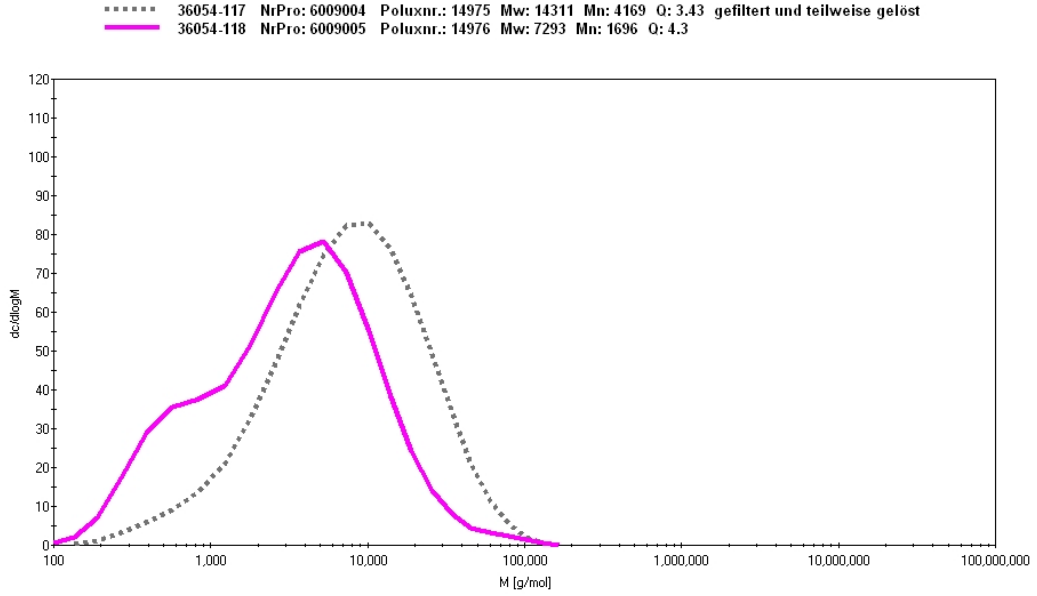

This result indicated the presence of a separate catalytic species making a different polymer than obtained from the polymer made without UV. UV irradiation alone did not produce bimodal polymer with the (**102**) catalyst.

One hypothesis to explain the bimodal peak is that some population of the catalyst molecules in the polymerization experiment has been transformed by the irradiation. The shift to lower molecular weight polymer, and therefore broadened molecular weight, would be possible using (**80**) at a photo-activated state, where some portion of the catalyst population was in the irradiated (closed) position.

Under these conditions the open (**80)** catalyst made higher molecular weight polymer than the (**102**). After irradiation, the (**80**) polymer shoulder having the lowered molecular weight is comparable to that of (**102**) polymer molecular weight. This could be expected since (**102**) and the closed form of the (**80**) have similar structural features (see Figure 10).

Figure 34. Proposed catalyst structures used in these experiments:

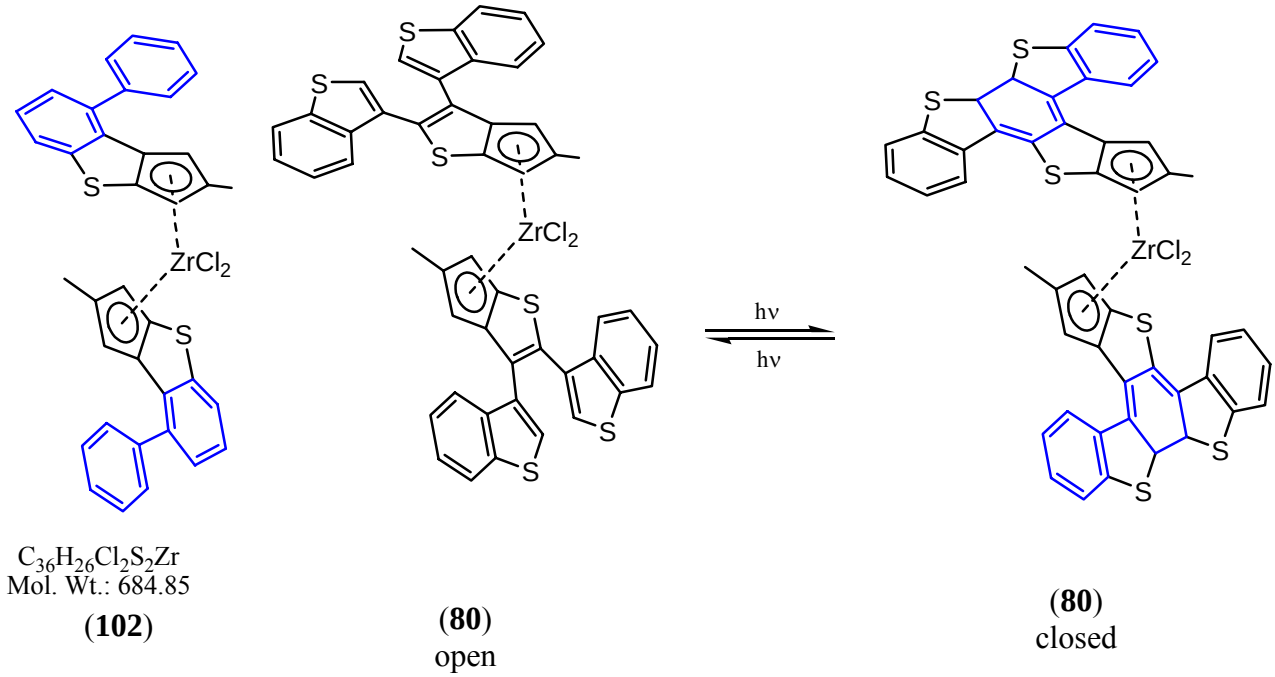

The lowered activity in the last experiment with (**80**) (entry 118) could be due to a loss of a part of the low molecular weight fraction during work-up.

In order to further understand and characterize the lower M_w shift seen in the GPC trace, the above experiments were repeated and the toluene soluble fraction collected and characterized. Polymerizations were done at higher Al/Zr ratio. The results are presented in Table 2.

The control using (**102**), (entries 156,162, and 164) show deviations within the normal polymerization and analytical testing methods found for this system. There is no significant impact from UV irradiation on the polymer made from the (**102**) catalyst. Entries 134 and 159 insoluble and soluble fractions are within experimental error, showing only a slight decrease in the soluble fraction with 254 UV irradiation. Catalyst activities are consistent at ~92 g/mmol cat*h^{-1}, this does not change under UV irradiation conditions. Activities were higher for both (**80**) and (**102**).

The (**80**) catalyst system produces a higher amount of insoluble polymer than does (**102**). Polymerization reproducibility was lower and the soluble fraction was higher at the higher Al/Zr levels.

When treated with UV irradiation (**80**) produced increased amounts of insoluble polymer. This is indicated in the higher insoluble polymer at the lower Al/Zr ratio.

Table 2. Solution propylene polymerization results with (**80**)/ MAO with and without 254 nm UV irradiation.

run ID (catalyst)	UV	time [h]	Cat Load [mg]	activity [g PP/mmol cat/h]	total Mass [g PP]	**insolubles** Mass [gm]	IV[(a)] [dl/g]	M_w [g/mol]	M_n [g/mol]	Q[(b)]	**solubles** Mass [gm]	IV[(a)] [dl/g]	M_w [g/mol]	M_n [g/mol]	Q[(b)]
Al/Zr = 1000:															
164 (**102**)	OFF	2.0	15	114	5.0	2.6	0.01	12051	4480	2.7	2.4	0.06	9837	3424	2.9
162 (**102**)	OFF	2.0	15	103	4.5	2.4	0.03	10870	4725	2.3	2.1	0.06	10559	3914	2.7
156 (**102**)	OFF	2.0	15	89	3.9	2.0	0.03	13835	5731	2.4	1.9	0.18	11661	3646	3.2
average				102±13	4.5±0.6	2.3±0.3					2.1±0.2				
134 (**102**)	ON	2.0	15	81	3.5	2.1	0.1	9016	3363	2.7	1.5	0.1	7180	2651	2.7
159 (**102**)	ON	2.0	15	107	4.7	2.9	0.03	8319	3616	2.3	1.8	0.13	8108	3076	2.6
average				94±19	4.1±0.8	2.5±0.6					1.6±0.2				
132 (**80**)	OFF	2.0	15	50	1.6	0.2	0.1	26421	8398	3.2	1.4	0.1	26246	8762	3.0
135 (**80**)	OFF	2.0	15	203	6.3	0.1	0.2	28884	7159	4.0	6.2	0.2	29428	8797	3.4
average				126±108	3.9±3.4	0.1±0.1					3.8±3.4				
131 (**80**)	ON	2.0	15	188	5.9	1.4	0.1	18670	8121	2.3	4.5	0.1	19111	7066	2.7
Al/Zr = 500:															
137 (**80**)	ON	1.5	10	217	3.4	2.8	0.1	28966	11809	2.5	0.6	0.2	24806	6251	4.0
138 (**80**)	ON	1.5	10	144	2.2	2.2	0.2	35289	6257	5.6	0.0	-	-	-	-
average				180±52	2.8±0.8	2.5±0.4					0.3±0.4				

(a) Intrinsic viscosity: [dl/g] (see analytical methods), (b) $Q = M_w/M_n$.

Differences in the polymerization products from this experiment can be rationalized by considering the rotation of the η^5-cyclopentadienyl ring (Cp) in the irradiated vs. the non-irradiated catalyst. The closed (flattened), irradiated form of the catalysts should have less hindered rotation around the ligand-metal axis (dotted line, Figure 35) making atactic, low molecular weight polymer, whereas the open form (non-irradiated catalyst) would present benzothiopentyl- groups protruding into the plane of Cp rotation, restricting free rotation around the metal center and creating a pseudo –*rac* catalyst. The *pseudo -rac* catalyst would be more isospecific and make higher M_w more crystalline segments in the polymer chain.

Figure 35. Drawing of conformational isomers based on restricted rotation in open and closed form of (**80**).

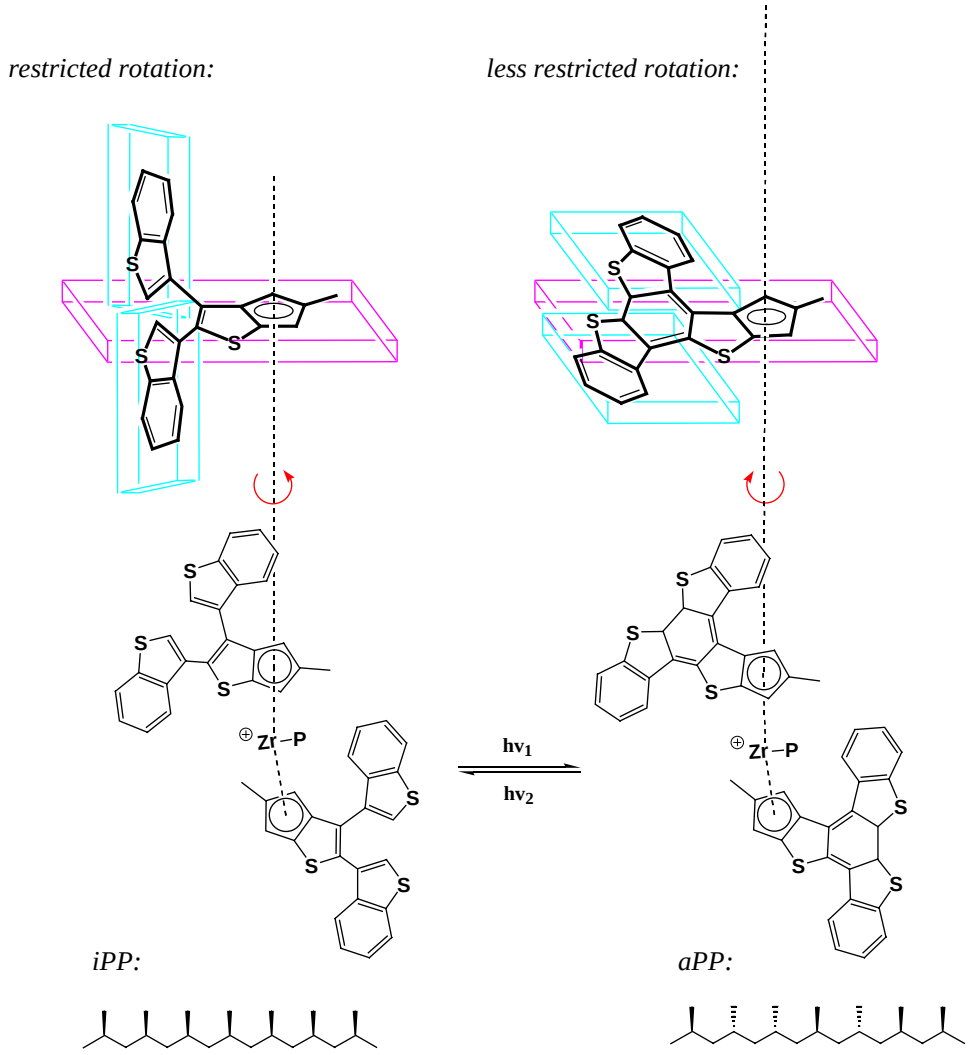

The hindered rotation presented by the open form of the (**80**) structure is rendered in Figure 35. The open structure would have restricted rotation around the central metal atom π-bonded Cp rings whereas the planar structure would be less restricted.

Larger substituents of this nature have been made and are known to have hindered rotation around the metal center due to steric interaction of the ligands[115]. In addition, this restricted rotation gives rise to isomers which have distinct relative structural orientations[116]. The polymers made from restricted rotation torsional isomers have been studied and characterized[117].

2.2.2 Bulk Propylene polymerizations using (22) and diarylethenes and (25), (26) and (27):

Polymerizations were done in liquid propylene with the diaryl substituted heterocenes (**25**), (**26**) and (**27**) (see Figure 9): as a control for this series (**22**) was polymerized in an identical procedure. A solution of the catalyst was prepared then transferred to a photochemical reactor (see Figure 124), and irradiated for between 5 to 6 h with a Heraeus (00-1725 TQ 150), 150 Watt medium pressure high intensity lamp. To a measured portion of this solution was added a solution containing MAO. As is typical with these metallocenes, the yellow catalyst solution turned violet with MAO addition. The mixture was added to a 1L reactor containing propylene and TiBAl (triisobutyl aluminium, scavenger) using 30 g liquid propylene. A portion of the irradiated solution was dried and analyzed by NMR.

2.2.2.1 Results from the polymerizations using $Me_2Si(2,5Me_2\text{-}3\text{-}PhTP)_2ZrCl_2$ (22).

As a control, experiments were done with catalyst (**22**) which contains no photo-switchable substitutions. The ^{1}H-NMR spectrum (Figure 36) indicates that under the conditions of irradiation (125 w medium pressure Hg lamp, 4 h), catalyst decomposition is taking place. In addition, in the ^{1}H-NMR spectrum of the starting complex and irradiated complex (Figure 36) show that ~86% of the -*rac* form of the complex has been converted to the -*meso* form as evidenced by the upfield shift in the single Cp proton from 6.60 to 6.48 ppm.

---

[115] G. Erker, B. Temme, "Use of Cholestanylindene-Derived Nonbridged Group 4 Bent Metallocene / Methylalumoxane Catalysts for Stereoselective Propene Polymerization", *J. Am. Chem. Soc.* (**1992**) *114*, 4004-4006.

[116] Krüger, M. Nolte, G. Erker, S. Thiele, C., "Torsional Isomerism of Bent Metallocene Complexes - The Molecular Structure of Bis(isopropylcyclopentadienyl)zirconiumdichloride in the Solid State", *Z. Naturforsch.* (**1992**) *47*b, 995-999.

[117] G. Erker, M. Aulbach, M. Knickmeier, D. Wingbermühle, C. Krüger, M. Nolte, S. Werner, "The Role of Torsional Isomers of Planarly Chiral Nonbridged Bis(indenyl)metal Type Complexes in Stereoselective Propene Polymerisation", *J. Am. Chem. Soc.* (**1993**) *115*, 4590-4601. b) C. Krüger, F. Lutz, M. Nolte, G. Erker, M. Aulbach, "Torsional isomerism of bent metallocene complexes. The structures of meso- and rac-bis(1-cyclohexyltetrahydroindenyl)zirconium dichloride in the solid state", *J. Organomet. Chem.* (**1993**) *452*, 79-86.

Figure 36. ^{1}H-NMR spectra of $Me_2Si(2,5\text{-}Me_2\text{-}3\text{-}PhTP)_2ZrCl_2$ (**22**) before and after irradiation.

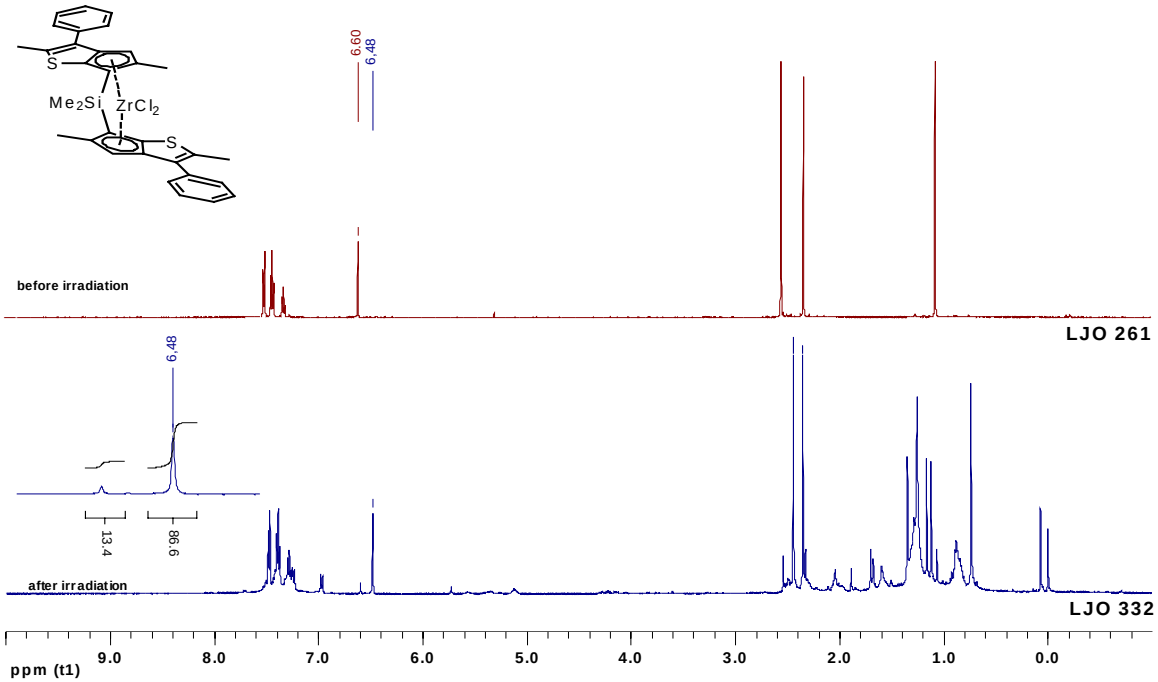

A limited number of polymerizations were done with the irradiated (**22**) complex: results are included in Table 3.

Table 3. Bulk propylene polymerization results with Dimethylsilylbis(2,5-dimethyl-3-phenylcyclopenta[b]thien-6-yl)zirconium dichloride (**22**)/ MAO, with and without irradiation treatment[(a)].

(cat) Run ID 36054-	UV	Cat. Load/ mg	MAO Al/Zr	Polym. Temp. [°C]	Mass /g PP	activity Kg PP/g cat/h	T_m2 [°C]	ΔH_c2 [J/g]	IV [dl/g]	M_w [10^{-3}]	Q[(c)]
(**22**) -68	-	1.0	1902	to 75	58.6	2929	154	93	2.3	374	4.2
(**22**) -160[(b)]	-	0.1	10569	65	62.4	4160	156	94	5.4	1171	2.4
(**22**) 111	+	0.1	10569	65	57.4	1145	155	67	2.1	361	2.4

(a) Polymerization conditions: 1l bulk, 4 mmol TiBAl, 30 min. (b) run stopped after 10 minutes, (c) $Q = M_w/M_n$.

The Q value for entry -68 is very high due to loss of temperature control at the higher activity (almost 3 million gPP/ g cat). The run-away temperature of the reaction caused the broadened M_w seen in the GPC trace (Figure 37).

Figure 37. GPC results from (**22**) liquid propylene polymerizations (see Table 3).

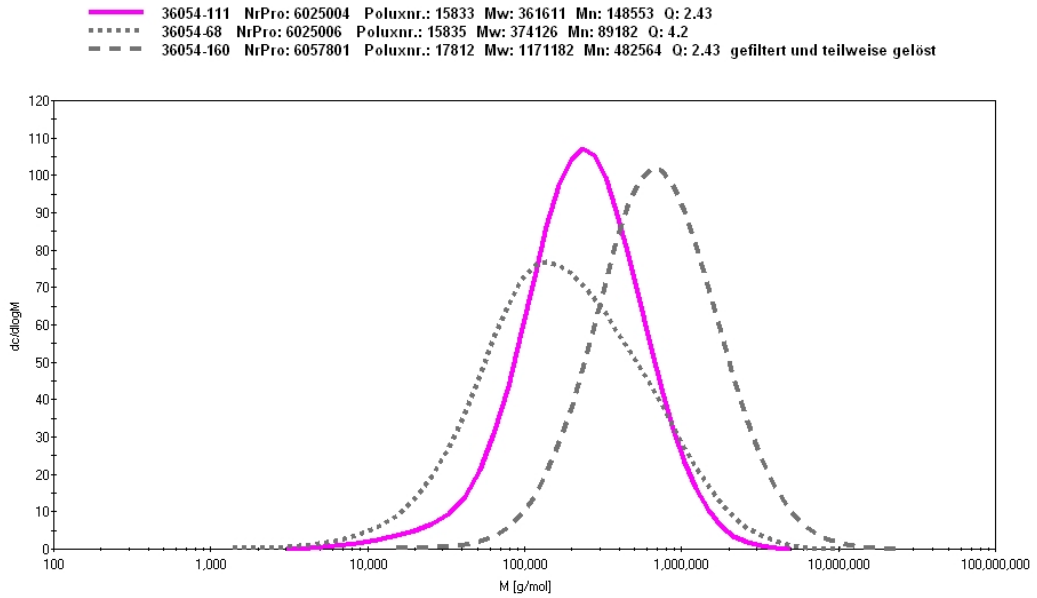

The melting point and crystallinity of the polymer made from the pre-irradiated catalyst reported here is typical for this system. In agreement with previously reported data[22], these are control runs and testing conditions partially qualifying the reactor system used in the experiments reported herein.

The high activity seen in the irradiated catalyst experiment (entry -111, although still high, shows the lowest activity among the three runs) is due to the small amount of -*rac* catalyst that remains in the irradiated mixture. The melting temperature of the polymer was 155°C and clearly did not originate from the -*meso* complex formed during irradiation.

2.2.2.2 Liquid propylene polymerizations with $Me_2Si[2\text{-}Ph\text{-}3\text{-}(2\text{-}Tolyl)TP]_2ZrCl_2$ (25)/MAO.

Results from the diaryl-thiopentalene catalyst $Me_2Si[2\text{-}Ph\text{-}3\text{-}(2\text{-}Tolyl)TP]_2ZrCl_2$ (**25**) in liquid propylene polymerizations are included in Table 4. The table contains 5 entries which include the polymerization campaigns made to determine the optimum levels of catalyst and system conditions. Entry -74 (at 65°C) and -75 (at 30°C) with non-irradiated catalyst and entry -100 with irradiated catalyst are best compared. In these cases, the activity of irradiated (**25**) was lower than the non- irradiated (**25**). The melting point and crystallinity of the polymer was decreased.

The ^{1}H-NMR of the irradiated (**25**) sample is –*meso* isomerised. The melting point at 155°C of the polymer from (**25**) irradiated originates from the small amount of -rac isomer of the complex that remains in the mixture from the irradiation experiment. The aromatic signals in the ^{1}H-NMR were not assigned, but signals from the aromatic region were similar to those found in the -*meso* complex.

Figure 38. ^{1}H-NMR spectra of $Me_2Si[2\text{-}Ph\text{-}3\text{-}(2\text{-}Tolyl)TP]_2ZrCl_2$ (**25**) before and after irradiation.

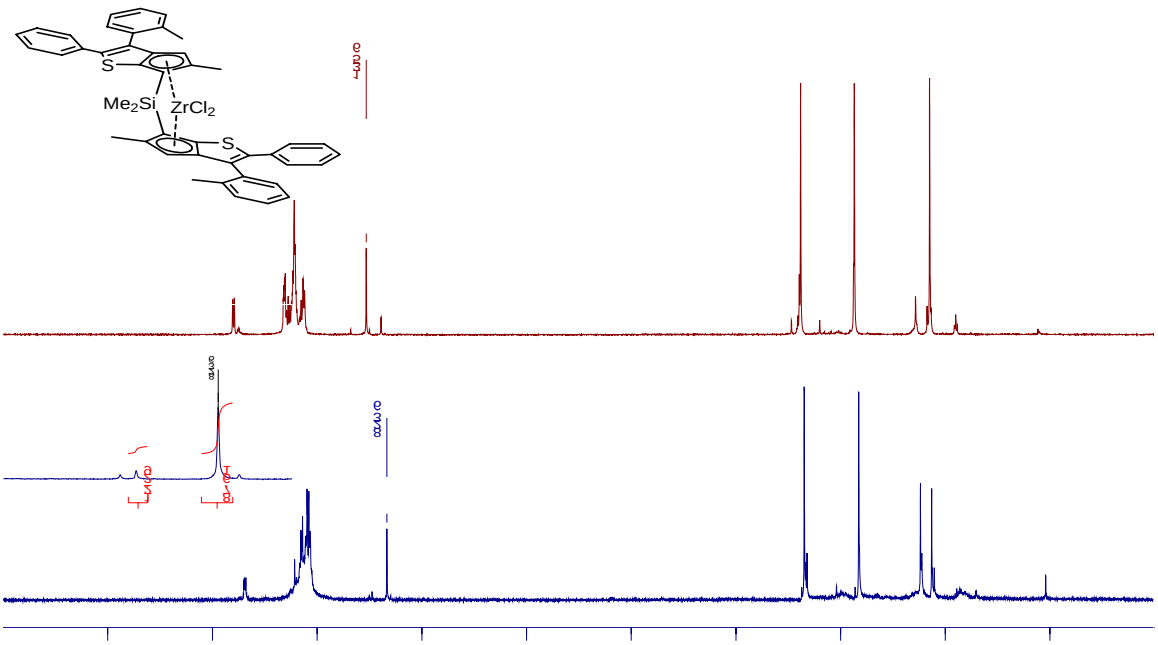

The decreasing melting temperature, if there had been cyclization, was predicted. The heterocenes containing increasing torsion angles from the substituted phenyl in the thiopentalene -3 position have made polypropylene having increasing melting point (from decreasing stereo and region irregularities) correlated with increasing torsion angel (see Figure 14). The flat torsion angle (0° isomer) would be made by irradiation (*vide supra*), and have a melting point a few degrees lower than that of (**22**). This hypothesis is supported with these experimental results.

Table 4. Bulk Propylene Polymerization results with $Me_2Si[2\text{-}Ph\text{-}3\text{-}(2\text{-}Tol)\text{-}5\text{-}MeTP]_2ZrCl_2$ (**25**), with and without irradiation treatment[(a)].

(cat) Run ID 36054-	UV	Cat. Load [mg]	MAO Al/Zr	Polym. Temp. [°C]	Mass [g PP]	activity [Kg PP/g cat/h]	T_m2 [°C]	ΔH_c2 [J/g]
(**25**) -73	-off	0.15	15600	65	52	2037	158	89
(**25**) -74	-off	0.1	23350	65	38	1260	159	94
(**25**) -100	5h 45m	1	2335	65	58	116	155	26

(a) Polymerization conditions: 1l bulk, 4 mmol TiBAl, 30 min.

Although difficult to assign, the ^{1}H-NMR of the catalyst during irradiation was collected at increasing time intervals during the experiment. These results are included in Figure 39. The conversion from -*rac* to -*meso* is followed by the change in signal intensity

originating from the cyclopentadienyl protons (at ~6.55 for the -*rac* protons and ~6.37 for the -*meso* protons).

Over the course of 150 minutes, the initial 82.7% -*rac*/ 17.5% -*meso* isomer ratio changes to 43.3% -*rac*/ 57.7% under the irradiation conditions. The conversion of the di-aryl system to the closed form is not determined by these spectra, however, this view of the kinetics of the conversion has application in processes where combinations of -*rac*/ -*meso* isomers are desired.

In further exploring the cyclization possibility, the olefin starting material used in making (**26**) was irradiated under identical conditions, The ^{1}H-NMR for this experiment is presented in Figure 40, which indicates compound decomposition, with loss of the methylene and methyl signals in the up field portion of the spectra and coalescence of the protons in the aromatic region.

Figure 39. ^{1}H-NMR spectra of irradiation of (**25**).

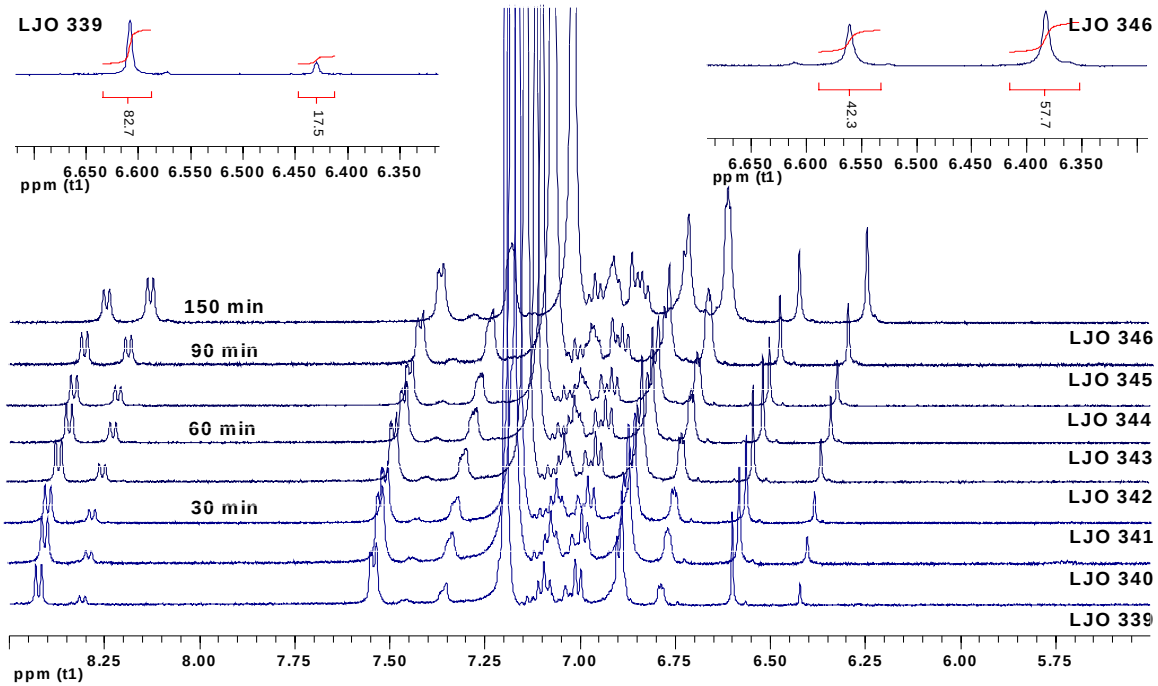

Figure 40. ^{1}H-NMR of 2,3-diphenyl-5-methyl-6-hydrocyclopenta[b]thiophene before (blue) and after (red) irradiation (see text for explanation of results).

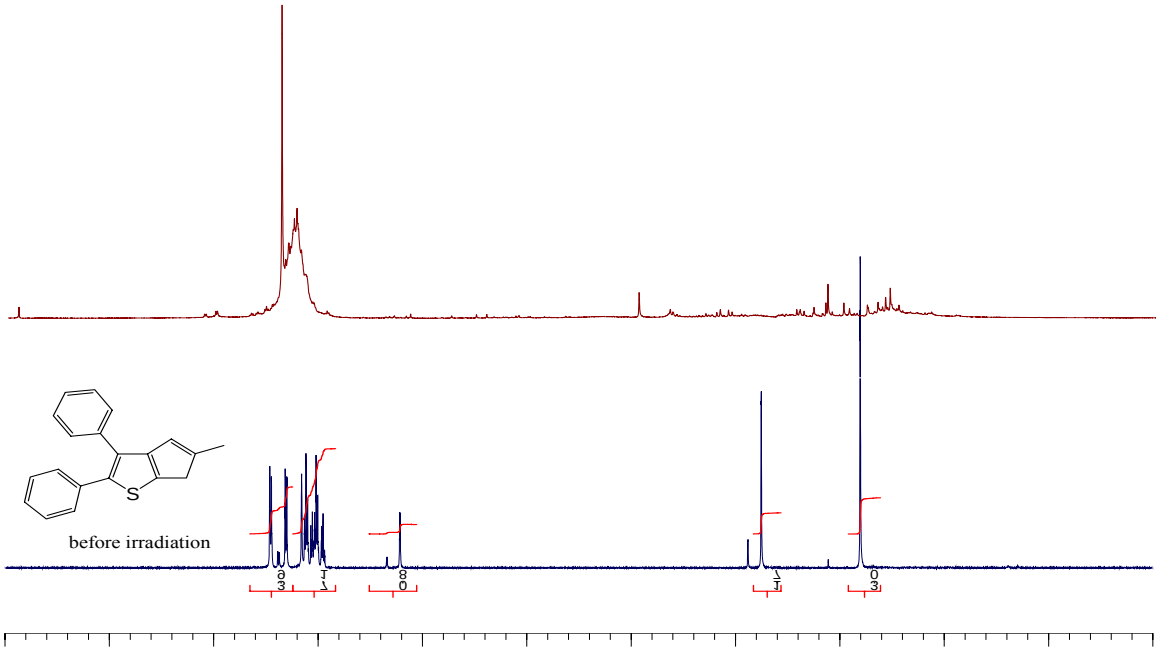

2.2.2.3 Bulk Propylene Polymerization results with $Me_2Si(2,3\text{-}Ph_2\text{-}5\text{-}MeTP)_2ZrCl_2$ (26)/MAO.

There was a large decrease in activity with (**26**) catalyst which had been irradiated, probably due to catalyst decomposition. Decomposition is seen in the ^{1}H-NMR spectrum region between 1.6 and 2.4, with broadening and coalescence of the peaks into un-assignable signals. To be certain, higher catalyst amounts were required for polymerizations with the irradiated catalyst.

Figure 41. ^{1}H-NMR spectra of $Me_2Si(2,3\text{-}Ph_2\text{-}5\text{-}MeTP)_2ZrCl_2$ (**26**) before and after irradiation.

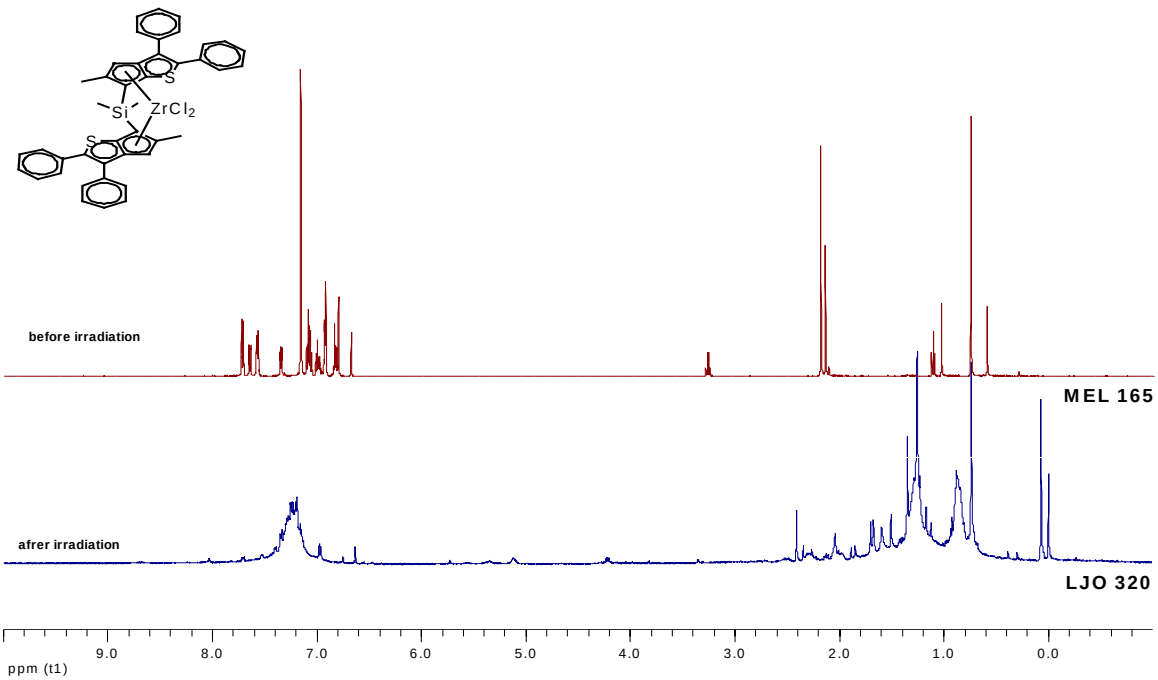

Liquid propylene polymerization results are listed in Table 5. The typical result with the un-irradiated catalyst shows good homogeneous activity, an uninteresting melting temperature, but good M_w and slightly higher than expected molecular weight distribution (Q). The irradiated catalyst, with an increase in an order of magnitude in catalyst reactor loading, had less activity, but still high melting temperature, molecular weight and even narrower polymer dispersion (Q).

In probing this result further, adding hydrogen to increase activity and increasing the Al/Zr ratio did not increase activity, but did (interestingly) increase M_w, with polymer melting temperature remaining about the same.

Table 5. Liquid Propylene Polymerization results with $Me_2Si(2,3\text{-}Ph_2\text{-}5\text{-}MeTp)_2ZrCl_2$ (**26**), with and without irradiation treatment[(a)].

36054-ID	UV	Cat Load [mg]	MAO Al/Zr	Mass [g PP]	activity [Kg PP/g cat/h]	T_m2 [°C]	ΔH_c2 [J/g]	M_w [10^{-3}]	Q[(b)]
-085	-	0.1	22555	20.8	417	153	89	1260	2.9
-086	+	1.0	10171	43.7	87	154	76	506	2.6
-109	$+H_2$	1.0	22555	28.3	57	153	87	999	2.8

(a) Polymerization conditions: 1l bulk, 4 mmol TiBAl, 30 min, 65°C, (b) $Q = M_w/M_n$.

Although the molecular weight distribution, (MWD or Q value) from the treated polymer is still narrow (ie, the MWD did not increase with UV treatment), indicating that decomposition products did not interfere other active polymerization components. In fact, the activity increased at the lower Al/Zr and the M_w was decreased by 1/2: this also indicates that chain transfer to aluminum was not substantial at the higher Al/Zr concentrations.

The GPC results all show the polymer to be single site (not bimodal, see Figure 42).

Figure 42. GPC results from catalyst polypropylene made from catalyst (**26**), (from Table 5).

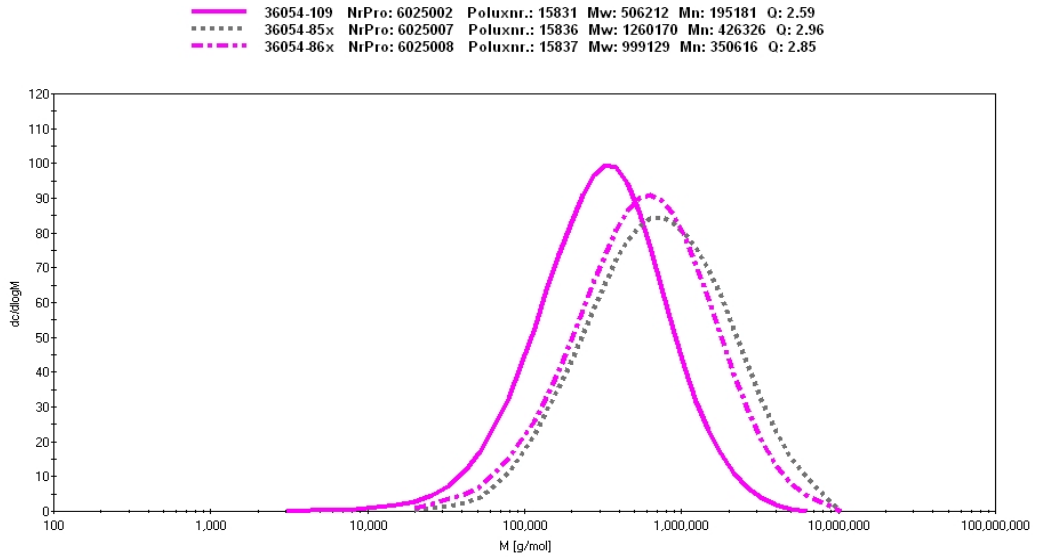

2.2.2.4 Bulk Propylene Polymerization results with $Me_2Si(2,3\text{-}Ph_2\text{-}5\text{-}MeTP)(2\text{-}iPr\text{-}4\text{-}tBuPhInd)ZrCl_2$ (**27**)/ MAO.

The final catalyst tested in the diarylethene series was a C_1 symmetric catalyst originally designed and studied for increasing molecular weight in ethylene propylene copolymers[118]. The addition of the diaryl-heterocene was for increasing isospecificity in the crystalline segment of the copolymer. The regulation of this event could be valuable, and this candidate was included.

---

[118] a) Y. Okumura, S. Sakuragi, M. Ono, S. Inazawa, "Catalyst for polyolefin production and process for producing polyolefin" to Japan Polyolefins, WO97/40075, EP845519B1, US6121182, JP9701387B (Priority: 22.04.**1996**), b) J. Schottek, M. Oberhoff, C. Bingel, D.Fischer, H. Weiss, A. Winter, V. Fraaije "Transition metal compound, ligand system, catalyst system and the use of the latter for the polymerization and copolymerization of olefins, WO01/48034 (Priority: 23.12.**1999**) c) Y. Okumura, M. Oberhoff, J. Schottek, J. Schulte "Organometallic transition metal compound, biscyclopentadienyl ligand system, catalyst system and preparaton of polyolefins", WO 03/045551 (Priority: 30.11.**2001**), d) Y. Okumura, N. Seidel, L. Kölling, "Organometalloc transition metal compound having a specific substitution pattern, biscyclopentadienyl ligand system, catalyst system and process for preparing polyolefins", International application number PCT/EP2004/005688 (Priority: 28.05.**2003**), e). Y. Okumura, I. Nifantèv, P. Ivchenko, V. Bagrav "Organometallic transition metal compound, biscyclopentadienyl ligand system, catalyst system and preparation of polyolefins" German application number DE 10358082.4 (Priority: 10.12.**2003**).

^{1}H-NMR from the irradiated and un-irradiated catalyst is included in Figure 43. Unfortunately as with the other diarylethene-thiopentalenes in the series, irradiation of the complex converted -*rac* to -*meso*, to decomposition products, and unassignable signals in the ^{1}H-NMR. Never the less, the polymerization data was collected and is presented in Table 8.

Catalyst decomposition can account for the dramatic drop in activity. The catalyst activity the polymer melting point was lowered and the MWD increased: the polymers were not bimodal. The broadened M_w for the irradiated sample was probably due to catalyst decomposition in the irradiation reactor, not multiple species of the open and closed form of the photoswitch (see Figure 44) although as with (**25**) the lower melting temperature of the polymer supports the theory of the flat isomer making lower melting point polymer. The decomposition makes interpretation in the aromatic region of the ^{1}H-NMR spectrum challenging.

Figure 43. ^{1}H-NMR of (**27**), before and after irradiation.

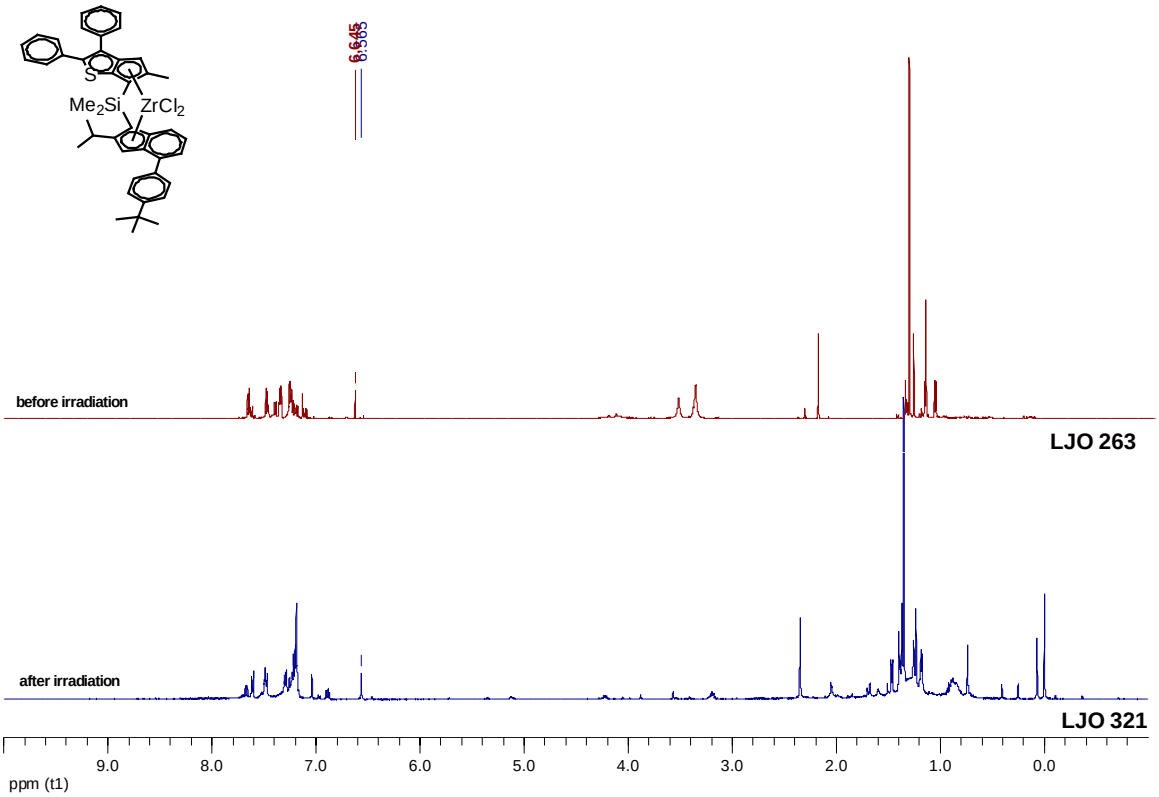

Table 6. Polymerization results with $Me_2Si(2,3\text{-}Ph_2\text{-}5\text{-}MeTp)(2\text{-}iPr\text{-}4\text{-}tBuPhInd)ZrCl_2$ (**27**), with and without irradiation treatment[(a)].

36054-ID	UV	Cat. Load [mg]	MAO Al/Zr	Mass [g PP]	activity [Kg PP/g cat/h]	T_m2 [°C]	ΔH_c2 [J/g]	M_w [10^{-3}]	Q[(b)]
-106	-	0.1	10050	5.3	106	156	81	171	1.9
-110	+	1.0	10197	1.4	2.7	133	126	415	4.1

(a) Polymerization conditions: 1l bulk, 4 mmol TiBAl, 30 min, 65°C., (b) $Q = M_w/M_n$.

The activity of this complex is lower than the previously encountered heterocenes due to the crowding at the metal center by the isopropyl group on the indenyl-Cp ring. The melting temperature, molecular weight, and polymer molecular weight distribution are normal expected values for this catalyst in this system (unsupported homogeneous homo-polymerization in bulk).

Irradiation of the catalyst resulted in much lower activity and produced a much broader molecular weight polymer, further indicating the decomposition taking place in the irradiation reaction. This is further confirmed in the graph of the polymer molecular weight distribution, where the broadening is graphically illustrated.

Figure 44. GPC of polymer made from catalyst (**27**) without (106, grey, dashed line) and with (110, magenta) 254 nm UV irradiation:

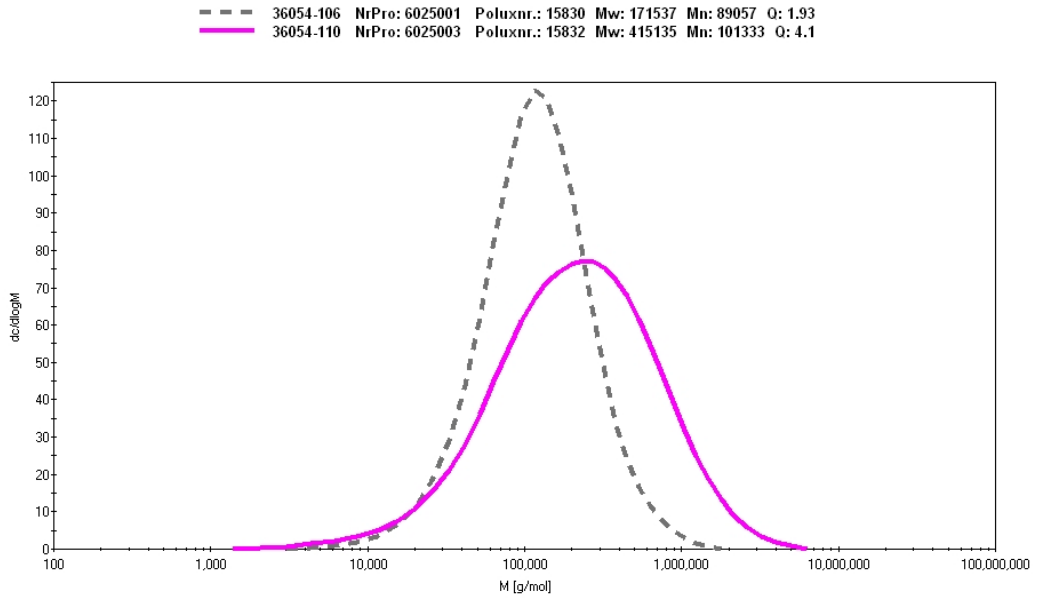

In summary, the irradiation of the diarylethyene (as opposed to heteroarylethyene) metallocene complexes above did not produce polymers which definitively demonstrate an operative molecular switch type mechanism. The ^{1}H-NMR of all complexes indicated decomposition, and interpretation of the polymer results was difficult at best.

In the Wynberg photo-cyclization experiments described earlier, aryl substituted thiophene cyclization reactions "tend towards a steady state concentration after 6 h". Many of the complexes he described slowly decomposed under the irradiation conditions[71]. Brintzinger stated that photo-steady state was reached with his metallocene complexes in 1 to 2 h. Irradiations of the complexes reported here were for 4 to 5 h: a competition may exist between ring cyclization and decomposition. Shortened periods of time may not be effective in aryl substituted ring formation with the irradiation required. The *rac*- to -*meso* conversion and photocyclization for the aryl ring systems may be competitive reactions that eliminate aryl substitutions as being candidates for photoswitches in these complexes.

The diaryl substituted thiopentalenes did not exhibit changes in absorption with 254 nm UV (see Figure 45). The substituted thiophenes (dihetero-arylethenes) on the thiopentalene ligand do cyclize at low energy UV wavelengths as demonstrated by the UV-visible spectral data (presented in the experimental section as part of the characterization of these complexes). In this context, the data shows that for the ligand components (diheteroaryl substituted thiopentalenes) and for the metallocene complexes (see Figure 74 for example), the change in absorbance which is typical of complexes containing heteroaryl-photoswitching substitutions, is below the wavelength of interference with the Cp-metal bonding, and that changing the ligand geometry using this mechanism does effect catalytic polymerization behavior.

Figure 45. UV/Visible absorption spectra of 2,3-di(2-tolyl)-5-methylcyclopenta[b]thiophene (olefin starting material for (**25**) without (–) and with (–) UV irradiation.

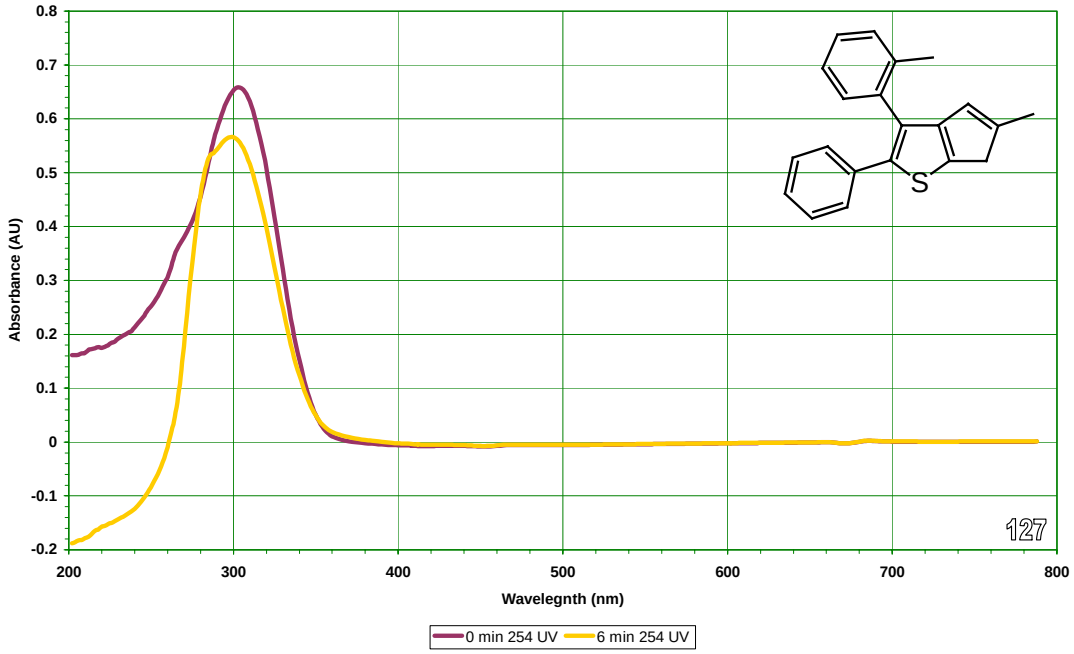

2.2.3 Solution propylene polymerization with $Me_2Si(2,3\text{-}BzTP)(2,5\text{-}Me_2\text{-}3\text{-}PhTP)ZrCl_2$/MAO (86).

In further probing the validity of the polyolefin catalysis photoswitch hypothesis, a bridged C_1 ligand and metallocene structure was prepared and tested in different polymerization conditions. Having available the photoactive olefin component (**79**) from catalyst preparations described above, dimethylsilyl-2,5-dimethyl-6-phenylcyclopenta[b]thienyl ligand was added and the bridged metallocene made by methods previously discussed.

As was typical with heterocene/metallocene complexes, the yellow toluene catalyst solution changes color to violet after MAO addition. Results from polymerizations with this complex in toluene solution with and without irradiation are included in Table 7.

Table 7. Solution Propylene polymerization results with $Me_2Si(2,3\text{-}BzTP)(2,5\text{-}Me_2\text{-}3\text{-}PhTP)ZrCl_2$ (**86**)/MAO with and without 254 nm UV irradiation during the polymerization.

36054-ID	UV	Cat. Load. [mg]	MAO Al/Zr	time [min]	polym. temp. [°C]	Mass [g PP]	activity [Kg PP/g cat/h]	T_m2 [°C]	ΔH_c2 [J/g]	IV [dl/g]	M_w [10^{-3}]	Q[(a)]
-146	OFF	10	1030	15	60	4.4	880	144	84	0.2	44	2.4
-149	OFF	5	950	60	40	10.4	2088	148	88	0.6	85	3.2
-151	OFF	2.5	530	15	30	0.5	360	155	87	0.3	66	2.0
-153	ON	5	555	120	55	2.7	270	154	87	1.6	272	2.2
-154	ON	2.5	530	15	30	0.2	144	151	71	1.3	235	2.1

(a) $Q = M_w/M_n$

Irradiation causes a dramatic increase in the molecular weight of the polymer made from this catalyst: The molecular weight distribution was not bimodal, but narrow and typical of a single site catalyst.

Figure 46. GPC from polypropylene made with catalyst (**86**), with and without 254 nm UV irradiation (see table 7).

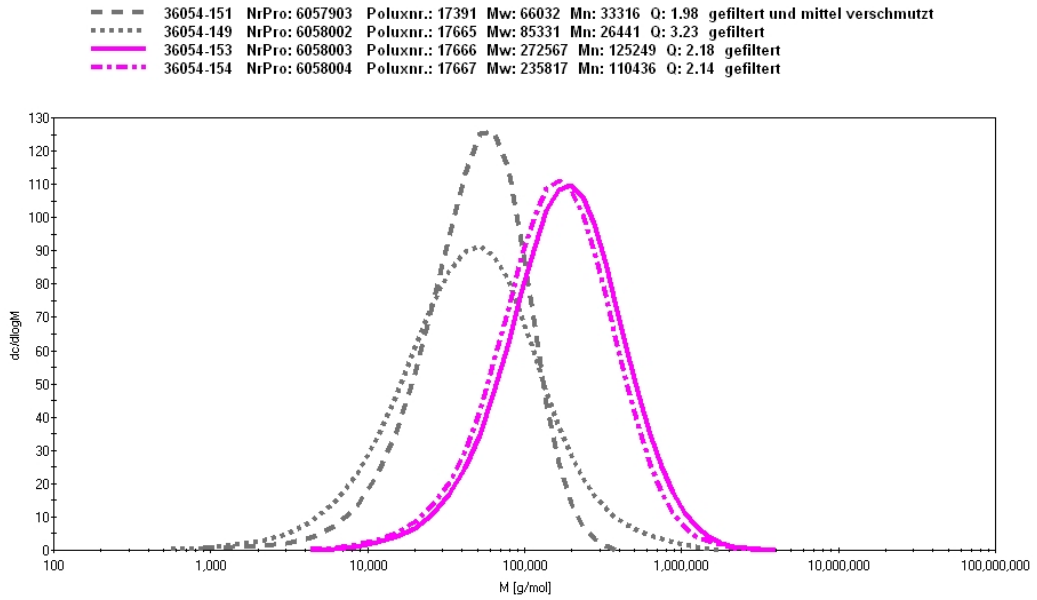

2.2.4 Bulk Propylene polymerization with catalyst $Me_2Si(2,3\text{-}BzTpTP)(2,5\text{-}Me\text{-}3\text{-}Ph_2)ZrCl_2$ (86).

The liquid propylene polymerization activity of (**86**) was high, typical of thiopentalene ligand containing metallocenes. In initial bulk propylene polymerizations activity of the complex was 878 Kg/g cat*h^{-1} (721.6 Kg/mmol cat*h^{-1}). The amount of catalyst used in these experiments had to be limited such that the levels of poisons in the reactor competed with the amount of activated catalyst and make accurate measurement challenging (entry -158). Convincing polymerization results were obtained by finding optimum ratio between the amount of activator (methylaluminoxane, MAO) and catalyst loading.

Polymerizations were done in a stainless steel reactor which had no means of irradiation treatment during the polymerization. Instead, the catalyst was irradiated for 2 h then kept in the (dark) photo-activated state during MAO activation and transfer into the 1L autoclave.

Polymerization results are shown in Table 8. Entry 144 was a run-away reaction and had to be stopped. The data is indicative, but not reliable. It is included for demonstrating the high activity encountered with this catalyst complex. Entry -158 illustrates the opposite extreme. By restricting the catalyst amount put in to the reactor in an effort to control the polymerization, the catalyst is inactivated by the reaction medium.

Table 8. Bulk Propylene Polymerization Results with (**86**)[(a)].

36054-ID	UV	Cat. Load [mg]	MAO Al/Zr	time [min]	pol temp [°C]	Mass [g PP]	activity [Kg PP/g cat/h]	T_m2 [°C]	ΔH_c2 [J/g]	IV [dl/g]	M_w (10^{-3})	Q[(b)]
144	NO	1.0	10000	4	to 70°	52.6	878	155	86	3.9	718	2.2
157	NO	0.2	1000	30	65	3.2	32	154	66	4.1	1160	4.3
145	NO	0.1	5000	30	65	4.8	97	150	80	5.0	1112	4.0
168	NO	0.2	5000	30	65	15	150	153	85	5.4	1319	3.7
158	YES	0.2	1000	30	65	0.5	5	150	53	3.9	828	3.9
169	YES	0.2	5000	30	65	5.6	50	152	78	5.4	1315	3.9

(a) Polymerization conditions: 1l bulk, 4 mmol TiBAl, 30 min. (b) $Q = M_w/M_n$.

Comparable polymerization data was collected and included in entries **157** and **158** (Al/Zr = 1000) and entries **168** and **169** (Al/Zr = 5000)**.** The data shows that there is a decrease in catalyst activity and a slight increase in the molecular weight polymer dispersity with catalyst UV irradiation at the higher Al/Zr ratio (see Figure 48). This could be due to the changing ligand structure made by the closed form of the catalyst. All other properties of the polymer are only slightly changed.

Decreased activity could be due to the aging of the catalyst solution while spending time in the presence of the irradiation source. Similar experiments with catalyst solutions aged without UV exposure however, did not loose activity after 18 h under ambient conditions.

Figure 47. GPC trace from bulk propylene polymerizations with (**86**): entry 145 and 157 without UV(dashed, grey): and 158 with 254 UV (magenta):

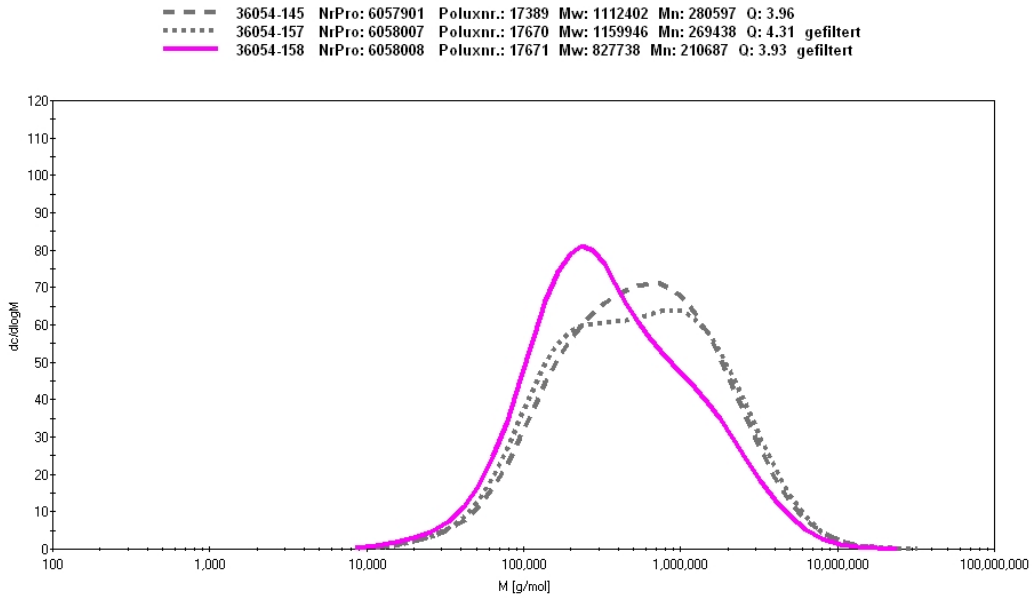

Figure 48. GPC trace from bulk propylene polymerizations with (**86**): entry 168 without UV (grey, dashed): and 169 with 254 UV (magenta), Al/Zr = 5000:

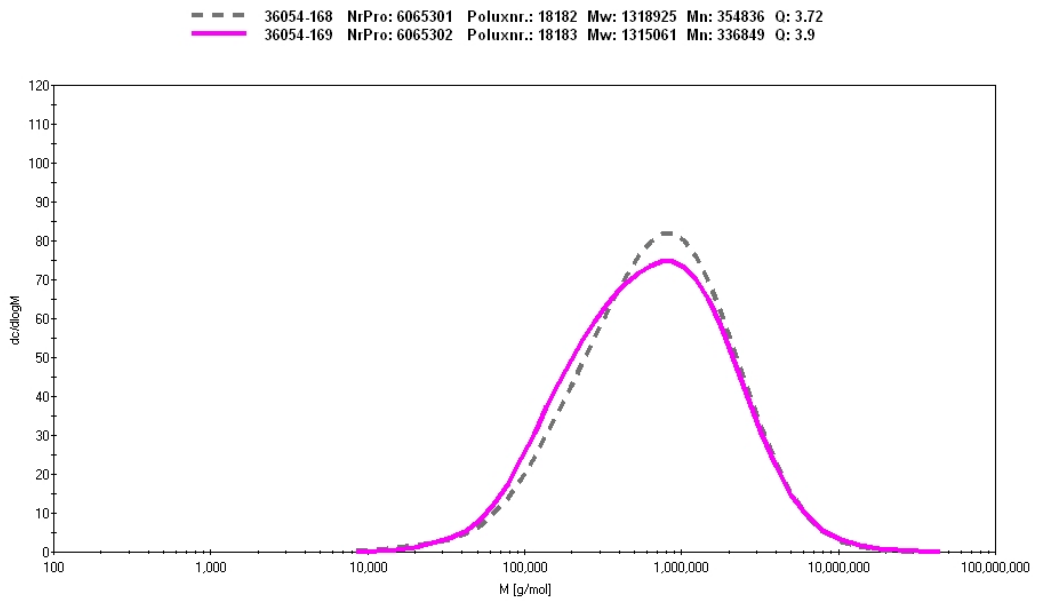

The increase in MWD of the irradiated catalyst is typical of multiple catalyst species making a different polymer. This effect is less pronounced in the polymers made at Al/Zr = 5000 than those made at Al/Zr = 1000.

2.2.5 Ethylene and Ethylene-Hexene co-polymerizations

Polymerizations were made at 1 atm ethylene pressure in toluene solution with and without hexene co-monomer at 40°C for varying times. Polymerizations were done in the presence of UV irradiation or without: results are listed in Table 9.

The data does not indicate that at these levels or under these conditions there is an effect of co-monomer uptake by (**80**) catalyst activation. The levels of co-monomer are slightly increased for both the (**102**) and for (**80**) with UV irradiation. The GPC curves are similar in the control and test case, with no indication of broadening or bimodality as was seen in propylene polymerizations.

The selection of catalyst and type of co-monomer used for this experiment does not demonstrate control of co-monomer incorporation in these polyethylene experiments. The effect may be below the detection limit or the ligand geometry is not dramatically enough affected. The sensitivity of co-monomer insertion into the growing polymer chain may be less affected by changes in this ligand type at these levels.

Table 9. Ethylene and ethylene-hexene polymerization results with (**102**) and (**80**)[(a)].

Run ID	Catalyst [mg]	Hexene [mL]	time [min]	Mass [g PP]	Activity [Kg PE/ mol Zr/h]	T_m2 [°C]	ΔH_c2 [J/g]	IV [dl/g]	IR Density [g/cm^3]	IR % hexene	GPC M_w [g/mol]	GPC M_n [g/mol]	Q[(b)]
120	(**102**)	0	10	5.6	1485	133	234	0.56	0.9722	-	22157	6134	3.6
118	(**102**)	5	15	13.4	2802	103	77	0.97	0.9016	15.1	45683	10047	4.6
144	(**102**)+UV	5	16	12.7	2381	102	77	0.75	0.9049	25	33023	11112	3.0
134	(**80**)	0	15	3.7	949	135	186	3.0	0.9527	-	202590	41610	4.9
136	(**80**)	5	15	1.9	477	77	61	1.0	0.9853	16.6	42456	15351	2.8
138	(**80**)+UV	5	12	3.1	832	74	43	1.3	nm	~18.5	46859	15045	3.1

(a) Polymerization conditions: 1L glass reactor, 40°C, Al/Zr = 500, (b) $Q = M_w/M_n$.

Figure 49. GPC trace from Ethylene/Hexene polymerization results with (**102**):

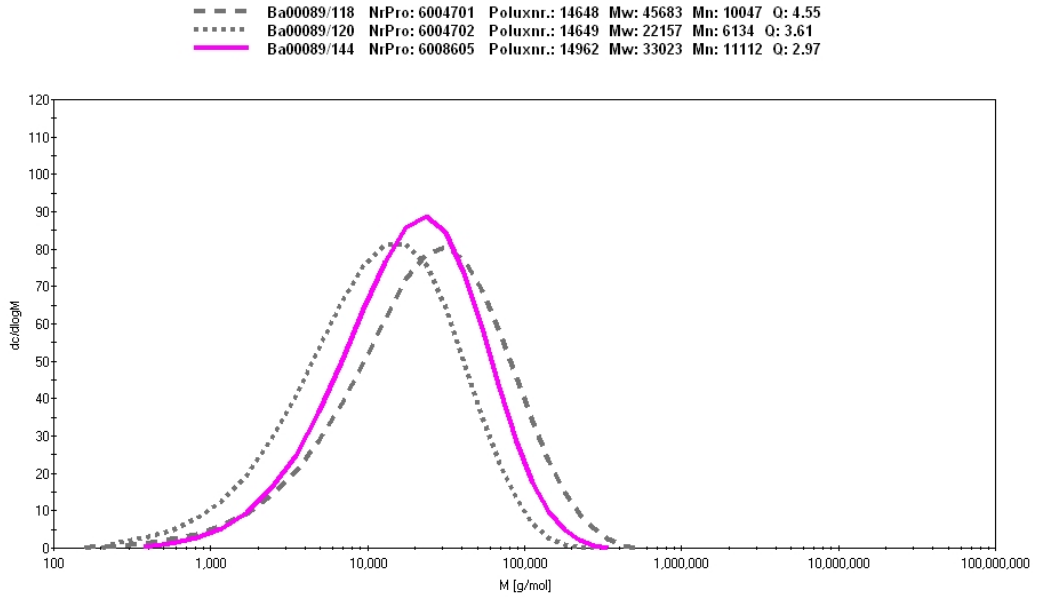

Figure 50. GPC trace from Ethylene/Hexene polymerization results with (**80**):

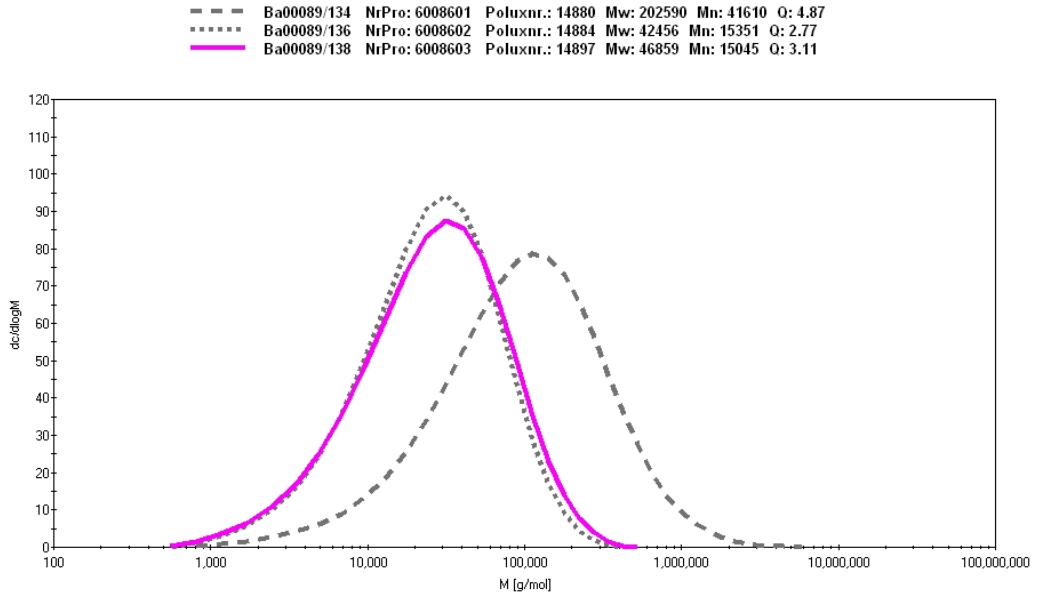

2.2.6 Ethylene and Ethylene/Hexene Polymerization Results with $Me_2Si(2,5\text{-}Me\text{-}3\text{-}Ph_2)ZrCl_2$ (22) and $Me_2Si(2,3\text{-}BzTpTP)(2,5\text{-}Me\text{-}3\text{-}PhTP)_2ZrCl_2$ (86).

Ethylene polymerizations in toluene solution at atmospheric pressure were made with either (**22**) or (**86**) with or without 254 nm irradiation under identical conditions. The data from the polymers is included in Table 10.

The control catalyst $Me_2Si(2,5\text{-}Me_2\text{-}3\text{-}PhTP)_2ZrCl_2$ (**22**) has good activity in the ethylene/hexene co-polymerizations (compared to the unbridged catalysts tested above, see Table 9), making high molecular weight copolymers having good co-monomer incorporation. There is a slight increase in activity with 254 nm UV irradiation, but no increase in hexene incorporation as measured by IR. This result is reiterated in the measure of $-CH_3$ groups per 1000 carbons: both values being the same.

In the ethylene or ethylene/hexene polymerizations with $Me_2Si(2,3\text{-}BzTpTP)(2,5\text{-}Me\text{-}3\text{-}PhTP)_2ZrCl_2$ (**86**) there was a substantial increase in activity with UV irradiation. The values for polymer melting temperature and crystallinity differ indicating increased co-monomer incorporation, and this is verified by IR values for % co-monomer incorporation which also increase for the irradiated polymer. This result is seen again in the IR measurement for $-CH_3$/1000C which is substantially higher for the irradiated polymer, again indicating increased co-monomer uptake. The molecular weight of the polymer remains the same with or without irradiation and there is a decrease in the MWD.

Broadened MWD could be due to hexene oligomers, but the decreasing values for UV treated polymer for either catalyst are interesting. The GPC curves for these polymers do not indicate bimodality: the polymers are homogeneous.

Table 10. Toluene solution ethylene and ethylene-hexene polymerization results with $Me_2Si[2,5\text{-}Me_2\text{-}3\text{-}(Ph)TP]_2ZrCl_2$ (**22**) and dimethylsilyl bis(2,3-di(benzo[b]thiophen-3-yl)-5-methyl-cyclopenta[b]thien-6-yl)][2,5-dimethyl-6-phenylcyclopenta[b]thien-6-yl)]zirconium(IV) chloride (**86**)[(a)].

Run ID (cat.)	Cat. Load [mg]	hexene [mL]	time [min]	Mass [g PE]	activity [Kg PE/ mol Zr/h]	T_m2 [°C]	ΔH_c2 [J/g]	IV [dl/g]	IR Density [g/cm^3]	IR % hexene	IR CH_3 1/1000C	GPC M_w [10^{-3}]	GPC M_n [10^{-3}]	Q[(b)]
264 (**22**)	5.3	4	9	9.5	7997	122	85	4.2	0.9097	~14	29.1	492	85	5.8
266 (**22**)	5.3	5	12	15.2	9596	121	74	3.9	0.9027	~16	29.4	373	97	3.8
258 (**86**)	2	0	20	0.8	1013	133	142	8.2	0.9382	-	<0.7	800	204	3.9
260 (**86**)	5.2	5	20	1.1	535	79	45	3.8	0.8953	~16	~22	436	68	6.4
262 (**86**)	5.3	5	20	6.5	3100	86	48	3.4	0.885	~20	36.5	433	109	4.0

(a) see text for polymerization conditions and explanation of results, (b) $Q = M_w/M_n$.

2.2.7 Piano Stools: 2,3(BzTp)TP-$ZrBr_3$ and 2,5MeTp-$ZrBr_3$

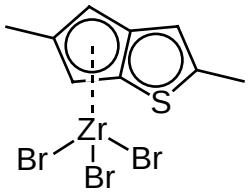

(**103**)
2,5-Me_2TPZrBr_3

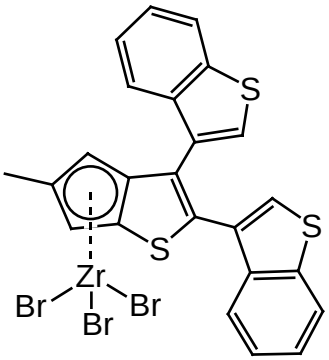

(**104**)
2,3-BzTp-5-MeTPZrBr_3

Complexes 2,5-Me_2TPZrBr_3 (**103**) and 2,3-BzTp-5-MeTPZrBr_3 (**104**) were prepared and tested in ethylene solution polymerizations. The data is included in Table 11.

The catalyst complex 2,3-BzTp-5-MeTPZrBr_3 (**104**) had very low initial activity when compared to 2,5-Me_2TPZrBr_3 (**103)** due to low solubility in toluene. When (**104**) was dissolved directly in the toluene/ MAO solution, the activity became better than the control. Polymer melting point and IV are similar, with (**104**) making a slightly higher molecular weight (by IV).

When the polymerization was done in with (**104**) in the presence of 254 nm UV irradiation, the molecular weight of the polymer was increased from an IV of 3 to an IV of 6.2: a little more than doubled. GPC results further verify this result: the molecular weight increases from 207,000 to 357,000. This result is accompanied with an increase in the polymer dispersity, from 3.9 in the un-irradiated sample to 7.0 in the polymer made with irradiation. This `could be due to cross-linking or some other physical modification of the polymer as a result of this catalyst complex: it is an interesting result.

Table 11 Toluene solution ethylene polymerization results with 2,5-Me_2TP-$ZrBr_3$ (**103**) and 2,3$(BzTp)_2$TP-$ZrBr_3$ (**104**)[(a)].

Run ID (cat)	Cat. Load. [mg]	time [min]	Mass [g PE]	activity [Kg PE/ mol Zr/h]	T_m2 [°C]	ΔH2 [J/g]	IV [dl/g]	IR Density [g/cm^3]	IR CH_3 1/1000C	GPC M_w [10^{-3}]	GPC M_n [10^{-3}]	Q[(c)]
286 (**103**)	18	20	2.8	225	135	200	2.2	0.9067	<0.7	105	11	9.7
304 (**104**)[(b)]	22	10	2.2	438	135	188	3.0	0.9545	<0.7	207	53	3.9
302 (**104**)[(b)]	20	20	2.5	274	135	184	6.2	0.9634	2	357	51	7.0

(a) complex (**104**) was dissolved directly in the toluene/MAO solution due to limited solubility in toluene, see text for polymerization conditions and explanation of results, (c) $Q = M_w/M_n$.

3.0 Conclusions and Prospects

Different polymers were produced with the same catalyst by incorporating and activating a molecular switch. I have demonstrated that the heterocene-diarylethenes, particularly those substituted with a benzothiophene group were suitable candidates and demonstrated the photoswitching polyolefin catalyst hypothesis. Catalysts activated with MAO made different polymers with the same catalyst after irradiation with 254 nm UV.
.
Using rational catalyst design, the incorporation of a photomolecular switch provided control over the type of polymer produced using two independent catalyst examples.

There are alternative polyolefin and functional group tolerant catalysts that are available and could be tested. Expanding the application of this technology into other catalyst systems is obvious.

It may be possible to affect living polymerizations using the Mitsui/Coates phenoxy-imine FI catalysts. Long lived polymerization centers have recently been demonstrated[119]. It is entirely feasible to change the orientation of ligand conformations using a photoswitch and affect the polymer product produced from this reaction using these types of catalyst.

Information storage in product from a polymerization reaction using these types of catalyst:

Busico has described the polymerization reaction as making:

"A linear macromolecule, in particular, is like a tape on which the complete reaction story is sequentially and permanently recorded"….

The "tape" is a binary information sequence consisting of methyl groups placed in mesomeric dyads on either side of the polymer chain (backbone). Although reading the tape (polymer microstructure) with current technology is accessible at the undecad level at best (with NMR for polypropylene), movement towards reading the tape is progressing. Precise similar placement of copolymerized molecules may present an alternative.

In either case, the placement of information of this type into the growing polymer chain would depend on the ability of the catalyst to insert monomer at a rate faster than chain termination. Analyzing this scenario, we consider the insertion reaction to be taking place at "10-100 propene insertions per second at the same temperature and [C_3H_6] 1-10 mol/L)"…[120]

---

[119] Junichi Mori, Terunori , *Organometallic News*, **2003** (4), 132 – 137.
[120] Quote from Busico *et. al*., reference 37 (and references therein).

whereas depending on the radiation type and amount, the ring opening and ring closing reaction which could lead to alternative stereochemical monomer insertions occur on a picosecond time scale[121]. This was as well reviewed by Lucas, where she noted:

" Typically, "dithienyl*perfluoro*cyclopentene switches have revealed ring closure time constants of 1-3 ps"[122].

In the right environment, these values are well within a range so as to create a possible synergy and effect the monomer placement reaction.

Reactor Blends

Should the commercial reactor be modified to have an irradiation source located in an area where during the polymerization reaction irradiative exposure was possible, the switching of the catalytic system from one form to another would lead to reactor blends. Reactor blending technology is currently accomplished on an industrial scale using multiple catalysts in the reaction sequences, multiple reactors operated at different conditions, or by blending polymers post-reactor. Using a photo-switchable catalyst in a reactor having irradiation capabilities would produce such a desired product. In a continuous process (such as UV sterilization of drinking water) application of such continuous UV irradiative systems are well known.

Multiple types of photoswitching components have been described (see photoswitching references). Each component has a characteristic wavelength that it operates. It should be possible to construct a catalyst having multiple addressable photoswitching capabilities which could control monomer or co-monomer insertion rates into the polymer chain, thereby further controlling the reactor blending methodology.

Different metallocene catalysts have different co-monomer incorporation rates[123]. Control over the type of co- or –ter - polymer made by changing orientations using photoswitching catalysts could provide control over polymer properties in a reaction mixture. Combining this scenario with multiple switches having different addressability could also provide unique structures.

---

[121] Feringa, B. L. Molecular Switches, Wiley-Vch GmbH, Weinheim, 2001.
[122] Linda Nienke Lucas, "Dithienylcyclopentene optical switches : towards photoresponsive supramolecular materials", Dissertation (**2001**) University of Groningen, Netherlands.
[123] Monomer reactivity ratio: for ideal copolymerization r1/r2 = 1: for alternating copolymers r1 = r2 = 0, for block copolymers r1>1, r2>1

4.0 Experimental

4.1 General Procedures

The synthesis of organic and organometallic compounds involving air sensitive materials were performed under nitrogen atmosphere in pre-dried glassware unless stated otherwise. Manipulations such as filtration and handling, weighing and drying were performed in a Vacuum Atmospheres dri-box with nitrogen flow through arrangement. Solvents used in the synthesis of air-sensitive compounds were Aldrich anhydrous grade. In some cases solvents were further purified by filtration through molecular sieves, activated alumina, or supported copper catalyst in a procedure similarly described by Grubbs, et al.[124].

The (tetrakis-(triphenylphosphine)palladium) used in the coupling experiments and zirconium(IV) chloride were purchased from Strem Chemical Co. (MA, USA): Bis(diphenylphosphino)propane nickel(II) chloride (NiDPPP) was purchased from Aldrich.

Methylalumoxane (solution in toluene; 30% by weight of MAO) used in the polymerizations was procured from Albemarle Corp. and Al(iso-Bu)$_3$ (1 M solution in toluene) was procured from Aldrich Chemical Company.

4.2 Synthesis and Experimental Protocols

4.2.1 Intermediates and Catalysts:

2-methylbenzo[b]thiophene (**53**).
(ID: 001-010P1):

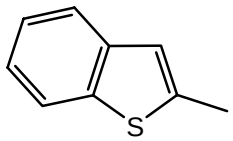

To a flask containing 70.06 g (520 mmol) benzo[b]thiophene (**52**) (Aldrich) dissolved in 500 ml diethyl ether at -10°C was added a solution containing n-butyllithium (210 ml, 525 mmol, 2.5M in hexane). After addition was completed the reaction mixture was allowed to warm to ambient and stirred an additional 1 h. The reaction mixture was cooled to -10°C, and then a solution containing 75 g (532 mmol) iodomethane dissolved in 100 ml diethyl ether was added dropwise. The reaction mixture was allowed to warm to room temperature: stirring was continued for 18 h. The reaction mixture was poured into an equal volume of water; organics were collected with a 20% dichloromethane/hexane solution, washed with water, dried over magnesium sulfate, filtered, then solvents removed in vacuo. Slight yellow oil which crystallizes upon

---

[124] Amy B. Pangborn, Michael A. Giardello, Robert H. Grubbs, Robert K. Rosen, and Francis J. Timmers "Safe and Convenient Procedure for Solvent Purification", *Organometallics*, (**1996**) *15* (5), 1518 -1520.

standing:Yield 77.96 g (87% by GC FID = 88%: used in subsequent steps without further purification). EIMS, m/z (%): 149 (11), 148 (69), 147 (100), 115 (8), 104 (1), 103 (6), 102 (3). ^{1}H-NMR δ ($CDCl_3$): 7.7 (d, 1H), 7.6 (d, 1H), 7.29 (t, 1H), 7.22 (t, 1H), 6.9 (s, 1H), 2.55 (s, 3H).

Figure 51. ^{1}H-NMR of the starting material (for reference); benzo[b]thiophene (**52**)

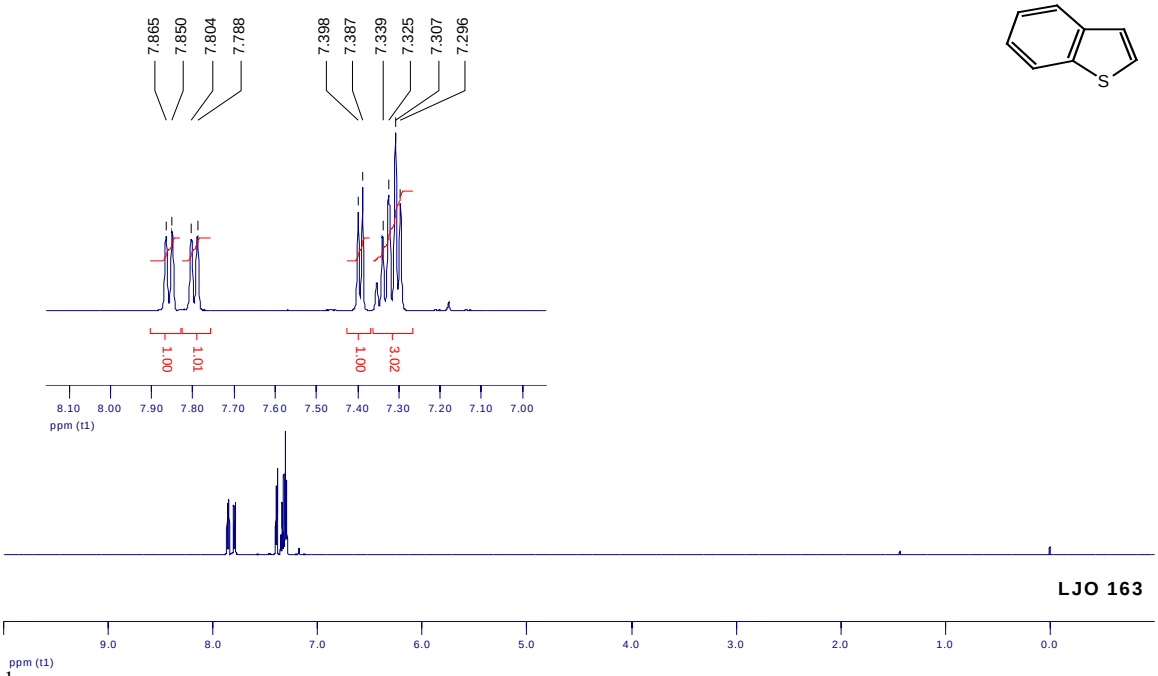

^{1}H-NMR δ ($CDCl_3$): 7.85 (d, 1H), 7.78 (d, 1H), 7.39 (d, 1H), 7.34 – 7.25 (m, 3H).

Figure 52. ^{1}H-NMR of 2-methylbenzo[b]thiophene (**53**) in $CDHCl_3$.

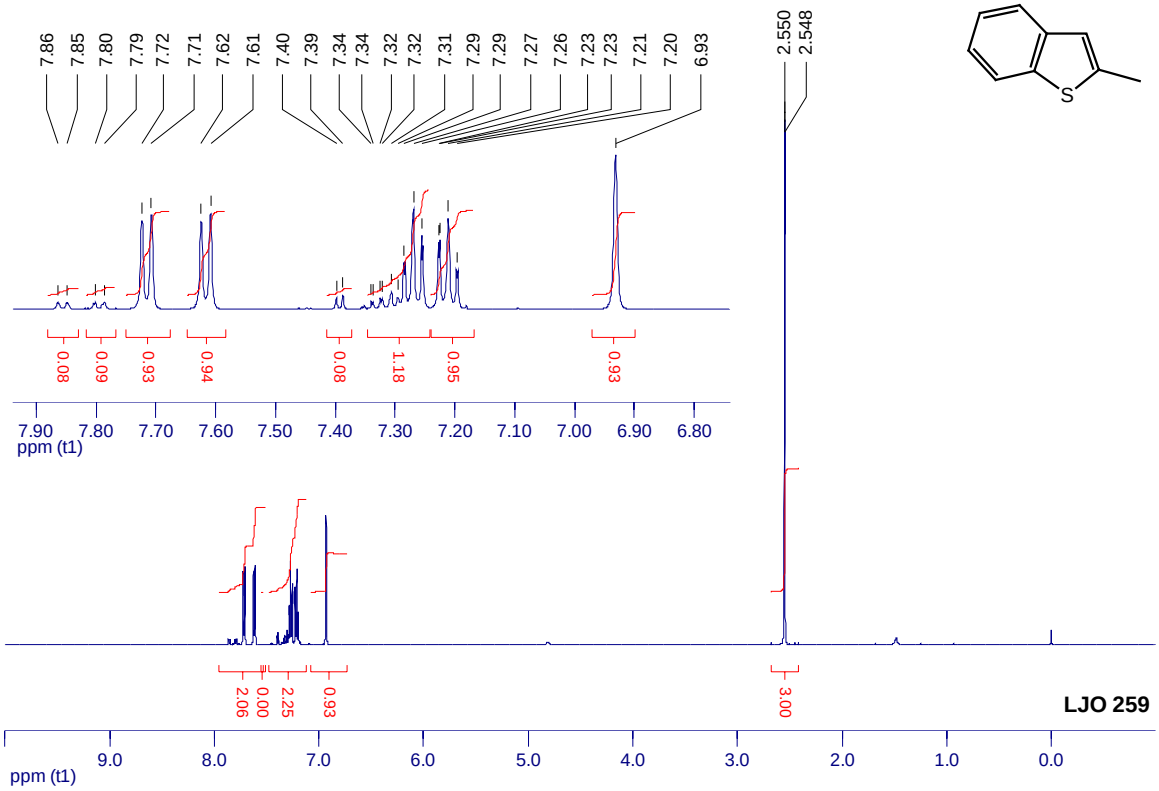

^{1}H-NMR δ ($CDCl_3$): 7.7 (d, 1H), 7.6 (d, 1H), 7.29 (t, 1H), 7.22 (t, 1H), 6.9 (s, 1H), 2.55 (s, 3H).

3-bromo-2-methylbenzo-[b]thiophene (**54)**
(ID: 001-068)

A flask containing 62.58 g (422.8 mmol) 2-methylbenzo[b]thiophene (**2)** dissolved in 300 mL 1:1 dichloromethane: acetic acid was cooled to -10°C (ice/acetone), then 75.25 g (423 mmol) *N*-bromosuccinimide was added (slowly) as a dry powder. The reaction mixture was stirred for 20 minutes, then sampled (the reaction had completed). The reaction mixture was poured into an equal volume of water, organics were extracted with dichloromethane. The organics were washed with a saturated solution containing sodium bicarbonate, water, then dried over magnesium sulphate. The organics were filtered then solvents removed from the filtrate in vacuo. In this fashion, 128.44 g were collected (dark brown oil) which was then filtered through silica (100 g) using hexane. Solvents were removed in vacuo. Yield: 105.76 g recovered (GC FID: 87%). EIMS, m/z (%):229 (7), 228 (68), 226 (20), 225 (12). 149 (5), 148 (11), 147 (100). ^{1}H-NMR δ ($CDCl_3$): 7.65 (t, 2H), 7.33 (t, 1H), 7.25 (t, 1H), 2.48 (s, 3H).

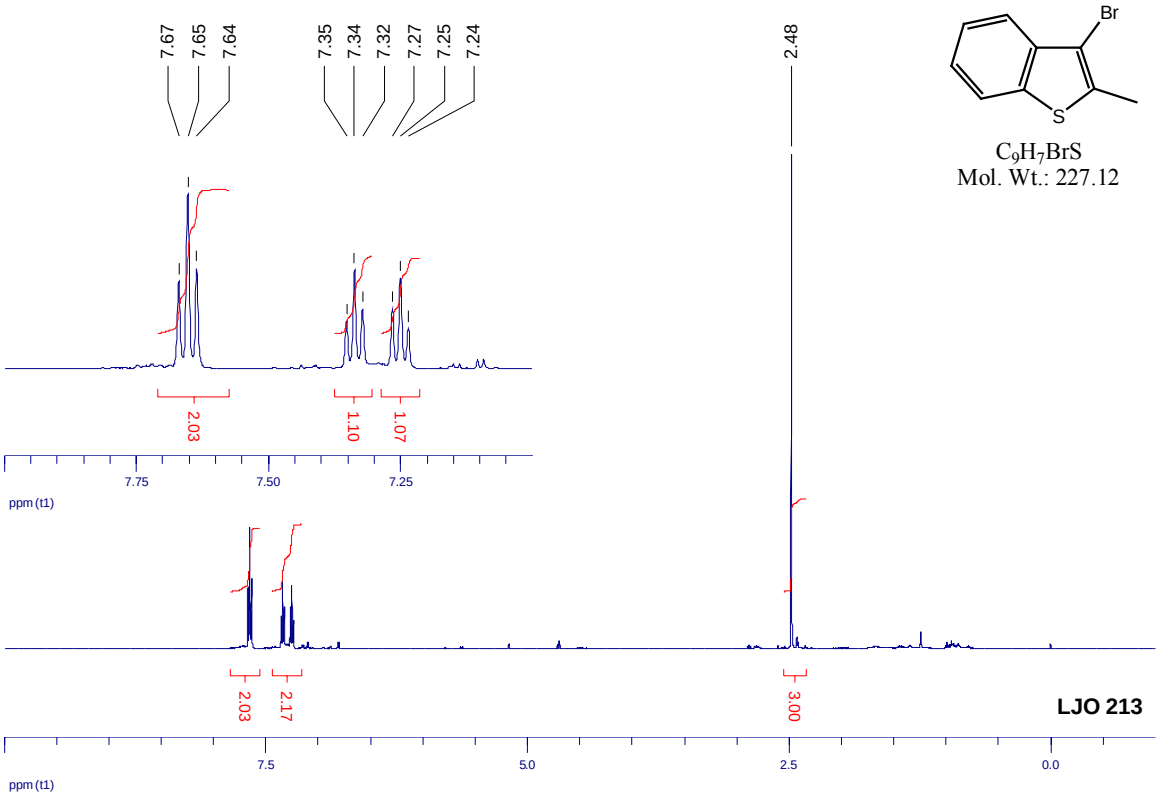

2-methyl-3-(thiophen-3-yl)benzo[b]thiophene (**63**).
(ID: 001-020)

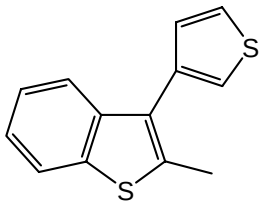

In a flask containing 5.03 g (22 mmol) 3-bromo-2-methylbenzo[b]thiophene (**54**) dissolved in 80 mL diethyl ether at -10°C (ice/acetone) was added a solution containing n-butyllithium (8.8 mL, 22 mmol, 2.5M in hexane): a white precipitate formed.

A 2nd flask was prepared containing 5.67 g (22 mmol) magnesium bromide etherate dissolved (with sonication) in 80 mL diethyl ether. This solution was added to the above flask via cannula. After 15 min., the slurry had become a solution.

A 3rd flask was prepared containing 3-bromothiophene and 0.75 g (1.3 mmol) 1,3-bis(diphenylphosphino)propane nickel(II) chloride (Strem), (**50**) slurried in 80 mL diethyl ether and the temperature lowered to -10°C. The above solution was added by cannula. After addition was completed the ice bath was removed and stirring continued for 7 days. The contents were poured into water, organics collected with w 20% dichloromethane/ hexane solution, dried over magnesium sulphate, filtered, then solvents removed in vacuo to yield a dark brown oil. Yield: 4.42 g (80% by FID-GC).

Figure 53. FID-GC and GC-MS analytical results for 2-methyl-3-(thiophen-3-yl)benzo[b]thiophene (**63**):

```
                    Area Percent Report
Data Path : D:\MSDCHEM\1\DATA\Jones\100DISS\020\
Data File : 020CP1.D
Acq On    : 22 Mar 2005   9:35 (#1); 22.03.2005 09:35:18 AM (#2)
Operator  : JONES
Sample    : 020CP1
Misc      : 3Tp2MeBzTp at P1 4.42 g (Sig #1);  (Sig #2)
ALS Vial  : 1   Sample Multiplier: 1

Integration Parameters: autoint1.e
Integrator: ChemStation   6890 Scale Mode: Large solvent peaks clipped
Smoothing : OFF                    Filtering: 5
Sampling  : 1                      Min Area: 5 % of largest Peak
Start Thrs: 0.2                    Max Peaks: 100
Stop Thrs : 0                      Peak Location: TOP

If leading or trailing edge < 100 prefer < Baseline drop else tangent >
Peak separation: 5

Method    : D:\MSDCHEM\1\METHODS\MSHIGH.M
Title     : install
```

Signal : TIC

peak #	R.T. min	first scan	max scan	last scan	PK TY	peak height	corr. area	corr. % max.	% of total
1	8.094	642	648	655	BB	3583671	40075785	10.29%	8.318%
2	8.985	757	763	769	BB	577633	6177109	1.59%	1.282%
3	12.004	1146	1153	1167	BB	25372354	389307706	100.00%	80.799%
4	13.893	1392	1397	1404	BB	1680496	18586402	4.77%	3.858%
5	15.062	1541	1548	1553	BV	2008324	27673213	7.11%	5.743%

Sum of corrected areas: 481820215

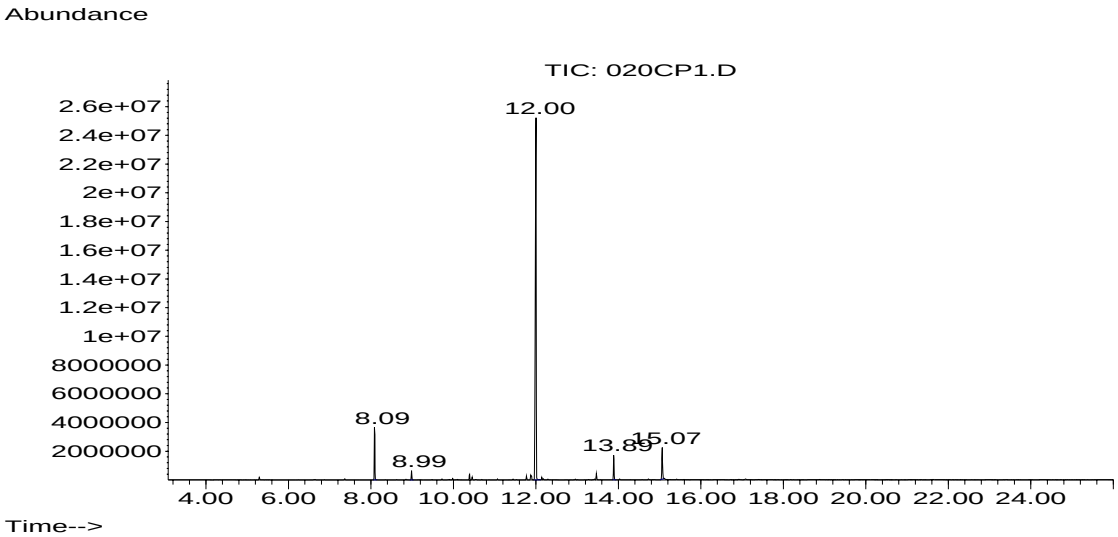

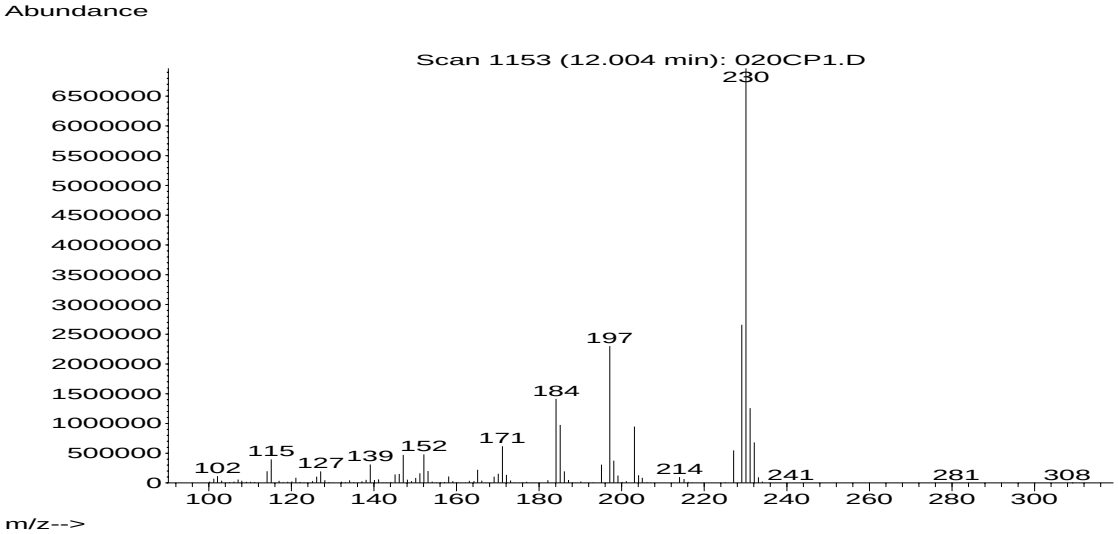

Signal : 020CP1.D\FID1A.CH

peak #	R.T. min	Start min	End min	PK TY	peak height	corr. area	corr. % max.	% of total
1	2.380	2.342	2.458	BV	7561952	126292662	18.66%	9.016%
2	2.487	2.458	2.523	VV	12731073	172746915	25.53%	12.332%
3	2.547	2.523	2.594	VV	14770658	233210870	34.46%	16.649%
4	2.626	2.594	2.738	VB	54058324	676681843	100.00%	48.308%
5	2.779	2.749	2.854	BB	9925101	120039346	17.74%	8.570%
6	8.142	8.109	8.172	BB	780574	7853236	1.16%	0.561%
7	12.050	11.990	12.082	BB	4481889	63927917	9.45%	4.564%

Sum of corrected areas: 1400752789

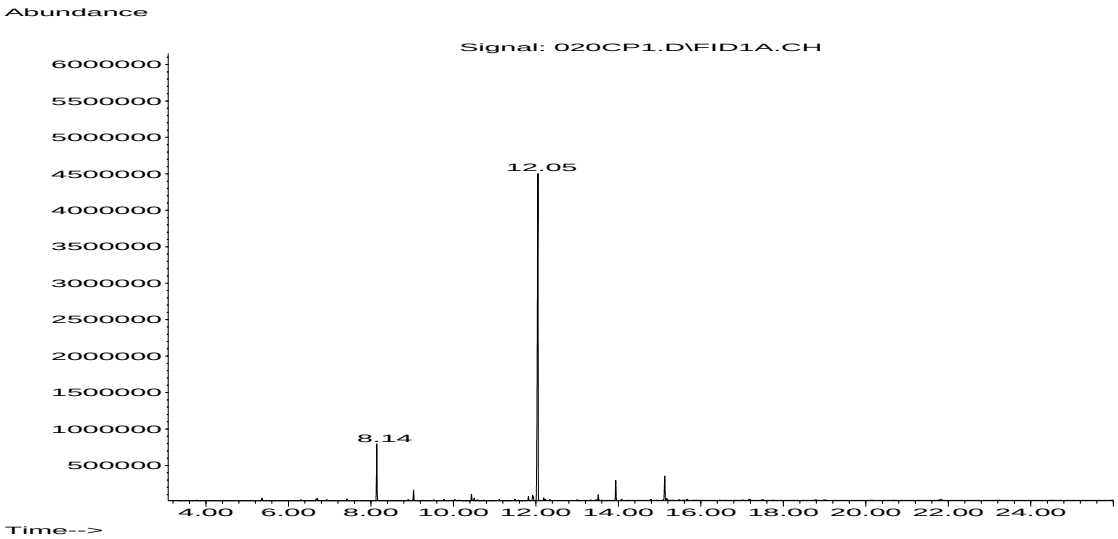

MSHIGH.M Wed Jun 29 18:45:16 2005 CHEMSTATION

3-(2-bromothiophen-3-yl)-2-methylbenzo[b]thiophene (**64**).
(ID 001-022)

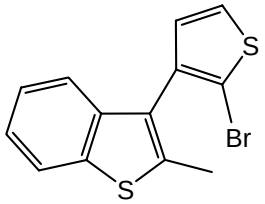

In a flask containing 4.39 g (19.1 mmol) 2-methyl-3-(thiophen-3-yl)benzo[b]thiophene () dissolved in a 1:1 solution containing dichloromethane and glacial acetic acid was added 3.4 g (19.1 mmol) *N*- bromosuccinimide. The reaction mixture was stirred for 2 h, then the reaction mixture was poured into an equal volume of water. Organics were extracted with dichloromethane. The organics were washed with a saturated solution containing sodium bicarbonate, water, then dried over magnesium sulphate. The organics were filtered then solvents removed from the filtrate in vacuo. In this fashion, 5.16 g were collected (dark brown oil) which was then filtered through silica (100 g) using hexane. Solvents were removed in vacuo. Yield: 2.43 g recovered (GC FID:94%). EIMS, m/z (%): 313 (1), 312 (9)‘, 311 (16), 310 (100), 309 (19), 308 (95), 232 (1), 231 (7), 230 (14), 229 (77), 228 (32), 227 (42), 195 (11), 185 (50), 184 (47). ^{1}H-NMR δ ($CDCl_3$): 7.69 (m, 1H), 7.27 (m, 2H), 7.19 (m, 2H), 6.85 (d, 1H), 2.36 (s, 3H).

Figure 54. ^{1}H-NMR of 3-(2-bromothiophen-3-yl)-2-methylbenzo[b]thiophene (**64**).

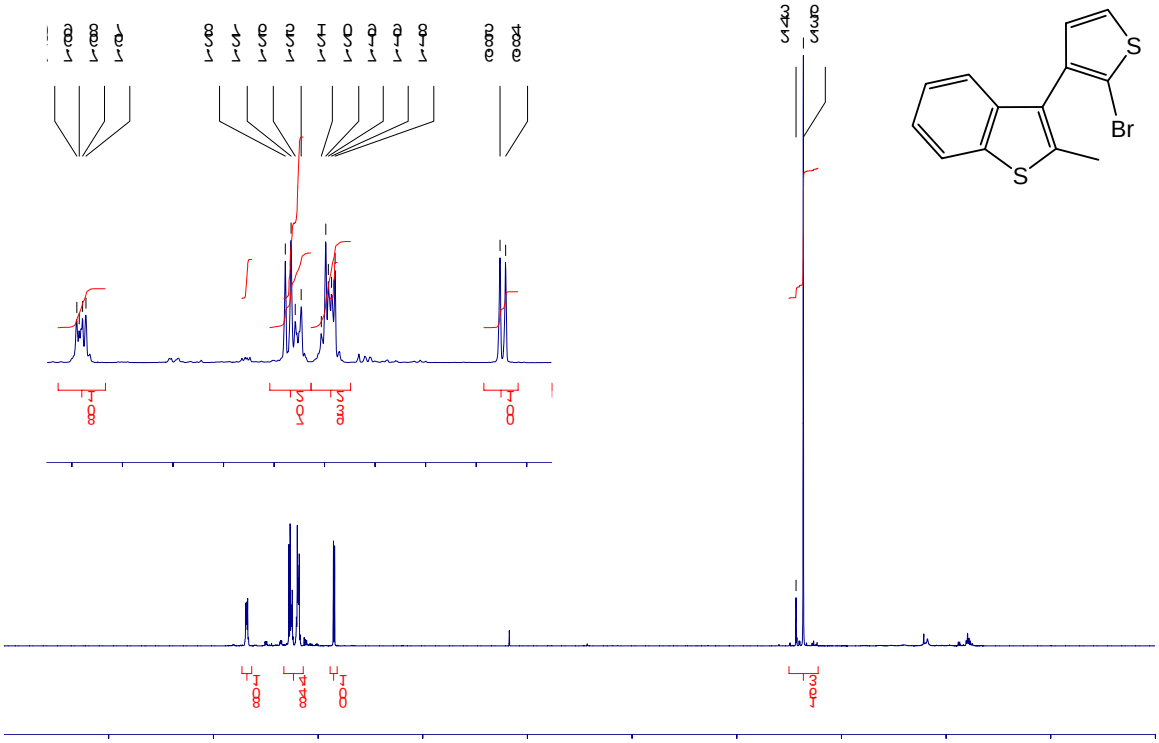

2,3-di(2-methyl-benzo[b]thiophen-3-yl)thiophene (**65**).

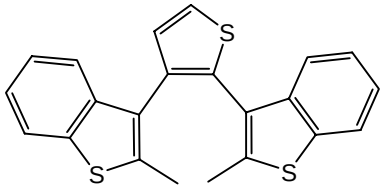

In a flask containing 7.2 g (31.7 mmol) 3-bromo-2-methylbenzo-[b]thiophene (**3**) dissolved in 100 mL diethyl ether at -10°C (ice/acetone) was added a solution containing n-butyllithium (13 mL, 32.5 mmol, 2.5M in hexane). The reaction mixture was stirred for 1 h, then the contents of the flask were transferred to a 2nd flask containing 8.17 g (31.7 mmol) magnesium bromide etherate slurried in 50 mL diethyl ether at -78°C. The flask contents were allowed to warm to -10°C, and stirred an additional 90 m (the reaction mixture became a colourless solution). The solution was then transferred via cannula to a flask containing 9.81 g (32 mmol) 3-(2-bromothiophen-3-yl)-2-methylbenzo[b]thiophene (**7**), 0.87 g (1.6 mmol) 1,3-bis(diphenylphosphino)-propane nickel(II) chloride slurried in 100 mL diethyl. After addition was completed stirring continued for 7 days. The contents were poured into water, organics collected with 20% dichloromethane/hexane solution, dried over magnesium sulphate, filtered, then evaporated to a dark brown oil. In this manner 13.25 g were recovered then purified (twice) over silica gel (HPLC): 240 mg of the targeted product were recovered (87% by FID-GC). EIMS, m/z (%): 379 (4), 378 (16), 377 (26), 376 (100), 349 (13), 348 (23), 347 (79), 346 (41), 328 (5), 327 (14), 326 (19), 325 (2), 315 (9), 314 (26).

Figure 55 FID-GC and GCMS analytical results for 2,3-di(2-methyl-benzo[b]thiophen -3-yl)thiophene (**65**).

```
Data Path : D:\MSDCHEM\1\DATA\Jones\100DISS\030\
Data File : 030BF5RAW.D
Acq On    : 11 Apr 2005  15:02 (#1); 11.04.2005 03:02:46 PM (#2)
Operator  : JONES
Sample    : 030BF5RAW
Misc      : 2,3-(2MeBzTp)2Tp   2nd sepn. frac 5 raw (Sig #1);  (Sig #2)
ALS Vial  : 1   Sample Multiplier: 1

Integration Parameters: autoint1.e
Integrator: ChemStation   6890 Scale Mode: Large solvent peaks clipped
Smoothing : OFF                Filtering: 5
Sampling  : 1                  Min Area: 5 % of largest Peak
Start Thrs: 0.2                Max Peaks: 100
Stop Thrs : 0                  Peak Location: TOP

If leading or trailing edge < 100 prefer < Baseline drop else tangent >
Peak separation: 5

Method    : D:\MSDCHEM\1\METHODS\MSHIGH.M
```

Signal : TIC

peak #	R.T. min	first scan	max scan	last scan	PK TY	peak height	corr. area	corr. % max.	% of total
1	13.088	1288	1293	1305	BB	1410488	20371998	10.71%	9.673%
2	15.395	1578	1591	1614	BB	8171110	190231772	100.00%	90.327%

Sum of corrected areas: 210603769

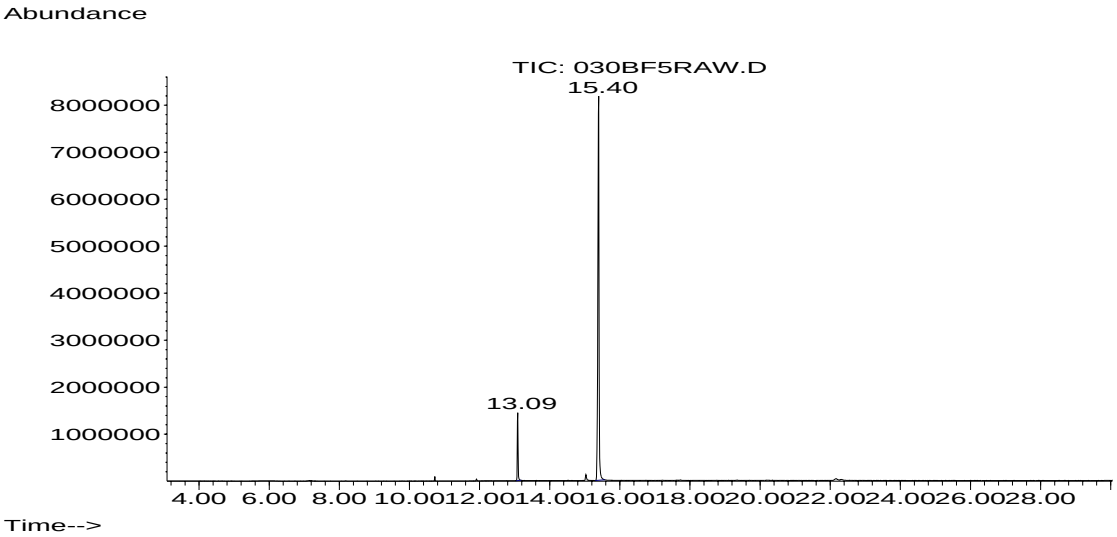

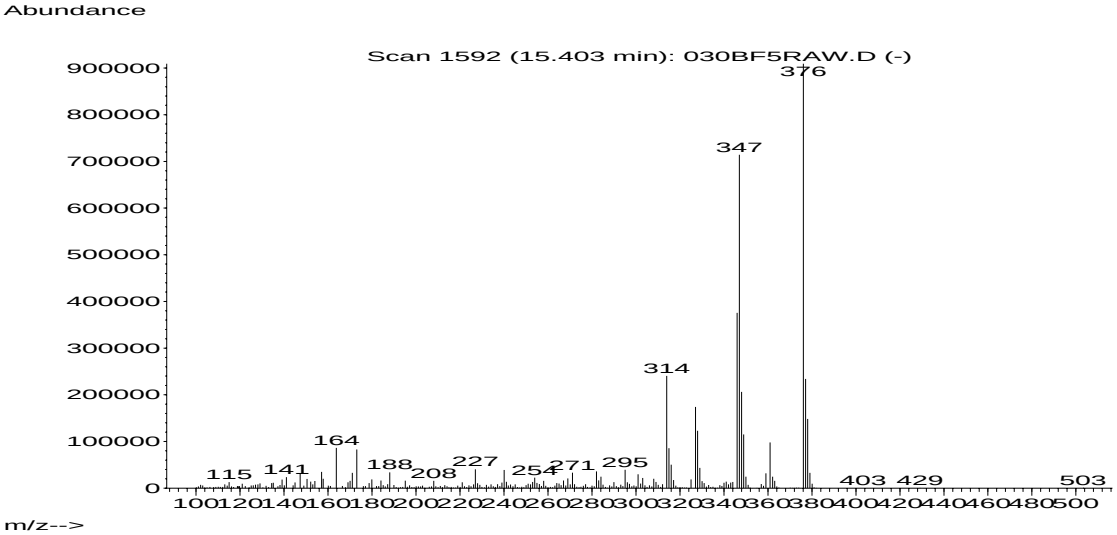

Signal : 030BF5RAW.D\FID1A.CH

peak #	R.T. min	Start min	End min	PK TY	peak height	corr. area	corr. % max.	% of total
1	13.150	13.111	13.188	BB	246629	3142233	15.11%	13.130%
2	15.502	15.419	15.559	BB	877721	20790030	100.00%	86.870%

Sum of corrected areas: 23932263

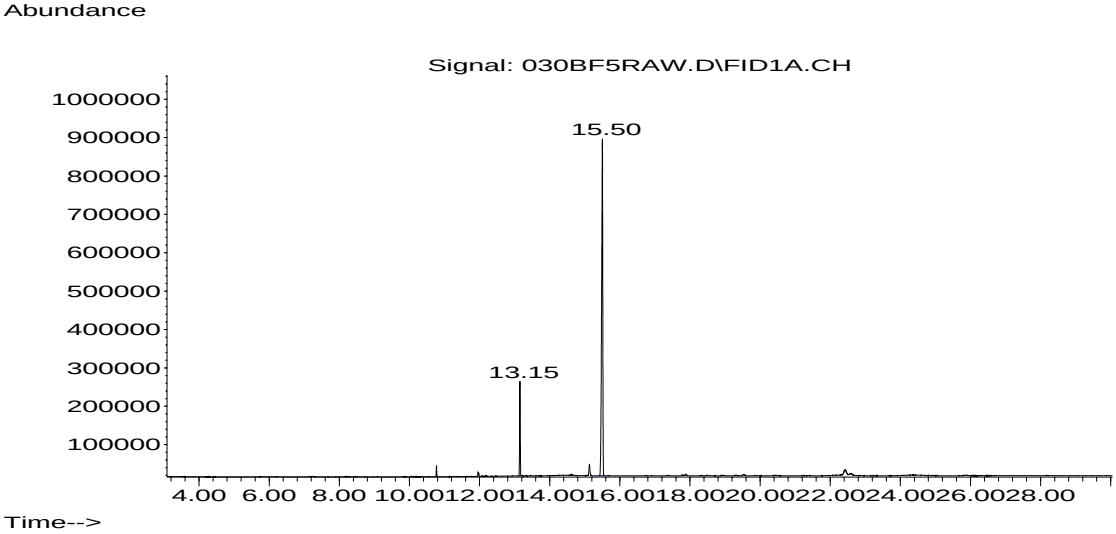

MSHIGH.M Wed Jun 29 19:53:28 2005 CHEMSTATION

Figure 56. ^{1}H-NMR of 2,3-di(2-methyl-benzo[b]thiophen-3-yl)thiophene (**65**).

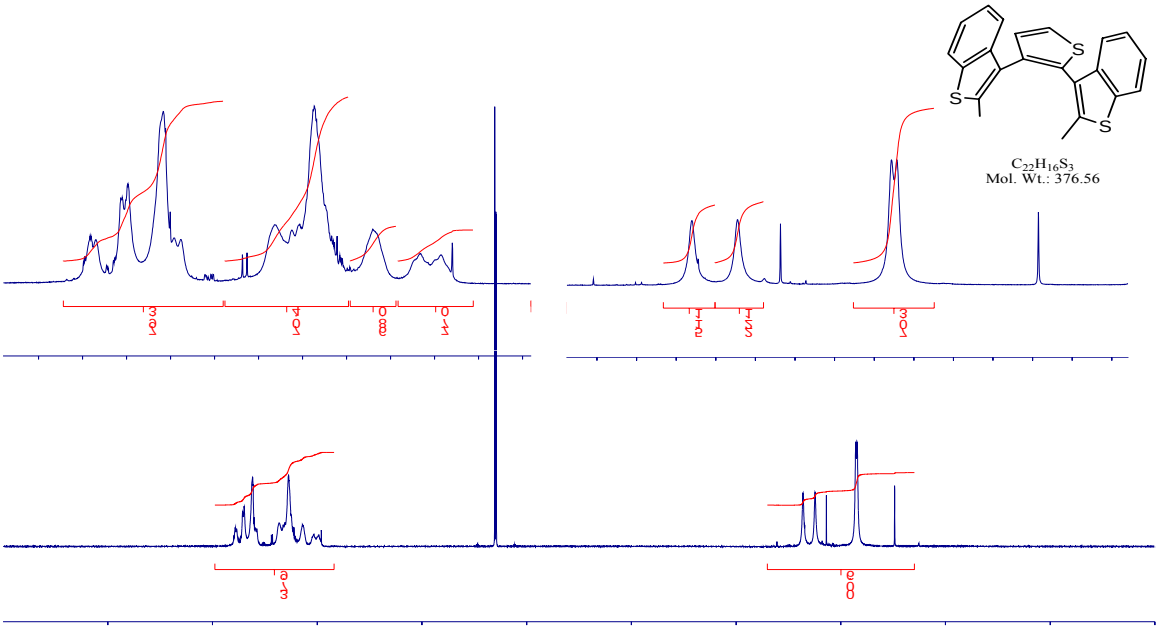

note: this spectra was taken from the same flask containing crystals that were selected for x-ray characterization.

Figure 57. UV/Vis absorption spectra of 2,3-di(2-methyl-benzo[b]thiophen-3-yl) thiophene (**65**) in benzene, 5.3x10^{-2}M (0.053 mmol/ml), without (-) and with (-) UV irradiation.

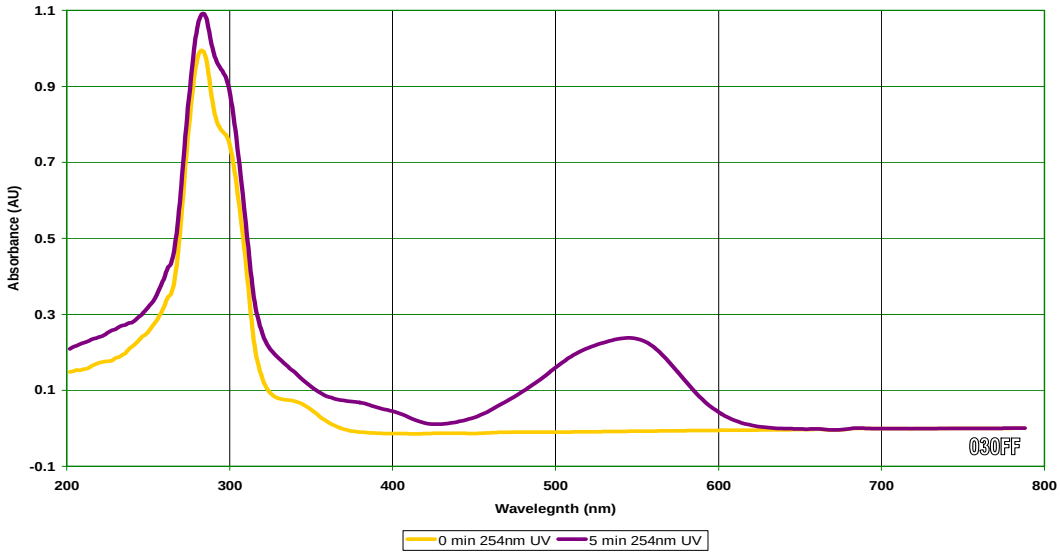

:

Figure 58. Structure of (**65**) from crystallographic analysis:

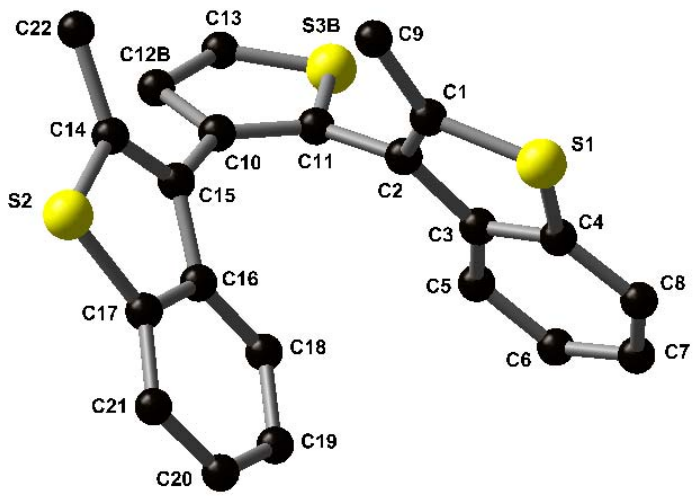

Table 12. Crystal data and structure refinement for (**65**):

Identification code	ex_lj3
Empirical formula	$C_{22}H_{16}S^{3}$
Formula weight	376.53
Temperature	100(2) K
Wavelength	0.71073 Å
Crystal system	Orthorhombic
Space group	$P\,2_1\,2_1\,2_1$
Unit cell dimensions	a = 8.7657(5) Å α = 90°
	b = 11.7411(6) Å β = 90°
	c = 17.2059(9) Å γ = 90°
Volume	1770.81(16) Å^3
Z	4
Density (calculated)	1.412 Mg/m^3
Absorption coefficient	0.420 mm^{-1}
F_{000}	784
Crystal size	0.17 x 0.15 x 0.15 mm^3

ϑrange for data collection	2.10 to 32.01°
Index ranges	-13 <= *h* <= 13, 0 <= *k* <= 17, 0 <= *l* <= 25
Reflections collected	30971
Independent reflections	6092 [R_{int} = 0.0517]
Completeness to ϑ = 32.01°	99.8 %
Absorption correction	Semi-empirical from equivalents
Max. and min. transmission	0.9397 and 0.9301
Refinement method	Full-matrix least-squares on F^2
Data / restraints / parameters	6092 / 4 / 247
Goodness-of-fit on F^2	1.065
Final *R* indices [$I>2\sigma(I)$]	*R* = 0.0404, *wR*2 = 0.0922
R indices (all data)	*R* = 0.0482, *wR*2 = 0.0954
Absolute structure parameter	-0.08(6)
Largest diff. peak and hole	0.510 and -0.227 e/Å^3

Table 13. Atomic coordinates (x 10^4) and equivalent isotropic displacement parameters (Å^{2}x 10^3) for (**65**): U_{eq} is defined as one third of the trace of the orthogonalized U^{ij} tensor.)

	x	*y*	*z*	U_{eq}
C(1)	4589(2)	4478(1)	1426(1)	16(1)
C(2)	3624(2)	5039(1)	1918(1)	15(1)
C(3)	3280(2)	6185(1)	1657(1)	15(1)
C(4)	4031(2)	6455(1)	959(1)	16(1)
C(5)	2304(2)	6994(1)	1996(1)	18(1)
C(6)	2130(2)	8046(2)	1640(1)	21(1)
C(7)	2918(2)	8312(2)	956(1)	23(1)
C(8)	3875(2)	7527(2)	609(1)	20(1)
C(9)	5266(2)	3317(1)	1527(1)	22(1)
C(10)	2239(2)	3582(1)	2759(1)	16(1)
C(11)	3072(2)	4570(1)	2657(1)	16(1)
C(13)	2799(2)	4331(2)	4033(1)	39(1)
C(14)	1763(2)	1683(1)	2139(1)	16(1)
C(15)	1571(2)	2840(1)	2155(1)	16(1)
C(16)	599(2)	3238(1)	1532(1)	16(1)
C(17)	44(2)	2332(1)	1073(1)	16(1)
C(18)	173(2)	4354(1)	1340(1)	18(1)
C(19)	-746(2)	4534(2)	697(1)	22(1)
C(20)	-1290(2)	3628(2)	246(1)	24(1)
C(21)	-920(2)	2520(2)	438(1)	21(1)
C(22)	2777(2)	963(2)	2629(1)	23(1)
S(1)	5116(1)	5311(1)	631(1)	18(1)
S(2)	714(1)	1031(1)	1405(1)	18(1)
S(3A)	1919(4)	3289(3)	3715(2)	19(1)
C(12A)	3449(18)	5052(12)	3446(7)	23(3)
S(3B)	3571(5)	5209(4)	3504(2)	19(1)
C(12B)	2040(20)	3425(13)	3605(7)	35(4)

Table 14. Bond lengths [Å] and angles [°] for (**65**).

C(1)-C(2)	1.365(2)	C(16)-C(18)	1.403(2)
C(1)-C(9)	1.497(2)	C(16)-C(17)	1.411(2)
C(1)-S(1)	1.7439(17)	C(17)-C(21)	1.399(2)
C(2)-C(3)	1.450(2)	C(17)-S(2)	1.7338(16)
C(2)-C(11)	1.468(2)	C(18)-C(19)	1.384(2)
C(3)-C(5)	1.405(2)	C(18)-H(18)	0.9500
C(3)-C(4)	1.406(2)	C(19)-C(20)	1.399(3)
C(4)-C(8)	1.402(2)	C(19)-H(19)	0.9500
C(4)-S(1)	1.7404(17)	C(20)-C(21)	1.381(3)
C(5)-C(6)	1.386(2)	C(20)-H(20)	0.9500
C(5)-H(5)	0.9500	C(21)-H(21)	0.9500
C(6)-C(7)	1.401(3)	C(22)-H(22A)	0.9800
C(6)-H(6)	0.9500	C(22)-H(22B)	0.9800
C(7)-C(8)	1.381(3)	C(22)-H(22C)	0.9800
C(7)-H(7)	0.9500	C(12A)-H(12A)	0.9500
C(8)-H(8)	0.9500	C(12B)-H(12B)	0.9500
C(9)-H(9A)	0.9800	C(2)-C(1)-C(9)	127.77(15)
C(9)-H(9B)	0.9800	C(2)-C(1)-S(1)	112.36(12)
C(9)-H(9C)	0.9800	C(9)-C(1)-S(1)	119.77(13)
C(10)-C(11)	1.382(2)	C(1)-C(2)-C(3)	112.58(14)
C(10)-C(12B)	1.477(13)	C(1)-C(2)-C(11)	124.08(15)
C(10)-C(15)	1.477(2)	C(3)-C(2)-C(11)	123.22(15)
C(10)-S(3A)	1.703(4)	C(5)-C(3)-C(4)	119.14(15)
C(11)-C(12A)	1.507(13)	C(5)-C(3)-C(2)	128.70(15)
C(11)-S(3B)	1.696(4)	C(4)-C(3)-C(2)	112.13(14)
C(13)-C(12A)	1.434(13)	C(8)-C(4)-C(3)	121.59(15)
C(13)-C(12B)	1.457(14)	C(8)-C(4)-S(1)	127.39(13)
C(13)-S(3B)	1.532(4)	C(3)-C(4)-S(1)	111.02(12)
C(13)-S(3A)	1.546(4)	C(6)-C(5)-C(3)	119.10(16)
C(13)-H(13)	0.9500	C(6)-C(5)-H(5)	120.4
C(14)-C(15)	1.369(2)	C(3)-C(5)-H(5)	120.4
C(14)-C(22)	1.489(2)	C(5)-C(6)-C(7)	121.02(17)
C(14)-S(2)	1.7394(17)	C(5)-C(6)-H(6)	119.5
C(15)-C(16)	1.446(2)	C(7)-C(6)-H(6)	119.5

C(8)-C(7)-C(6)	120.93(16)	C(22)-C(14)-S(2)	118.49(12)
C(8)-C(7)-H(7)	119.5	C(14)-C(15)-C(16)	112.19(15)
C(6)-C(7)-H(7)	119.5	C(14)-C(15)-C(10)	123.41(15)
C(7)-C(8)-C(4)	118.18(16)	C(16)-C(15)-C(10)	124.36(14)
C(7)-C(8)-H(8)	120.9	C(18)-C(16)-C(17)	118.69(15)
C(4)-C(8)-H(8)	120.9	C(18)-C(16)-C(15)	129.30(15)
C(1)-C(9)-H(9A)	109.5	C(17)-C(16)-C(15)	112.01(14)
C(1)-C(9)-H(9B)	109.5	C(21)-C(17)-C(16)	121.79(15)
H(9A)-C(9)-H(9B)	109.5	C(21)-C(17)-S(2)	126.95(13)
C(1)-C(9)-H(9C)	109.5	C(16)-C(17)-S(2)	111.26(12)
H(9A)-C(9)-H(9C)	109.5	C(19)-C(18)-C(16)	119.06(15)
H(9B)-C(9)-H(9C)	109.5	C(19)-C(18)-H(18)	120.5
C(11)-C(10)-C(12B)	107.1(6)	C(16)-C(18)-H(18)	120.5
C(11)-C(10)-C(15)	127.95(15)	C(18)-C(19)-C(20)	121.69(16)
C(12B)-C(10)-C(15)	124.9(6)	C(18)-C(19)-H(19)	119.2
C(11)-C(10)-S(3A)	112.27(16)	C(20)-C(19)-H(19)	119.2
C(12B)-C(10)-S(3A)	5.2(7)	C(21)-C(20)-C(19)	120.23(16)
C(15)-C(10)-S(3A)	119.69(15)	C(21)-C(20)-H(20)	119.9
C(10)-C(11)-C(2)	126.78(15)	C(19)-C(20)-H(20)	119.9
C(10)-C(11)-C(12A)	108.5(5)	C(20)-C(21)-C(17)	118.49(16)
C(2)-C(11)-C(12A)	124.6(5)	C(20)-C(21)-H(21)	120.8
C(10)-C(11)-S(3B)	113.50(17)	C(17)-C(21)-H(21)	120.8
C(2)-C(11)-S(3B)	119.56(17)	C(14)-C(22)-H(22A)	109.5
C(12A)-C(11)-S(3B)	5.0(6)	C(14)-C(22)-H(22B)	109.5
C(12A)-C(13)-C(12B)	104.9(9)	H(22A)-C(22)-H(22B)	109.5
C(12A)-C(13)-S(3B)	8.3(7)	C(14)-C(22)-H(22C)	109.5
C(12B)-C(13)-S(3B)	113.2(5)	H(22A)-C(22)-H(22C)	109.5
C(12A)-C(13)-S(3A)	114.6(6)	H(22B)-C(22)-H(22C)	109.5
C(12B)-C(13)-S(3A)	9.7(6)	C(4)-S(1)-C(1)	91.91(8)
S(3B)-C(13)-S(3A)	122.9(2)	C(17)-S(2)-C(14)	91.73(8)
C(12A)-C(13)-H(13)	122.7	C(13)-S(3A)-C(10)	95.7(2)
C(12B)-C(13)-H(13)	132.4	C(13)-C(12A)-C(11)	109.0(10)
S(3B)-C(13)-H(13)	114.4	C(13)-C(12A)-H(12A)	125.5
S(3A)-C(13)-H(13)	122.7	C(11)-C(12A)-H(12A)	125.5
C(15)-C(14)-C(22)	128.70(16)	C(13)-S(3B)-C(11)	95.6(3)
C(15)-C(14)-S(2)	112.74(13)	C(13)-C(12B)-C(10)	110.6(9)

C(13)-C(12B)-H(12B)	124.7
C(10)-C(12B)-H(12B)	124.7

Symmetry transformations used to generate equivalent atoms:

Table 15. Anisotropic displacement parameters (Å^2 x 10^3) for (**65**).

The anisotropic displacement factor exponent takes the form: $-2\pi^2[\, h^2\, a^{*2} U^{11} + ... + 2\, h\, k\, a^*\, b^*\, U^{12}\,]$

	U^{11}	U^{22}	U^{33}	U^{23}	U^{13}	U^{12}
C(1)	18(1)	17(1)	14(1)	2(1)	-2(1)	0(1)
C(2)	16(1)	15(1)	14(1)	1(1)	-2(1)	-1(1)
C(3)	15(1)	15(1)	15(1)	0(1)	-2(1)	-2(1)
C(4)	18(1)	17(1)	15(1)	-1(1)	-2(1)	-1(1)
C(5)	18(1)	17(1)	20(1)	0(1)	0(1)	-1(1)
C(6)	22(1)	16(1)	26(1)	-2(1)	0(1)	2(1)
C(7)	30(1)	15(1)	24(1)	3(1)	-3(1)	0(1)
C(8)	26(1)	18(1)	16(1)	3(1)	-2(1)	-2(1)
C(9)	29(1)	18(1)	20(1)	1(1)	1(1)	6(1)
C(10)	14(1)	19(1)	14(1)	2(1)	-1(1)	1(1)
C(11)	17(1)	16(1)	14(1)	1(1)	0(1)	2(1)
C(13)	29(1)	73(2)	15(1)	-3(1)	-2(1)	21(1)
C(14)	15(1)	17(1)	16(1)	3(1)	0(1)	0(1)
C(15)	14(1)	18(1)	15(1)	2(1)	1(1)	-1(1)
C(16)	14(1)	18(1)	16(1)	2(1)	1(1)	0(1)
C(17)	16(1)	17(1)	15(1)	1(1)	2(1)	1(1)
C(18)	18(1)	15(1)	20(1)	1(1)	0(1)	1(1)
C(19)	23(1)	21(1)	24(1)	6(1)	-2(1)	2(1)
C(20)	22(1)	30(1)	18(1)	4(1)	-5(1)	3(1)
C(21)	21(1)	26(1)	15(1)	-2(1)	-1(1)	0(1)
C(22)	22(1)	20(1)	27(1)	6(1)	-4(1)	-1(1)
S(1)	22(1)	19(1)	14(1)	1(1)	2(1)	2(1)
S(2)	18(1)	15(1)	19(1)	-1(1)	0(1)	1(1)
S(3A)	20(1)	22(1)	15(1)	4(1)	-1(1)	-2(1)
C(12A)	18(3)	15(4)	37(5)	-10(2)	6(3)	-4(2)
S(3B)	22(1)	18(1)	16(1)	2(1)	0(1)	-2(1)
C(12B)	27(4)	31(5)	47(8)	14(4)	-3(4)	-10(3)

Table 16. Hydrogen coordinates (x 10^4) and isotropic displacement parameters (Å^{2}x 10^3) for (**65**).

	x	*y*	*z*	U_{eq}
H(5)	1772	6823	2462	22
H(6)	1466	8594	1865	26
H(7)	2792	9042	727	27
H(8)	4413	7709	146	24
H(9A)	5148	3075	2069	34
H(9B)	6352	3340	1393	34
H(9C)	4740	2777	1186	34
H(13)	2901	4482	4572	47
H(18)	511	4979	1646	21
H(19)	-1014	5291	558	27
H(20)	-1916	3777	-193	28
H(21)	-1312	1900	145	25
H(22A)	3483	1451	2920	34
H(22B)	3360	444	2297	34
H(22C)	2158	520	2995	34
H(12A)	4023	5724	3540	28
H(12B)	1483	2818	3837	42

4,5-dihydro-5-methylcyclopenta[b]thiophen-6-one (**74**).
(ID: BSC-999-1-0001)

This material was purchased from Boulder Scientific and was synthesized according to previously reported methods (see reference 22).

Figure 59. ^{1}H-NMR of 4,5-dihydro-5-methylcyclopenta[b]thiophen-6-one (**74**).

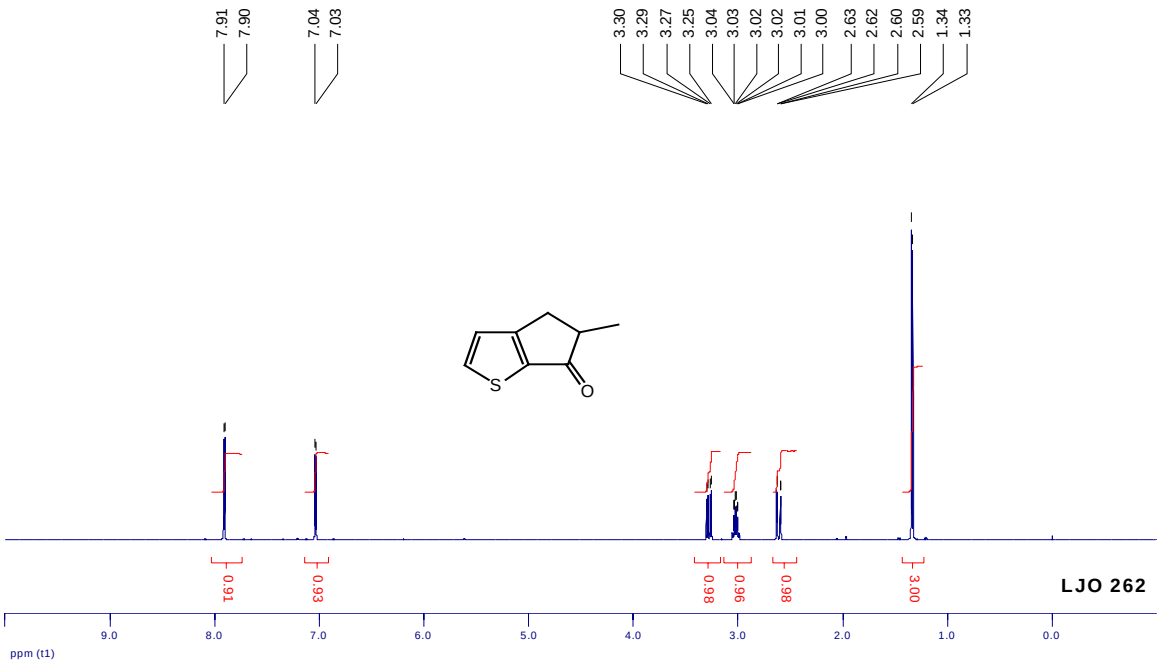

^{1}H-NMR δ ($CDCl_3$): 7.9 (d, 1H), 7.0 (d, 1H), 3.2 – 3.3 (m, 1H), 3.0 (m, 1H), 2.6 (m, 1H), 1.3 (s, 3H).

2,3-dibromo-4,5-dihydro-5-methylcyclopenta[b]thiophen-6-one (**75**).
(ID: 001-052P1):

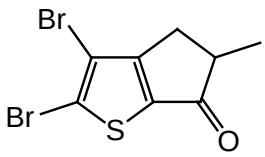

$C_8H_6Br_2OS$
Mol. Wt.: 310.01

In a flask containing 20.5 g (250 mmol) sodium acetate, 50 ml water, and 15.2 g (100 mmol) 5-methyl-6H-cyclopenta[b]thiophen-6-one was added 35.7 (225 mmol) bromine (dropwise). After addition was completed, the reaction mixture was stirred for 30 min, sampled (GCMS indicated only one bromine was "on"): an additional 15 g (94 mmol) of bromine was added (dropwise). The reaction mixture was stirred an additional 1 h, then poured into water. Organics were extracted with dichloromethane, washed with a saturated solution of sodium bicarbonate until pH neutral, then water. The organics were dried over magnesium sulphate, filtered, then solvents were removed in vacuo. 29.31 g dark purple free flowing solid was collected (95% by GCMS). The material was used in subsequent steps without further purification. ^{1}H-NMR δ ($CDCl_3$): 3.2 (m, 1H), 2.98 (m, 1H), 2.57 (m, 1H), 1.3 (t, 3H). EIMS: *m/e* (%) = 312.9 (3), 311.9 (32), 310.9 (10.0), 309.9 (62), 308.9 (11.0), 307.9 (31) 306.9 (4), 296.9 (51), 295.5 (9), 294.9 (100), 292.9 (51).

Table 17. GCMS analysis of 2,3-dibromo-4,5-dihydro-5-methylcyclopenta[b]thiophen-6-one (**75**).

Area Percent Report

```
Data Path : D:\MSDCHEM\1\DATA\Jones\100Diss 50-100\052\
Data File : 052P1DIL.D
Acq On    : 26 Apr 2005  13:37 (#1); 26.04.2005 01:37:31 PM (#2)
Operator  : JONES
Sample    : 052P1dil
Misc      : 2,3-Br2-5-MeTp=O @ P1 (29.31 g) diluted (Sig #1);  (Sig #2)
ALS Vial  : 1   Sample Multiplier: 1

Integration Parameters: autoint1.e
Integrator: ChemStation   6890 Scale Mode: Large solvent peaks clipped
Smoothing : OFF                    Filtering: 5
Sampling  : 1                      Min Area: 5 % of largest Peak
Start Thrs: 0.2                    Max Peaks: 100
Stop Thrs : 0                      Peak Location: TOP

If leading or trailing edge < 100 prefer < Baseline drop else tangent >
Peak separation: 5
```

Method : D:\MSDCHEM\1\METHODS\MSHIGH.M
Title : install

Signal : TIC

peak #	R.T. min	first scan	max scan	last scan	PK TY	peak height	corr. area	corr. % max.	% of total
---	-----	-----	----	----	---	-------	-------	------	-------
1	8.001	631	636	643	BB	1419314	16092673	5.00%	4.761%
2	9.217	781	793	806	BB	17982752	321923800	100.00%	95.239%

Sum of corrected areas: 338016474

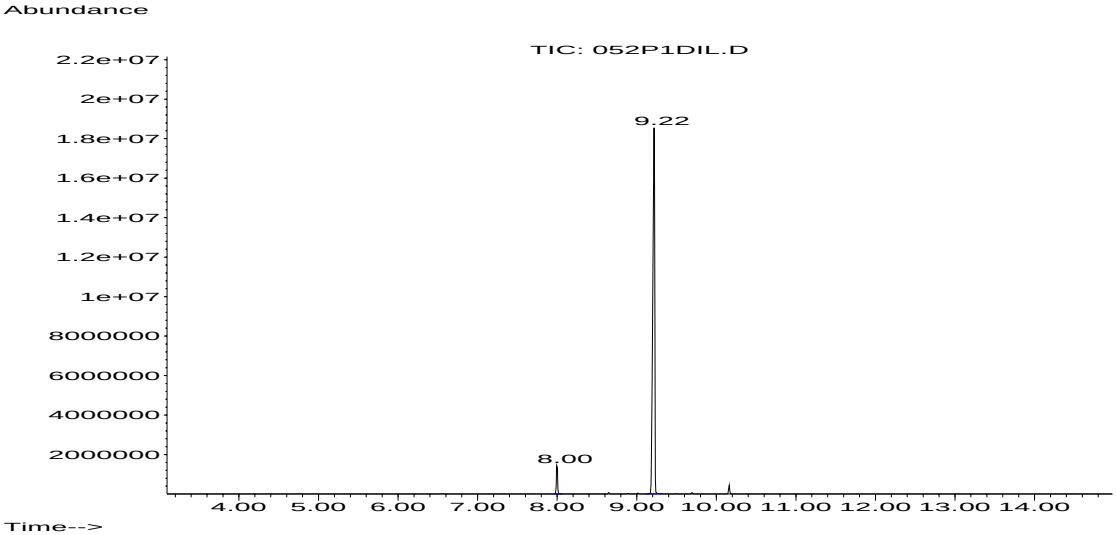

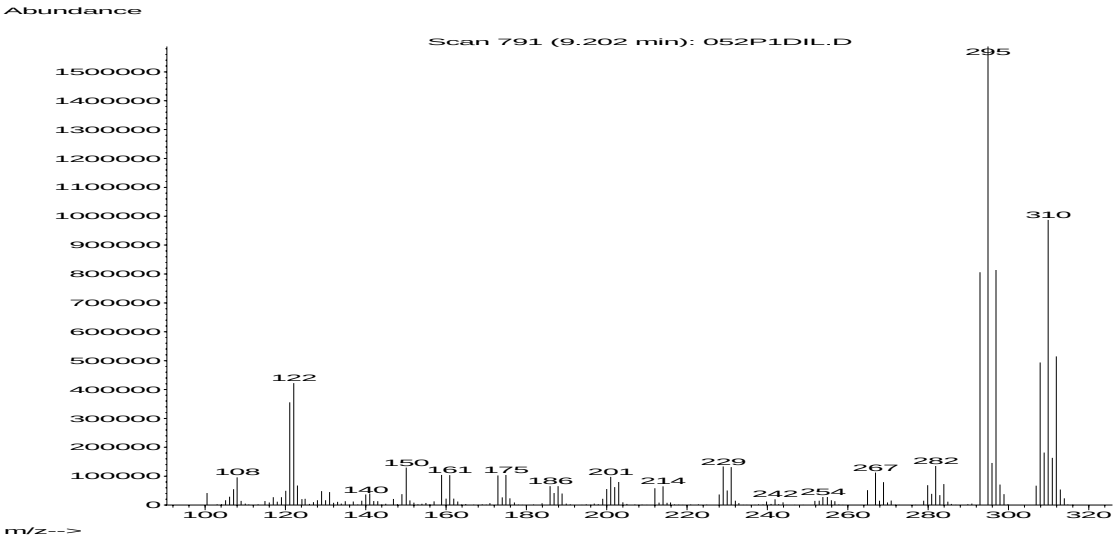

Signal : 052P1DIL.D\FID1A.CH

peak #	R.T. min	Start min	End min	PK TY	peak height	corr. area%	corr. max.	% of total
---	-----	-----	-----	---	-------	-------	------	------
1	8.046	8.013	8.078	BB	341481	3439965	8.12%	7.509%
2	9.267	9.202	9.307	BB	2698892	42373127	100.00%	92.491%

Sum of corrected areas: 45813092

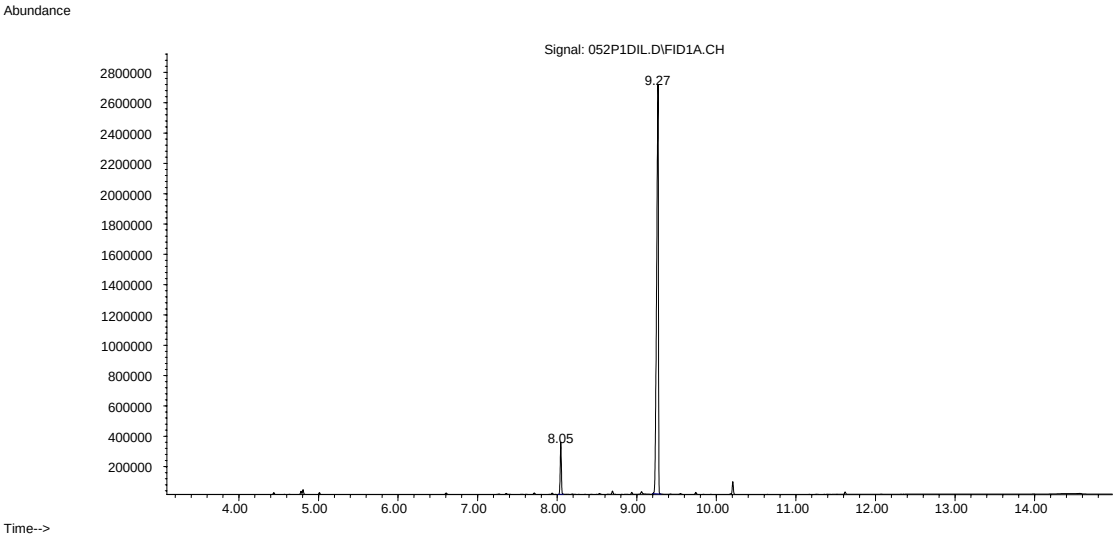

Figure 60. ^{1}H-NMR of 4,5-dihydro-5-methylcyclopenta[b]thiophen-6-one (**75**).

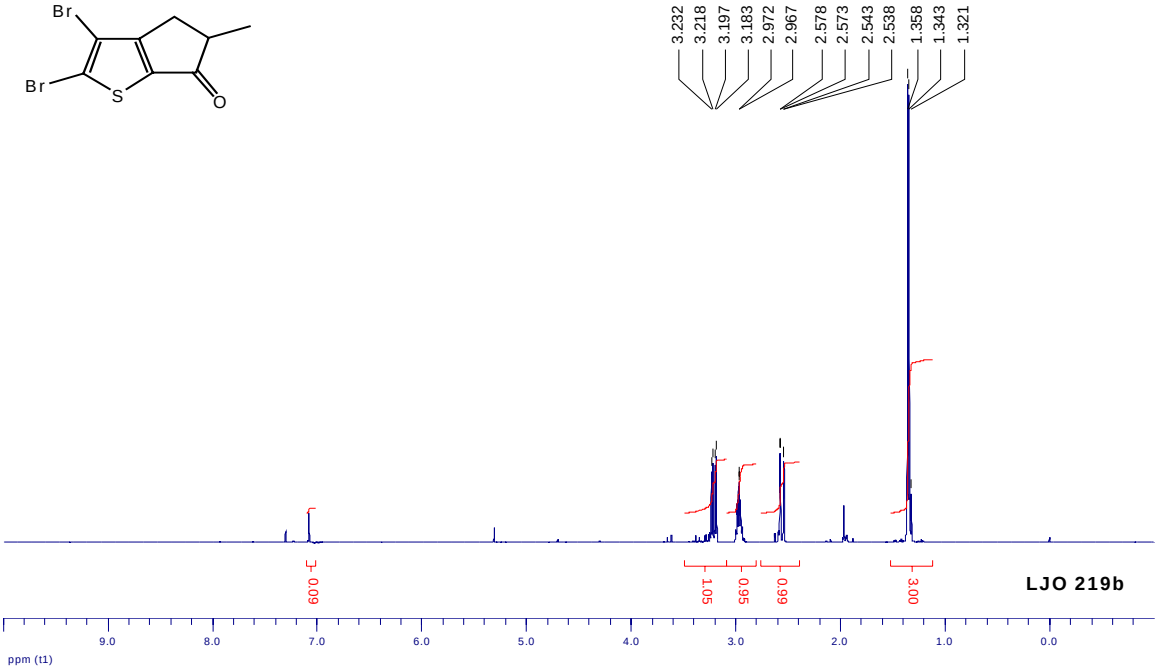

2,3-di(benzo[b]thiophen-3-yl)-5-methyl-6H-cyclopenta[b]thiophen-6-one (**77**).
ID: (001-092P1):

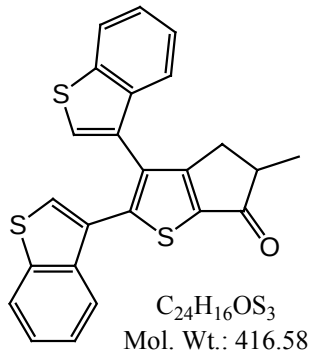

In a flask containing 1.7 g (5.78 mmol) 2,3-dibromo-5-methyl-6H-cyclopenta[b]-thiophen-6-one (**75**) dissolved in a degassed solution containing 70 ml dimethoxyethane/water (9:1) was added 5 g (28 mmol) thianaptahalene-3 boronic acid (**76**): (Aldrich), and 2.35 g (22.4 mmol) sodium carbonate. The flask atmosphere replaced with nitrogen (further degassing the reaction mixture), then under positive nitrogen flow, 0.7 g (0.6 mmol) tetrakis-(triphenylphosphine)palladium (Strem, 99.9%) was added. The reaction mixture was refluxed for 2 h and then cooled. The reaction mixture was then poured into a 1N HCl solution, washed with water, saturated bicarbonate solution, then water. The reaction mix was dried over magnesium sulphate, filtered through silica using 1) hexane, then 2) 50:50 dichloromethane/ hexane (to collect the product). Solvents removed in vacuo: 2.03 g (92.8% by GCMS) the product was used in subsequent reactions without further purification.

Scale-up synthesis of (**77**).

In a 250 ml flask with side arm and Teflon stirring bar was placed 9.3 g (30 mmol) 2,3-dibromocyclopenta[b]thiophen-6-one (**75**) dissolved in degassed 70 ml 10% water in ethyleneglycol-dimethylether solution. 25 g (140 mmol) thianapthalene-3-boronic acid (**76**) (Aldrich) was added followed by 11.7 g (110 mmol) sodium carbonate. 2.0 g (2 mmol) $Pd(PPh_3)_4$ (Strem) was added, (an additional 30 ml of the DME solution was used to wash in the components); the contents of the flask were then refluxed for 3 h. The mixture was cooled, poured into an iced 1N HCl solution, then the organics were collected with 50:50 dichloromethane/hexane solution. The organics were washed with water, dried over magnesium sulphate, filtered, then solvents removed in vacuo. Solids were then washed with hexane, and then dried. 15.8 g pale yellow powder was recovered, 91% product by FIDGC/GCMS. EIMS, m/z (%): 418 (17), 417 (29), 416 (100), 410 (11), 375 (2), 374 (3), 373 (9), 372 (2), 346 (10), 340 (16), 327 (11); ^{1}H-NMR δ ($CDHCl_3$) (isomers): 7.8 (m, 2H), 7.15 - 7.55 (m, 8H), 3.5 (2d, 1H), 3.2 (m, 1H), 3.05 (m, 1H), 2.6 (m, 1H), 1.3 (2s, 3H).

Gas Chromatographic analysis of reaction product for (**77**).

Area Percent Report

Data Path : D:\MSDCHEM\1\DATA\Jones\100Diss 50-100\092\
Data File : 092P1.D
Acq On : 9 Jun 2005 8:04 (#1); 09.06.2005 08:04:19 AM (#2)
Operator : JONES
Sample: 092P1
Misc: 3BOH2BzTp+2,3Br2Tp6=O Pd at P1 (2.03 g) (Sig #1); (Sig #2)
ALS Vial: 1 Sample Multiplier: 1

Integration Parameters: autoint1.e
Integrator: ChemStation 6890 Scale Mode: Large solvent peaks clipped
Smoothing : OFF Filtering: 5
Sampling : 1 Min Area: 5 % of largest Peak
Start Thrs: 0.2 Max Peaks: 100
Stop Thrs : 0 Peak Location: TOP

If leading or trailing edge < 100 prefer < Baseline drop else tangent >
Peak separation: 5

Method : D:\MSDCHEM\1\METHODS\MSHIGH.M
Title : install

Signal : TIC

Peak #	R.T min	First scan	Max scan	Last scan	PK TY	Peak height	Corr. area	Corr. % max.	% of total
1	8.303	664	675	695	BV	355475	15891039	3.68%	3.415%
2	10.866	1002	1006	1016	BB	1040329	11213849	2.60%	2.410%
3	13.584	1351	1357	1375	BB	313352	6259651	1.45%	1.345%
4	24.686	2735	2791	2881	BB	3907481	431908176	100.00%	92.829%

Sum of corrected areas: 465272715

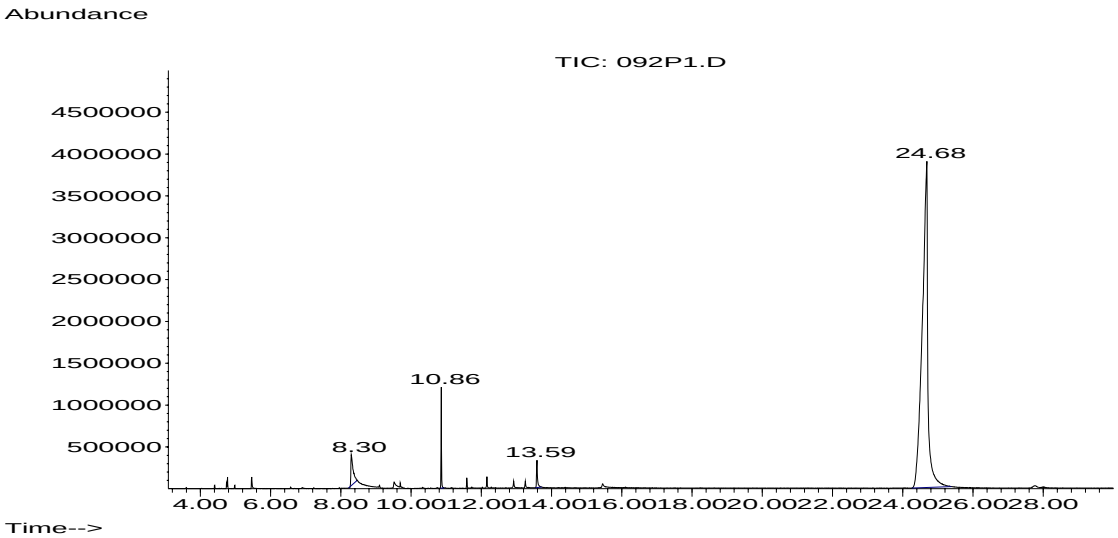

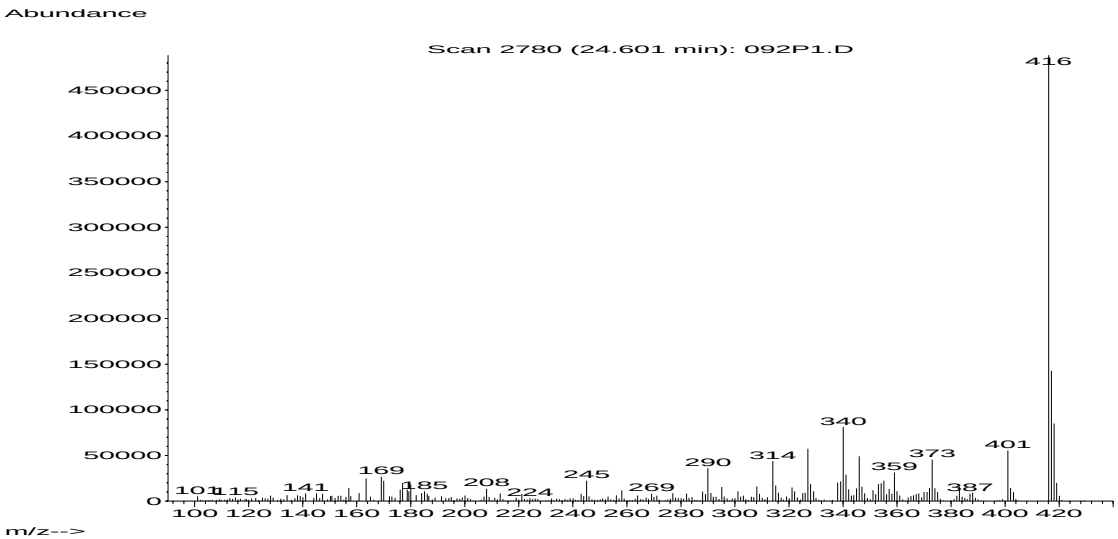

Signal : 092P1.D\FID1A.CH

Peak #	R.T min	Start min	End min	PK TY	Peak height	Corr. area	Corr. % max.	% of total
1	4.832	4.819	4.868	VB	129303	1265286	1.98%	1.822%
2	10.906	10.881	10.941	BB	271083	2559003	4.01%	3.684%
3	13.656	13.606	13.698	BB	122875	1772380	2.78%	2.552%
4	25.015	24.614	25.169	BB	522498	63865995	100.00%	91.943%

Sum of corrected areas: 69462664

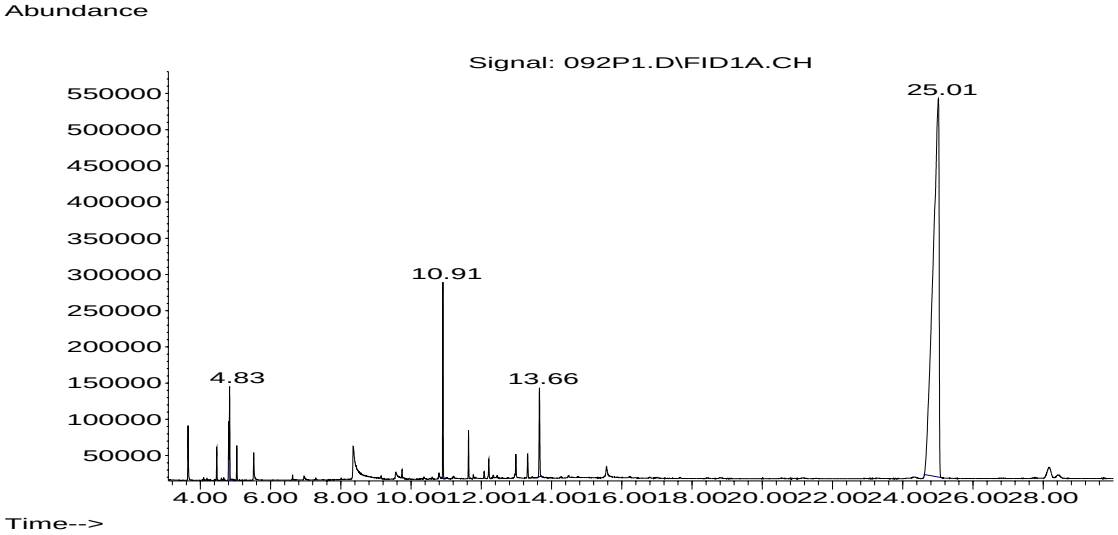

MSHIGH.M Wed Jun 29 13:38:43 2005 CHEMSTATION

Figure 61. ^{1}H-NMR of reaction product (**77**) ($CDHCl_2$):

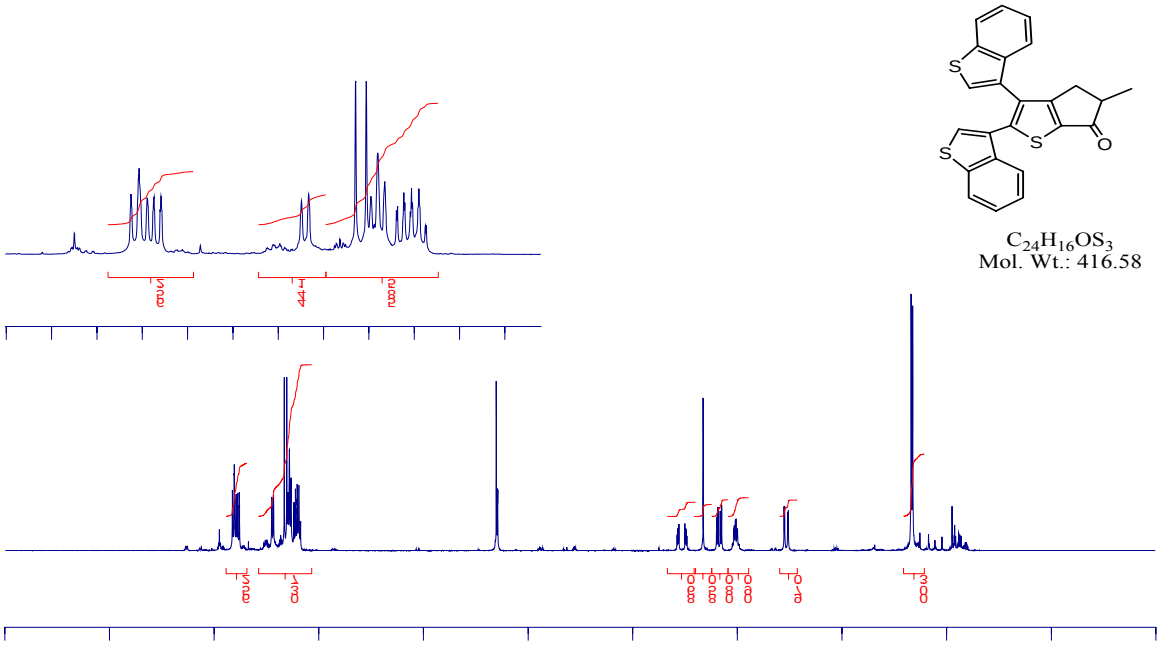

Figure 62. ^{1}H-NMR of reaction product (**77**) (THF-d_8):

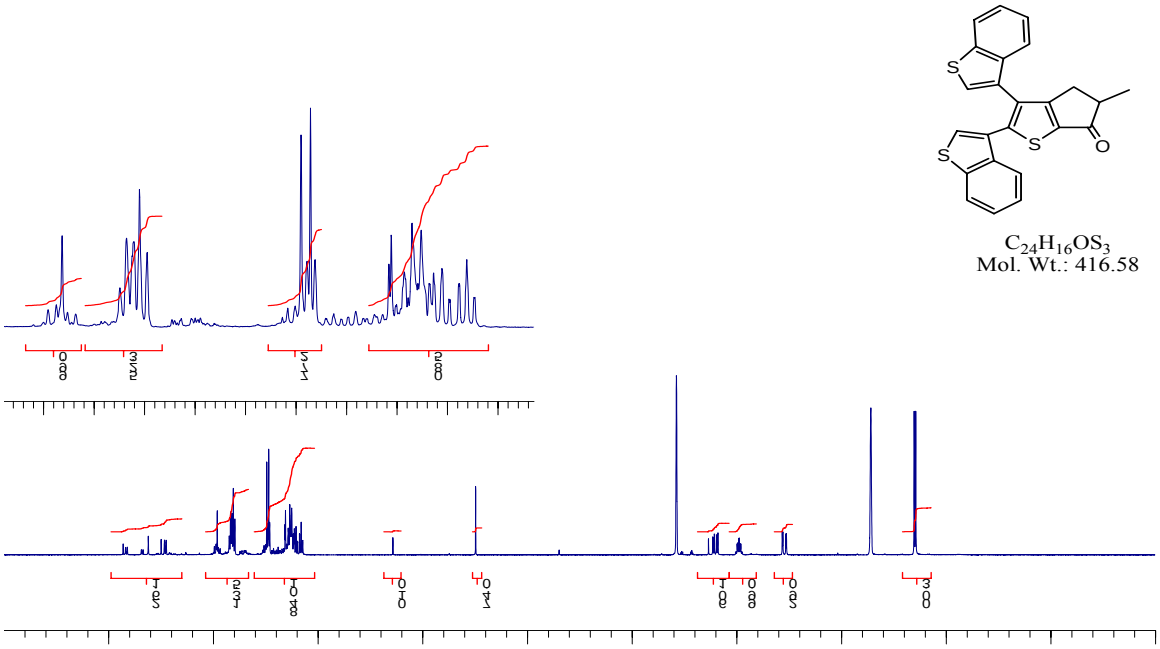

Figure 63. ^{13}C-NMR of open and closed form of ketone (**77**).

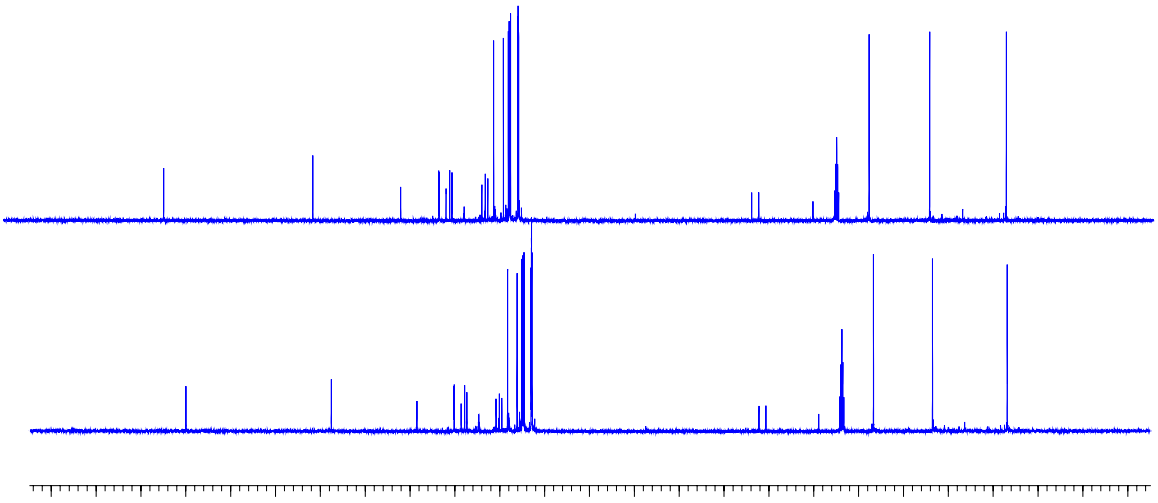

Figure 64. UV/Vis absorption spectra of 2,3-di(benzo[b]thiophen-3-yl)-5-methyl-*6H*-cyclopenta[b]thiophen-6-one (**77**) in benzene (4.8 x 10^{-5}M), without (–) and with (–) UV irradiation.

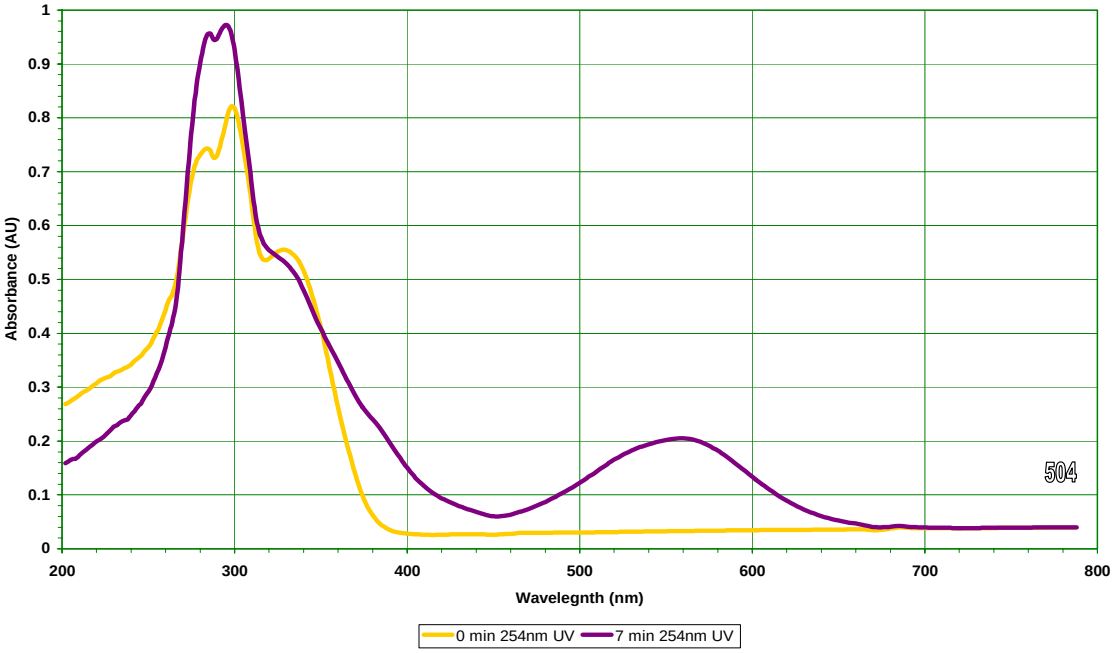

2,3-di(benzo[b]thiophen-3-yl)-5,6-dihydro-5-methyl-4H-cyclopenta[b]-thiophen-6-ol (**78**).
(001-093):

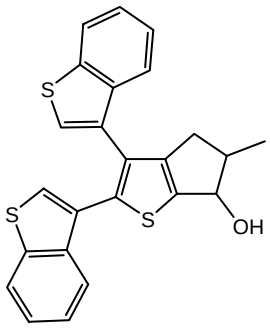

In a flask containing 1.59 g (3.8 mmol) 3-di(benzo[b]thiophen-3-yl)-5-methyl-6H-cyclopenta[b]thiophen-6-one (-092P1) dissolved in 70 ml diethyl ether was added a solution containing lithium aluminium hydride (1.8 mmol, 1.8 ml, 1M in diethyl ether), drop-wise. The reaction mixture was stirred for 1 h at room temperature, then poured onto ice. The organics were collected with diethyl ether, washed with water, dried over magnesium sulphate, then filtered. Solvents were removed in vacuo. 1.18 g light brown powder was recovered. GCMS analysis of this material indicated only olefin, which was possibly dehydrated in the instrument. ^{1}H-NMR δ ($CDHCl_2$): 7.7 (m, 2H), 7.45 (m, 1H), 7.2 (4H), 3.4 (m, 0.5H), 3.0 – 1.9 (7m, 3H), 1.3 (3m, 3H).

Scale-up synthesis:

In a flask containing 8.32 g (20 mmol) 2,3-(3-thianapthalene)cyclopenta[b]thiophen-6-one slurried in 100 ml diethyl ether was added a solution containing lithium aluminium hydride ($LiAlH_4$), (6.6 mmol, 7 ml, 1M solution in diethyl ether). The reaction mixture was stirred for 3 h, then a small amount (15 ml) anhydrous THF was added to help solublize the materials in the flask. The reaction mix was poured into water, washed with 1N HCl, water, dried over magnesium sulphate, filtered, then solvents removed in vacuo. 7.51 g were recovered (grey powder). Note: $CDCl_3$ solution photochromic: see Figure 68.

Figure 65. ^{1}H-NMR of 2,3-di(benzo[b]thiophen-3-yl)-5,6-dihydro-5-methyl-4H-cyclopenta[b]-thiophen-6-ol (**78**).

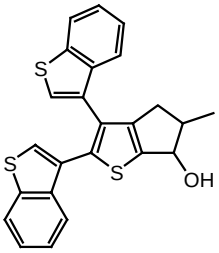

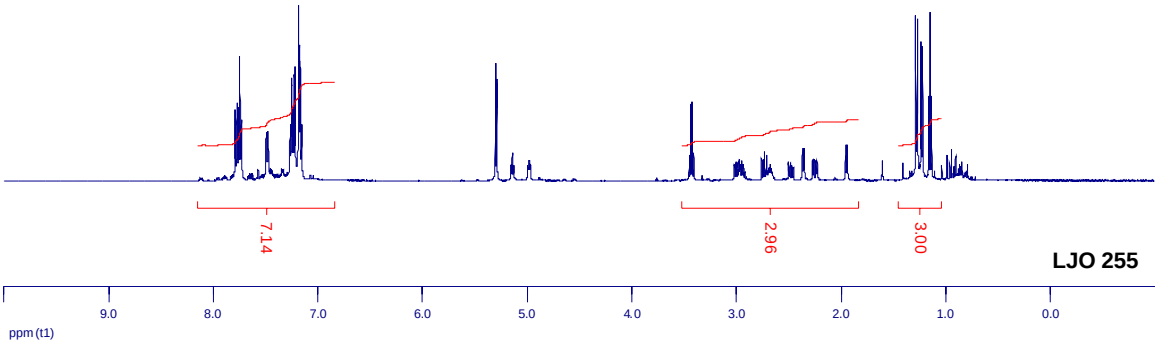

Figure 66. ^{13}C-NMR of 2,3-di(benzo[b]thiophen-3-yl)-5,6-dihydro-5-methyl-4H-cyclopenta[b]-thiophen-6-ol (**78**).

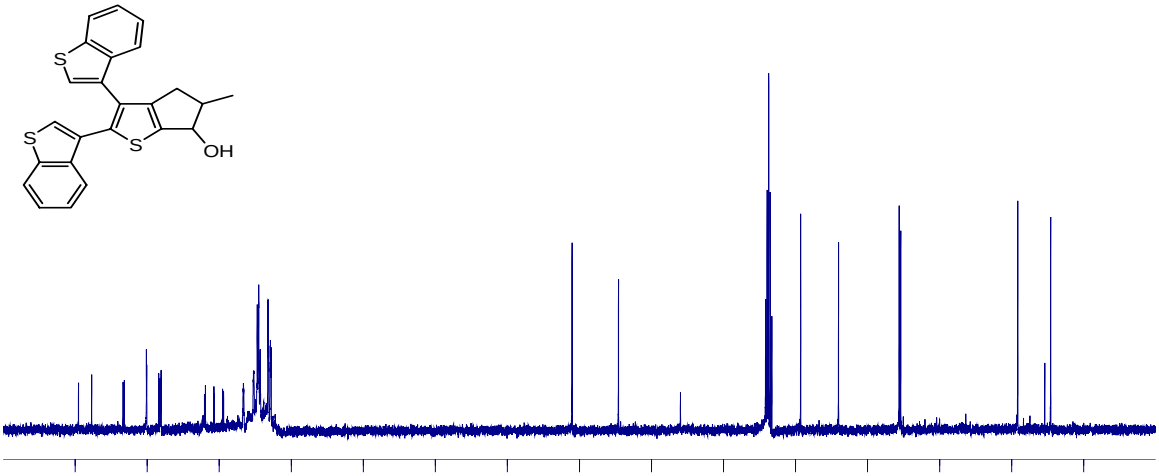

Figure 67. Decoupled ^{13}C-NMR of 2,3-di(benzo[b]thiophen-3-yl)-5,6-dihydro-5-methyl-4H-cyclopenta[b]-thiophen-6-ol (**78**) spectra:

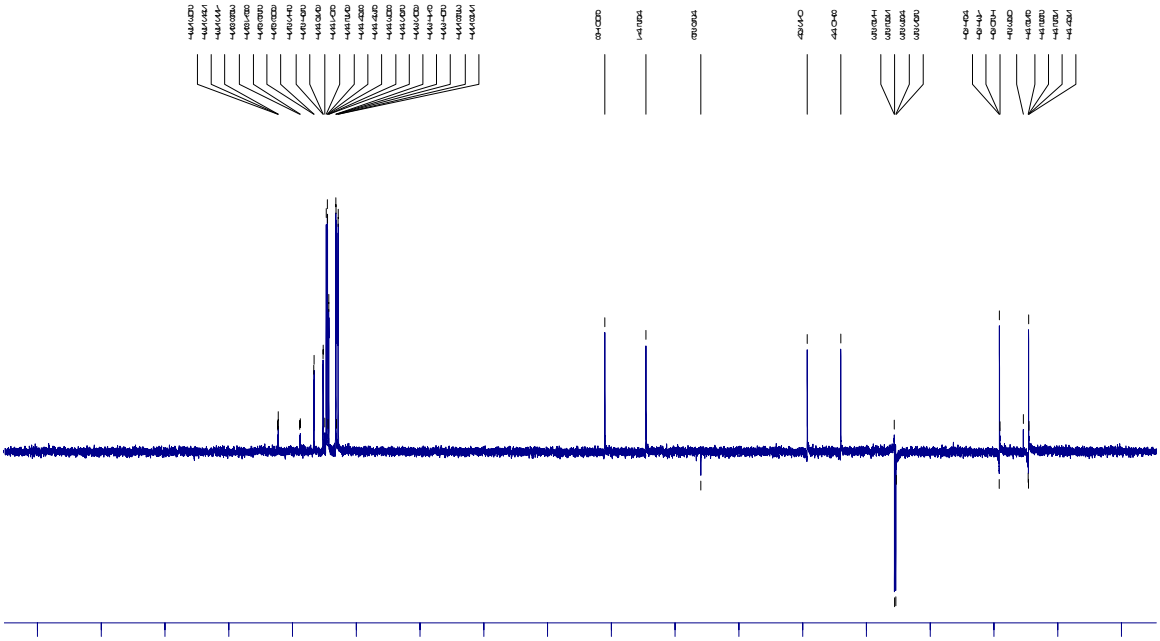

Figure 68. UV/Vis absorbance spectra of 2,3-di(benzo[b]thiophen-3-yl)-5,6-dihydro-5-methyl-4H-cyclopenta[b]-thiophen-6-ol (**78**) in benzene (5 x 10^{-5}M), without (-) and with (-) UV irradiation.

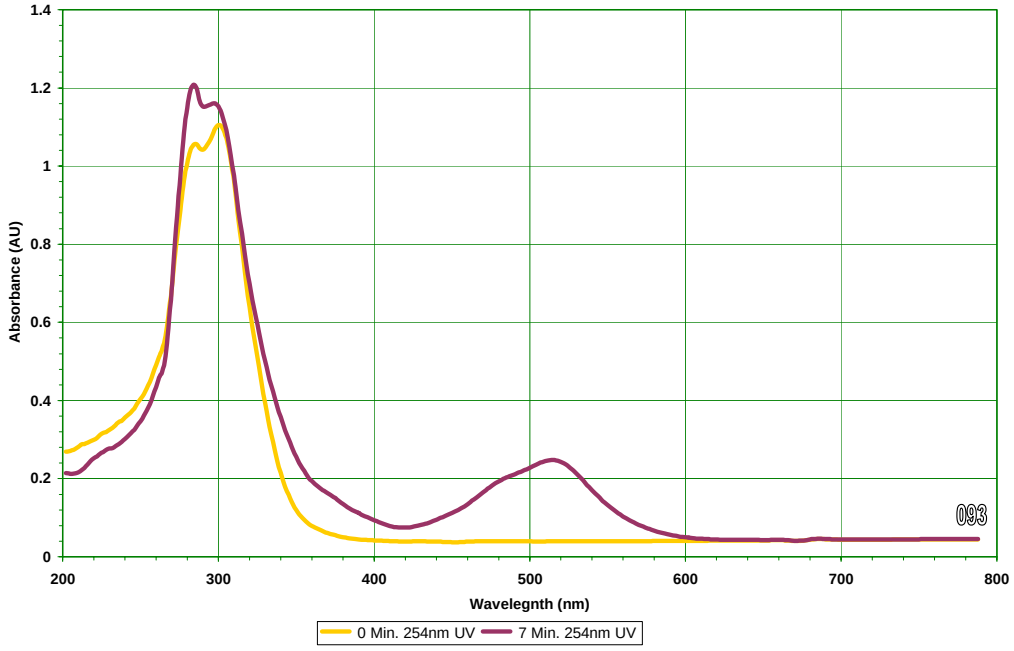

2,3-di(benzo[b]thiophen-3-yl)-5-methyl-4H-cyclopenta[b]thiophene (**79**).

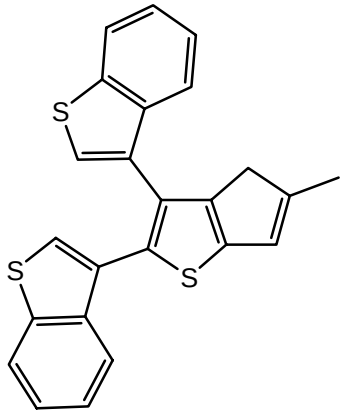

In a flask containing 1.1 g 2,3-di(benzo[b]thiophen-3-yl)-5,6-dihydro-5-methyl-4H-cyclopenta[b]-thiophen-6-ol dissolved in 50 ml toluene was added 0.6 g para-toluenesulfonic acid monohydrate. The mixture was refluxed for 1 h, cooled, and then poured into water. The organics were collected with a 50/50 mixture of dichloromethane/ hexane, washed with water, dried over magnesium sulphate, filtered, then solvents removed in vacuo. 1.18 g light brown powder was recovered which was then recrystallized from hexane. 0.44 g was recovered ; ^{1}H-NMR δ ($CDHCl_2$): 7.9 – 7.7 (m, 2H), 7.44 (d, 1H), 7.4 – 7.1 (m, 5H), 3.56 (m, 0.3H), 3.50 (m, 0.3H), 3.5 (s, 0.3), 3.17 (m, 1H), 3.02 (m, 1H), 2.53 (2d, 1H), 1.33 (2s, 3H).

Figure 69. ^{1}H-NMR of 2,3-di(benzo[b]thiophen-3-yl)-5-methyl-4H-cyclopenta[b]thiophene (**79**).

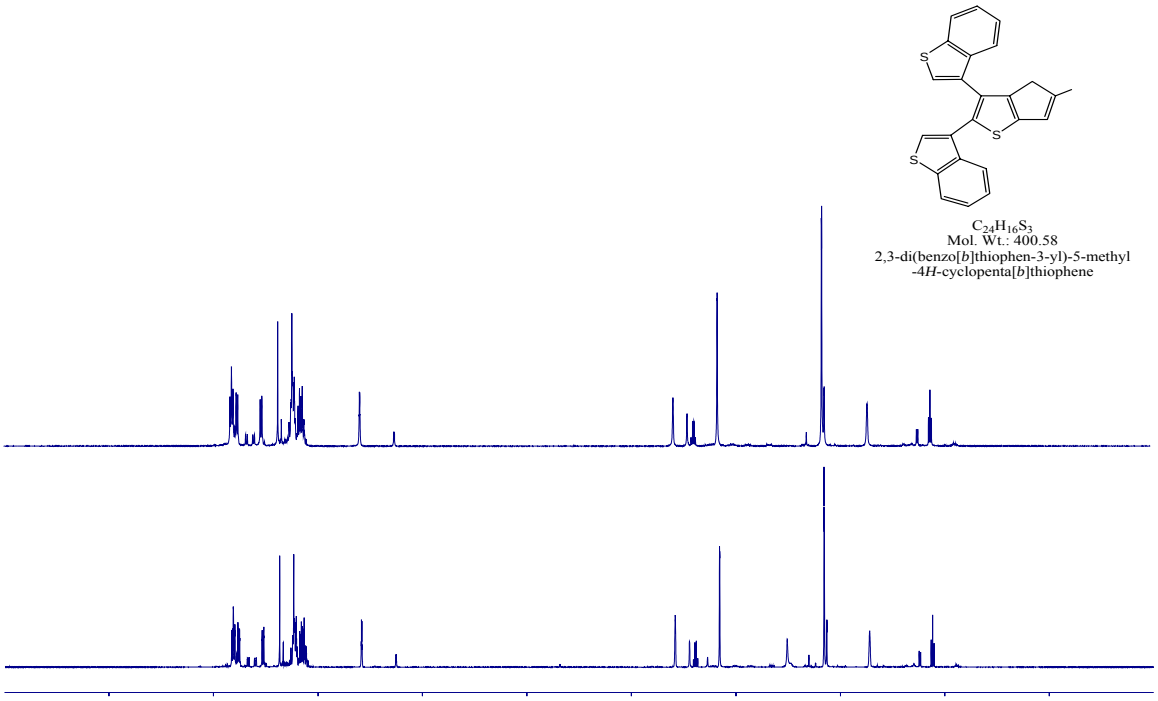

Figure 70. ^{13}C-NMR of 2,3-di(benzo[b]thiophen-3-yl)-5-methyl-4H-cyclopenta[b]-thiophene (**79**): decoupled.

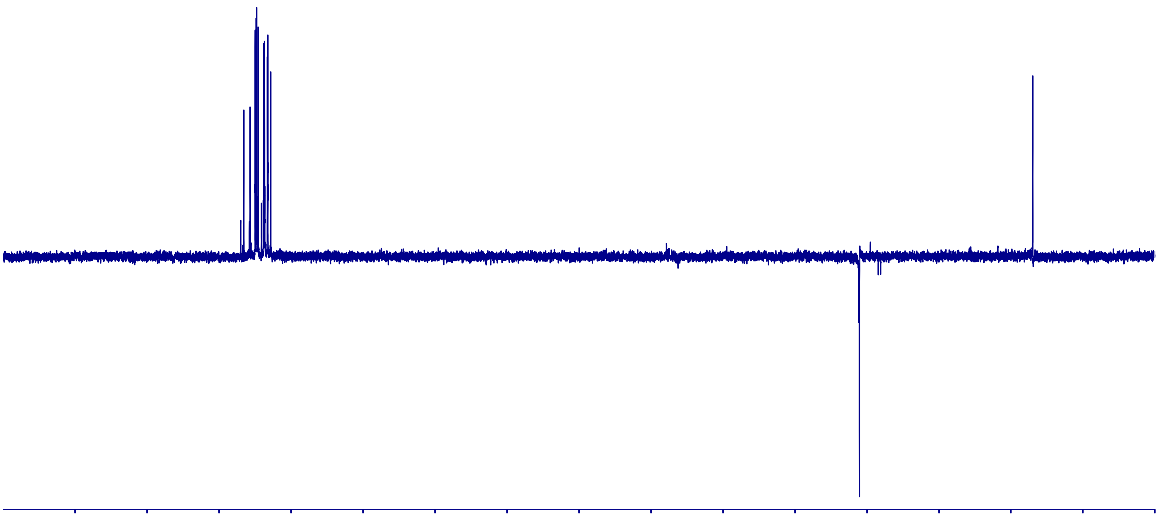

Figure 71. UV/Vis absorbance spectra of 2,3-di(benzo[b]thiophen-3-yl)-5-methyl-4H-cyclopenta[b]thiophene (**79**) in benzene (5 x 10^{-5}M), without (–) and with (–) UV irradiation.

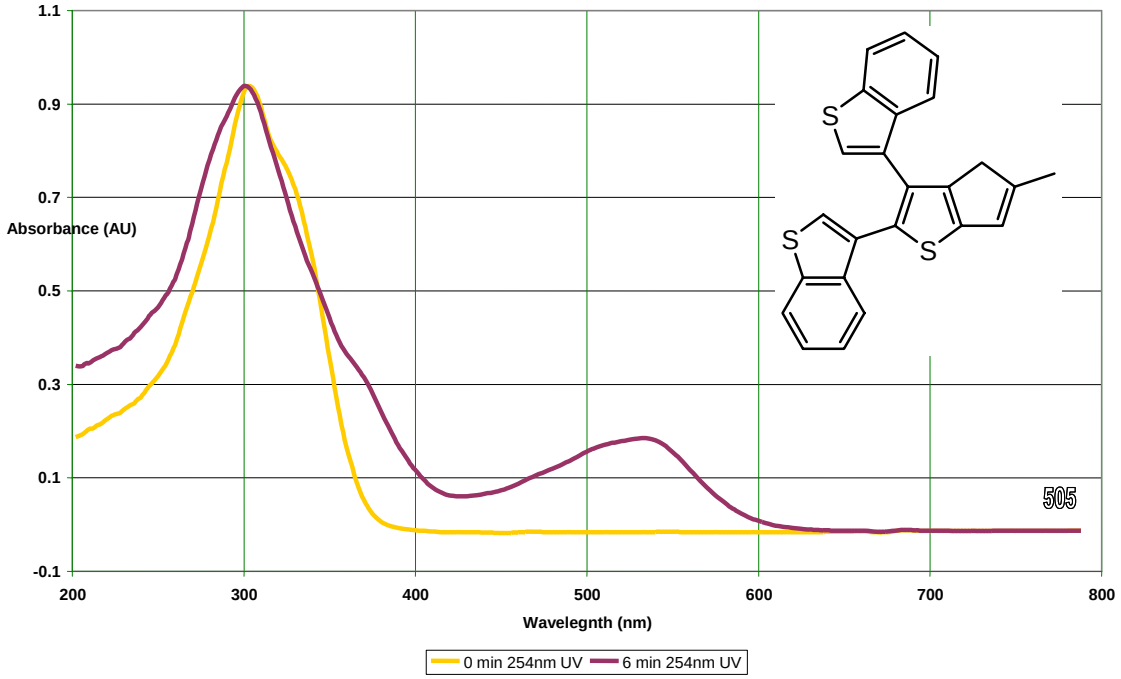

Figure 72. Structure of (**79**) from crystallographic analysis:

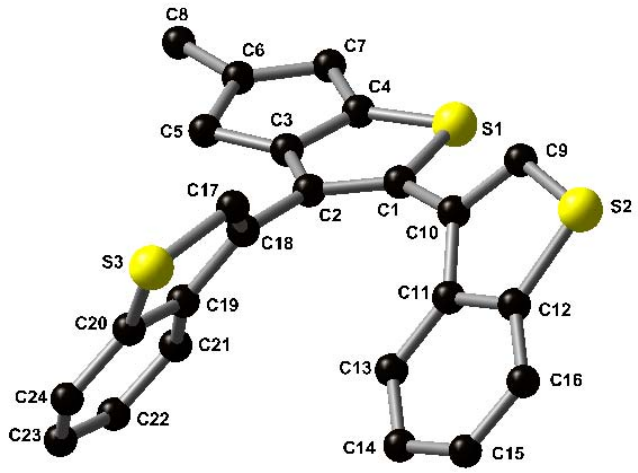

Table 18. Crystal data and structure refinement for (**79**).

Identification code	ex_lj4
Empirical formula	$C_{24}H_{16}S_3$
Formula weight	400.55
Temperature	446(2) K
Wavelength	0.71073 Å
Crystal system	Monoclinic
Space group	$P\,2_1$
Unit cell dimensions	a = 9.1874(7) Å α = 90°
	b = 7.8194(6) Å β = 94.467(2)°
	c = 13.0801(10) Å γ = 90°
Volume	936.82(12) Å^3
Z	2
Density (calculated)	1.420 Mg/m^3
Absorption coefficient	0.402 mm^{-1}
F_{000}	416
Crystal size	0.15 x 0.13 x 0.10 mm^3
ϑrange for data collection	1.56 to 30.51°
Index ranges	-13 <= h <= 13, -11 <= k <= 11, 0 <= l <= 18

Reflections collected	15507
Independent reflections	5461 [R_{int} = 0.0519]
Completeness to ϑ = 30.51°	100.0 %
Absorption correction	Semi-empirical from equivalents
Max. and min. transmission	0.9609 and 0.9422
Refinement method	Full-matrix least-squares on F^2
Data / restraints / parameters	5461 / 1 / 297
Goodness-of-fit on F^2	1.014
Final R indices [$I>2\sigma(I)$]	R = 0.0459, $wR2$ = 0.1016
R indices (all data)	R = 0.0559, $wR2$ = 0.1061
Absolute structure parameter	-0.01(6)
Largest diff. peak and hole	0.525 and -0.293 e/Å^3

Table 19. Atomic coordinates (x 104) and equivalent isotropic displacement parameters (Å2x 103) for (**79**).

U_{eq} is defined as one third of the trace of the orthogonalized U^{ij} tensor.)

	x	*y*	*z*	U_{eq}
S(1)	10672(1)	4989(1)	9370(1)	20(1)
S(2)	14342(1)	4453(1)	7015(1)	23(1)
S(3)	8715(1)	8695(1)	5077(1)	18(1)
C(1)	10707(3)	6069(3)	8211(2)	16(1)
C(2)	9416(2)	6957(3)	7965(2)	15(1)
C(3)	8424(3)	6745(3)	8747(2)	16(1)
C(4)	8953(3)	5707(3)	9538(2)	19(1)
C(5)	6895(3)	7230(4)	8927(2)	21(1)
C(6)	6624(3)	6359(4)	9902(2)	28(1)
C(7)	7841(3)	5451(3)	10267(2)	22(1)
C(8)	5203(3)	6477(4)	10383(2)	36(1)
C(9)	12759(3)	4373(3)	7637(2)	21(1)
C(10)	12032(2)	5891(3)	7660(2)	16(1)
C(11)	12779(2)	7226(3)	7138(2)	16(1)
C(12)	14065(2)	6606(3)	6742(2)	18(1)
C(13)	12429(3)	8954(3)	6993(2)	19(1)
C(14)	13329(3)	9986(4)	6458(2)	22(1)
C(15)	14593(3)	9338(4)	6071(2)	24(1)
C(16)	14979(3)	7655(3)	6212(2)	22(1)
C(17)	9163(2)	7250(3)	6051(2)	16(1)
C(18)	9065(2)	7903(3)	7004(2)	14(1)
C(19)	8606(2)	9668(3)	6969(2)	14(1)
C(20)	8384(2)	10281(3)	5959(2)	14(1)
C(21)	8426(3)	10798(3)	7783(2)	19(1)
C(22)	8009(3)	12471(3)	7567(2)	22(1)
C(23)	7784(3)	13047(3)	6560(2)	22(1)
C(24)	7970(2)	11979(3)	5746(2)	19(1)

Table 20. Bond lengths [Å] and angles [°] for (**79**).

S(1)-C(4)	1.706(2)	C(16)-H(16)	0.90(3)
S(1)-C(1)	1.737(2)	C(17)-C(18)	1.357(3)
S(2)-C(9)	1.722(2)	C(17)-H(17)	0.98(3)
S(2)-C(12)	1.735(3)	C(18)-C(19)	1.443(3)
S(3)-C(17)	1.729(2)	C(19)-C(21)	1.403(3)
S(3)-C(20)	1.737(2)	C(19)-C(20)	1.405(3)
C(1)-C(2)	1.391(3)	C(20)-C(24)	1.404(3)
C(1)-C(10)	1.469(3)	C(21)-C(22)	1.386(3)
C(2)-C(3)	1.432(3)	C(21)-H(21)	0.93(3)
C(2)-C(18)	1.473(3)	C(22)-C(23)	1.393(4)
C(3)-C(4)	1.374(3)	C(22)-H(22)	0.95(3)
C(3)-C(5)	1.491(3)	C(23)-C(24)	1.374(4)
C(4)-C(7)	1.465(3)	C(23)-H(23)	1.01(3)
C(5)-C(6)	1.484(4)	C(24)-H(24)	0.98(3)
C(5)-H(5A)	0.93(4)		
C(5)-H(5B)	0.96(4)	C(4)-S(1)-C(1)	91.90(12)
C(6)-C(7)	1.378(4)	C(9)-S(2)-C(12)	90.98(12)
C(6)-C(8)	1.495(4)	C(17)-S(3)-C(20)	91.19(11)
C(7)-H(7)	0.77(3)	C(2)-C(1)-C(10)	131.1(2)
C(8)-H(8A)	0.9600	C(2)-C(1)-S(1)	111.78(17)
C(8)-H(8B)	0.9600	C(10)-C(1)-S(1)	117.07(16)
C(8)-H(8C)	0.9600	C(1)-C(2)-C(3)	110.9(2)
C(9)-C(10)	1.364(3)	C(1)-C(2)-C(18)	125.1(2)
C(9)-H(9)	0.96(3)	C(3)-C(2)-C(18)	124.0(2)
C(10)-C(11)	1.449(3)	C(4)-C(3)-C(2)	113.5(2)
C(11)-C(13)	1.399(3)	C(4)-C(3)-C(5)	108.3(2)
C(11)-C(12)	1.412(3)	C(2)-C(3)-C(5)	138.0(2)
C(12)-C(16)	1.396(3)	C(3)-C(4)-C(7)	110.3(2)
C(13)-C(14)	1.384(4)	C(3)-C(4)-S(1)	111.96(18)
C(13)-H(13)	0.87(3)	C(7)-C(4)-S(1)	137.6(2)
C(14)-C(15)	1.398(4)	C(6)-C(5)-C(3)	104.0(2)
C(14)-H(14)	0.84(4)	C(6)-C(5)-H(5A)	113(2)
C(15)-C(16)	1.371(4)	C(3)-C(5)-H(5A)	113(2)
C(15)-H(15)	0.99(3)	C(6)-C(5)-H(5B)	114(2)

C(3)-C(5)-H(5B)	109(2)	C(15)-C(14)-H(14)	119(2)
H(5A)-C(5)-H(5B)	104(3)	C(16)-C(15)-C(14)	120.8(2)
C(7)-C(6)-C(5)	110.4(2)	C(16)-C(15)-H(15)	123.1(18)
C(7)-C(6)-C(8)	126.7(3)	C(14)-C(15)-H(15)	116.1(18)
C(5)-C(6)-C(8)	122.9(3)	C(15)-C(16)-C(12)	118.2(2)
C(6)-C(7)-C(4)	107.0(2)	C(15)-C(16)-H(16)	123(2)
C(6)-C(7)-H(7)	128(3)	C(12)-C(16)-H(16)	118(2)
C(4)-C(7)-H(7)	124(2)	C(18)-C(17)-S(3)	113.71(18)
C(6)-C(8)-H(8A)	109.5	C(18)-C(17)-H(17)	127.7(16)
C(6)-C(8)-H(8B)	109.5	S(3)-C(17)-H(17)	118.4(16)
H(8A)-C(8)-H(8B)	109.5	C(17)-C(18)-C(19)	111.8(2)
C(6)-C(8)-H(8C)	109.5	C(17)-C(18)-C(2)	124.7(2)
H(8A)-C(8)-H(8C)	109.5	C(19)-C(18)-C(2)	123.5(2)
H(8B)-C(8)-H(8C)	109.5	C(21)-C(19)-C(20)	118.8(2)
C(10)-C(9)-S(2)	114.3(2)	C(21)-C(19)-C(18)	129.0(2)
C(10)-C(9)-H(9)	130.4(18)	C(20)-C(19)-C(18)	112.1(2)
S(2)-C(9)-H(9)	115.3(17)	C(24)-C(20)-C(19)	121.8(2)
C(9)-C(10)-C(11)	111.5(2)	C(24)-C(20)-S(3)	127.02(18)
C(9)-C(10)-C(1)	121.3(2)	C(19)-C(20)-S(3)	111.21(16)
C(11)-C(10)-C(1)	127.2(2)	C(22)-C(21)-C(19)	119.1(2)
C(13)-C(11)-C(12)	118.2(2)	C(22)-C(21)-H(21)	119.0(19)
C(13)-C(11)-C(10)	130.3(2)	C(19)-C(21)-H(21)	121.8(19)
C(12)-C(11)-C(10)	111.5(2)	C(21)-C(22)-C(23)	121.1(2)
C(16)-C(12)-C(11)	122.2(2)	C(21)-C(22)-H(22)	119.6(17)
C(16)-C(12)-S(2)	126.01(19)	C(23)-C(22)-H(22)	119.4(17)
C(11)-C(12)-S(2)	111.78(18)	C(24)-C(23)-C(22)	121.2(2)
C(14)-C(13)-C(11)	119.4(2)	C(24)-C(23)-H(23)	120.7(16)
C(14)-C(13)-H(13)	115(2)	C(22)-C(23)-H(23)	118.0(16)
C(11)-C(13)-H(13)	125(2)	C(23)-C(24)-C(20)	118.0(2)
C(13)-C(14)-C(15)	121.2(3)	C(23)-C(24)-H(24)	120.1(19)
C(13)-C(14)-H(14)	120(2)	C(20)-C(24)-H(24)	121.9(19)

Table 21. Anisotropic displacement parameters ($Å^2$ x 10^3) for (**79**).

The anisotropic displacement factor exponent takes the form: $-2\pi^2[\, h^2\, a^{*2} U^{11} + ... + 2\, h\, k\, a^*\, b^*\, U^{12}\,]$).

	U^{11}	U^{22}	U^{33}	U^{23}	U^{13}	U^{12}
S(1)	24(1)	20(1)	15(1)	5(1)	2(1)	4(1)
S(2)	19(1)	20(1)	31(1)	0(1)	5(1)	4(1)
S(3)	22(1)	19(1)	13(1)	1(1)	4(1)	0(1)
C(1)	22(1)	12(1)	14(1)	3(1)	3(1)	-1(1)
C(2)	18(1)	12(1)	15(1)	0(1)	3(1)	1(1)
C(3)	21(1)	14(1)	14(1)	-1(1)	4(1)	0(1)
C(4)	24(1)	17(1)	16(1)	0(1)	4(1)	-1(1)
C(5)	20(1)	21(1)	21(1)	-1(1)	6(1)	0(1)
C(6)	28(1)	29(1)	26(1)	-5(1)	10(1)	-9(1)
C(7)	31(1)	23(1)	13(1)	3(1)	5(1)	-4(1)
C(8)	34(2)	37(2)	38(2)	-5(1)	19(1)	-10(1)
C(9)	20(1)	17(1)	25(1)	3(1)	5(1)	3(1)
C(10)	18(1)	16(1)	15(1)	2(1)	1(1)	1(1)
C(11)	17(1)	17(1)	15(1)	0(1)	-1(1)	-1(1)
C(12)	15(1)	17(1)	22(1)	-1(1)	0(1)	0(1)
C(13)	18(1)	18(1)	20(1)	-4(1)	2(1)	1(1)
C(14)	24(1)	15(1)	26(1)	2(1)	1(1)	-3(1)
C(15)	18(1)	29(1)	25(1)	1(1)	3(1)	-9(1)
C(16)	15(1)	25(1)	26(1)	0(1)	4(1)	-1(1)
C(17)	18(1)	14(1)	15(1)	1(1)	4(1)	-1(1)
C(18)	16(1)	13(1)	15(1)	2(1)	3(1)	1(1)
C(19)	12(1)	15(1)	16(1)	2(1)	2(1)	1(1)
C(20)	14(1)	14(1)	15(1)	0(1)	4(1)	-2(1)
C(21)	22(1)	17(1)	18(1)	1(1)	3(1)	2(1)
C(22)	25(1)	14(1)	26(1)	-3(1)	4(1)	2(1)
C(23)	19(1)	15(1)	34(1)	2(1)	6(1)	2(1)
C(24)	15(1)	19(1)	23(1)	6(1)	2(1)	-1(1)

Table 22. Hydrogen coordinates (x 10^4) and isotropic displacement parameters (Å^{2}x 10^3) for (**79**).

	x	*y*	*z*	U_{eq}
H(8A)	5246	5787	10991	53
H(8B)	4430	6075	9907	53
H(8C)	5021	7646	10559	53
H(21)	8600(30)	10460(40)	8470(20)	21(8)
H(17)	9520(30)	6120(40)	5870(20)	16(7)
H(15)	15190(30)	10170(40)	5720(20)	22(7)
H(9)	12520(30)	3270(40)	7900(20)	20(7)
H(5A)	6220(40)	6940(50)	8390(30)	41(10)
H(16)	15780(30)	7190(40)	5980(20)	18(7)
H(7)	7970(30)	4990(50)	10780(30)	33(9)
H(14)	13110(30)	11010(50)	6350(20)	28(8)
H(23)	7520(30)	14290(40)	6440(20)	19(7)
H(13)	11670(30)	9460(40)	7220(20)	28(8)
H(24)	7840(30)	12420(40)	5040(20)	23(8)
H(5B)	6830(40)	8450(50)	8960(30)	45(10)
H(22)	7900(30)	13240(40)	8110(20)	15(7)

Bis(2,3-(3'-benzothiophen-yl)]cyclopenta[b]thienyl)zirconium dichloride (**80**).

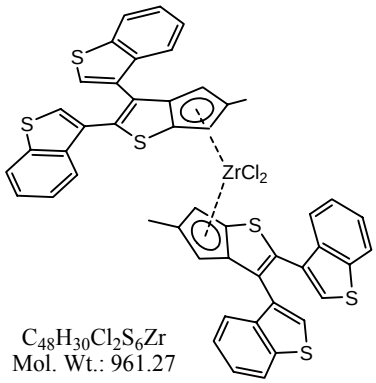

$C_{48}H_{30}Cl_2S_6Zr$
Mol. Wt.: 961.27

In a 50 ml glass vial with Teflon stirring bar was placed 1.04 g (2.5 mmol) 3-hydro-[2,3-(3'-benzothiaphen-yl)]cyclopenta[b]thiophene slurried in 30 ml diethyl ether. The solution was irradiated with 254 nm lamps for 90 minutes (color changes from off white to purple during irradiation), then a solution of n-butyllithium was added dropwise (2.5 mmol, 1 ml, 2.5M in hexane). The reaction mixture was stirred an additional 1 h, then 0.3 g (1.25 mmol) zirconium tetrachloride was slowly added as a dry powder. The reaction mixture was stirred overnight, and then filtered. Solids were washed with fresh diethyl ether. The solids were then slurried in dichloromethane, filtered, then solvents removed in vacuo. Finally, the solids recovered from the dichloromethane filtrate were washed with pentane, and then dried in vacuo. Yield: 0.90 g orange free flowing powder. ^{1}H-NMR δ ($CDCl_3$): 8.0 – 6.9 (m, 16H), 6.9 – 6.1 (4m, 4H), 2.1 (2s, 6H).

Figure 73. ^{1}H-NMR of Bis(2,3-(3'-benzothiaphen-yl)]cyclopenta[b]thiophen-yl)zirconium dichloride (**80**).

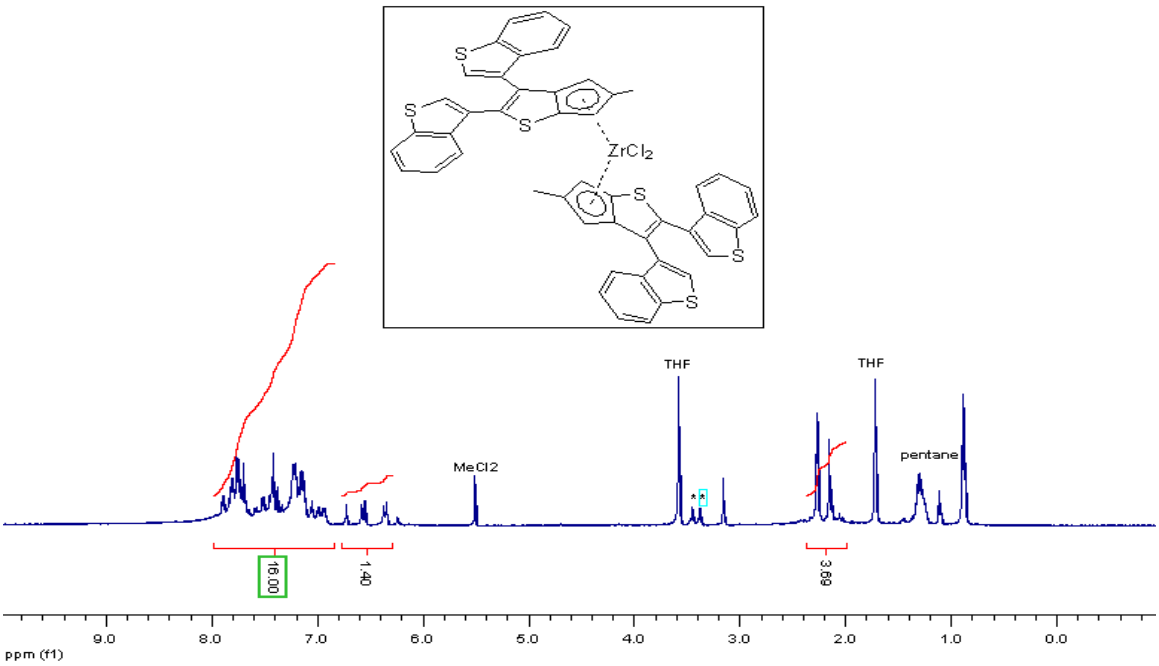

Figure 74. UV-visible absorbance spectrum of Bis(2,3-(3'-benzothiaphen-yl)]cyclopenta[b]thiophen-yl)zirconium dichloride (**80**) in benzene (5 x 10^{-5}M), without (-) and with (-) UV increasing irradiation time intervals.

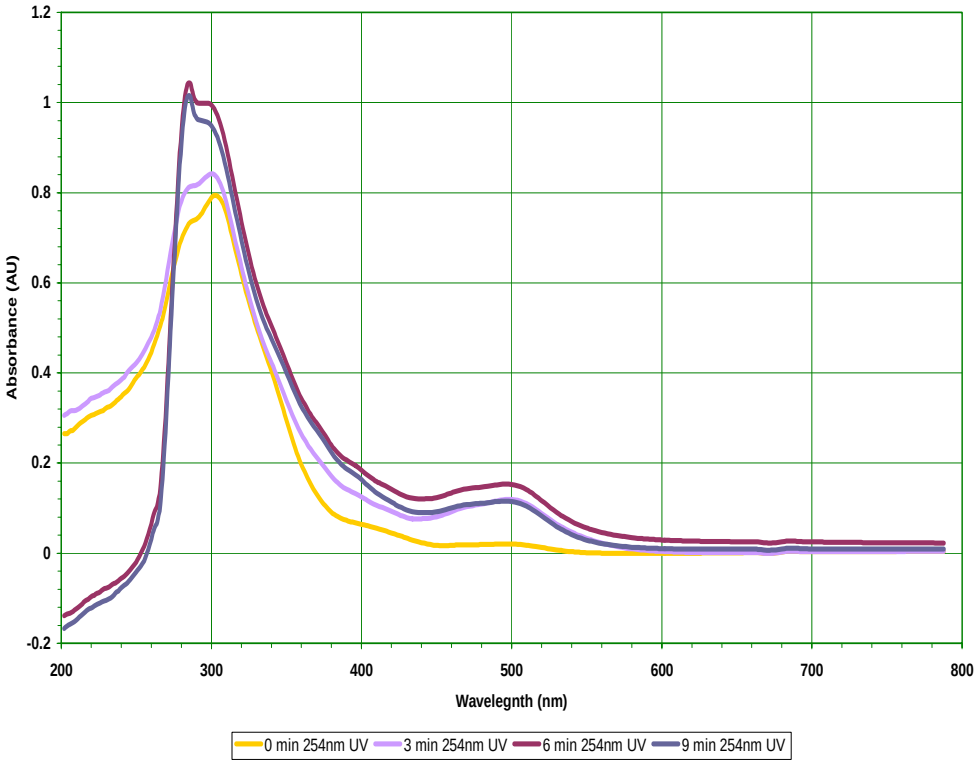

5-methyl-2,3-bis(benzo[b]thiaphen-3-yl)-4,5-dihydrocyclopenta[b]thiophene (**69**).

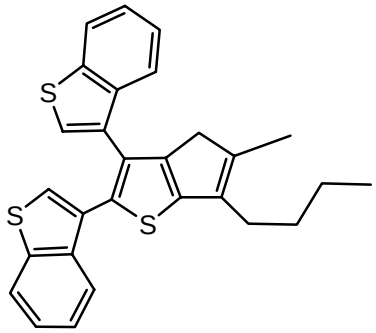

In a flask containing 2.08 g (5 mmol) 2,3-di(benzo[b]thiophen-3-yl)-5-methyl-6H-cyclopenta[b]thiophen-6-one (**11**) dissolved in 80 mL diethyl ether was added a solution containing n-butyllithium (5 mmol, 2 mL, 2.5M in hexane). The reaction mixture was stirred for 18 h, then poured into water. Organics were collected with a 1:1 solution containing dichloromethane and hexane, washed with water, dried over magnesium sulfate, filtered, then solvents were removed in vacuo. In this manner 1.35 g of an orange paste was collected and fractionated by preparative HPLC on 35 g silica using an

increasing hexane then dichloromethane gradient. Yield: 0.23 g target complex: 3 isomers by FIDGC/GCMS. EIMS, m/z (%): (major isomer): 459 (5), 458 (19), 457 (33), 456 (100), 454 (1), 430 (10), 430 (10), 429 (16), 429 (16), 428 (29), 427 (93). ^{1}H-NMR δ ($CDHCl_2$): 7.6 – 8.0 (m, 3H), 7.6 (d, 1H), 7.65 – 7.20 (m, 6H), 3.18 (s, 1H), 2.6 (t, 3H), 2.1 (s, 1H), 1.75 (m, 2H), 1.5 (m, 2H), 1.03 (t, 3H).

Figure 75. ^{1}H-NMR of 6-*n*butyl-5-methyl-2,3-bis(benzo[b]thiophen-3-yl)-*6H*-cyclopenta[b]thiophene (**83**).

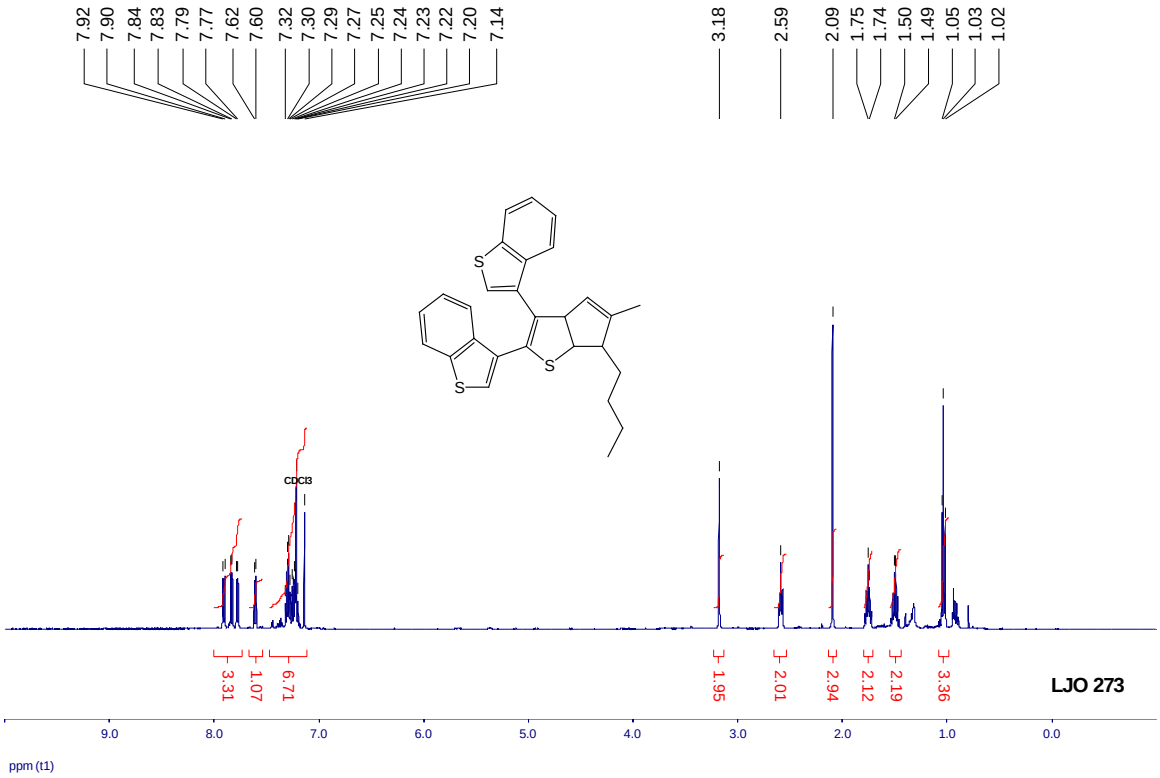

Figure 76. GC analysis of 5-methyl-2,3-bis(benzo[b]thiophen-3-yl)-4H-cyclopenta[b]thiophene (**69**).

Area Percent Report
Data Path : D:\MSDCHEM\1\DATA\Jones\Diss500\506\
Data File : 506FC1.D
Acq On : 28 Jun 2005 12:42 (#1); 28.06.2005 12:42:01 PM (#2)
Operator : JONES
Sample : 506FC1
Misc : PS1nBu frac 4 to 8 (0.2 g) (Sig #1); (Sig #2)
ALS Vial : 1 Sample Multiplier: 1

Integration Parameters: autoint1.e
Integrator: ChemStation 6890 Scale Mode: Large solvent peaks clipped
Smoothing : OFF Filtering: 5
Sampling : 1 Min Area: 5 % of largest Peak

Start Thrs: 0.2 Max Peaks: 100
Stop Thrs : 0 Peak Location: TOP

If leading or trailing edge < 100 prefer < Baseline drop else tangent >
Peak separation: 5

Method : D:\MSDCHEM\1\METHODS\MSHIGH.M
Title : install
Signal : TIC

peak #	R.T. min	first scan	max scan	last scan	PK TY	peak height	corr. area	corr. % max.	% of total
1	5.431	298	304	313	BB	3264084	37530785	3.31%	1.459%
2	6.120	387	393	399	BB	734561	7926277	0.70%	0.308%
3	14.489	1467	1474	1486	BB	593316	12112608	1.07%	0.471%
4	25.948	2882	2954	3022	BB	2 6577455	1011914360	89.27%	39.340%
5	27.334	3048	3133	3153	BV	6562585	1133602139	100.00%	44.071%
6	27.783	3153	3191	3256	VB	2 3176444	369144475	32.56%	14.351%

Sum of corrected areas: 2572230644

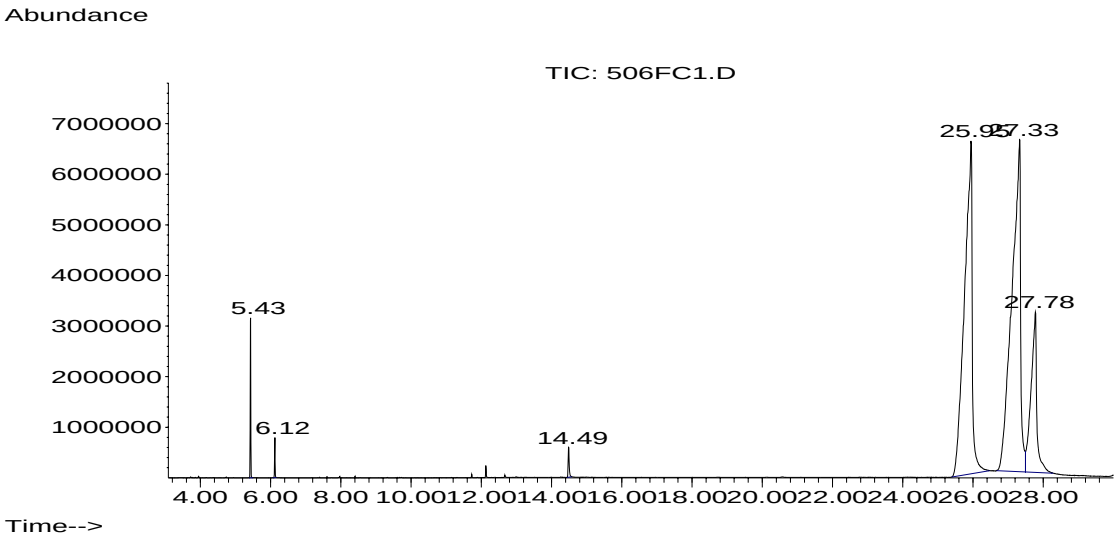

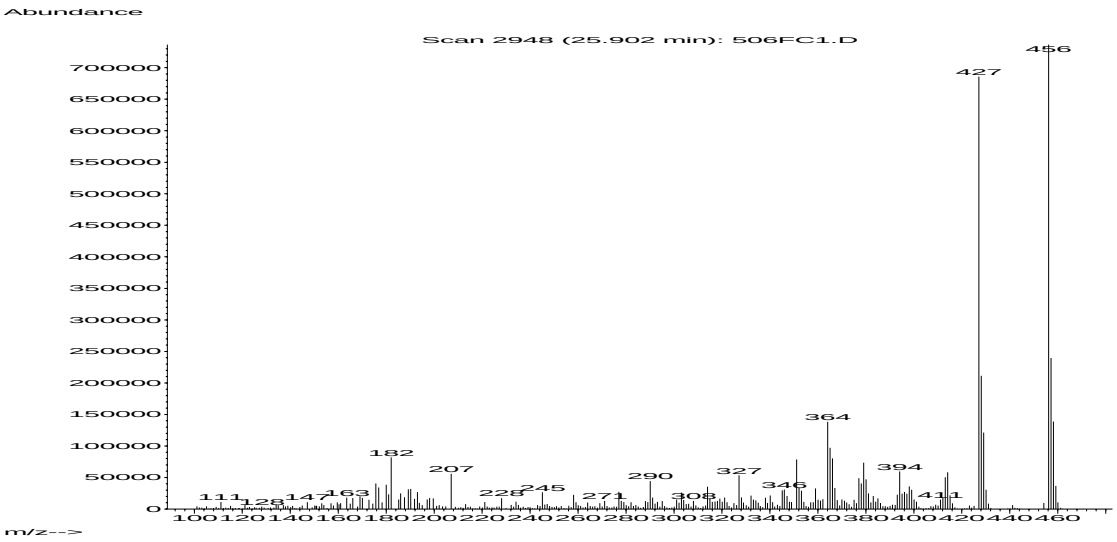
Abundance
Scan 2948 (25.902 min): 506FC1.D
456
427
364
182
207
394
290
327
346
245
228
271
308
411
111
129
147
163
m/z-->

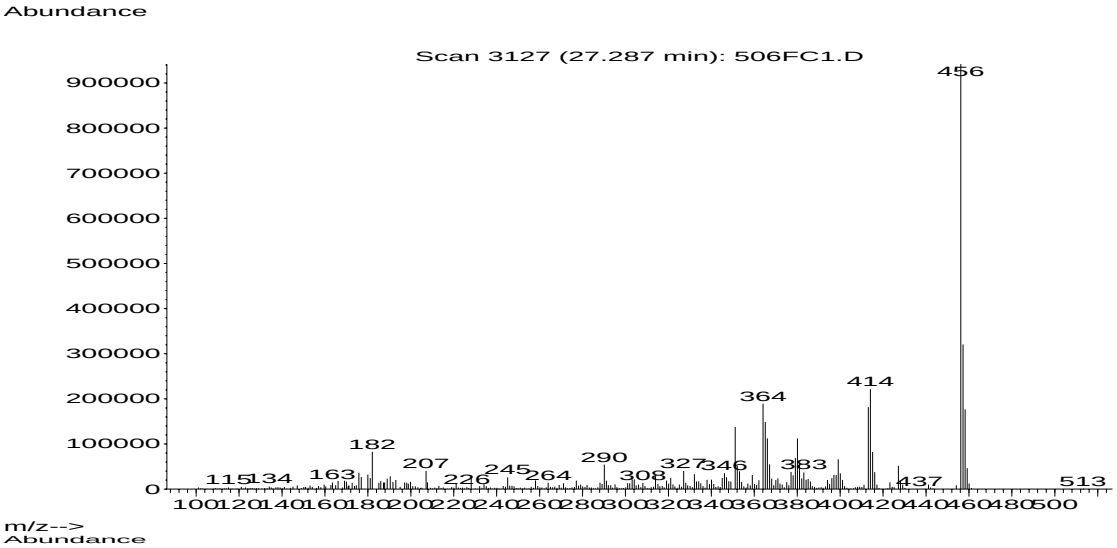
Abundance
Scan 3127 (27.287 min): 506FC1.D
456
414
364
182
207
290
327
346
383
245
264
308
226
163
134
115
437
513
m/z-->

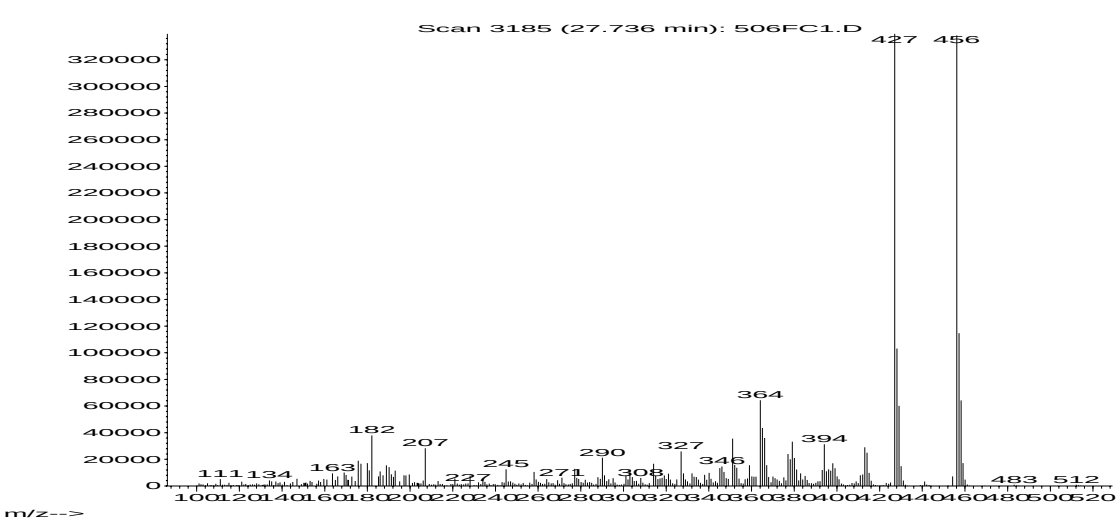
Abundance
Scan 3185 (27.736 min): 506FC1.D
427
456
364
182
207
394
327
290
346
245
271
308
227
163
134
111
483
512
m/z-->

Signal : 506FC1.D\FID1A.CH

peak #	R.T. min	Start min	End min	PK TY	peak height	corr. area	corr. % max.	% of total
---	-----	-----	-----	---	-------	-------	------	------
1	5.482	5.448	5.522	BB	1071425	11179355	7.34%	3.186%
2	6.172	6.137	6.203	BB	182659	1825755	1.20%	0.520%
3	14.571	14.517	14.616	BB	175531	3126764	2.05%	0.891%
4	26.312	25.796	26.450	BB	837096	137294839	90.12%	39.124%
5	27.727	27.098	27.818	BV	825372	152339416	100.00%	43.411%
6	28.175	27.818	28.288	VB	415896	45157782	29.64%	12.868%

Sum of corrected areas: 350923911

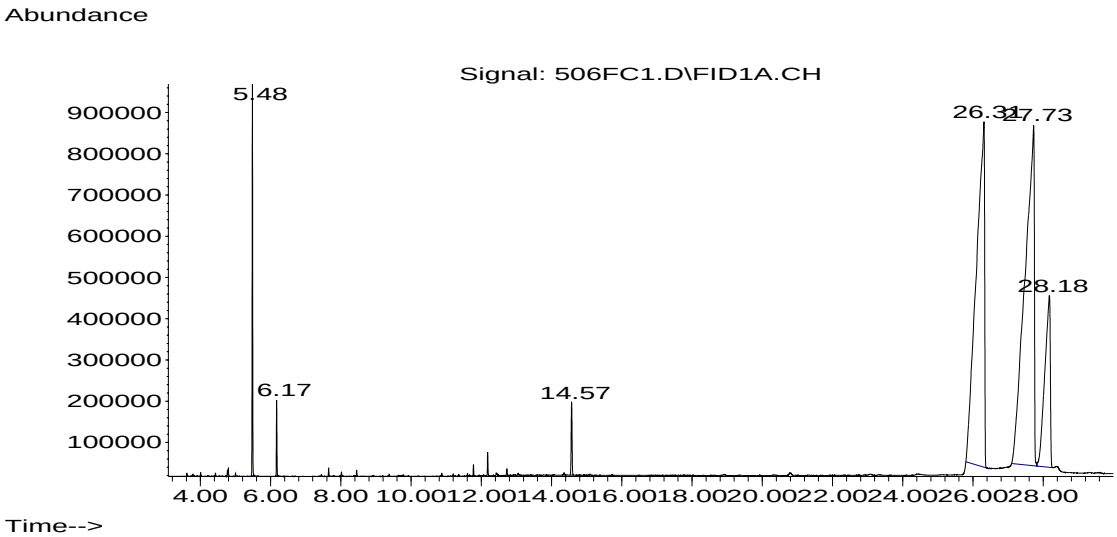

MSHIGH.M Thu Jun 30 08:06:47 2005 CHEMSTATION

Figure 77. Reaction product from the lithium salt of (**83**) and $nBuCpZrCl_3$.

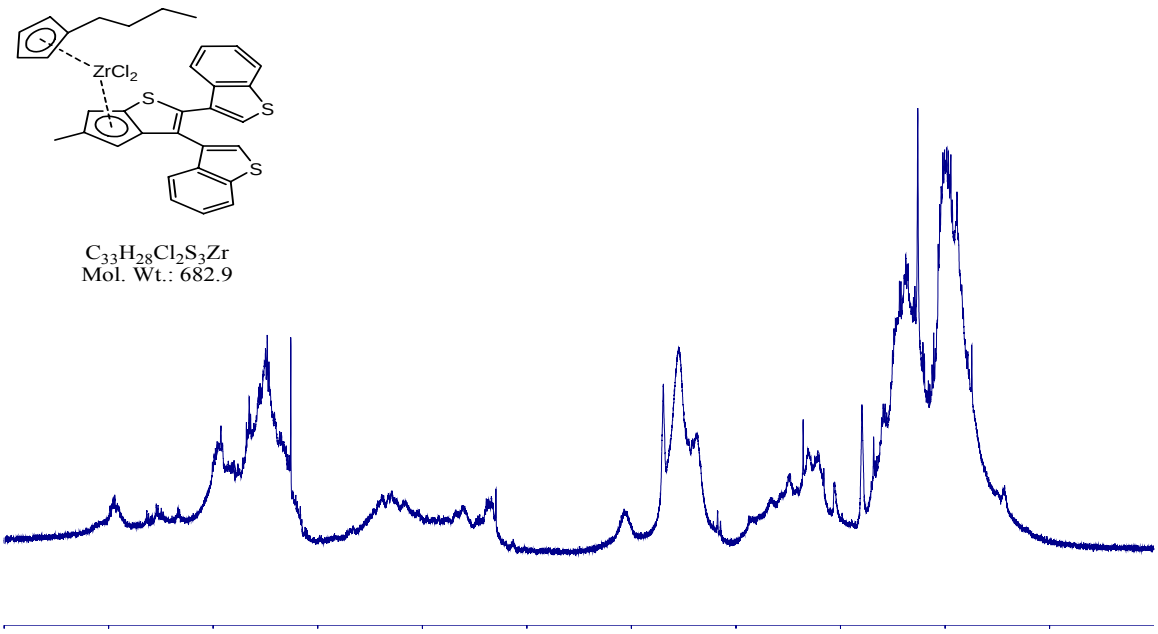

2,3-bis(thiophen-3-yl)-4,5-dihydrocyclopenta[b]thiophen-6-one (**105**).

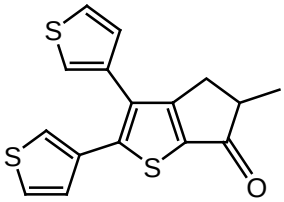

In a flask containing 3.1 g (10 mmol) 2,3-dibromo-4,5-dihydro-5-methylcyclopenta[b]thiophen-6-one (**10**), and 0.7 g tetrakis(triphenylphosphine) palladium in 80 ml dimethoxyethane was added 2.54 g (20 mmol) thiophene-3-boronic acid followed by a degassed solution containing 2.11 g sodium carbonate in 30 mL water. The reaction mixture was refluxed for 4 h., then cooled while stirring overnight. The reaction mixture was poured into an equal volume of 1N HCl, organics were collected with a 20% dichloromethane/hexane solution, washed with water, dried over magnesium sulfate, filtered through a plug of silica gel, then solvents were removed from the filtrate in vacuo. 1.82 g (89% by GCMS). EIMS, m/z (%): 288 (7), 301 (21), 315 (33), 316 (100), 317 (23), 318 (14).). ^{1}H-NMR δ ($CDHCl_2$): 7.4 - 7.2 (3H), 6.95 (m, 2H), 3.2 (m, 1H), 2.9 (m, 1H), 2.58 (m, 1H), 1.3 (2s, 3H).

Figure 78. ^{1}H-NMR of 2,3-bis(thiophen-3-yl)-4,5-dihydrocyclopenta[b]thiophen-6-one (**105**).

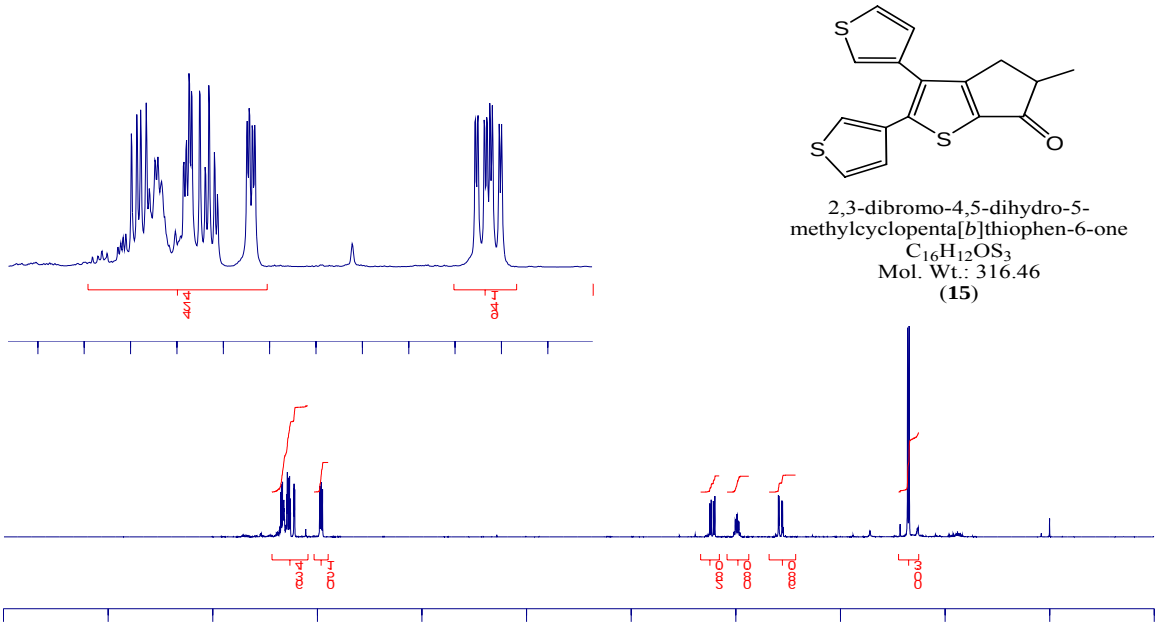

Figure 79. ^{1}H-NMR of 2,3-bis(thiophen-3-yl)-4,5-dihydrocyclopenta- [b]thiophen-6-one (**105**) after irridation (1h).

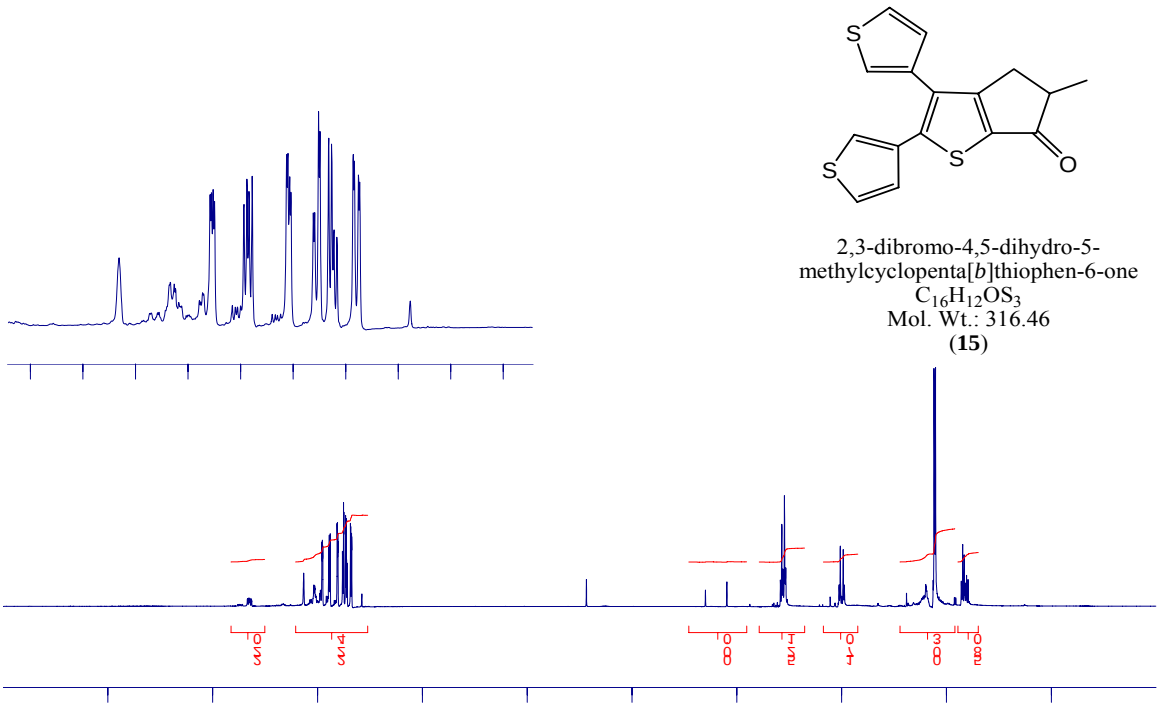

Synthesis of 2,3-di(thiophene-3-yl)cyclopenta[b]thiophenene (**106**):

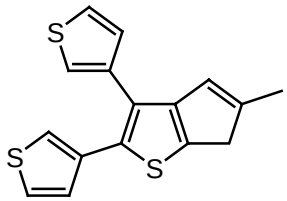

In a flask containing 1.52 g (4.8 mmol) 2,3-di(thiophene-3-yl)cyclopenta[b]thiophen-6-one (**105**) slurried in 80 ml diethyl ether was added a solution containing $LiAlH_4$ (1.6 mmol, 1.6 ml, 1M solution in diethyl ether), dropwise. The reaction mixture was stirred for 3 h., then 30 ml 1N HCl was slowly added. The reaction mixture was washed with water, organics were collected with diethyl ether, dried over magnesium sulphate, then solvents removed in vacuo. GC analysis showed no trace of the starting ketone.
The product was dissolved in 40 ml toluene, a catalytic amount of *para*-toluene sulfonic acid monohydrate was added (~0.2 g) and the reaction mixture was heated to reflux for 5 minutes. The reaction mixture was stirred for 18 h., then poured into an equal volume of water. Organics were collected with diethyl ether, dried over magnesium sulphate, then solvents removed in vacuo. 1.21 g viscous brown oil was filtered through silica gel (HPLC: 35 g SiO_2 column ISCO, hexane/dichloromethane, gradient): 0.72 g of a crystalline yellowish powder was recovered. EIMS, m/z (%): [300], ^{1}H-NMR δ ($CDHCl_2$): 7.3 (m, 1H), 7.25 (m, 1H), 7.15 (m, 1H), 7.05 (m, 1H), 6.95 (m, 1H), 6.45 (s, 1H), 3.2 (s, 2H), 2.2 (d, 3H).

Figure 80. ^{1}H-NMR 2,3-di(thiophene-3-yl)cyclopenta[b]thiophene (**106**):

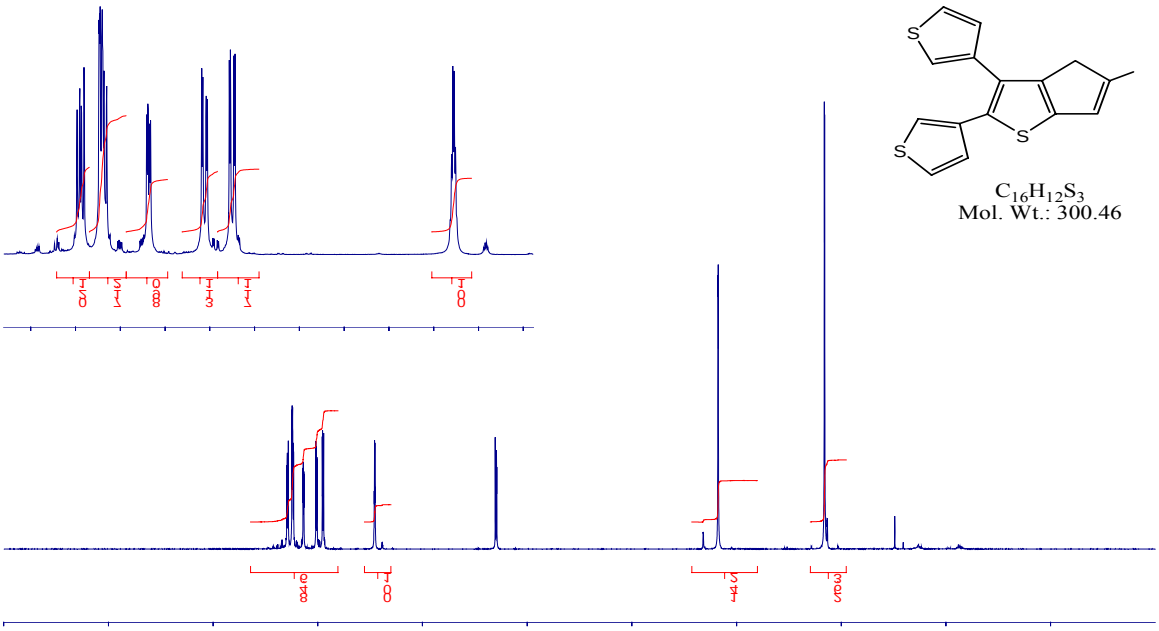

2-(benzothiophene-3-yl)-3-bromocyclopenta[b]thiophen-6-one (**107**).

This compound was isolated as part of the synthesis of (**77**) where only one of the intended benzothiophene substitutions was successfully added. The identical procedure was followed with the exception that 3 equivalents of boronic acid were added instead of 5.

Figure 81. ^{1}H-NMR of 2-(benzothiophene-3-yl)-3-bromocyclopenta[b]thiophen-6-one (**107**).

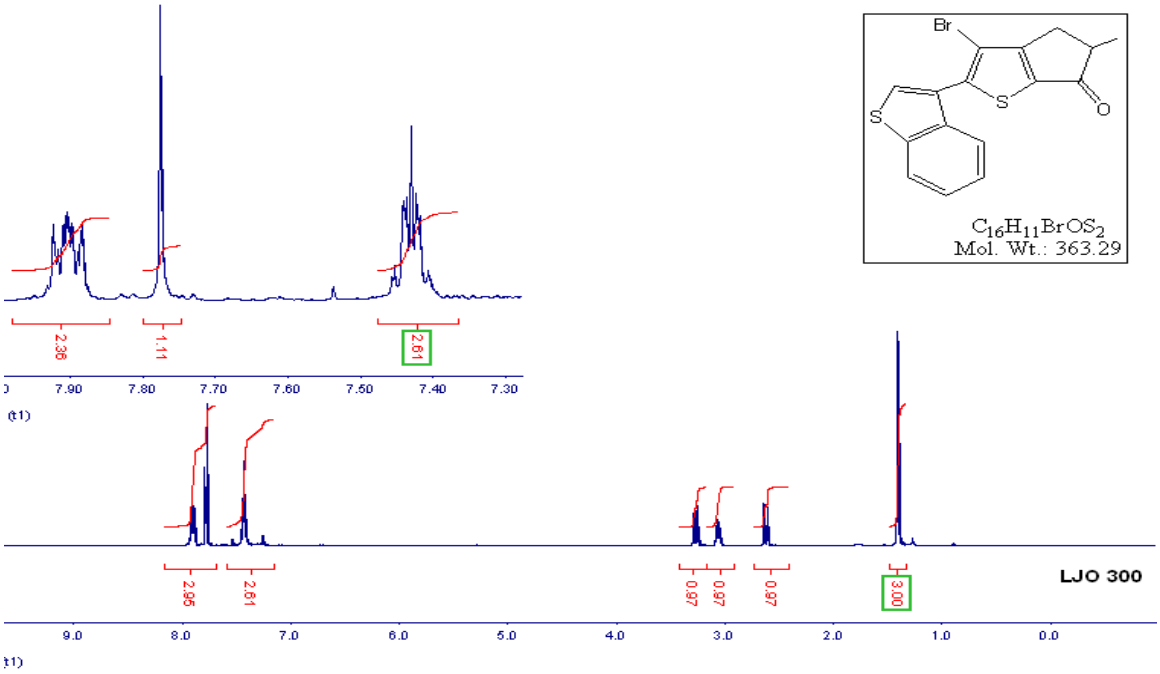

Chlorodimethyl(2,3-dimethyl-3-phenyl-6-hydrocyclopenta[b]thien-6-yl)silane (**84**).
(11527-35)

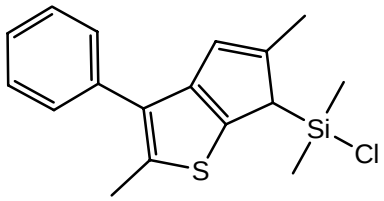

In a flask containing 12.7 g (56.2 mmol) 2,3-dimethyl-3-phenyl-6-hydrocyclopenta[b]thiophene dissolved in 100 ml diethyl ether was added a solution containing n-butyllithium (60 mmol, 24 ml, 2.5M in hexene). An additional 100 ml of diethyl ether was added to facilitate stirring. The reaction mix was stirred for 5 h, becoming a white slurry.

In a separate flask, a solution containing 10.9 g (86 mmol) dichlorodimethylsilane dissolved in 50 ml diethyl ether was prepared. The contents from the flask above were added via cannula, stirred for 18h, then solvents removed in vacuo. The solids were slurried in dichloromethane, then filtered. Solvents were removed from the filtrate: 6.37 g dark brown viscous oil recovered. EIMS, m/z (%): [M] 318, (100%).

Note: this compound was made in 1999, and was only slightly decomposed, as evidenced by the NMR and GC analysis.

Figure 82. ^{1}H-NMR of Chlorodimethyl(2,3-dimethyl-3-phenyl-6-hydrocyclopenta[b]thien-6-yl)silane (**84**).

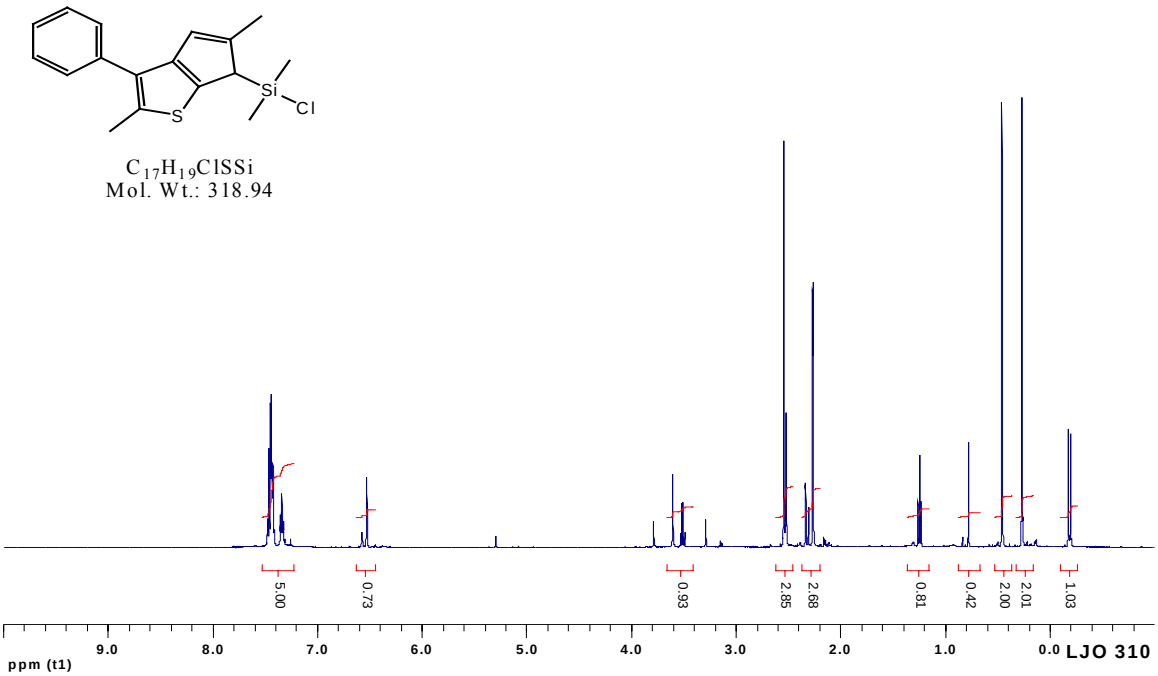

Table 23. Gas Chromatographic report from synthesis of chlorodimethyl(2,3-dimethyl-3-phenyl-6-hydrocyclopenta[b]thien-6-yl)silane (**108**).

Area Percent Report

Data Path : D:\MSDCHEM\1\DATA\Jones\Diss500\509\
Data File : 509SM1.D
Acq On : 23 Jun 2005 14:04 (#1); 23.06.2005 02:04:38 PM (#2)
Operator : JONES
Sample : 509SM1
Misc : Tp3SiMe2Cl from Elkton (Sig #1); (Sig #2)
ALS Vial : 5 Sample Multiplier: 1

Integration Parameters: autoint1.e
Integrator: ChemStation 6890 Scale Mode: Large solvent peaks clipped
Smoothing : OFF Filtering: 5

Sampling : 1 Min Area: 5 % of largest Peak
Start Thrs: 0.2 Max Peaks: 100
Stop Thrs : 0 Peak Location: TOP

If leading or trailing edge < 100 prefer < Baseline drop else tangent >
Peak separation: 5
Method : D:\MSDCHEM\1\METHODS\MSHIGH.M
Title : install
Signal : TIC

peak #	R.T. min	first scan	max scan	last scan	PK TY	peak height	corr. area	corr. % max.	% of total
1	9.519	826	832	841	BV	2035254	23725961	2.15%	1.840%
2	9.744	855	861	878	BB	10134950	156290155	14.17%	12.121%
3	9.999	887	894	898	BV	570557	6425486	0.58%	0.498%
4	11.191	1032	1048	1064	BV	20321799	1102942366	100.00%	85.540%

Sum of corrected areas: 1289383968

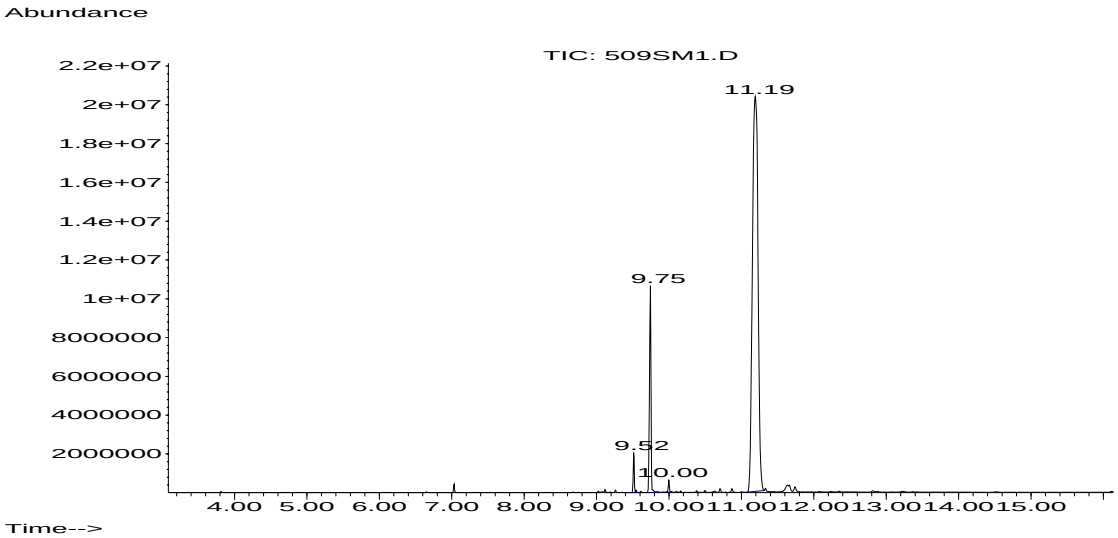

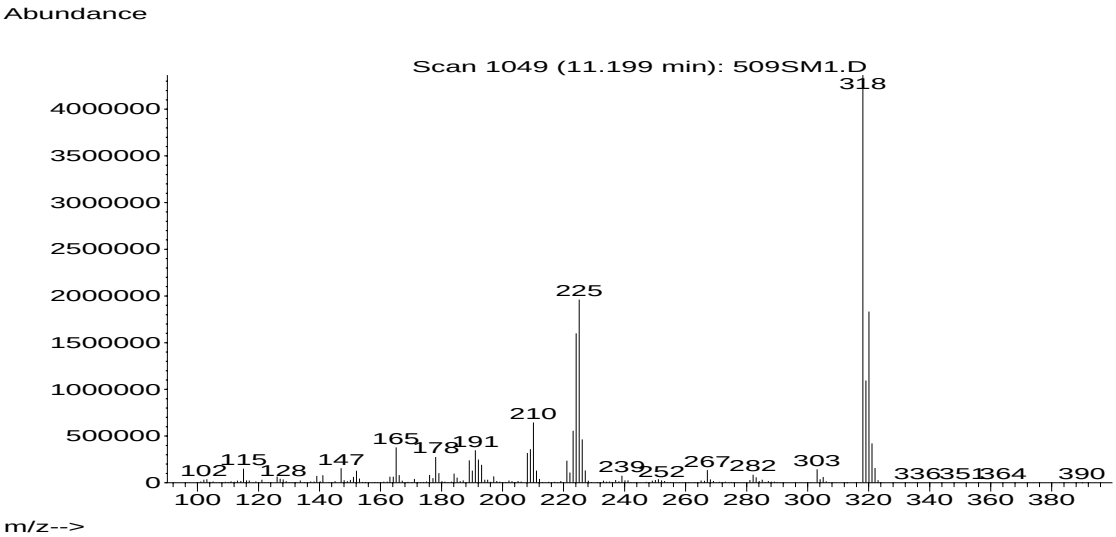

Signal: 509SM1.D\FID1A.CH

peak #	R.T. min	Start min	End min	PK TY	peak height	corr. area	corr. % max.	% of total
---	-----	-----	-----	---	-------	-------	------	------
1	7.082	7.049	7.111	BB	156876	1464635	0.47%	0.413%
2	9.563	9.523	9.582	BV	584692	5512771	1.78%	1.553%
3	9.790	9.739	9.817	BV	2625560	37544333	12.15%	10.575%
4	10.046	10.023	10.068	BV	157170	1524120	0.49%	0.429%
5	11.246	11.118	11.363	BV	6889531	308983009	100.00%	87.030%

Sum of corrected areas: 355028869

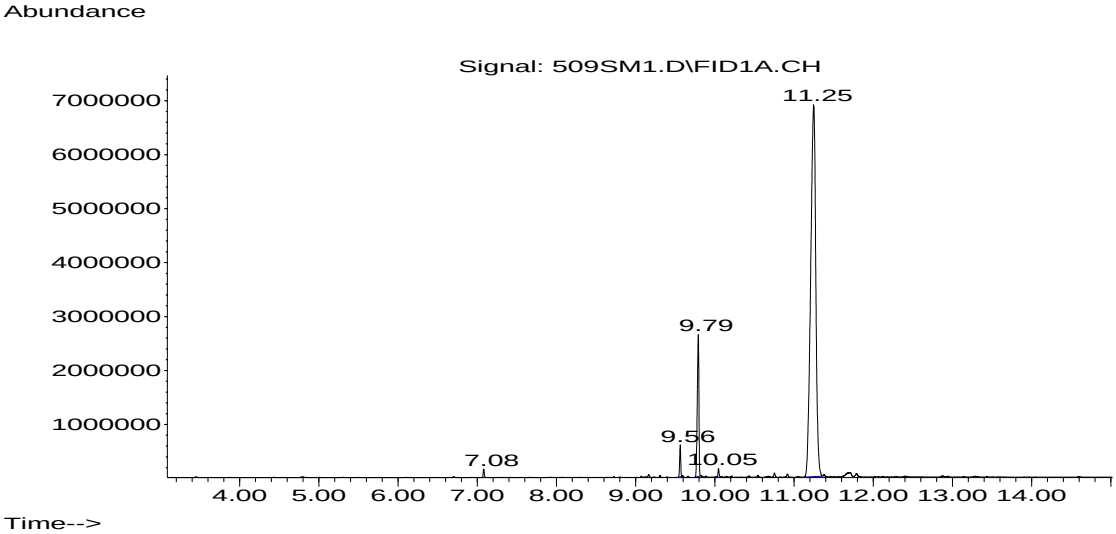

MSHIGH.M Tue Aug 30 10:16:05 2005 CHEMSTATION

Synthesis of Dimethyl-[5-methyl-[(2,3-bis(benzothiaphen-3-yl)hydrocyclopenta[b]thiophen-6-yl)][(2,5-dimethyl-3-phenylhydrocyclopenta[b]thiophen-6-yl)]silane (isomers) (**85**). (509L)

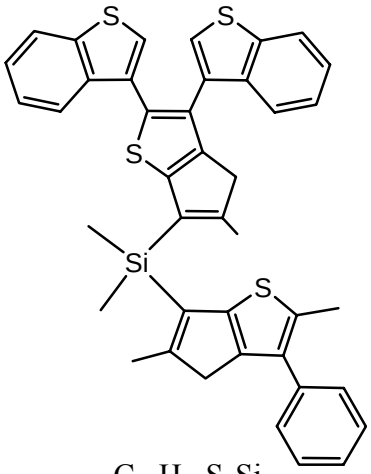

$C_{41}H_{34}S_4Si$
Mol. Wt.: 683.05

In a flask containing 1.04 g (2.5 mmol) (2,3-bis(benzothiaphen-3-yl)cyclopenta[b]-thiophene (**13**) was added 80 mL diethyl ether. The solution was stirred under 254 nm UV light for 90 min., then a solution containing n-butyl lithium was added (2.5 mmol, 1 ml, 2.5M in hexane). The reaction mix was stirred for 2 h, then a solution containing 0.82 g (2.6 mmol) chlorodimethyl-(2,5-dimethyl-3-phenylcyclopenta[b]thiophen-6-yl)]silane dissolved in diethyl ether was added slowly. The reaction mixture was stirred for 72 h, then poured into water. Organics were collected with a 20% dichloromethane/hexane solution, the organics were washed with water, dried over magnesium sulfate, filtered, the solvents removed in vacuo. 1.75 g of the product was filtered (HPLC) through silica gel (Isco column, 110 g) using hexane and dichloromethane gradient. In this fashion, 0.21 g of a light pink free flowing powder was recovered. ^{1}H-NMR δ ($CDHCl_2$): 8.0 - 7.6 (m, 5H), 7.6-7.0 (m, 10 H), 6.6 - 6.4 (2s, 2H), 4.2-3.8 (1d, 2s, 2H), 2.5 (s, 3H), 2.5 (m, 6H), -0.5 (m, 6H); LCMS, [M] = 683.

Figure 83. TLC analysis of products from Dimethyl-[5-methyl-[(2,3-bis(benzothiaphen-3-yl)hydrocyclopenta[b]thiophen-6-yl)][(2,5-dimethyl-3-phenylhydrocyclopenta[b]thiophen-6-yl)]silane (isomers).

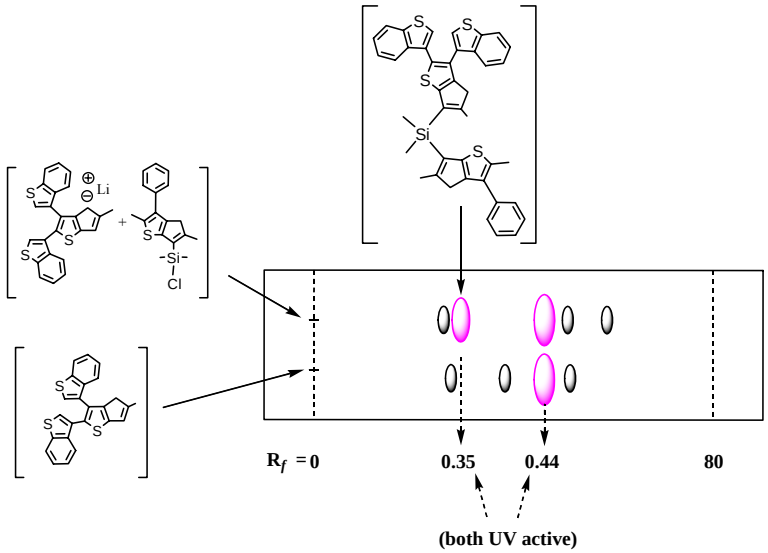

Figure 84. ^{1}H-NMR of fraction 2 from Dimethyl-[5-methyl-[(2,3-bis(benzothiaphen-3-yl)hydrocyclopenta[b]thiophen-6-yl)][(2,5-dimethyl-3-phenylhydrocyclopenta[b]thiophen-6-yl)]silane (isomers).

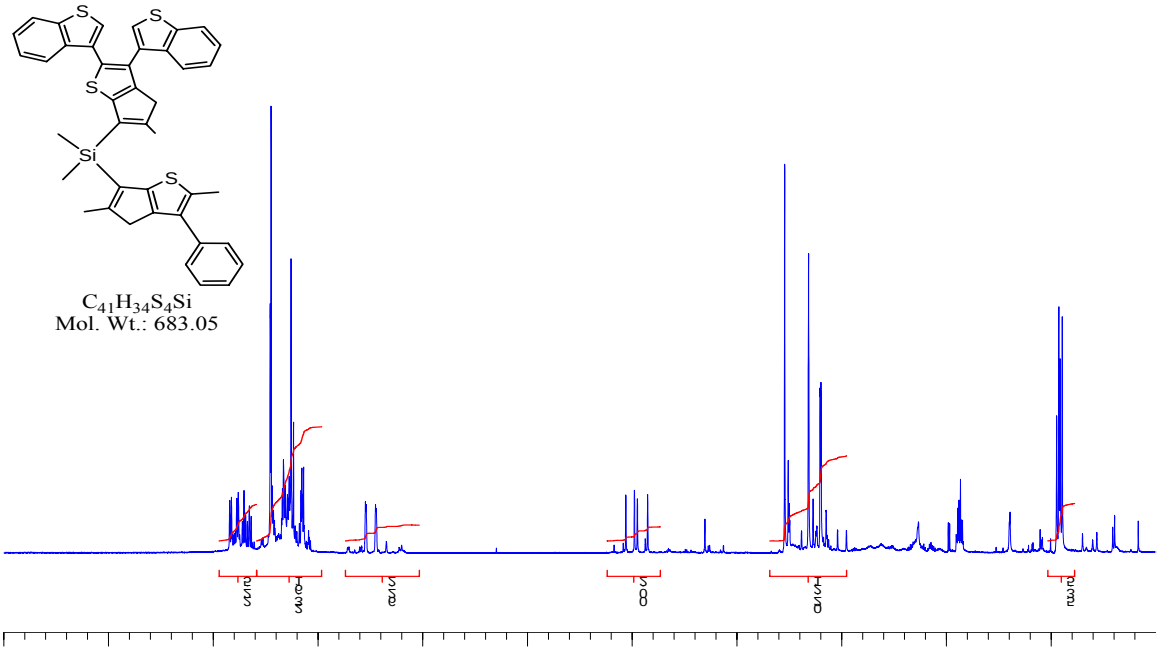

Figure 85. HPLC/MS analysis of products from Dimethyl[5-methyl-[(2,3-bis(benzothiaphen-3-yl)hydrocyclopenta[b]thiophen-6-yl)][(2,5-dimethyl-3-phenylhydrocyclopenta[b]thiophen-6-yl)]silane (isomers).
(Sample: 509F3)

Chromatogram: diode array detector (DAD) at 238nm

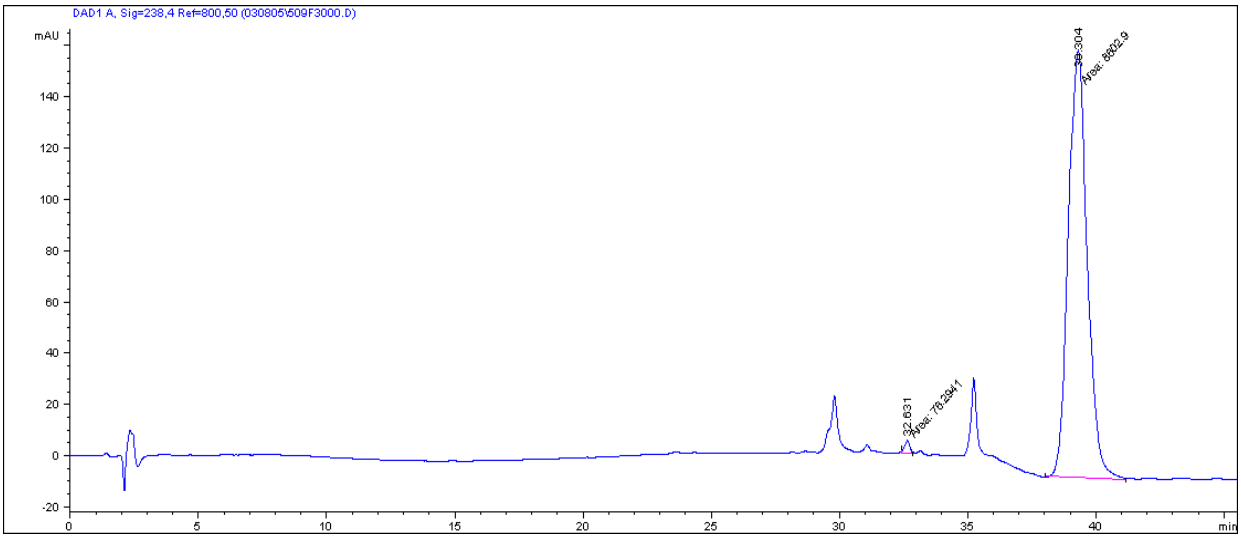

Peaktable (DAD at 238nm):

#	Time	Area	Height	Area%
1	32.631	76.3	5.2	0.879
2	39.304	8602.9	166.9	99.121

MS-Spektrum (pos. Mode):

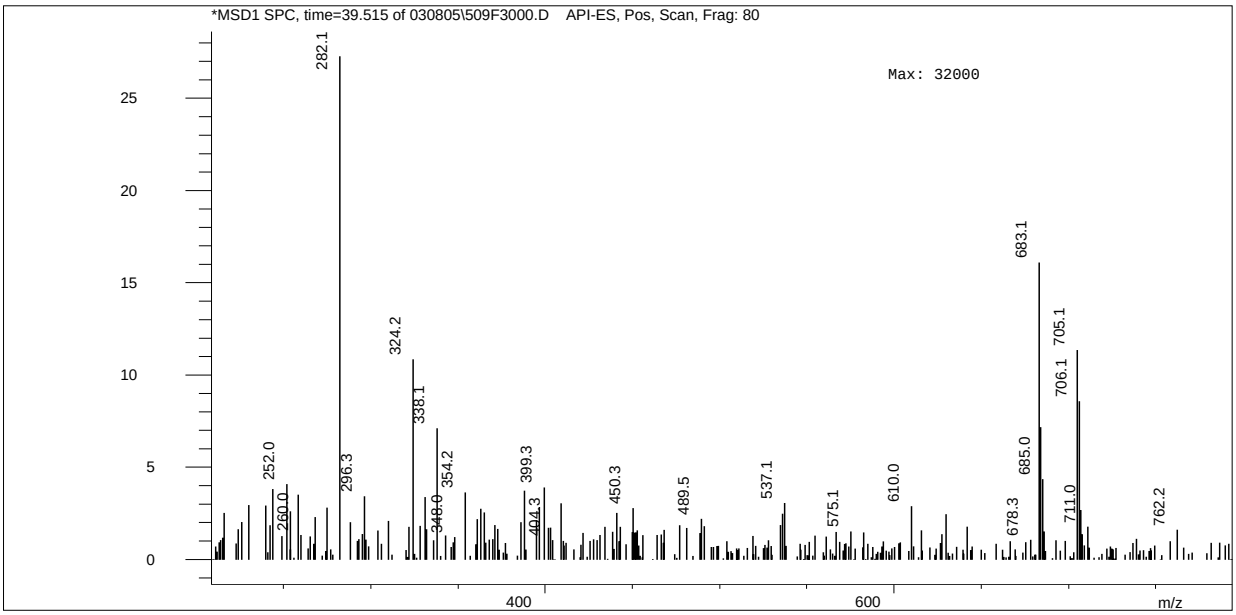

Synthesis of dimethylsilyl[(5-methyl-(2,3-bis(benzothiaphen-3-yl) cyclopenta[b]thien-6-yl)][(2,5-dimethyl-3-phenyl-cyclopenta[b]thien-6-yl)]zirconium dichloride (**86**).

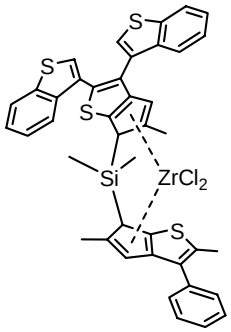

$C_{41}H_{32}Cl_2S_4SiZr$
Mol. Wt.: 843.17

A flask containing 0.18 g (0.26 mmol) Dimethyl-[5-methyl-[(2,3-benzothiaphen-3-yl)cyclopenta[b]thiophen-6-yl][(2,5-dimethyl-3-phenylthiophen-yl) cyclopenta[b]thiophen-6-yl]silane dissolved in 40 ml diethyl ether was irradiated for 4 h with two 254 nm lamps. Under irradiation, a solution containing n-butyllithium was added (0.6 mmol, 0.25 ml, 2.5M in hexane). The reaction mixture was stirred for 18 h, then 0.06 g (0.26 mmol) zirconium tetrachloride was added as a dry powder. The reaction mixture was stirred for 18 h, then filtered. Solvents were removed from the yellow ethereal solution and solids remaining were dried in vacuo: 0.02 g. (Yield = 9%); ^{1}H-NMR δ ($CDHCl_2$): 7.9 (d, 0.5H), 7.8 (d, 0.5H), 7.74 (t, 2H), 7.5 (t, 2H), 7.46-7.1 (m, 10H), 7.0 (m, 1H), 6.6, 2s, 1H), 6.5 (2s,1H), 2.5-2.3 (m, 6H), 1.1 (m, 6H), 0.05 (s, 3H); Mass by Laser Desorption Ionization-Time of Flight spectroscopy (LDI-TOF, negative mode): [M] = 839.

Figure 86. Laser Desorption Ionization-Time of Flight spectrum (LDI-TOF, positive mode) for (**86**).

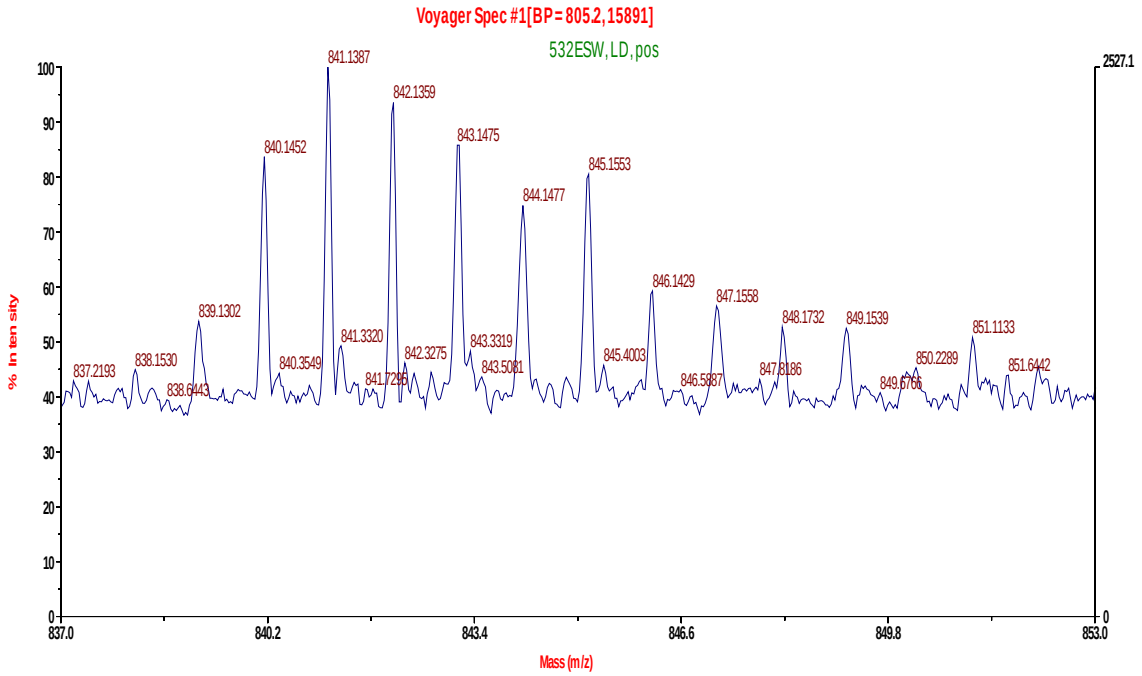

Figure 87. Laser Desorption Ionization-Time of Flight spectrum (LDI-TOF, negative mode for (**86**).

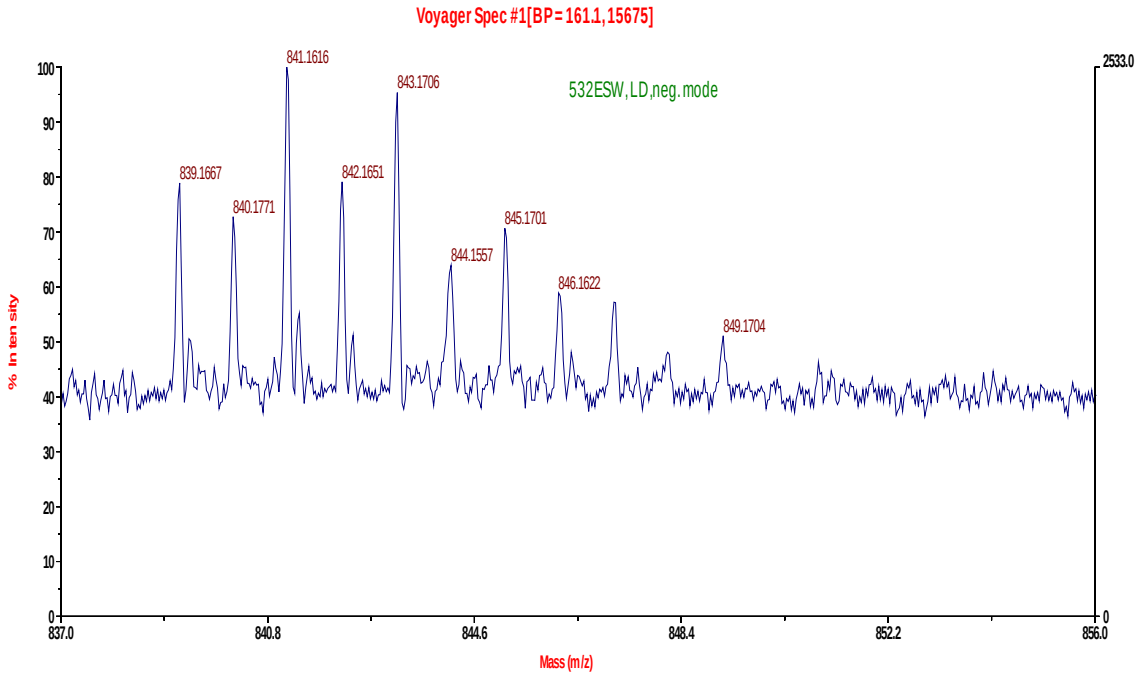

Figure 88. Laser Desorption Ionization-Time of Flight spectrum (LDI-TOF, negative mode for (**86**).

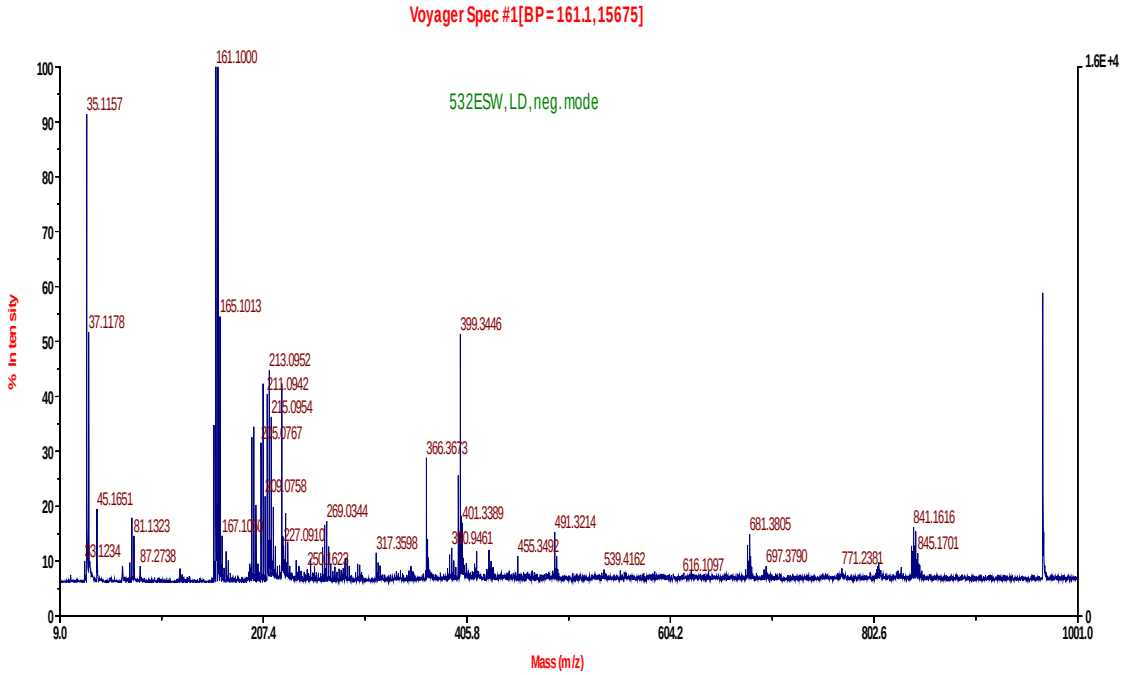

Figure 89. ^{1}H-NMR of dimethylsilyl[(5-methyl-(2,3-bis(benzothiaphen-3-yl) cyclopenta[b]thiaphen-6-yl)][(2,5-dimethyl-3-phenyl-cyclopenta[b]thiaphen-6-yl)]zirconium dichloride (**86**).

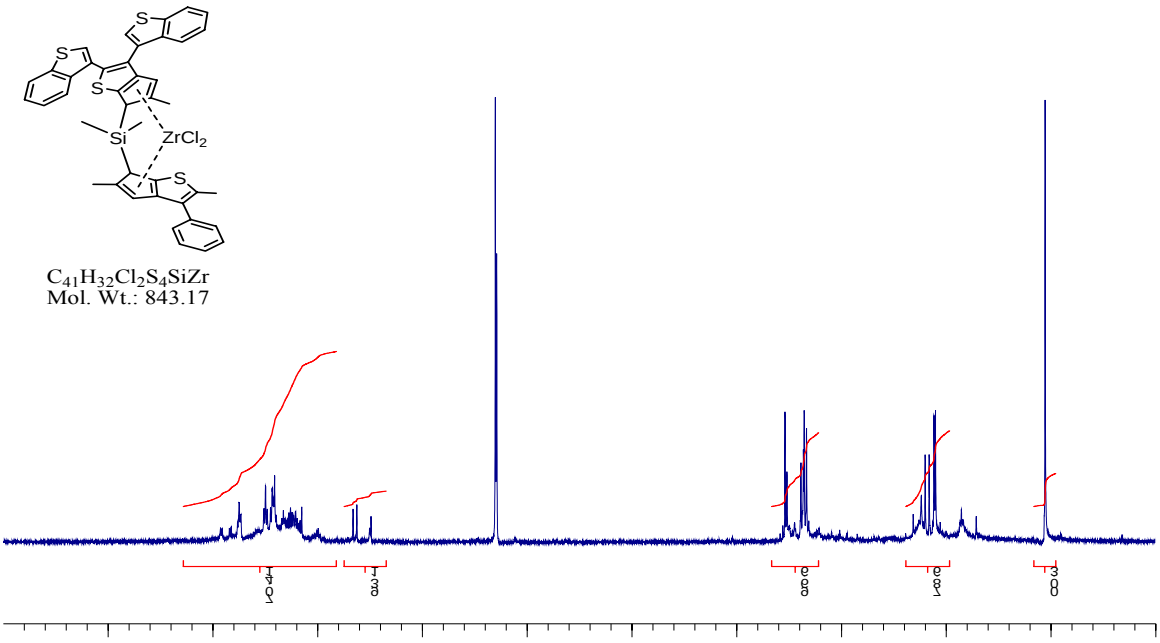

Notes on the ^{1}H-NMR spectrum of dimethylsilyl[(5-methyl-(2,3-bis(benzothiaphen-3-yl) cyclopenta[b]thiaphen-6-yl)][(2,5-dimethyl-3-phenyl-cyclopenta[b]thiaphen-6-yl)]zirconium dichloride (**86**): The spectrum was taken in deuterated dichloromethane.

There should be 15 aromatic protons, including the 2 on the Cp ring: 8 aromatic protons from the [benzo]thiophene, and 5 from the phenyl substitution. In addition, there should be 2 signals from the protons at the 2- position on the benzothiophene rings, which (according to Figure 50 and Figure 69) should come about 7.8 ppm. The signals from the Cp protons are found at 6.5 to 6.8: There are 2 sets of 2 singlets: the indication that -*rac* -*meso* isomers are present or that the spectra is complicated by torsional conformers from the benzothiophenes.

There should be 5 separate sets of methyl signals, all singlets. Instead we find a complicated ménage of coalesced peaks corresponding to the Cp- methyl signals (which are usually shifted more upfield (in the range of 2.2 to 2.6 ppm). The thiopentalene thiophene methyl signal is at 1,1, and the methyl signals from one of the two groups on the Si- bridge are split at 1.2. The remaining singlet at 0.0 is the methyl group on the clean side of the bridge, away from the benzothiophene substitutions.

Figure 90. UV-visible absorbance spectrum of dimethylsilyl[(5-methyl-(2,3-bis(benzothiaphen-3-yl) cyclopenta[b]thiophen-6-yl)][(2,5-dimethyl-3-phenyl-cyclopenta[b]thiophen-6-yl)]zirconium dichloride (**86**) in benzene (5 x 10^{-5}M), without (-) and with (-) UV irradiation.

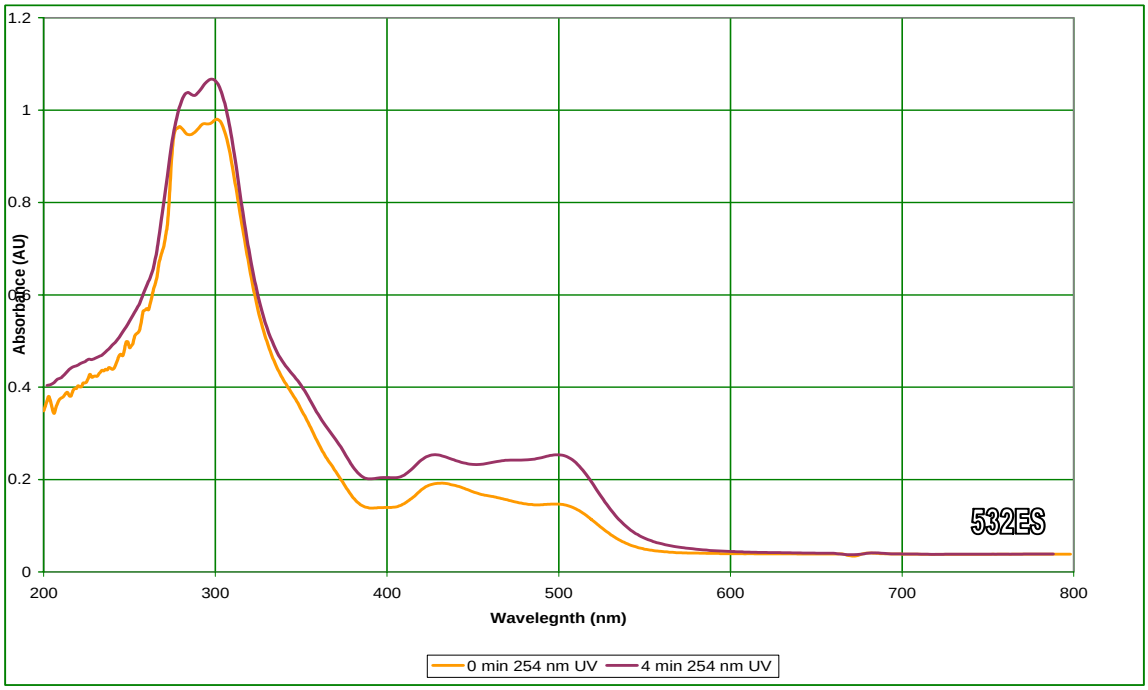

Note on UV-visible absorbance spectrum of dimethylsilyl[(5-methyl-(2,3-bis(benzothiaphen-3-yl) cyclopenta[b]thiophen-6-yl)][(2,5-dimethyl-3-phenyl-cyclopenta[b]thiophen-6-yl)]zirconium dichloride (**86**): the color of the metallocene complex is already slightly violet and irradiation changes the color even more, as evidenced in the UV-visible spectrum. The slight increase in color that is measured is an indication that the photochromic switch is closing under the influence of UV, similar to the olefin (starting material) seen in Figure 71.

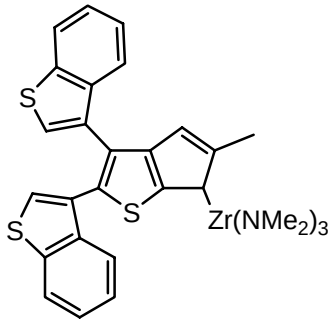

$C_{30}H_{33}N_3S_3Zr$
Mol. Wt.: 623.02

Synthesis of 2,3-bis(benzo[b]thiophen-3-yl)-5-methyl-thiopentalen-yl tris(dimethylamine)zirconium

In a flask containing 0.6 g (1.5 mmol) 2,3-bis(benzo[b]thiophen-3-yl)-5-methyl-cyclopenta[b]thiophene dissolved in 40 ml toluene was added 0.4 g (1.5 mmol) zirconium tetrakisdimethylamine. The reaction mixture was stirred for 18 h, then solvents were removed in vacuo. The dried material was slurried in hexane, then filtered and the hexane removed in vacuo: 0.64 g (530HS).

Solids remaining on the filter were slurried in dichloromethane and filtered: 0.46 g dark brown liquid which formed crystals upon standing.

Figure 91. ^{1}H-NMR of 2,3-bis(benzo[b]thiophen-3-yl)-5-methyl-thiopentalen-yl tris(dimethylamine)zirconium (**89**):

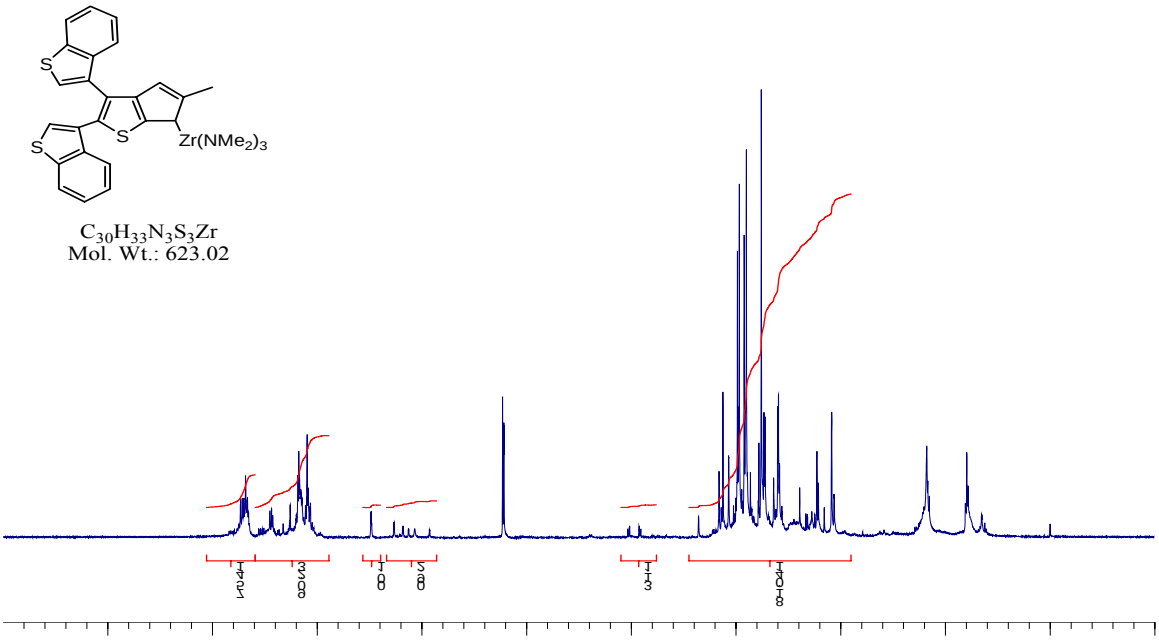

Figure 92. ^{1}H-NMR of 2,3-bis(benzo[b]thiophen-3-yl)-5-methyl-thiopentalen-yl zirconium tribromide (**90**).

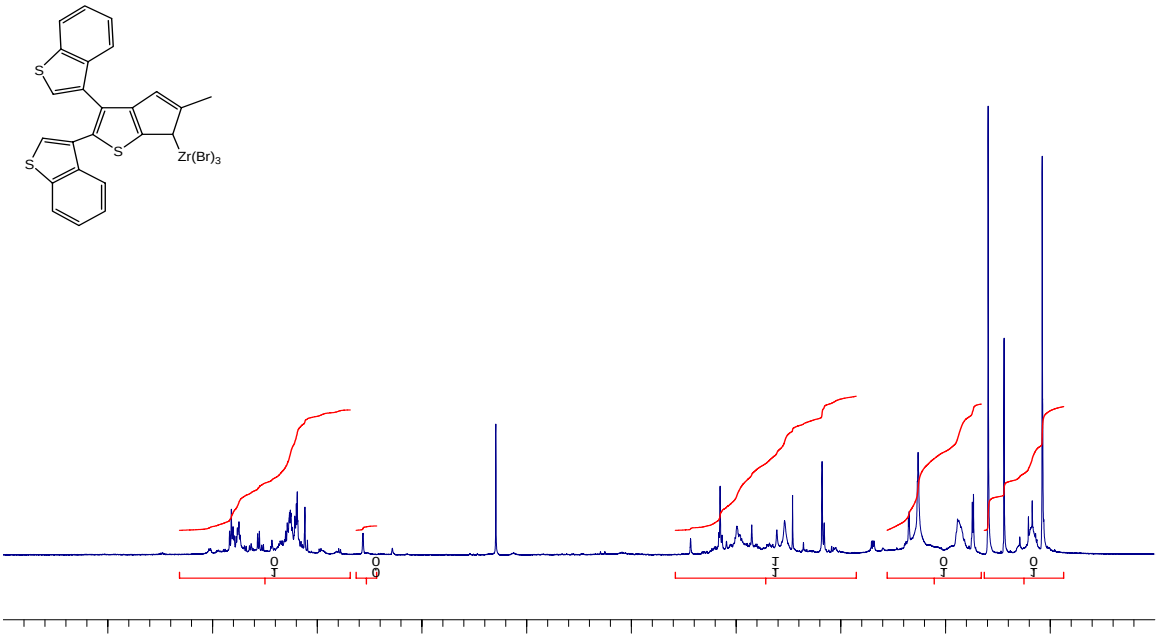

Synthesis of Benzo[b]tellurophene-3-boronic acid (boroxin)

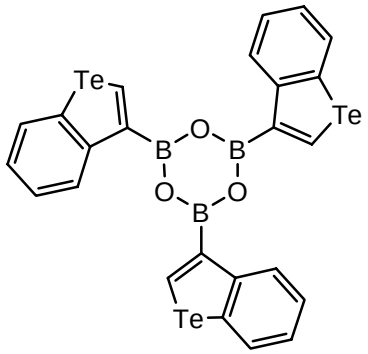

$C_{24}H_{15}B_3O_3Te_3$
Mol. Wt.: 766.61

In a flask containing 6.3 g (20.3 mmol) 3-bromobenzo[b]tellurophene dissolved in a solution containing 22 ml hexane and 4 ml THF was added 3.8 g (21 mmol) triisopropyl borate. The temperature was reduced to -78°C (dry ice/acetone) and a solution containing n-butyllithium was added dropwise (20 mmol, 8 ml, 2.5M in hexane). The reaction mixture was allowed to warm to about 0°C, then an aqueous solution containing HCl (1N) was added (22 mmol). The reaction mixture was dried in vacuo produced 6.54 g of a dark red oil which crystallized upon standing. 30% LC/UV: mass spectrum analysis at 20.46 m(21.966 m): [M] = [768].

Sample: 524P1
Chromatogram: DAD at 238nm
MS-TIC pos.Mode
MS-TIC neg.Mode

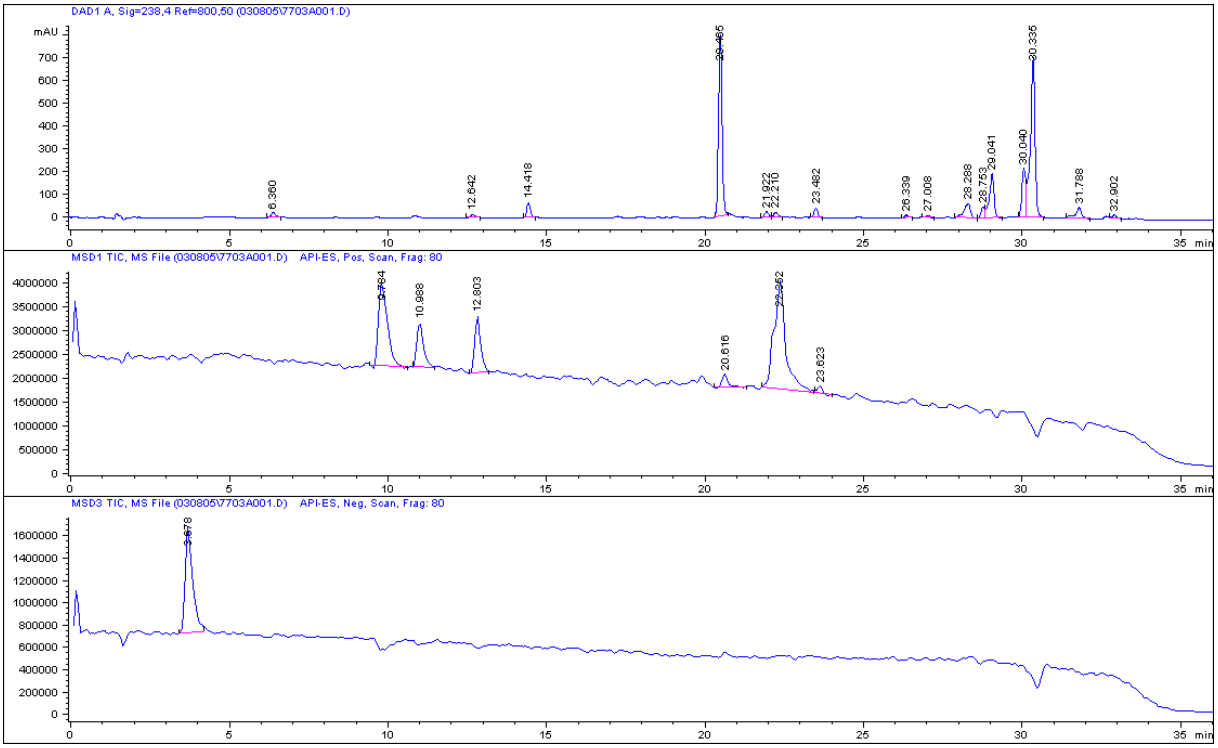

Peaktable (DAD at 238nm):

#	Time	Area	Height	Area%
1	6.36	216	21.6	0.999
2	12.64	128.6	13.2	0.595
3	14.41	516.6	65.7	2.389
4	20.46	6368.9	802.7	29.455
5	21.92	236.1	25.4	1.092
6	22.21	225.4	22.8	1.042
7	23.48	332.7	43.3	1.539
8	26.33	114.1	12.0	0.528
9	27.00	80.6	10.6	0.373
10	28.28	922.6	63.1	4.267
11	28.75	394.2	48.9	1.823
12	29.04	2023.8	193.8	9.360
13	30.04	1856	215.6	8.584
14	30.33	7338.1	704.7	33.937
15	31.78	689.5	48.8	3.189
16	32.90	179.2	17.8	0.829

MS-Spectra (pos. mode):

time	mass
3.743	161
6.529	339
9.796	301 (Te)
11.013	345 (Te)
12.807	470 (Te)
14.600	515
21.966	768 (Te)
20.621	701 (Te)
23.631	681 (Te)
26.514	981 (Te)
27.154	845 (Te)
28.499	867 (Te)
28.948	833 (Te)
29.204	835 (Te)
30.229	803 (Te)
30.485	807 (Te)

MS-Spektra (pos. Mode):

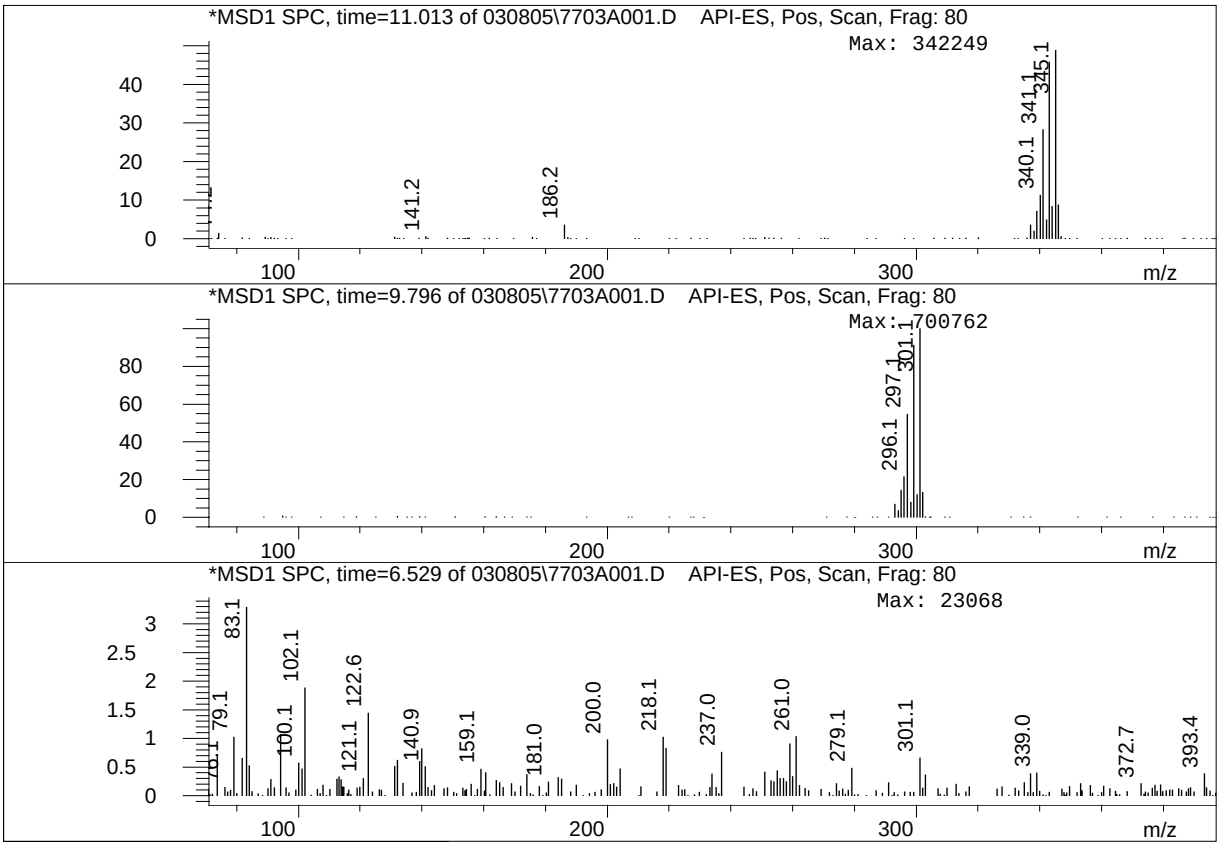

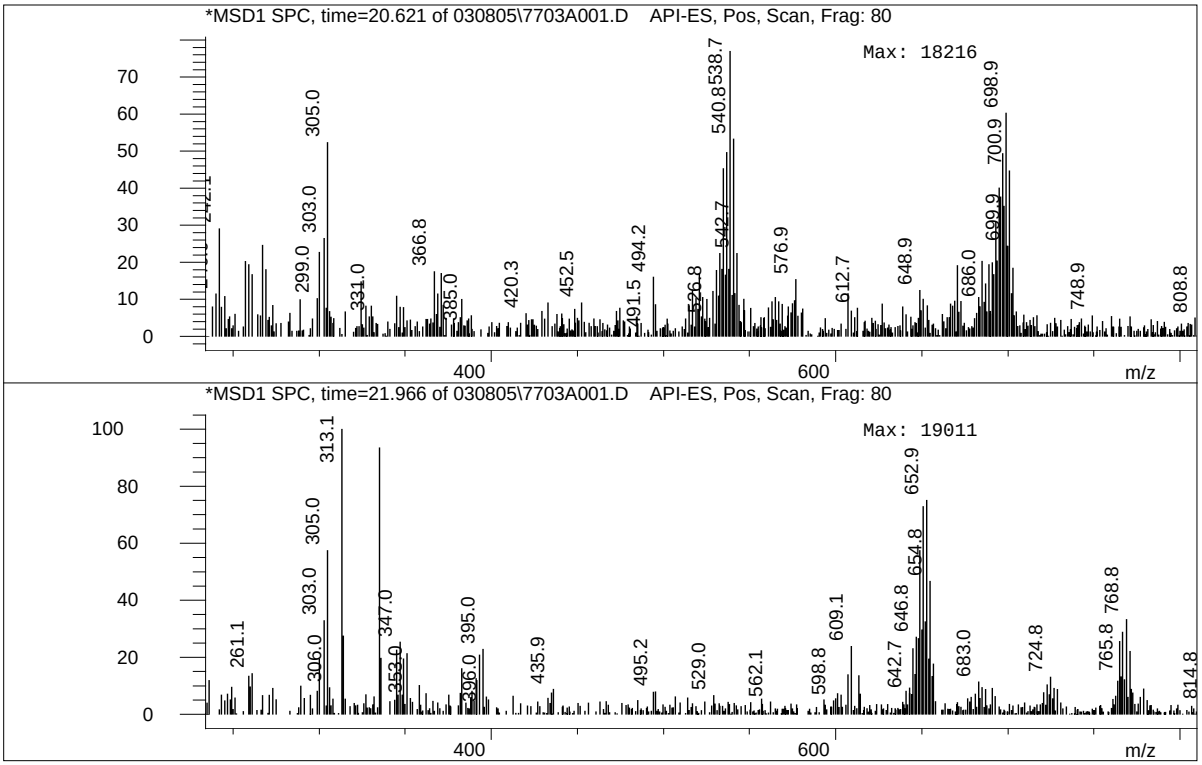
*MSD1 SPC, time=20.621 of 030805\7703A001.D API-ES, Pos, Scan, Frag: 80
Max: 18216
242.1
299.0
303.0
305.0
331.0
366.8
385.0
420.3
452.5
491.5
494.2
526.8
540.8
538.7
542.7
576.9
612.7
648.9
686.0
699.9
698.9
700.9
748.9
808.8
m/z
*MSD1 SPC, time=21.966 of 030805\7703A001.D API-ES, Pos, Scan, Frag: 80
Max: 19011
261.1
303.0
305.0
306.0
313.1
347.0
352.0
395.0
396.0
435.9
495.2
529.0
562.1
598.8
609.1
642.7
646.8
652.9
654.8
683.0
724.8
765.8
768.8
814.8
m/z

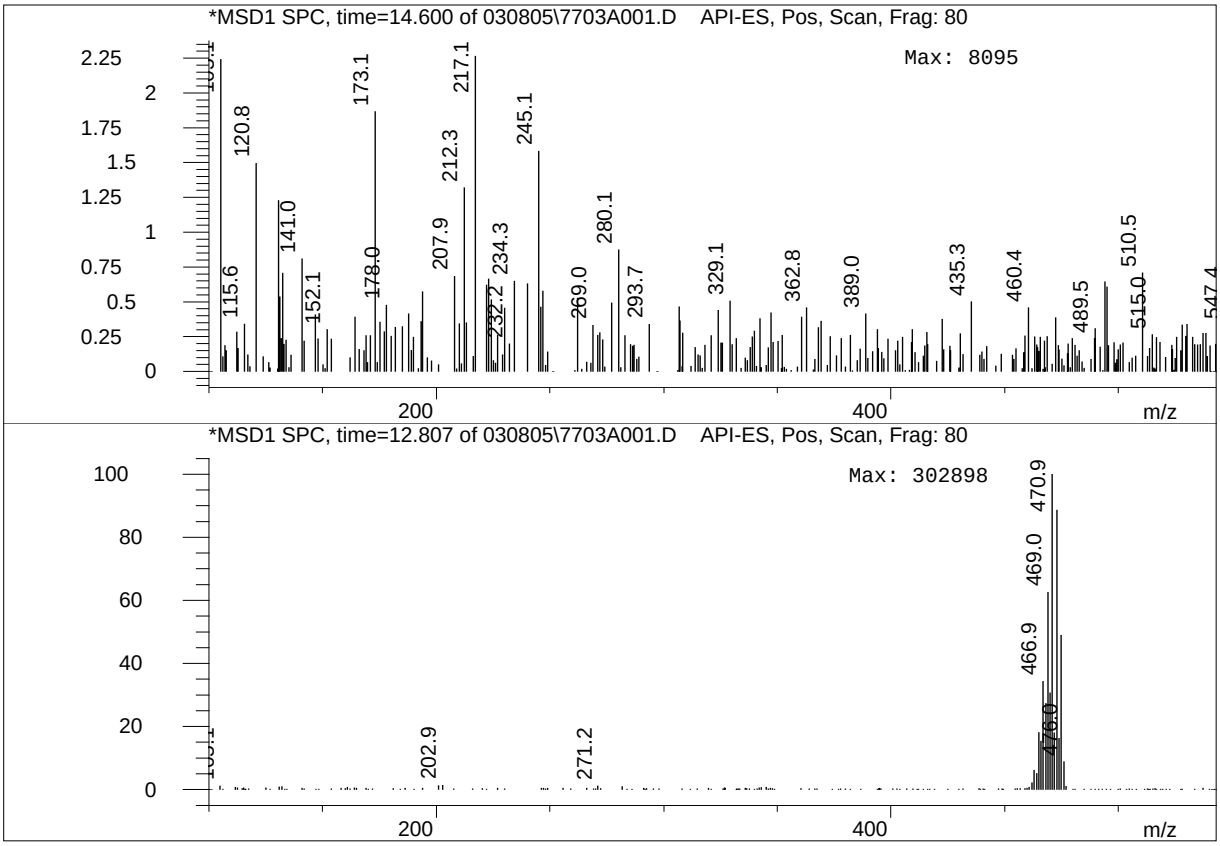
*MSD1 SPC, time=14.600 of 030805\7703A001.D API-ES, Pos, Scan, Frag: 80
Max: 8095
115.6
120.8
141.0
152.1
173.1
178.0
207.9
212.3
217.1
232.2
234.3
245.1
269.0
280.1
293.7
329.1
362.8
389.0
435.3
460.4
489.5
510.5
515.0
547.4
m/z
*MSD1 SPC, time=12.807 of 030805\7703A001.D API-ES, Pos, Scan, Frag: 80
Max: 302898
202.9
271.2
466.9
469.0
470.9
m/z

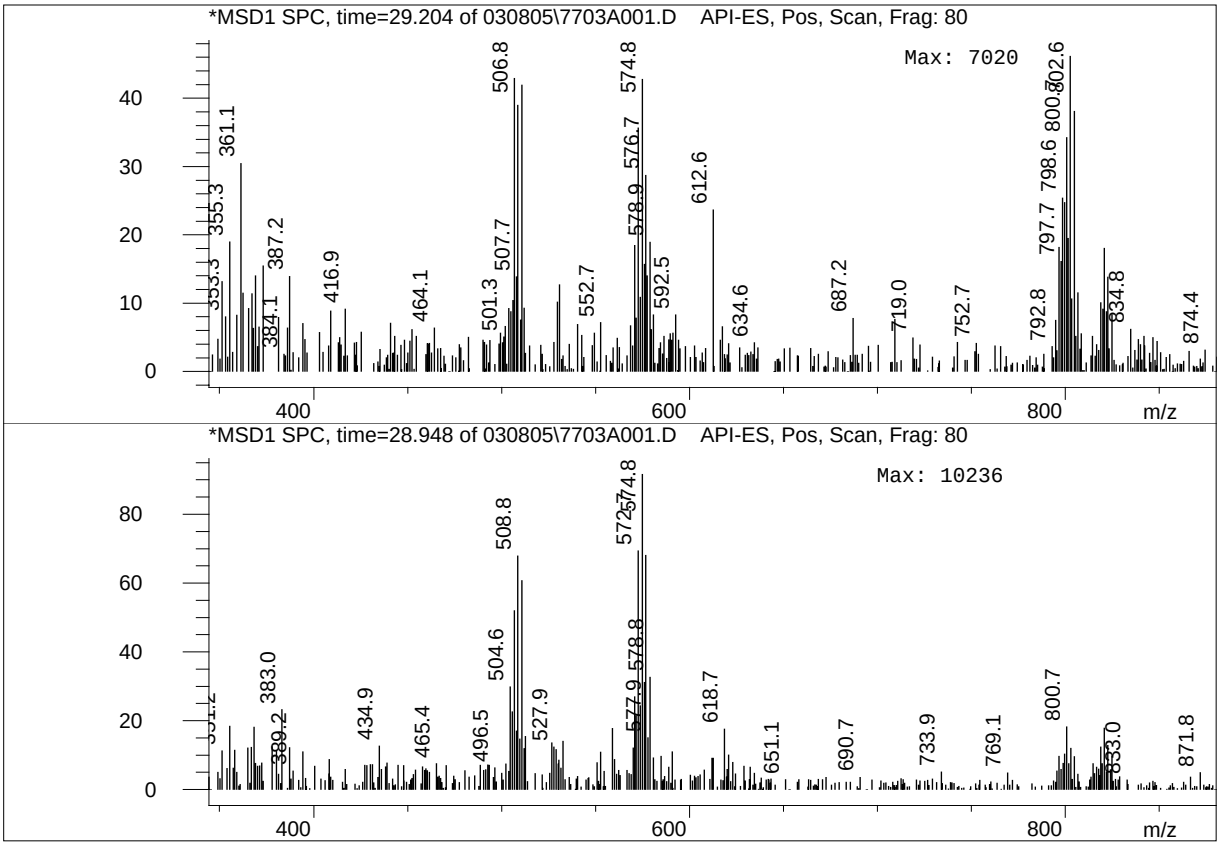
*MSD1 SPC, time=29.204 of 030805\7703A001.D API-ES, Pos, Scan, Frag: 80
Max: 7020
361.1
355.3
387.2
416.9
464.1
501.3
507.7
506.8
552.7
574.8
576.7
578.9
592.5
612.6
634.6
687.2
719.0
752.7
792.8
797.7
798.6
800.8
802.6
834.8
874.4
m/z
*MSD1 SPC, time=28.948 of 030805\7703A001.D API-ES, Pos, Scan, Frag: 80
Max: 10236
383.0
434.9
465.4
496.5
504.6
508.8
527.9
572.7
574.8
577.9
578.8
618.7
651.1
690.7
733.9
769.1
800.7
833.0
871.8
m/z

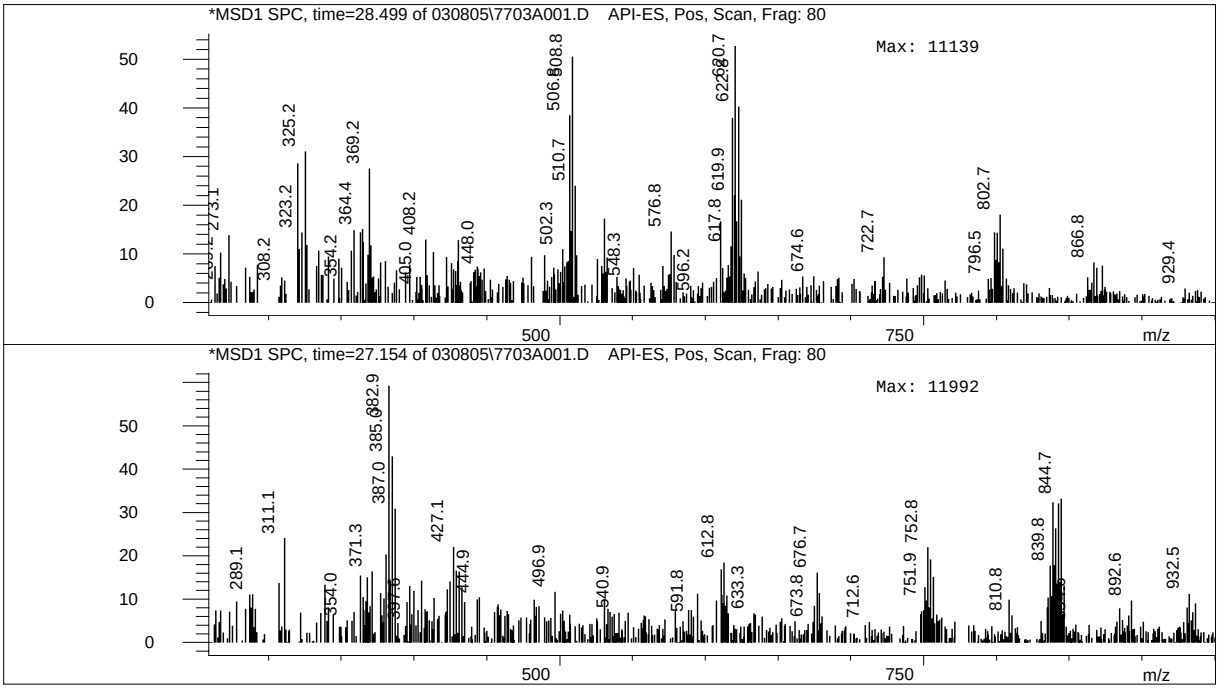
*MSD1 SPC, time=28.499 of 030805\7703A001.D API-ES, Pos, Scan, Frag: 80
Max: 11139
308.2
323.2
325.2
354.2
364.4
369.2
405.0
408.2
448.0
502.3
506.8
508.8
510.7
548.3
576.8
596.2
617.8
619.9
622.8
680.7
674.6
722.7
796.5
802.7
866.8
929.4
m/z
*MSD1 SPC, time=27.154 of 030805\7703A001.D API-ES, Pos, Scan, Frag: 80
Max: 11992
289.1
311.1
354.0
371.3
387.0
385.0
382.9
427.1
474.9
496.9
540.9
591.8
612.8
633.3
673.8
676.7
712.6
751.9
752.8
810.8
839.8
844.7
892.6
932.5
m/z

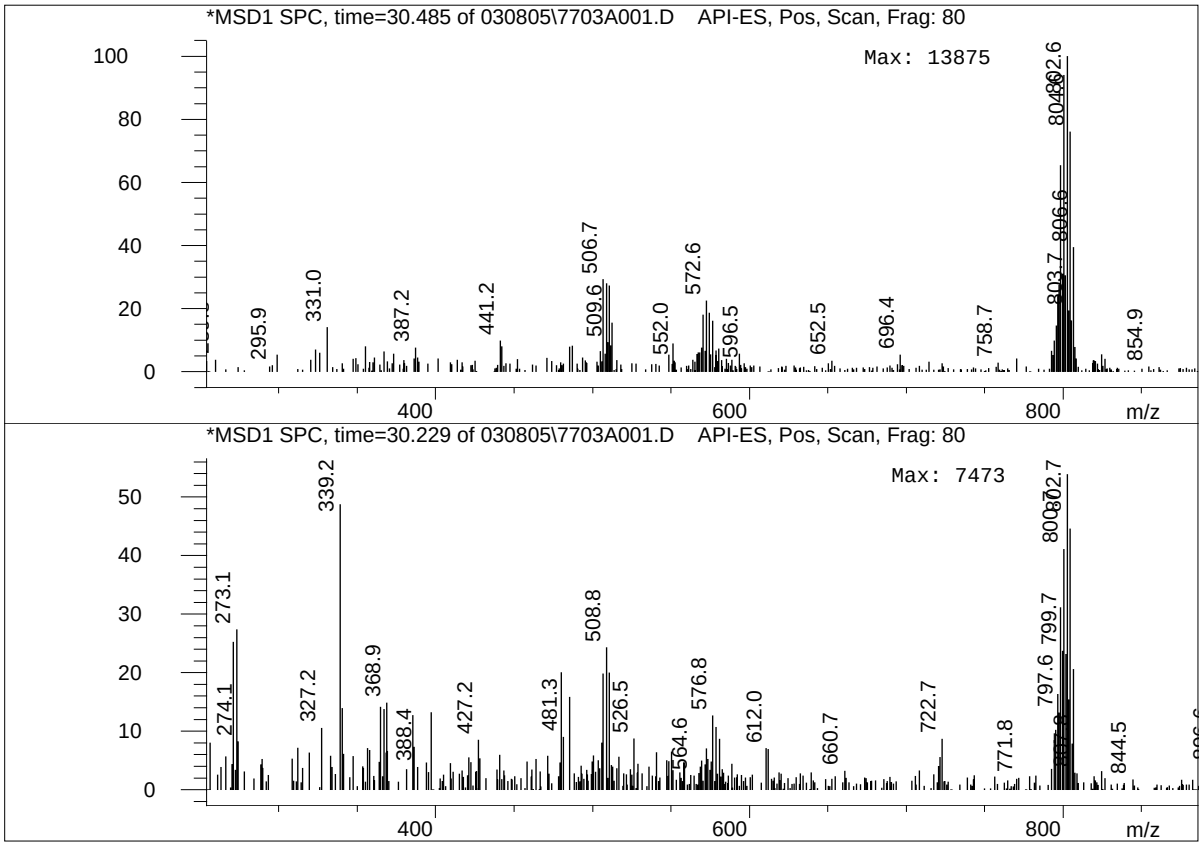

MS-Spectra (neg.Mode):

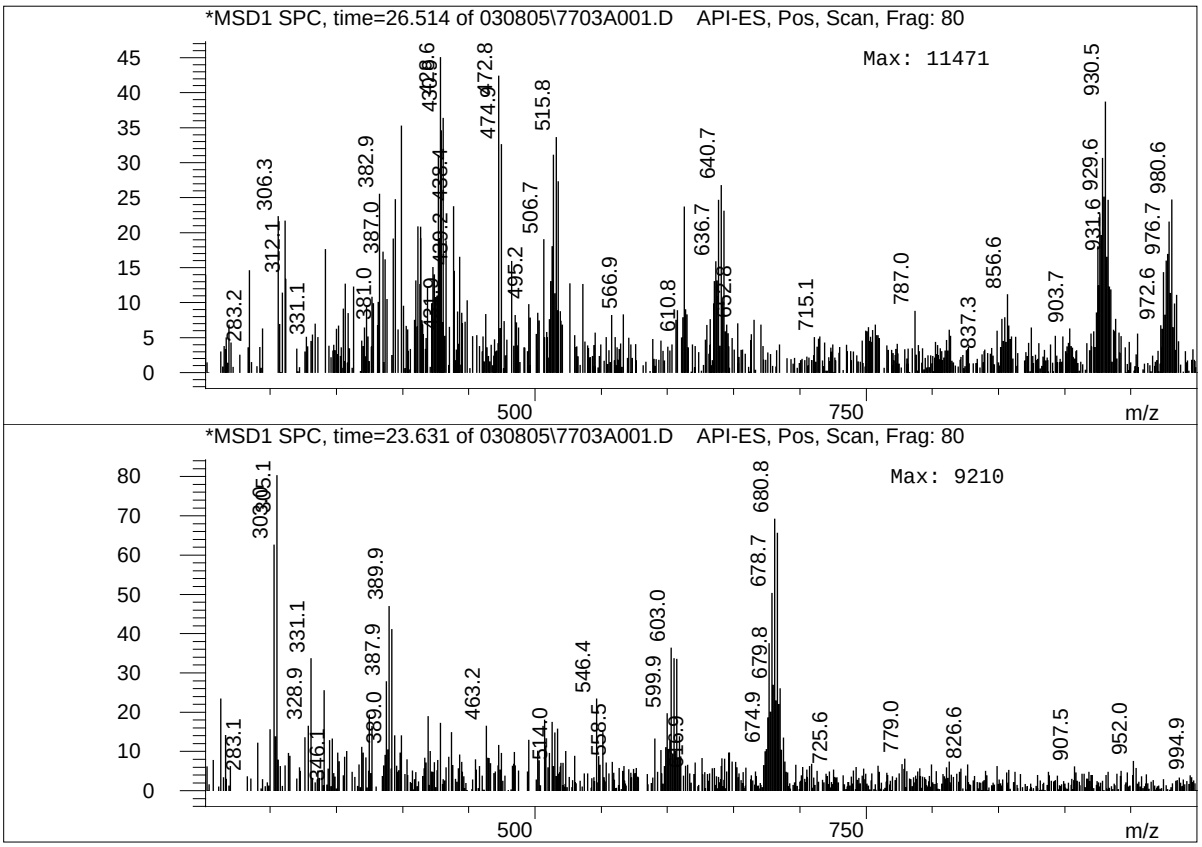

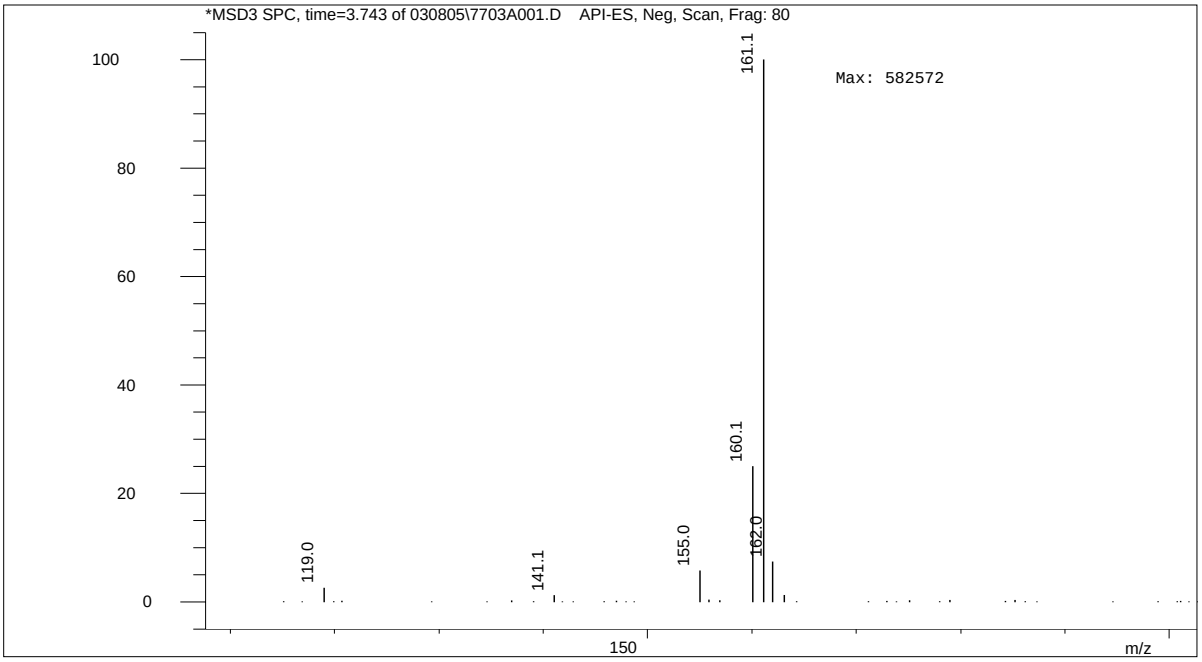
*MSD3 SPC, time=3.743 of 030805\7703A001.D API-ES, Neg, Scan, Frag: 80
Max: 582572
100
80
60
40
20
0
161.1
160.1
162.0
155.0
141.1
119.0
150
m/z

Figure 93. ^{1}H-NMR of product from benzotellurophene coupling experiment.

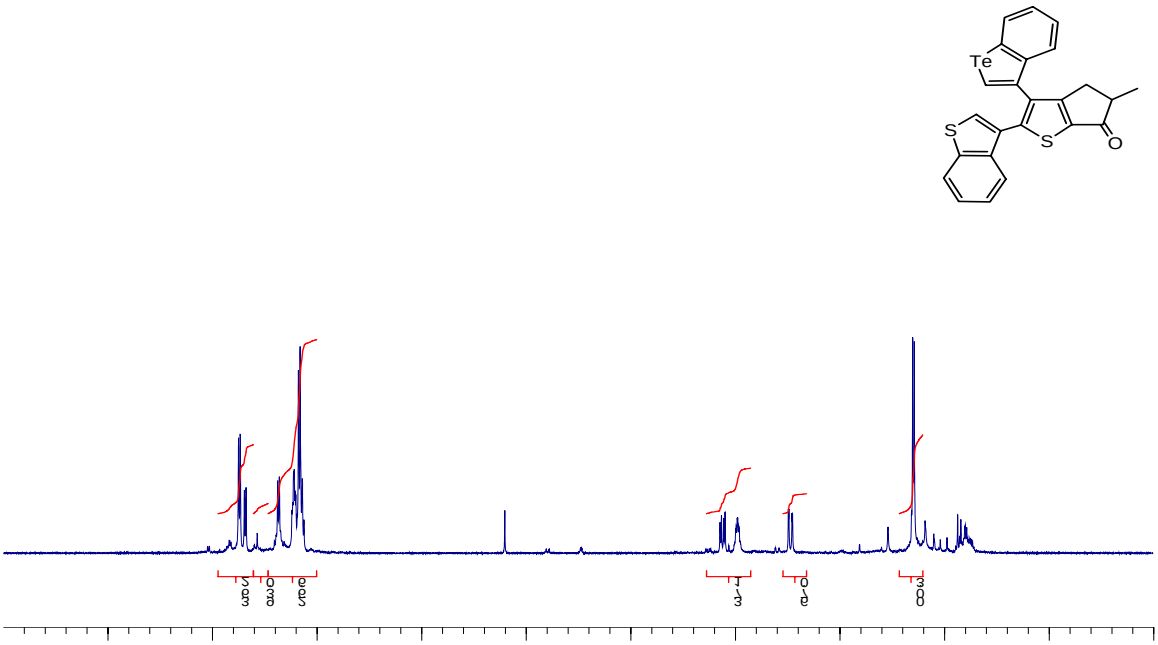

Figure 94. ^{1}H-NMR of comparative 2,3-dibenzthiophene substituted thiopentalene spectra.

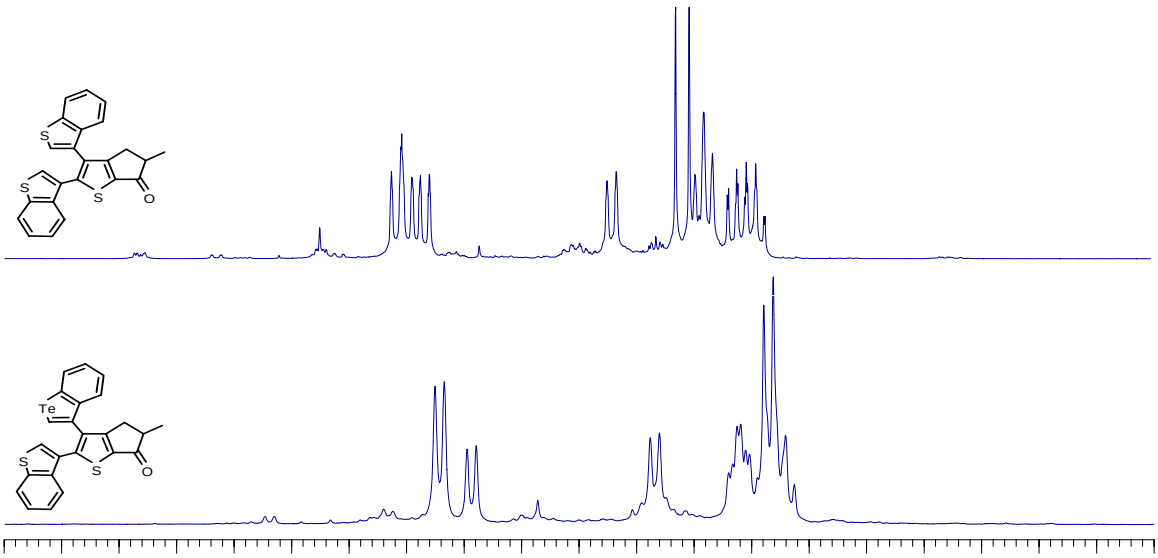

4.2.2 Additional Complexes Described and Tested:

The following complexes were available from the laboratory stockpile and were screened as candidates for photo-reactivity (available candidates and controls):

Numbering system and nomenclature for the olefin used in selected experiments:

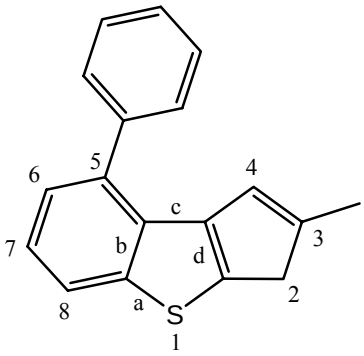 (**108**)	

Bis(3-methyl-5-phenyl-benzo[b]cyclopenta[d]thienyl)zirconium dichloride (**102**).
(ID: 200101-086)

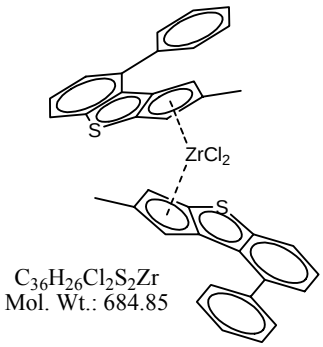

In a flask containing 2.62 g (10 mmol) 3-methyl-5-phenyl-benzo[b]cyclopenta[d]thiophene ("crab" olefin) dissolved in 70 mL diethyl ether was added a solution containing n-butyllithium (10 mmol, 4 mL, 2.5M in hexane), dropwise. The reaction mixture was stirred for 4 h, the 1.16 g (5 mmol) zirconium tetrachloride was slowly added as a dry powder. The reaction mixture was stirred for an additional 18 h, then filtered. The solids were washed with diethyl ether, then pentane. Solids were slurried in dichloromethane, filtered, then solvents removed from the filtrate. Yield: 3.04 g (80%).). ^{1}H-NMR δ ($CDHCl_2$): 8.0 – 7.0 (m, 16H), 6.0 – 5.7 (4d, 4H), 2.0 (s, 3H), 1.8 (s, 3H).

Figure 95. ^{1}H-NMR of Bis(3-methyl-5-phenyl-benzo[b]cyclopenta[d]thienyl)zirconium dichloride (**102**).

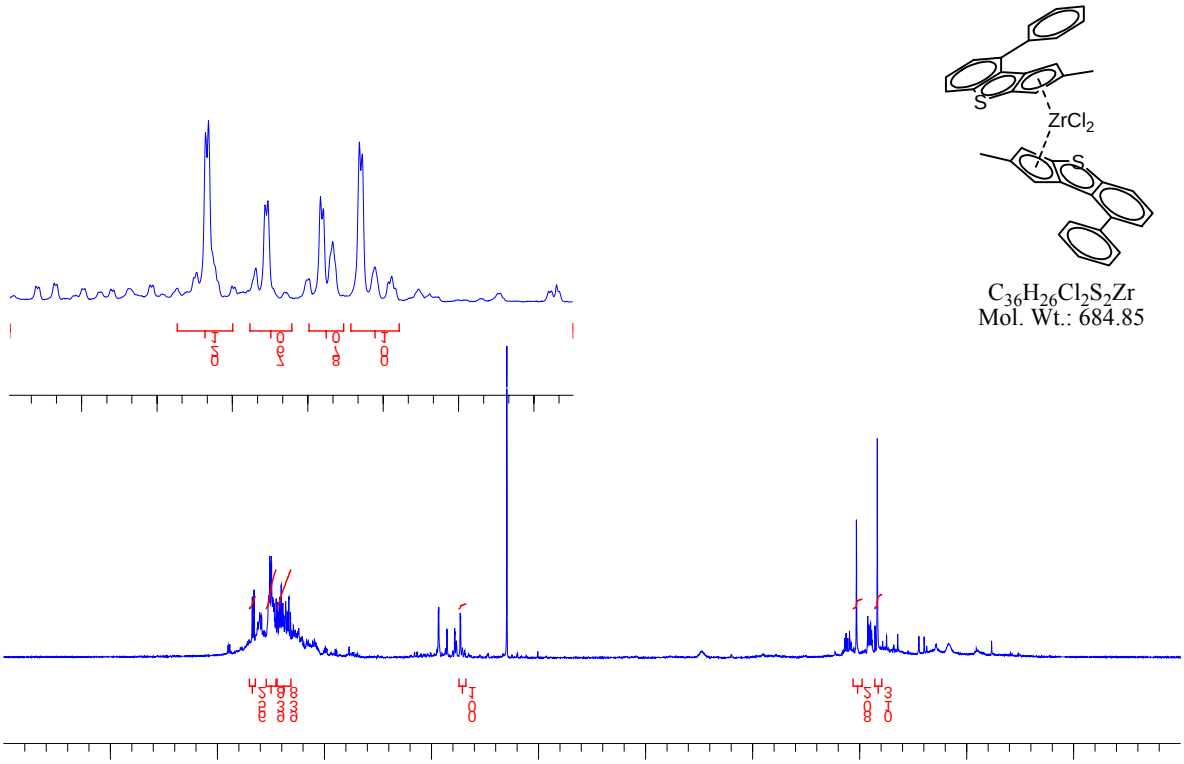

Dimethylsilysbis[2-phenyl-3-(2-tolyl)-5-methylcyclopent[b]thien-6-yl]zirconium dichloride

6, 6'-(Me_2Si)-{2-Ph-5-Me-3-(2-methylphenyl)-cyclopentadienyl[1,2-b]thiophene}$_2ZrCl_2$ (**25**). (from Basell Polyolefin: M.J. Elder synthesis)

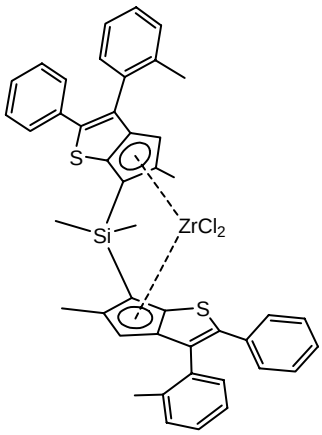

6, 6'-(Me_2Si)-{2-Ph-5-Me-3-(2-methylphenyl)-6-hydrocyclopenta[1,2-b]thiophene}$_2$ (6.73 g, 10.2 mmol) was dissolved in 80 mL of ether, cooled to –78°C, and treated with 8.5 mL of *n*-butyllithium in hexanes (2.5 M sol., 21.5 mmol). After stirring overnight at room temperature, solvents were removed *in vacuo* and $ZrCl_4$ (2.38 g) was added. The mixture was stirred in hexane (60 mL) / ether (60 mL) for 18 h. The reaction mixture was filtered through a closed frit and the yellow solids were washed with pentane and dried under vacuum (7.6 g of r/m mixture + LiCl*Et_2O). The crude product was extracted with CH_2Cl_2 and filtered through celite. The filtrate was concentrated; hexane was added and further concentrated to precipitate yellow solids. The first crop of yellow solids collected (2.2 g) were *ca*. 85% racemic isomer. ^{1}H-NMR δ (CD_2CL_2): 7.7 (m, 1H), 7.1-7.4 (m, 17H), 6.5 (s, 2H), 2.4 (s, 6H), 1.9 (s, 6H), 1.2 (s, 6H).

Dimethylsilylbis(2,3-diphenyl-5-methylcyclopenta[b]thienyl)zirconium dichloride (**26**):

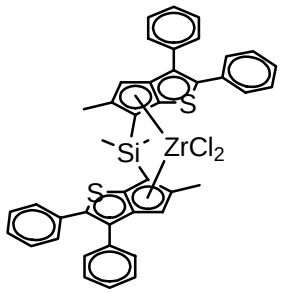

Catalyst was synthesized at the University of Moscow by the group of Dr. Ilya Nifant'ev in a manner similar to (**25**).

Synthesis of Me_2Si (4-(4-tert-Bu-Ph)-2-iPr-inden-1-yl)(2,3-Ph_2-5-Me-cyclopento[2,3-b]thiophen-6-yl)}$ZrCl_2$ (**27**).
(ref. 0008-170)[125]

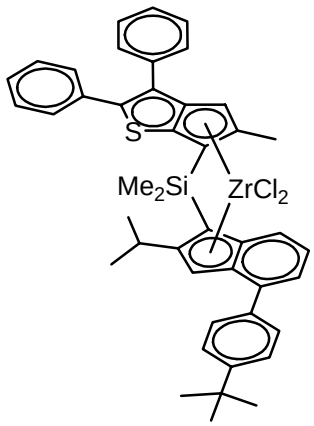

[4-(4-tert-Bu-Ph)-2-iPr-1H-inden-1-yl][2,3-Ph_2-5-Me-6H-cyclopenta [b]thiophen-6-yl]dimethylsilane (10.0 g, 15.8 mmol) was dissolved in 75 mL of ether, cooled to –78°C, and treated with 13 mL of butyllithium in hexanes (2.5 M, 32.5 mmol). After stirring at room temperature for 16 h, solvents were removed under reduced pressure giving a yellow glass-like solid. The solid was pulverized with a spatula in a glove box and zirconium (IV) chloride (3.68 g, 15.8 mmol) was added as a dry powder. The mixture was stirred in 60 mL of pentane for 1 h, then 1.5 mL of ether was added at -40°C and the mixture was warmed to room temperature and stirred for 18 h. The resulting yellow precipitate (12.5 g, ca. 91% of total mass) was collected on a closed frit funnel, washed with pentane, and dried in vacuo. Based on proton NMR spectra of this material, the metallocene yield was low (< 20%). Repeating the reaction in 100% ether improved the conversion to metallocene based on the proton NMR spectra of the precipitated product (67% of total mass, > 85% metallocene, ~2/1 *rac/meso* ratio). A sample of the *rac*-isomer was isolated by stirring at reflux 1 g of crude material with 200 mg of LiCl in 20 mL of DME. After cooling, the mixture was filtered and the yellow solids were washed with ether and pentane. The *rac*- zirconocene (400 mg) was extracted from the yellow soilds with dichloromethane. Running the LiCl reaction in THF gave only decomposition products. ^{1}H-NMR δ ($CDCl_3$): (*rac*- isomer) 7.1-7.7 (m, 19H), 6.6 (s, 1H), 3.4 (m, 1H), 2.2 (s, 3H), 1.4 (s, 9H), 1.35 (s, 3H), 1.2 (s, 3H),1.2 (d, 3H), 1.1 (d, 3H).

[125] Basell Polyolefins, Laboratory Notebook . 0008-170, M.J. Elder, 2005.

Figure 96. 2,5-Me_2TP-$ZrBr_3$ (spectra included for reference/comparison).

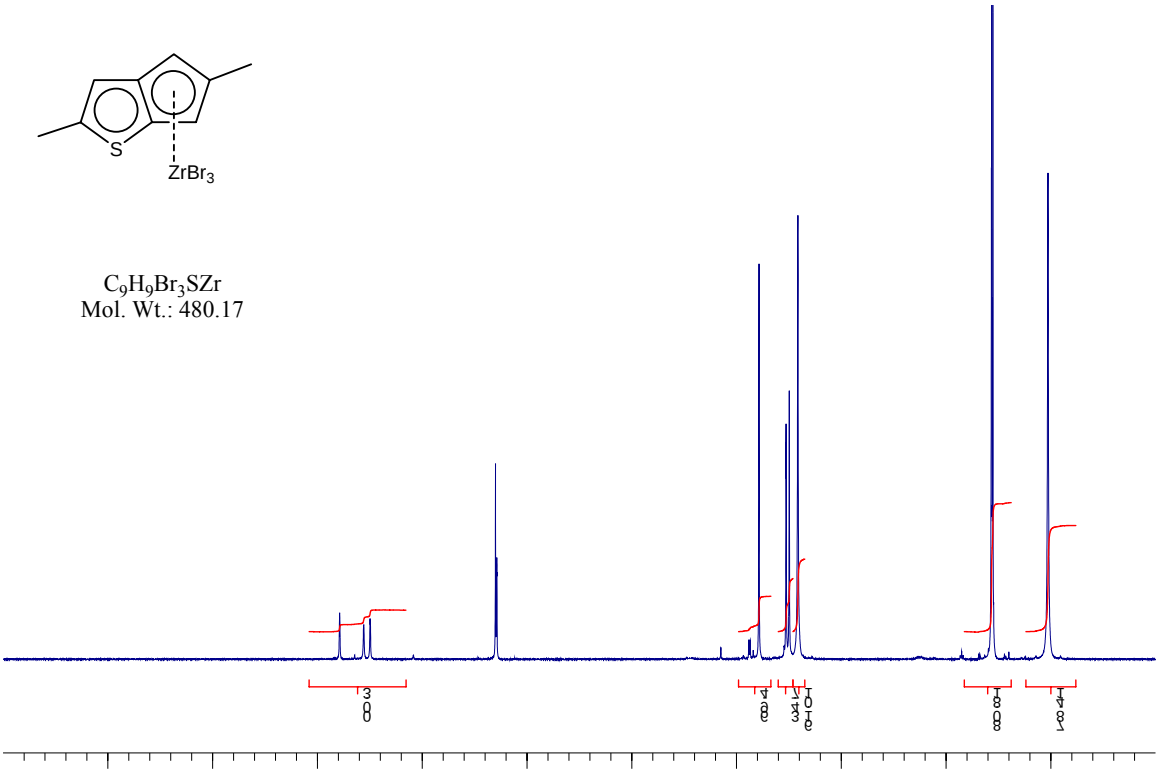

2-methylbenzo[b]thiophen-3-yl-3-boronic acid (**88**)
(ID: 079):

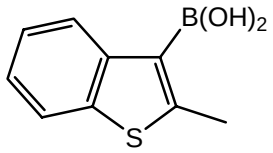

In a flask containing 2.3 g (10 mmol) 3-bromo-2-methylbenzo[b]thiophene (-068P2) dissolved in a solution containing 2.88 g THF and 10 g toluene) was added 2.25 g (12 mmol) triisopropyl borate. The reaction mixture was cooled to -78°C, then a solution containing n-butyllithium was added dropwise (12 mmol, 4.8 ml, 2.5M in hexanes). After addition was completed, the ice bath was removed and stirring was continued for an additional 1h. The reaction was quenched with 20 ml of 1N HCl, organics were collected with diethyl ether, dried over magnesium sulphate, filtered, then solvents were removed in vacuo. 1.98 g off white free flowing powder. Sample was further washed with acetonitrile and dried in vacuo: 0.94 g recovered (insoluble) from washing. Yield 50%. Elemental analysis of the boronic acid (Theo) found : %C = (56.29) 61.4, % H = (4.72) 4.6, %S = (16.7) 16.5. LCMS $[M]^+$ 191. (Ionization electrospray LCMS: Kromolith 10cm 0.3um 85% H_2O (0.1% HCOOH)/15% CH_3CN 2mL/min.)

Figure 97. ^{1}H-NMR Thianapthalene-3-boronic acid (Aldrich, for reference):

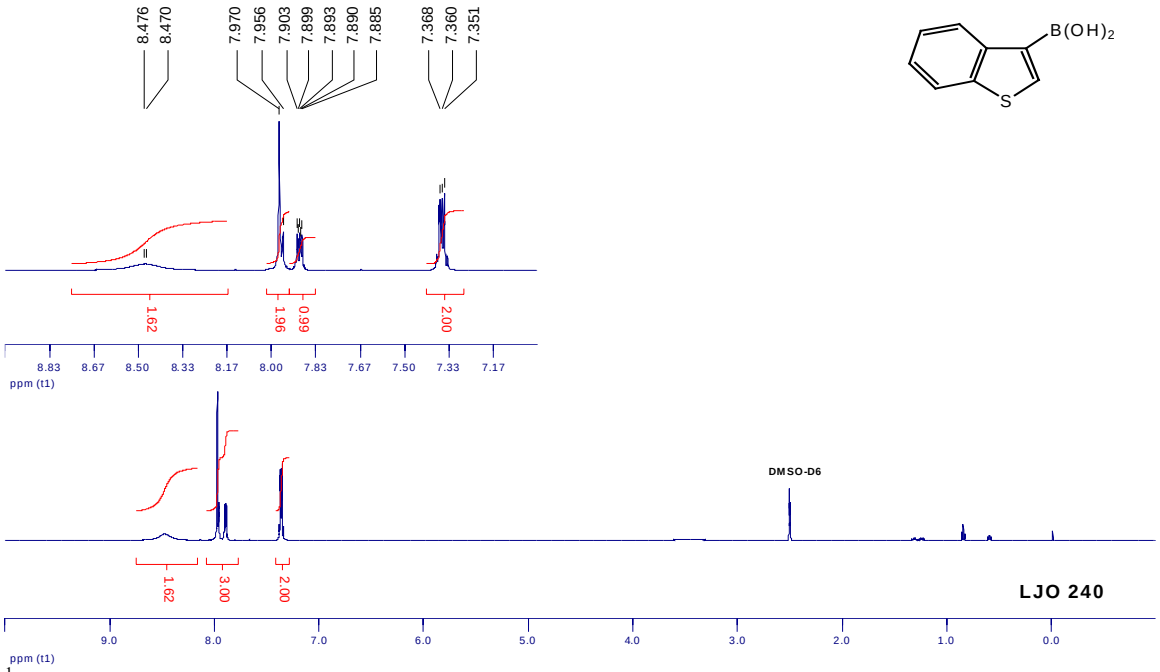

^{1}H-NMR δ (DMSO-D$_6$): 8.46 (s, 1H), 7.95 (m, 1H), 7.89 (m, 2H), 2.86 (m, 3H).

Figure 98. ^{1}H-NMR 2-methylbenzo[b]thiophen-3-yl-3-boronic acid (**88**).

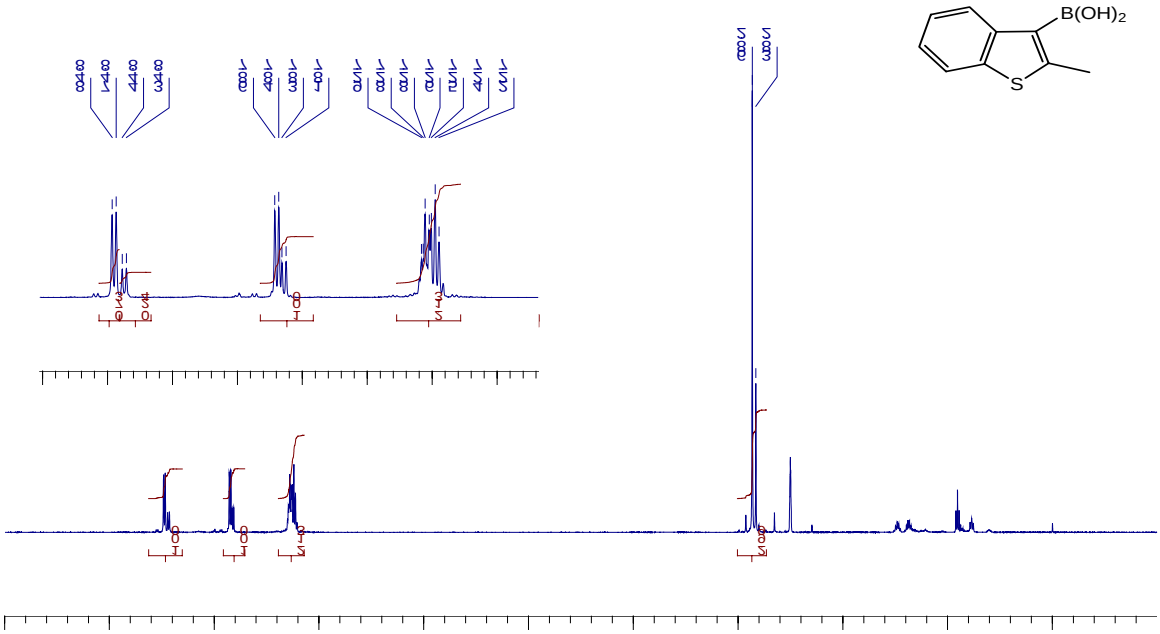

^{1}H-NMR δ (DMSO-D$_6$): 8.46 (m, 1H), 7.84 (m, 1H), 7.23 – 7.29 (m, 2H), 2.86 (m, 3H).

Figure 99. LC-MS ananytical results for (**88**)[126].

27/05/05 ALLIANCE/ZQ
MODE IONISATION ELECTRO SPRAY

Acide 2methyl thioindene 3boronique
O79P1-r1

ZQ05238 Kromolith 10cm 0.3um 85%H2O (0.1% HCOOH) / 15%CH3CN 2ml/mn splite
FV57047 DOSSIER 177 CAHIER21761 P10
zq05238 85%h2o0.01%hcooh-15%ch3cn chromolith

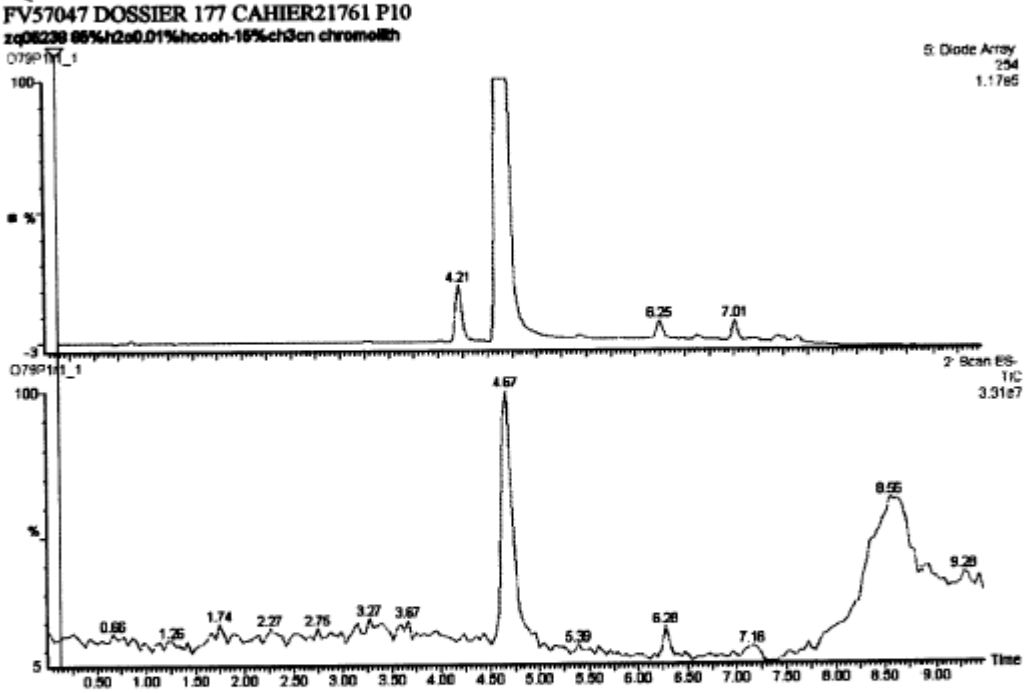

TR(SM)	Masse ES-	Masse supposee	STRUCTURE PROPOSEES
4.2	Pas d'ion	?	
4.7	191	192	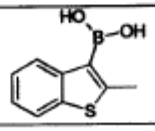
6.25	317	318?	Produit poly chlore ?
7.0	Pas d'ion	?	

[126] Analysis was provided by Clariant, LaMotte.

4.2.3 Preparation of the Dihydropyrene Photoswitch:

The synthesis of the dihydropyrene photoswitch followed the procedure published by Mitchell et al[127], as found in the Supporting Information, with the following modifications:

Synthesis of 5-tert-butyl-1,3-bis(bromomethyl)-2-methylbenzene.

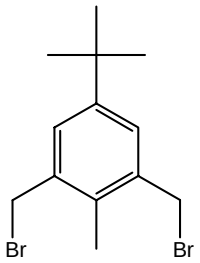

$C_{13}H_{18}Br_2$
Mol. Wt.: 334.09

In a 3-neck 1 liter Morton flask with mechanical stirrer under nitrogen atmosphere was placed 70.96 g (480 mmol) 4-tert-butyl toluene, 38.8 g (430 mmol) 1,3,5-trioxane, 15.77 g (70 mmol) zinc di-bromide, 250 ml of hydrogen bromide, and 10 ml glacial acetic acid. The mixture was heated to 85°C, then stirred for 14 d (cooling at night and over the weekends). The mixture was poured onto ice, washed with bicarbonate, water, dried over magnesium sulfate then solvents were removed in vacuo: 143.70 g dark brown oil which crystallizes upon standing: GCMS, EIMS, m/z (%): 257 (1), 256 (14) 254 (16), 253 (100):

[127] Reginald H. Mitchell, Timothy R. Ward, Yongsheng Chen, Yunxia Wang, S. Ananda Weerawarna, Peter W. Dibble, Michael J. Marsella, Adah Almutairi, and Zhi-Qiang Wang, "Synthesis and Photochromic Properties of Molecules Containing [e]-Annelated Dihydropyrenes. Two and Three Way ð-Switches Based on the Dimethyldihydropyrene-Metacyclophanediene Valence Isomerization", *J. Am. Chem. Soc.*, (**2003**), *125*, 2974-2988.

Figure 100. ^{1}H-NMR of 4-tert-butyltoluene (starting material: Aldrich)

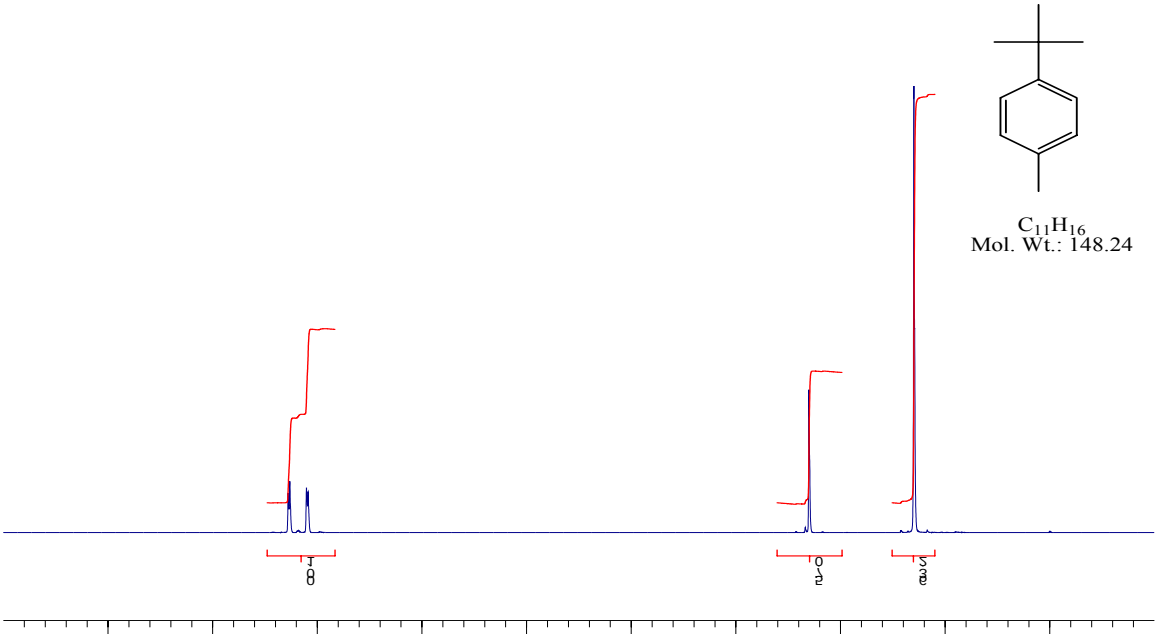

Figure 101. ^{1}H-NMR of 5-tert-butyl-1,3-bis(bromomethyl)-2-methylbenzene.

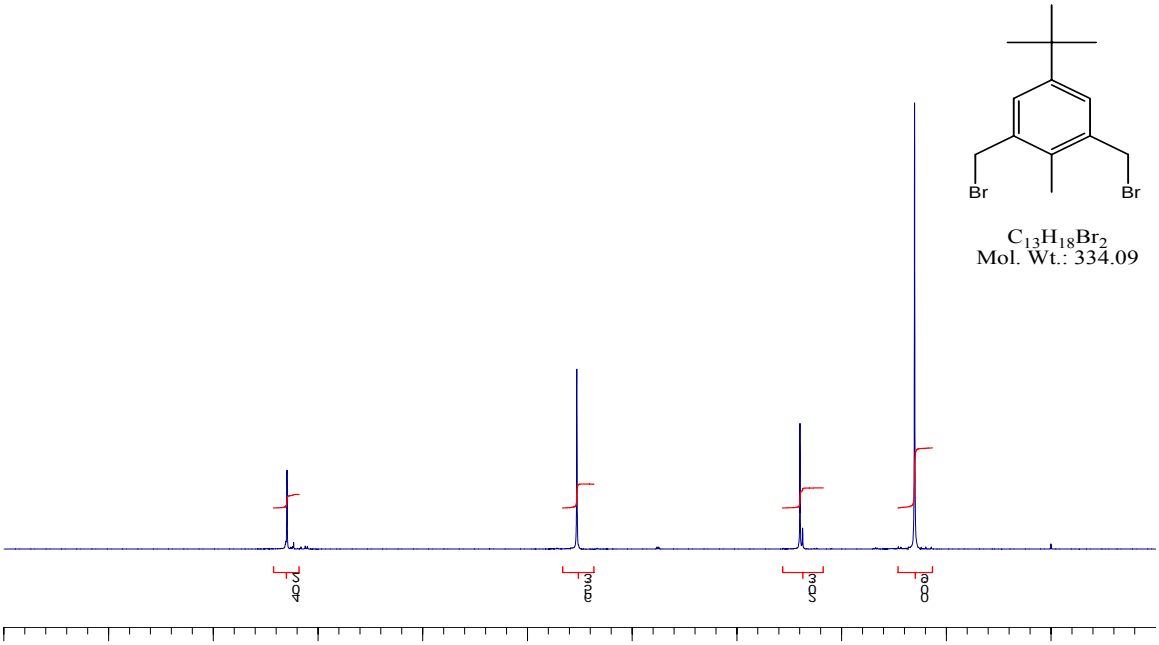

Synthesis of 2,6-Bis(mercaptomethyl)-4-tert-butyltoluene

(00038-199, 100-025)

Procedure was followed exactly as described in the literature:

Figure 102. ^{1}H-NMR of 2,6-Bis(mercaptomethyl)-4-tert-butyltoluene

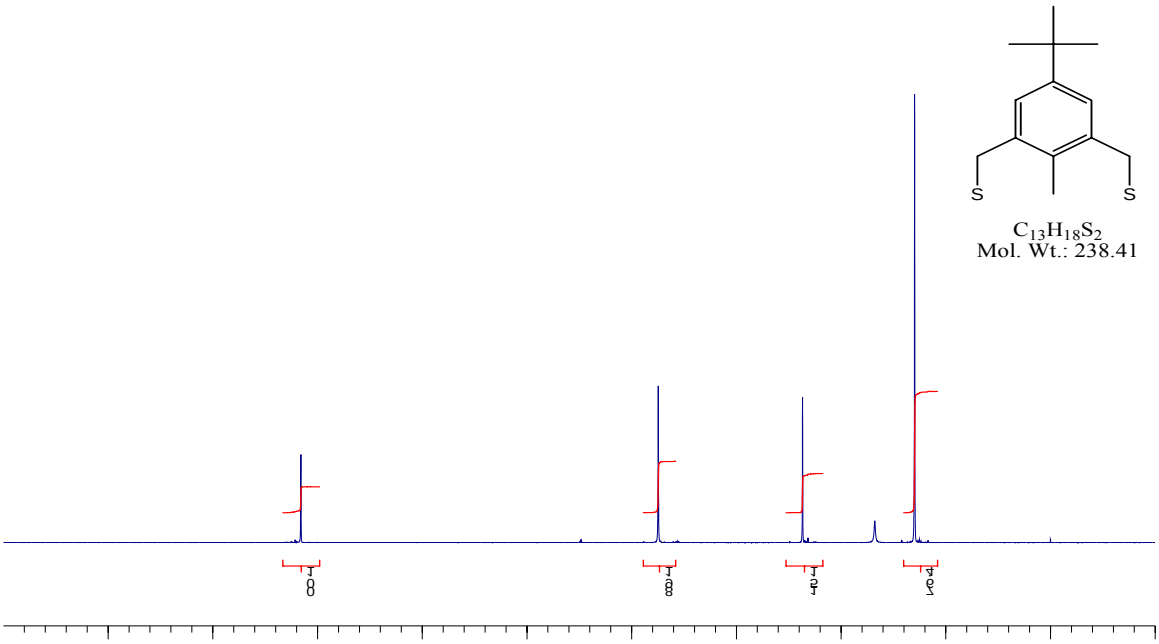

Synthesis of 1,15-di-tert-butyl-anti-9,18-dimethyl-2,11-dithia[3.3]metacyclophane

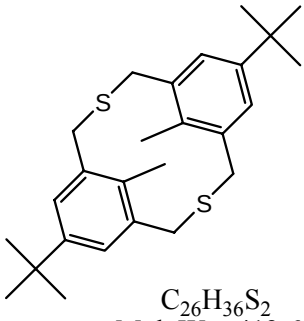

$C_{26}H_{36}S_2$
Mol. Wt.: 412.69

In a 2l flask with mechanical stirring was added 14 g KOH, 300 ml H2O, 500 ml Ethanol: the system was de-aerated then 3.8 g sodium borohydride was added. With rapid stirring, a solution containing 7.0 g (20.3 mmol) 5-tert-butyl-1,3-bis(bromomethyl)-2-methylbenzene and 4.88 g (20.3 mmol) 2,6-Bis(mercaptomethyl)-4-tert-butyltoluene in anhydrous toluene was added dropwise. The reaction mixture was stirred for 2 h (GCMS sample indicated no starting material remained): the sample was stirred an additional 18 h

(overnight), then solvents were removed in vacuo. Solids were dissolved in dichloromethane, washed with water, dried over magnesium sulphate, then solvents removed in vacuo: 9.03 g (white paste):

In a 6L flask with mechanical stirring and 1L addition funnel was added 500 ml H2), 2.5 L ethanol, 28 g KOH, the solution was de-aerated then 10.55 g sodium borohydride was added. A solution containing 39.29 g (117 mmol) of the dibromide and 28 g (117 mmol) of the disulfide dissolved in 800 ml toluene were added dropwise (over a 6 h time period). The reaction was stirred an additional 1h, then solvents removed in vacuo. The white chalky material remaining was emulsified in dichloromethane, washed with water, dried over magnesium sulphate, then filtered. The solids recovered for drying were re-crystallized from hot toluene: 52.2 g recovered.

Figure 103. ^{1}H-NMR of 1,15-di-tert-butyl-anti-9,18-dimethyl-2,11-dithia[3.3]metacyclophane.

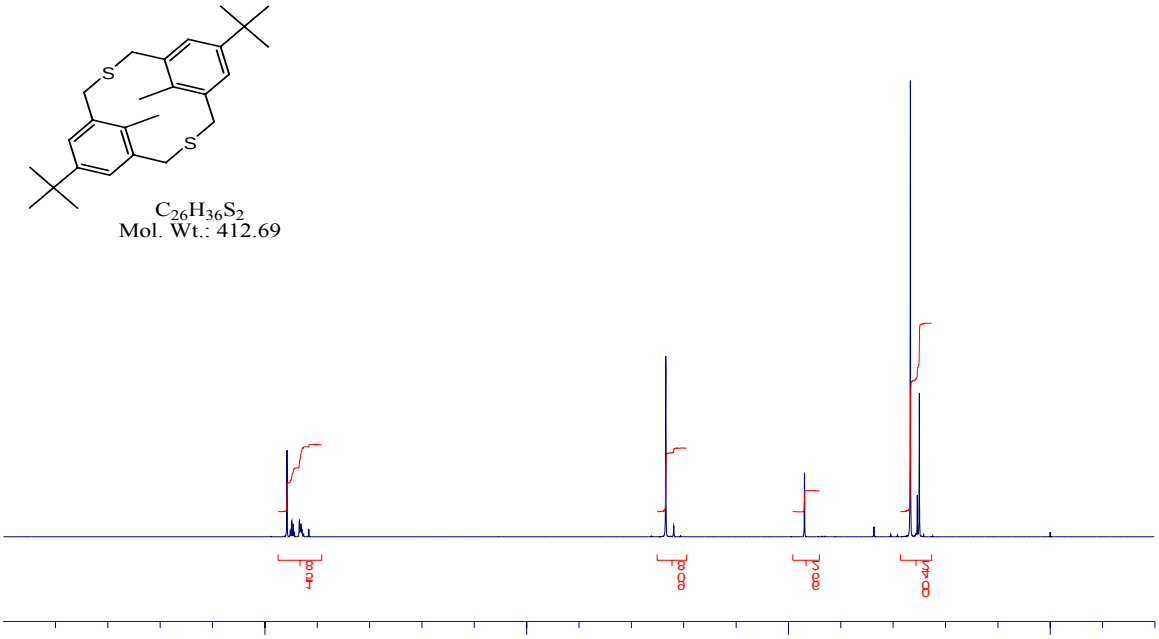

Wittig Re-arrangement of 1,15-di-tert-butyl-anti-9,18-dimethyl-2,11-dithia[3.3]metacyclophane

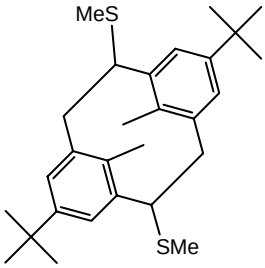

$C_{28}H_{40}S_2$
Mol. Wt.: 440.75

In a 1l flask with 125 ml addition funnel was added 30.36 g (73.4 mmol) of the coupled disulfide (above), dissolved in 500 ml THF at 0°. A solution containing n-butyllithium was added dropwise (300 mmol, 120 ml, 2.5M in hexane). After addition was complete the reaction mixture was stirred for an additional 2h at ambient temperature, then the reaction mixture was cooled and 45 g (320 mmol) iodomethane was added dropwise. After stirring an additional 1h, the reaction mixture was poured into water; organics were extracted with dichloromethane, washed with water, dried over magnesium sulphate, then solvents removed in vacuo: 31.03 g yellow solid.

Figure 104. ^{1}H-NMR of product from Wittig reaction:

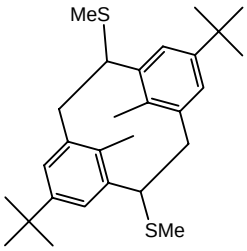

$C_{28}H_{40}S_2$
Mol. Wt.: 440.75

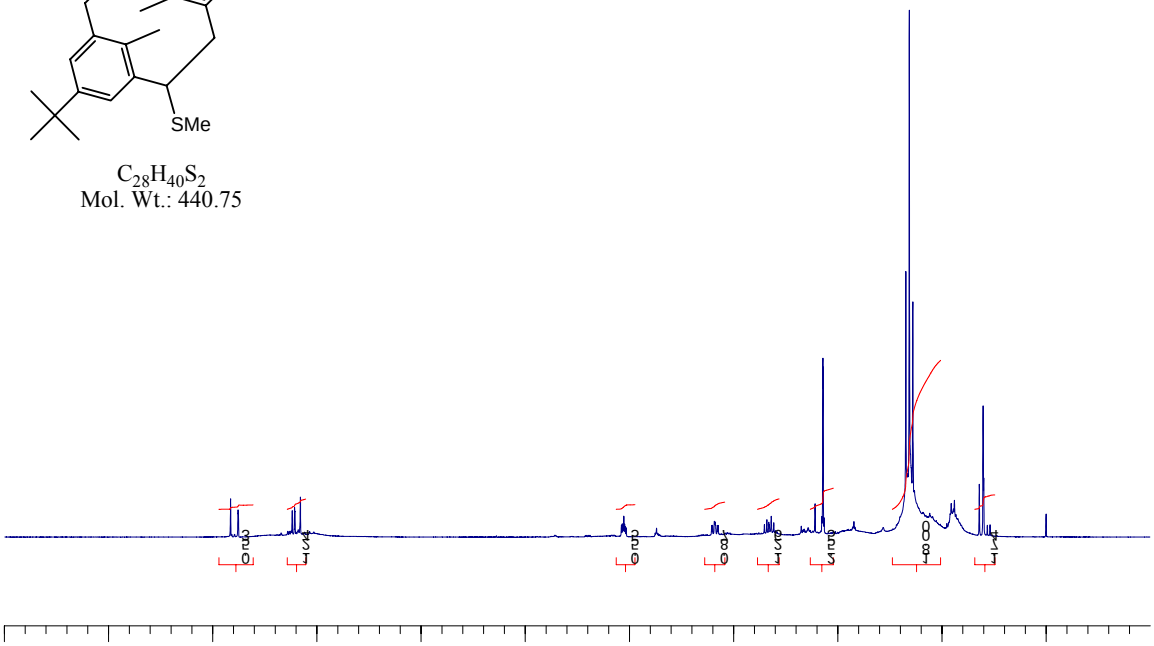

Preparation of Bosch's Reagent and (reaction product):

In a 500 ml flask with 60 ml addition funnel was added 23.3 g (220 mmol) triethylformate dissolved in 100 ml dichloromethane. Dropwise, at -47°C (dry ice/acetonitrile), a solution containing Boron trifloride-etherate was added (42 g, 298 mmol, 36 ml). After addition was complete the reaction mixture was stirred for 30 m at -10°C, then cooled to -40°C. The liquid in the flask which had not gelled was removed via cannula and the oily solids were suspended in dichloromethane (30 ml), then a solution containing the 31.03 g (70 mmol) dimethylsulfide (prepared above) dissolved in 60 ml dichloromethane was added (note: the reaction mixture turned dark purple). The reaction mixture was allowed to warm to ambient, stirring for 3h (note: turns brick red). Ethyl-acetate was added (180 ml) and stirring continued for an additional 2 h, then solids were collected by filtration. The solids were dried in vacuo: 15.8 g

15.8 g (28 mmol) was slurried in dry THF and a solution containing potassium *tert*-butoxide was added dropwise (86 mmol, 86 ml, 1M in THF). The reaction mixture was refluxed for 8 h, stirred at ambient temperature for 18 h (overnight), and then poured into iced dichloromethane. Organics were collected with dichloromethane, washed with water, dried over magnesium sulphate, filtered and solvents removed in vacuo: 8.32 g dark green powder.

Figure 105. ^{1}H-NMR of the dihydropyrene photoswitch:

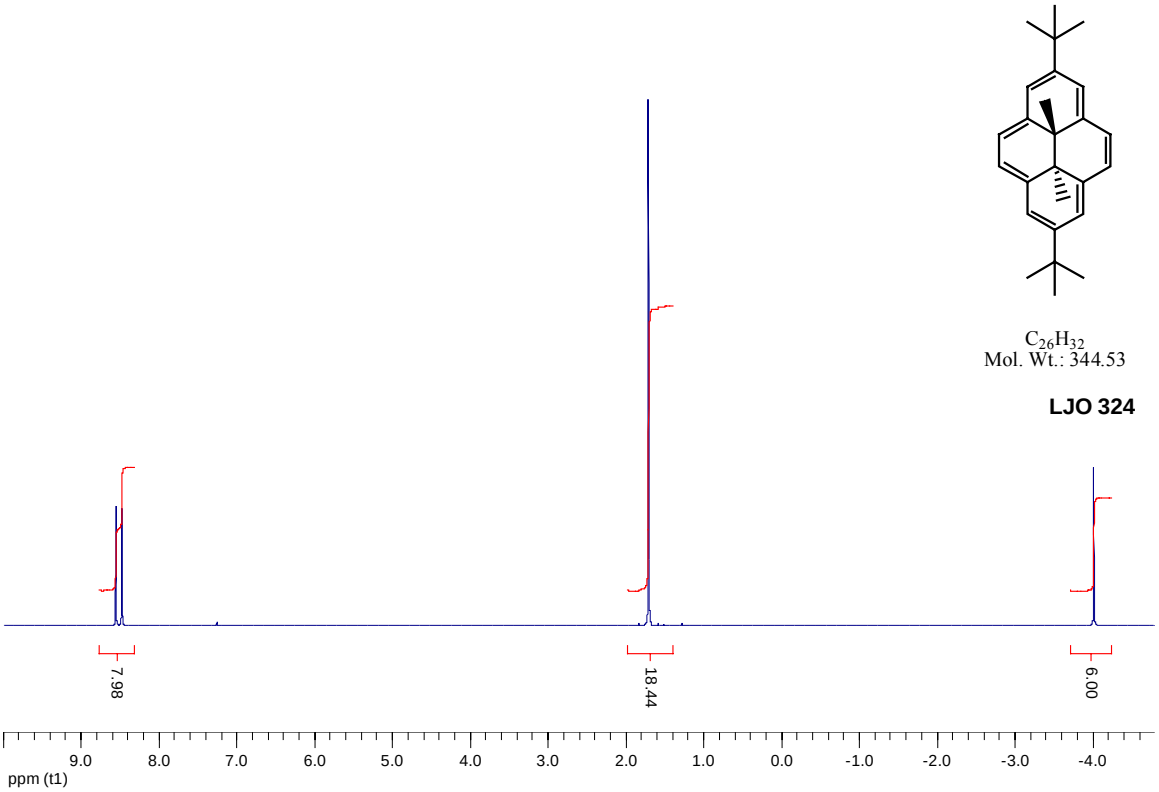

Figure 106. LCMS analysis of DHP synthesis:

(Sample: 100-031):

Chromatogram: DAD at 340 nm: MS-TIC positive Mode:

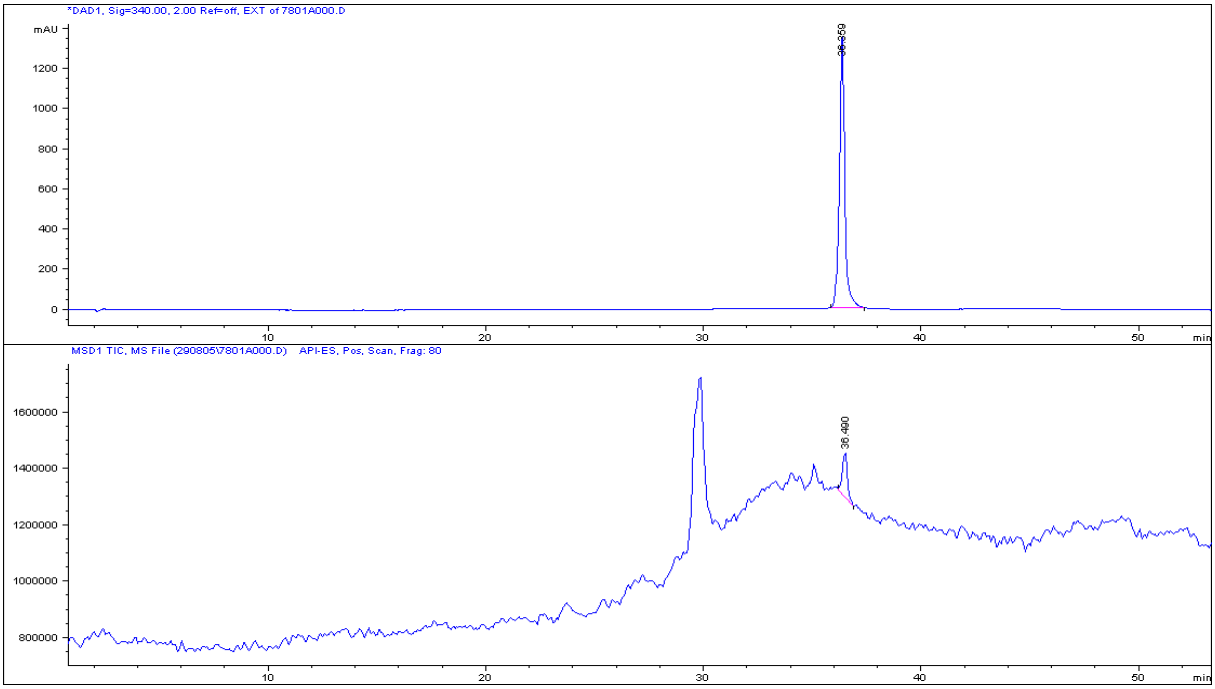

Peaktable (DAD at 340 nm):

#	Time	Area	Height
1	36.359	23070.6	1365

UV/vis-Spektra :

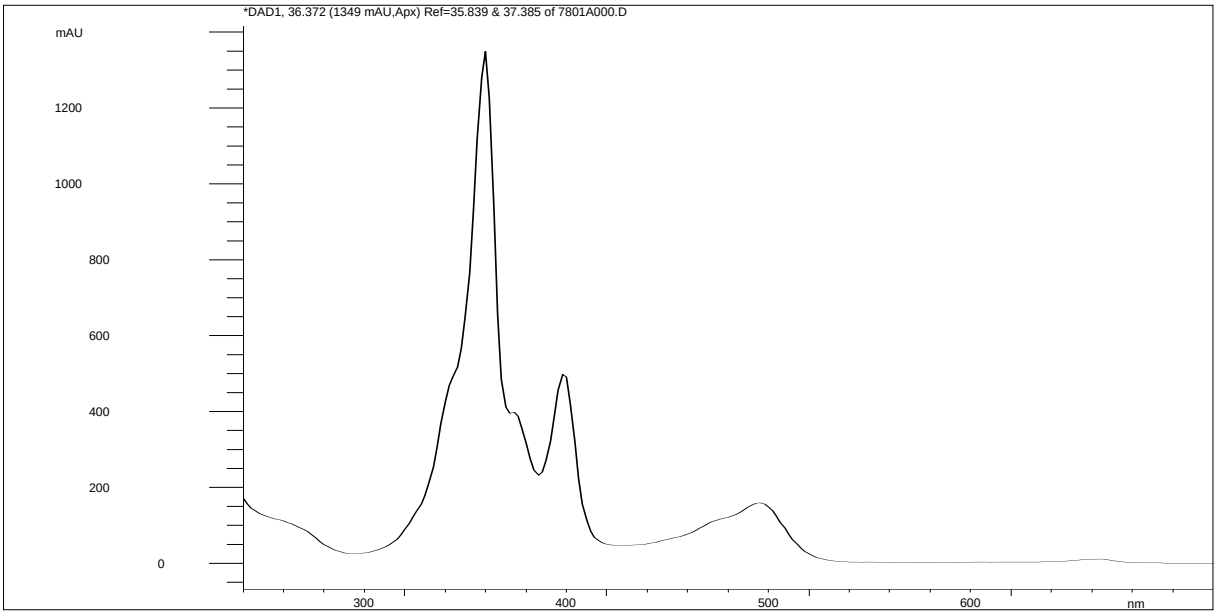

Peak mass spectrum at RT = 36.511:
MS-Spektra (pos. Mode):

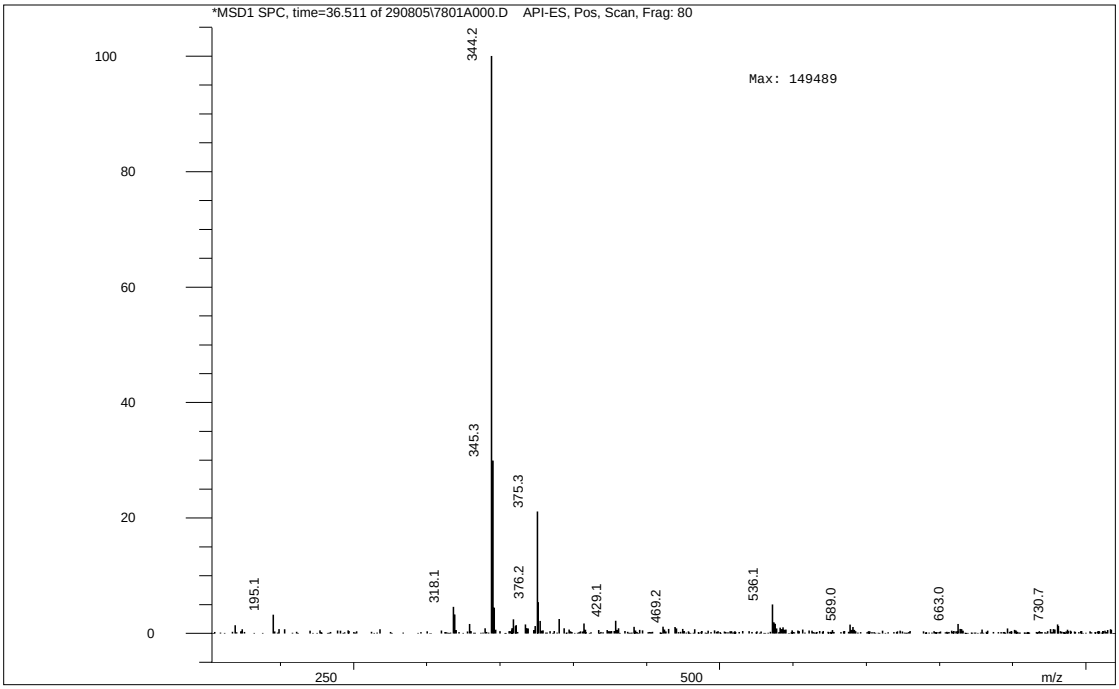

Bromination of the DHP photoswitch:

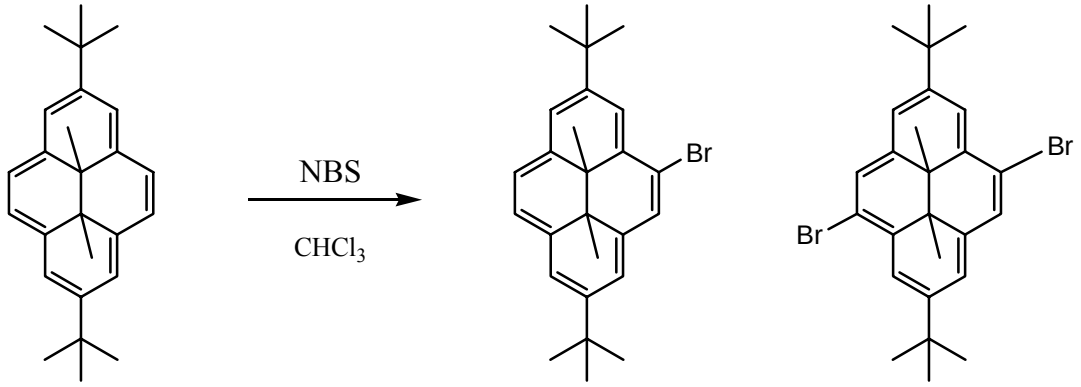

$C_{26}H_{32}$
Mol. Wt.: 344.53

$C_{26}H_{31}Br$
Mol. Wt.: 423.43

$C_{26}H_{30}Br_2$
Mol. Wt.: 502.32

In a flask containing 3.46 g (10 mmol) DHP dissolved in 150 ml chloroform was added 3.72 g (21 mmol: 2 equivalents) N-bromosuccinimide, slowly as a dry powder. The reaction mixture was stirred for 18 h, then poured into water. Organics were collected with dichloromethane, washed with water, then dried over magnesium sulphate, filtered, then solvents removed in vacuo. 7.2 g of a dark green powder was recovered which was further washed with hexane and then dried: 3.32 g recovered as hexane in-solubles, the remainder was dried in vacuo. LCMS analysis of the product shows it to contain a small amount of the mono-brominated product, chiefly containing a mixture di- and tri- brominated product (see Figure 104).

Figure 107. LCMS analysis of the DHP Bromination product: (Sample: 053RAW):

Chromatogram: DAD at 345 nm, DAD at 654 nm, MS-TIC pos.Mode

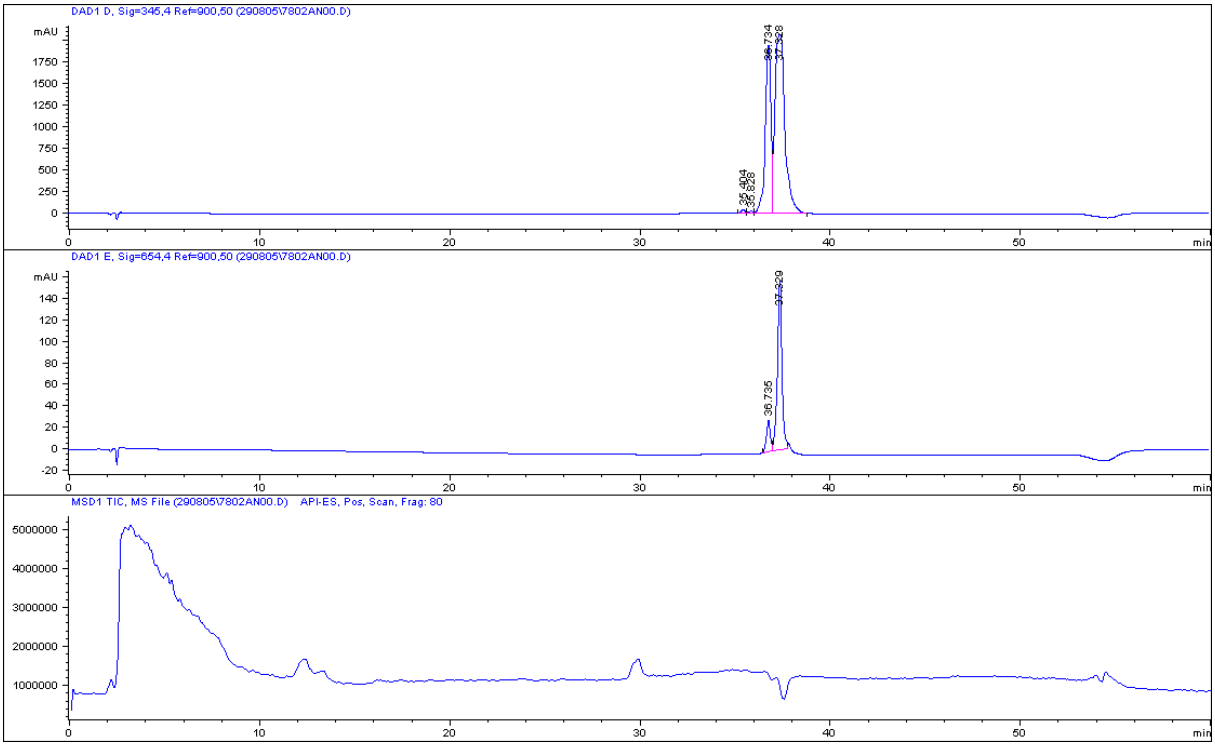

Analysis of LC results:

Peaktable (DAD at 345 nm):

#	Time	Area	Height
1	35.404	636.7	45.7
2	35.828	394.3	26.6
3	36.734	41099.1	1944
4	37.328	74952.7	2074

Peaktable (DAD at 654 nm):

#	Time	Area	Height
1	36.735	441.1	29.9
2	37.329	2821.7	160.7

UV/vis-Spektra :

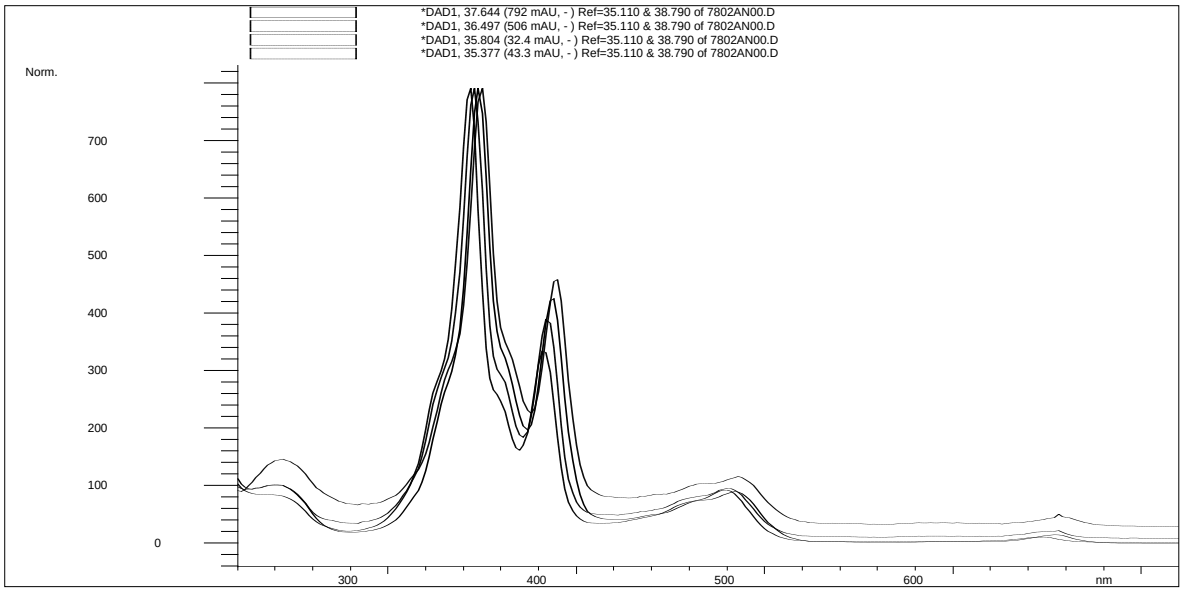

MS-Spektra (pos. Mode):

Peak mass spectrum at RT = 35.50:

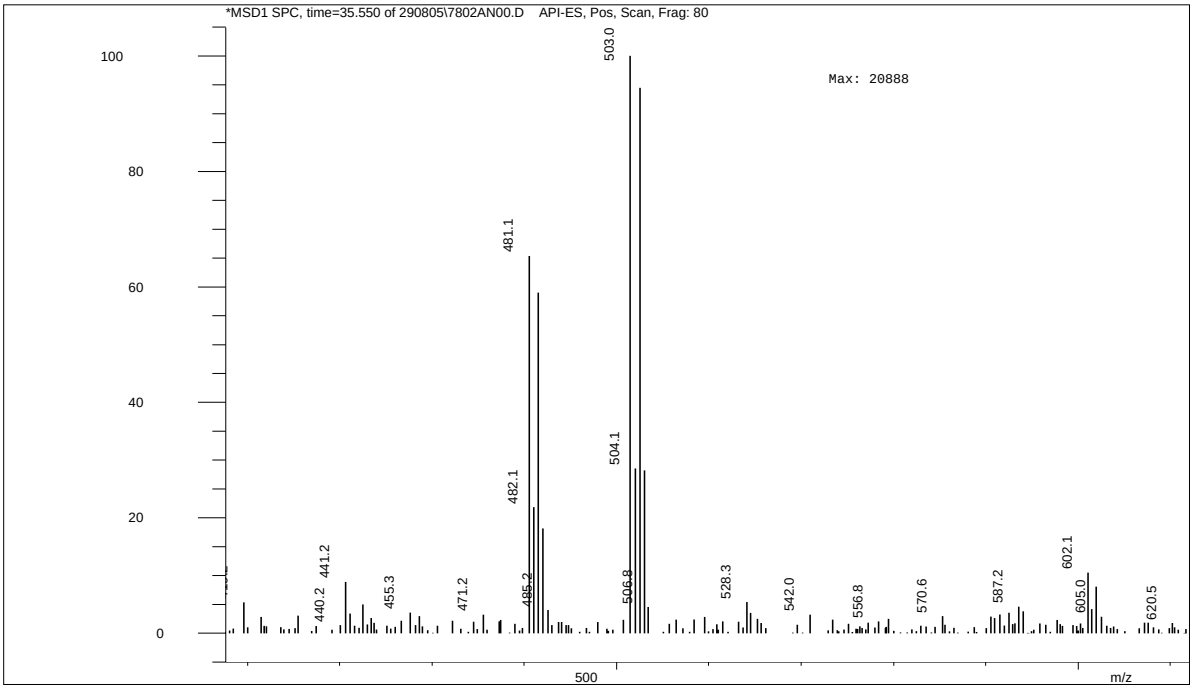

Peak mass spectrum at RT = 35.99:

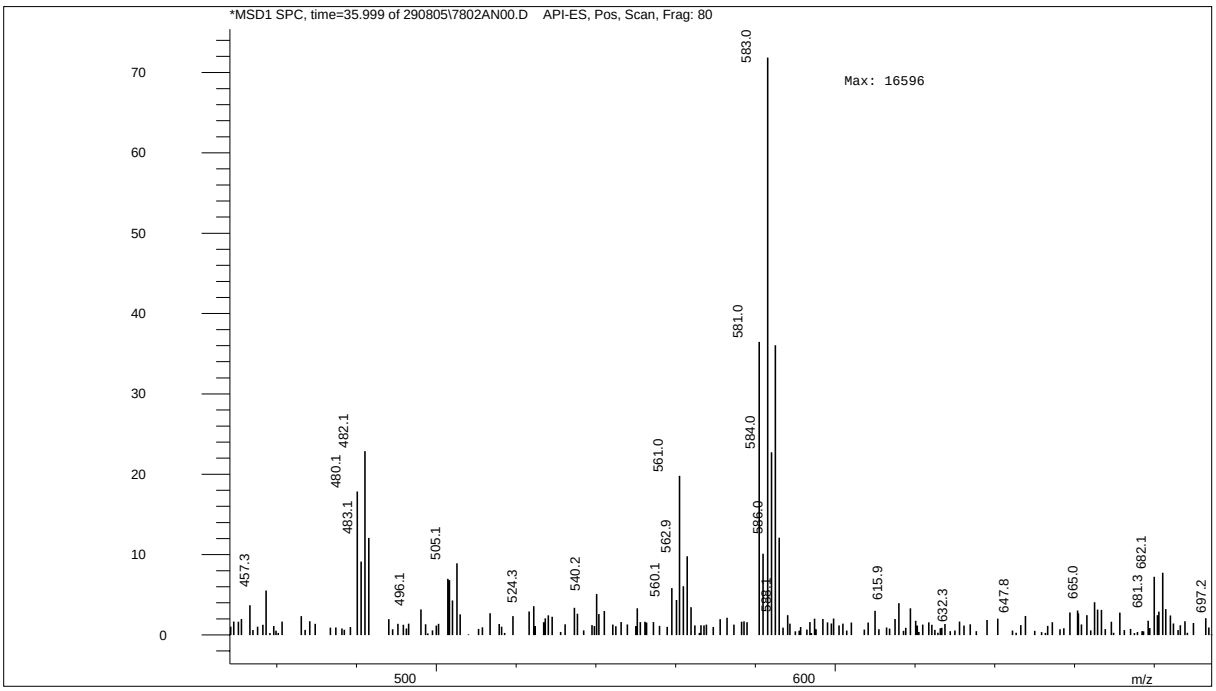

Peak mass spectrum at RT = 36.895:

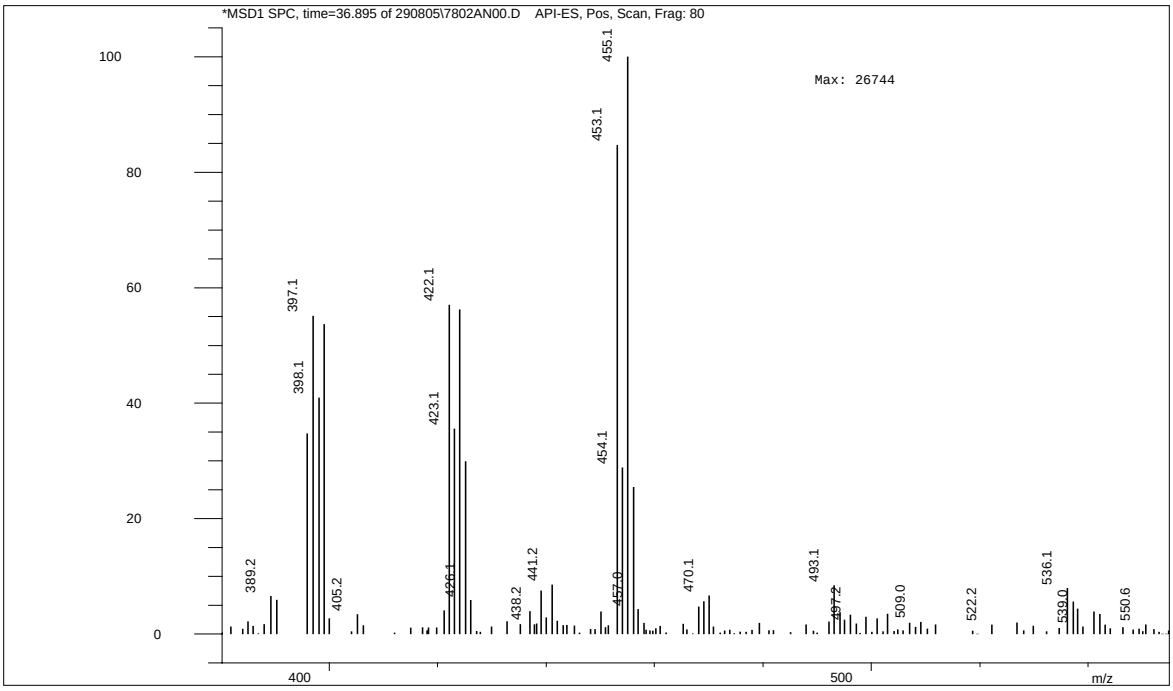

Peak mass spectrum at RT = 37.472

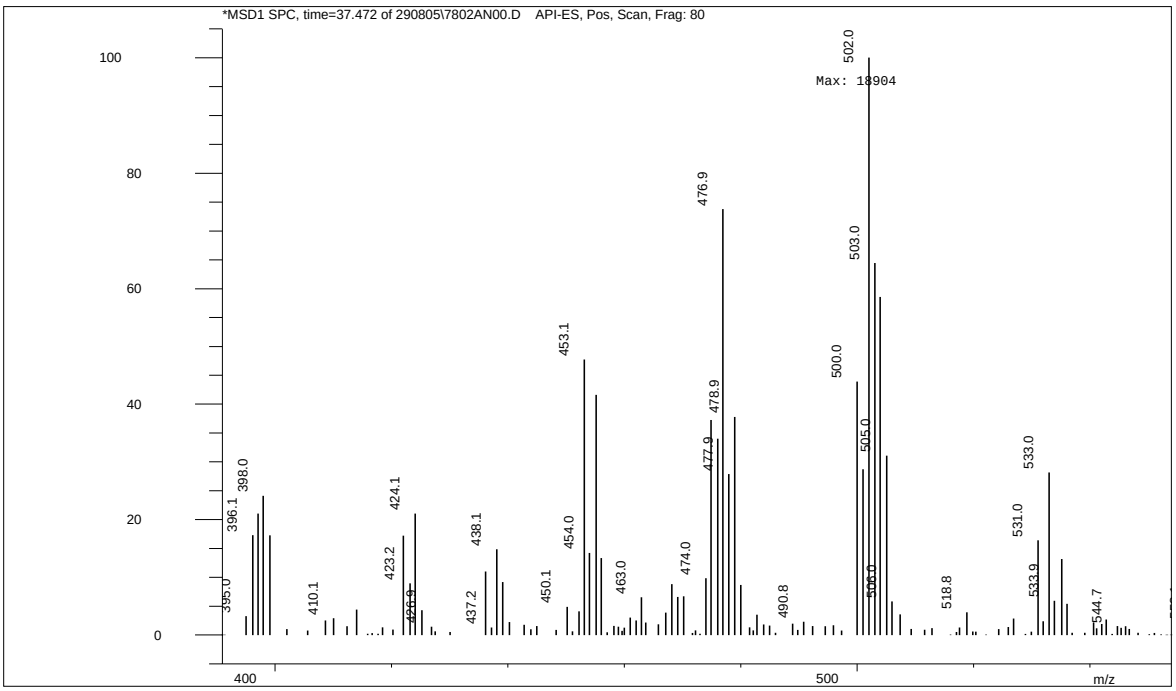

Lithiation of DHP-Br_n

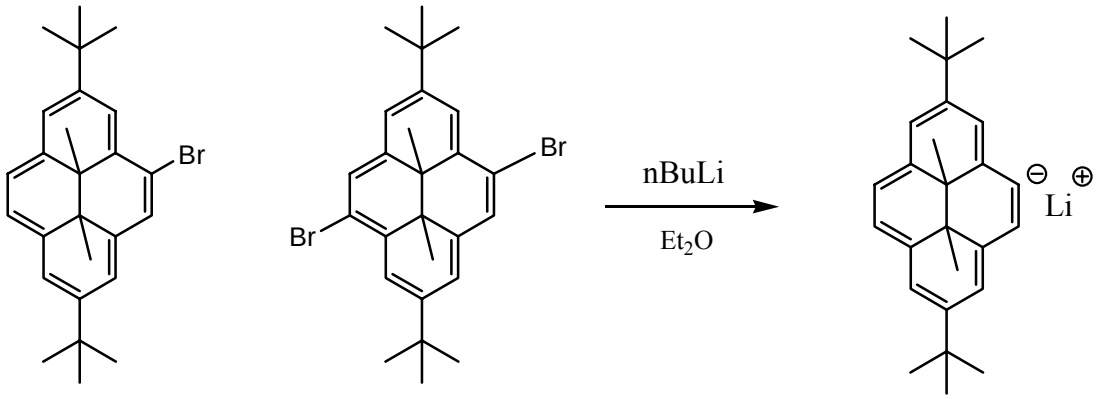

$C_{26}H_{31}Br$
Mol. Wt.: 423.43

$C_{26}H_{30}Br_2$
Mol. Wt.: 502.32

In a flask containing 3.09 g (6 mmol) DHP-Br_n (from above preparation) dissolved in diethyl ether was added a solution containing nBuLi (12 mmol, 4.8 ml, 2.5M in hexanes). The reaction mixture was stirred for 4 h, then solvents were removed in vacuo. The solids were washed repeatedly with pentane, the light brown solids were then slurried in fresh pentane.

4.2.4 Synthesis of the hafnium-pyridyl-imine complexes:

From the patent WO 03/040201 describing the synthesis of several complexes having the general structure related to the following:

6-(naphthalen-5-yl)pyridine-2-carbaldehyde

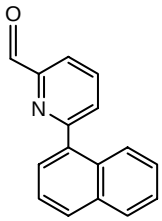

$C_{16}H_{11}NO$
Mol. Wt.: 233.26

In a (2L) 3-neck flask with mechanical stirrer charged with nitrogen was added 200 ml (500 ml) toluene, then 34.2 g (183 mmol) 6-bromo-2-pyridine carboxaldehyde (Aldrich, note: forms solution). Then 3.0 g (2.6 mmol) $Pd(PPh_3)_4$ (ABCR). The reactor contents were sparged with nitrogen while heating to 70°C. A de-gassed slurry containing 36 g (209 mmol) naphtylboronic acid and 46.6 g (582 mmol) sodium carbonate in 200 ml methanol/800 ml water was added via cannula. The reaction was stirred vigorously for 90 min, the flask contents were poured into a separatory funnel and the organic fraction separated. Organics were collected with diethyl ether, washed with water, dried over magnesium sulphate, filtered, then solvents removed in vacuo: 45.88 g yellow orange pasty solid recovered:

Figure 108. ^{1}H-NMR of 6-(naphthalen-5-yl)pyridine-2-carbaldehyde.

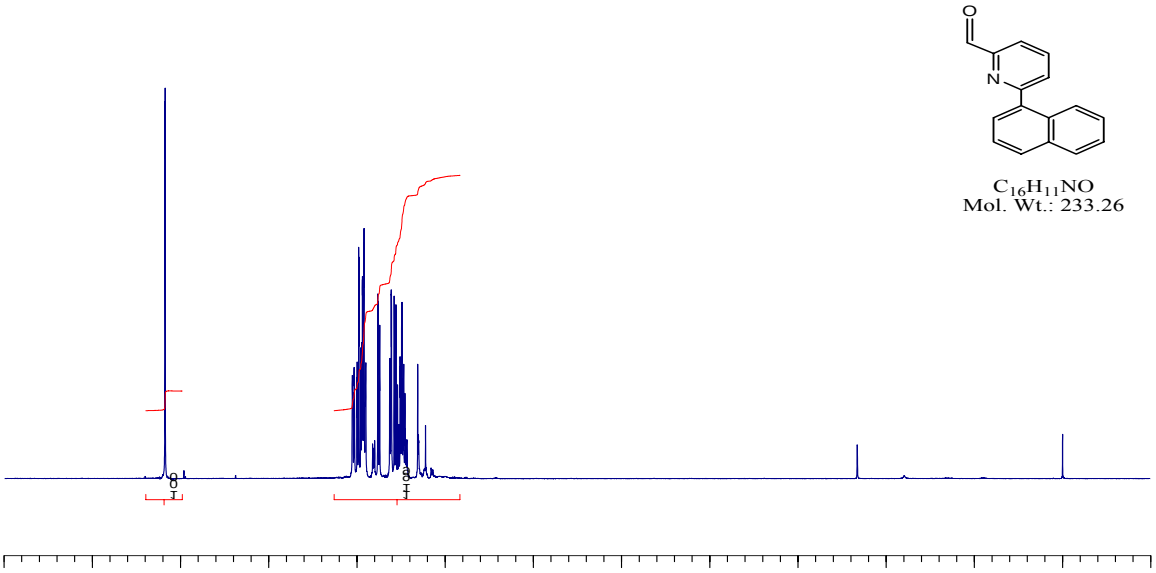

6-napthylpyridine-2-(2,6-diisopropylphenyl)imine

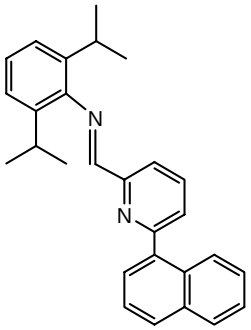

$C_{28}H_{28}N_2$
Mol. Wt.: 392.54

In a flask containing 25 g 3A molecular sieves, 350 ml THF, 23.95 g (102 mmol) 2-formyl-6-naphtylpyridine, 19.51 g (110.2 mmol) 2,6-diisopropylpyridine, was added 270 mg *para*-toluenesulfonic acid monohydrate. The reaction mixture was refluxed for 2 h., then filtered. Solvents were removed from the filtrate in vacuo forming dark red oil which was stirred with hexane forming a light pink precipitate which was collected by filtration and dried: 30.14 g (75.3%).

Figure 109. ^{1}H-NMR of 6-napthylpyridine-2-(2,6-diisopropylphenyl)imine.

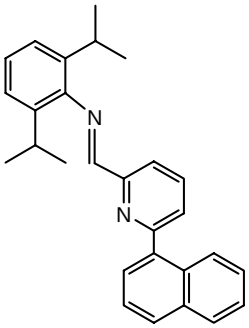

$C_{28}H_{28}N_2$
Mol. Wt.: 392.54

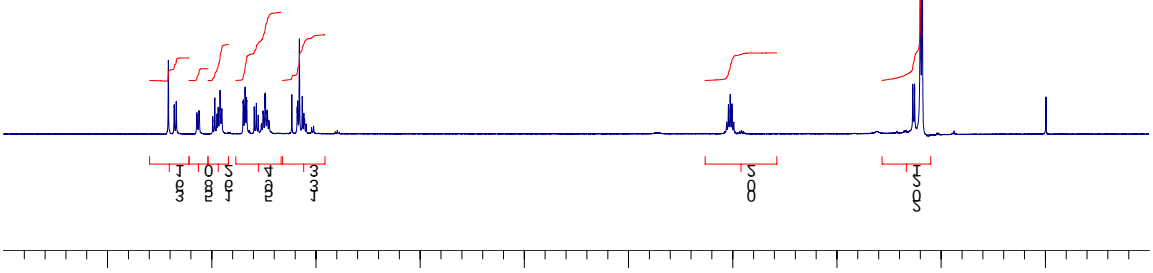

(6-naphtyl-2-pyridyl)-N-(2,6-diisopropylphenyl)benzylamine

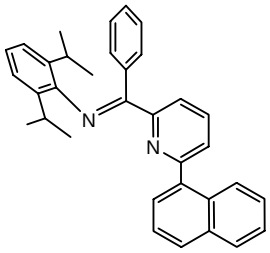

$C_{34}H_{32}N_2$
Mol. Wt.: 468.63

In a flask containing 19.6 g (50 mmol) 6-naphtylpyridine-2-(2,6-diisopropylphenyl)imine slurried in 250 ml diethyl ether at -78°C was added a solution containing phenyl lithium (50 mmol, 28 ml, 1.8M in diethyl ether). After addition was completed, the reaction mixture was stirred for an additional 10 m, then the flask contents were allowed to warm to ambient and stirred an additional 14 h. An additional amount of phenyl lithium was added (50 mmol, 28 ml, 1.8M in diethyl ether), and the reaction mixture stirred an additional 2h. The reaction mixture was quenched with 200 ml saturated ammonium chloride, organics were collected with diethyl ether, washed with water then dried over magnesium sulphate. Organics were filtered through silica with hexane and solvents removed in vacuo. 21.05 g (76% by GC/GCMS):

Figure 110. ^{1}H-NMR spectrum of (6-naphtyl-2-pyridyl)-N-(2,6-diisopropylphenyl)benzylamine

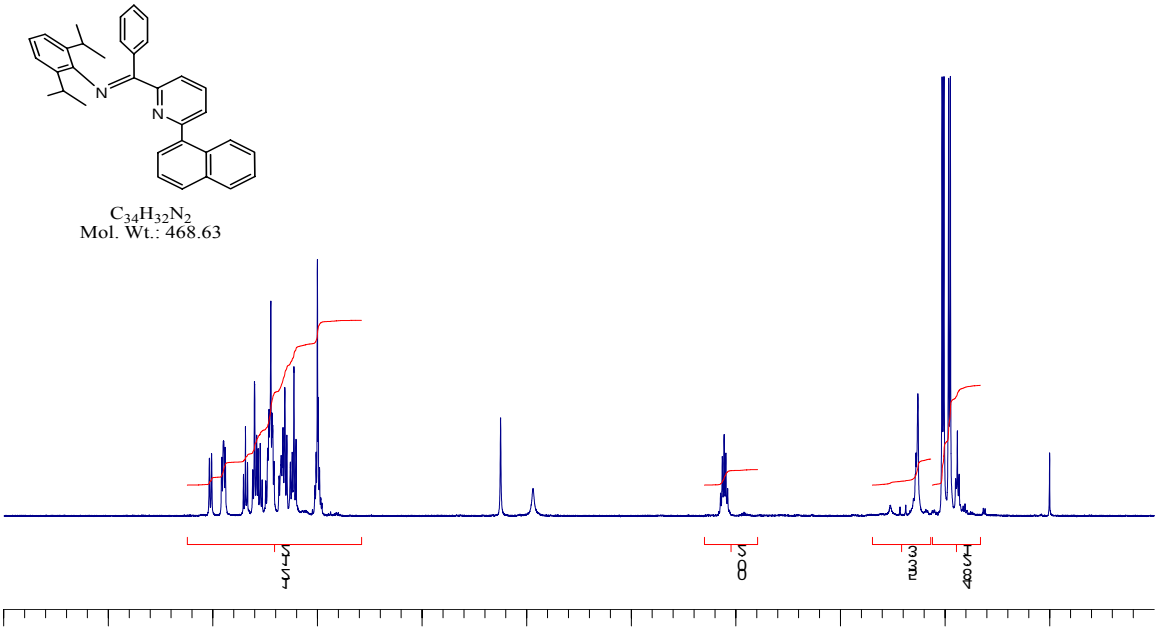

[(6-naphtyl-2-pyridyl)-N-(2,6-diisopropylphenyl)benzylamine]hafnium(tris-dimethylamine)

In a flask containing 4 g (11.3 mmol) hafnium tetrakisdimethylamine dissolved in 100 ml pentane was added a solution containing (6-napthyl-2-pyridyl)-N-(2,6-diisopropylphenyl)benzylamine dissolved in 20 ml pentane, dropwise. The reaction mixture was stirred overnight: a yellow precipitate was formed. The reaction mixture was filtered and the solids which were collected were washed with fresh pentane then dried: 4.22 g were collected. A second crop was collected from the filtrated: 0.62 g: total: 5.34 g (60.2 %):

Figure 111. ^{1}H-NMR spectrum of [(6-naphtyl-2-pyridyl)-N-(2,6-diisopropylphenyl)benzylamine]hafnium(tris-dimethylamine).

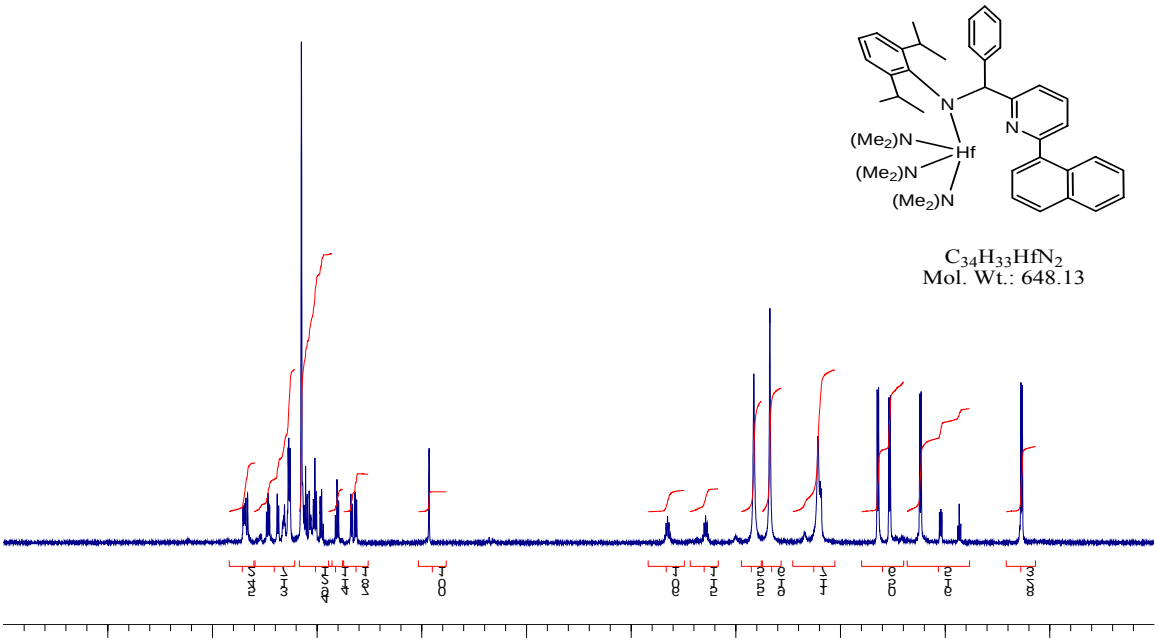

[(6-napthyl-2-pyridyl)-N-(2,6-diisopropylphenyl)benzylamine]methyl hafnium

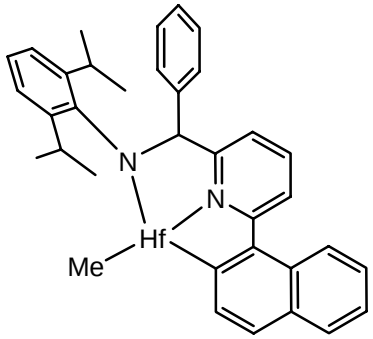

$C_{35}H_{35}HfN_2$
Mol. Wt.: 662.16

In a flask containing a solution of trimethylaluminum (106 mmol, 53 ml, 2M in hexane) dissolved in 140 ml pentane was added 4.28 g (6.3 mmol) of G4: *tris*-hafnium-amide adduct (from above) as a dry powder. The reaction mixture was stirred 18 h, then the yellow precipitate formed was collected by filtration: 2.93 g (68%).

Figure 112. ^{1}H-NMR Spectrum of [(6-napthyl-2-pyridyl)-N-(2,6-diisopropylphenyl)benzylamine]methyl hafnium

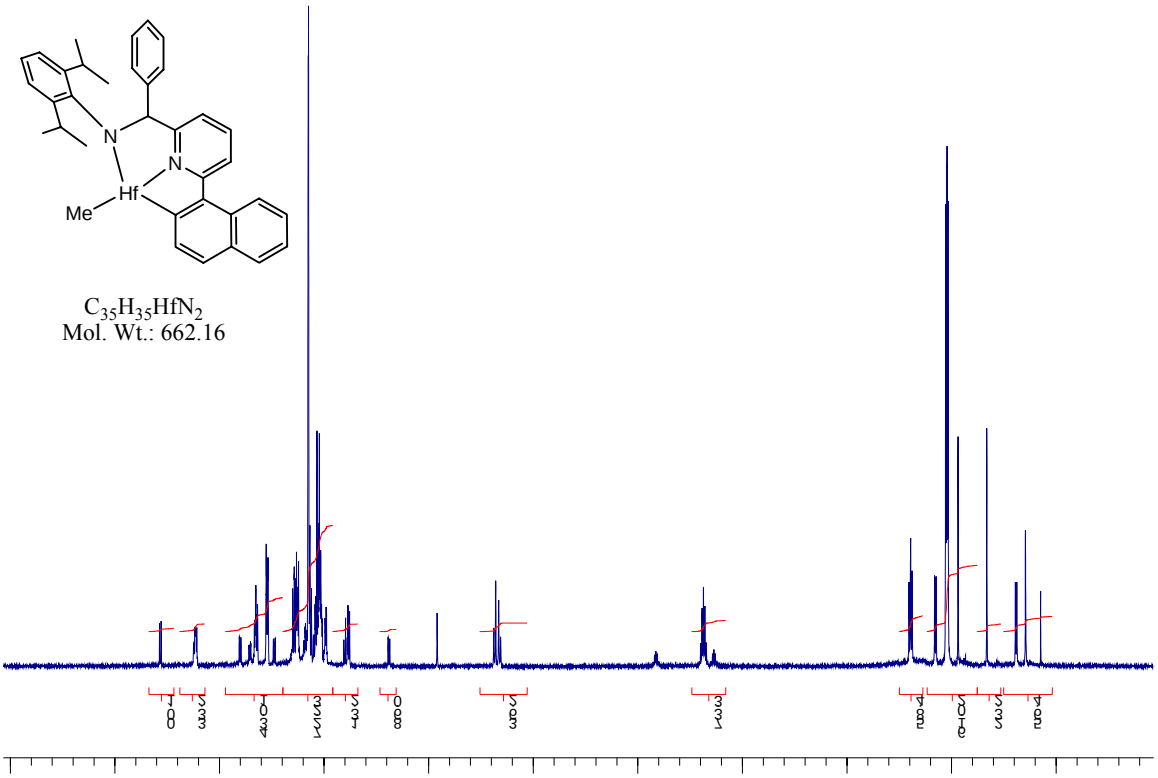
N
N
Hf
Me
$C_{35}H_{35}HfN_2$
Mol. Wt.: 662.16

The complex having the phenanthrene substitution (example H) was prepared according to the patent literature: analytical data is included for comparison and future reference:

Figure 113. ^{1}H-NMR Spectrum of 2H.

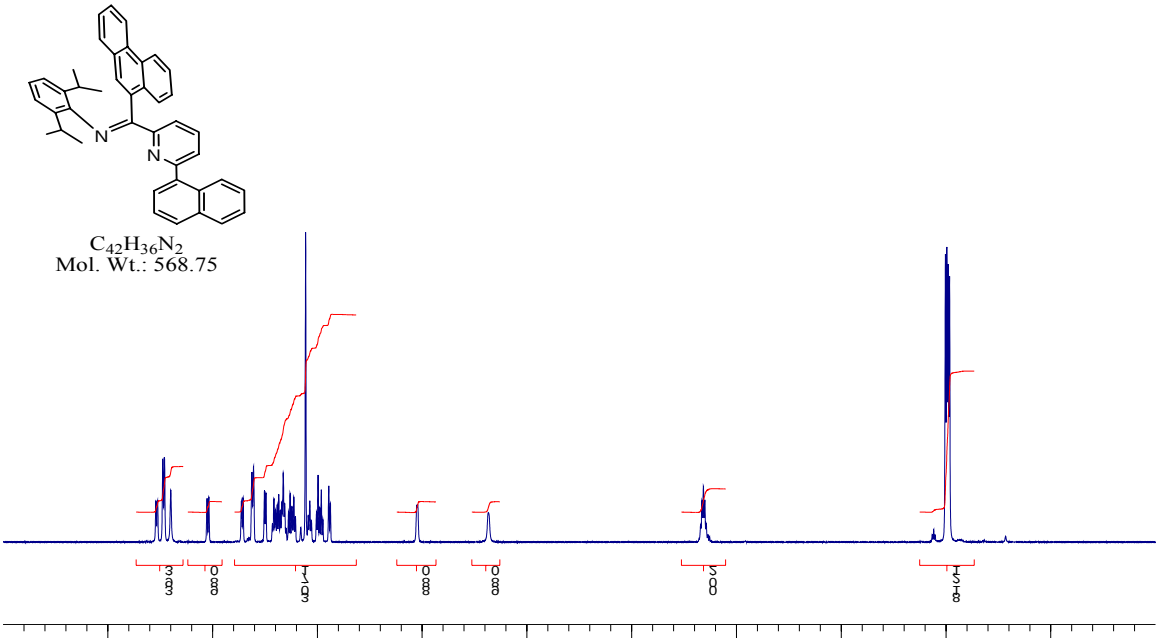

Figure 114. ^{1}H-NMR Spectrum of 3H.

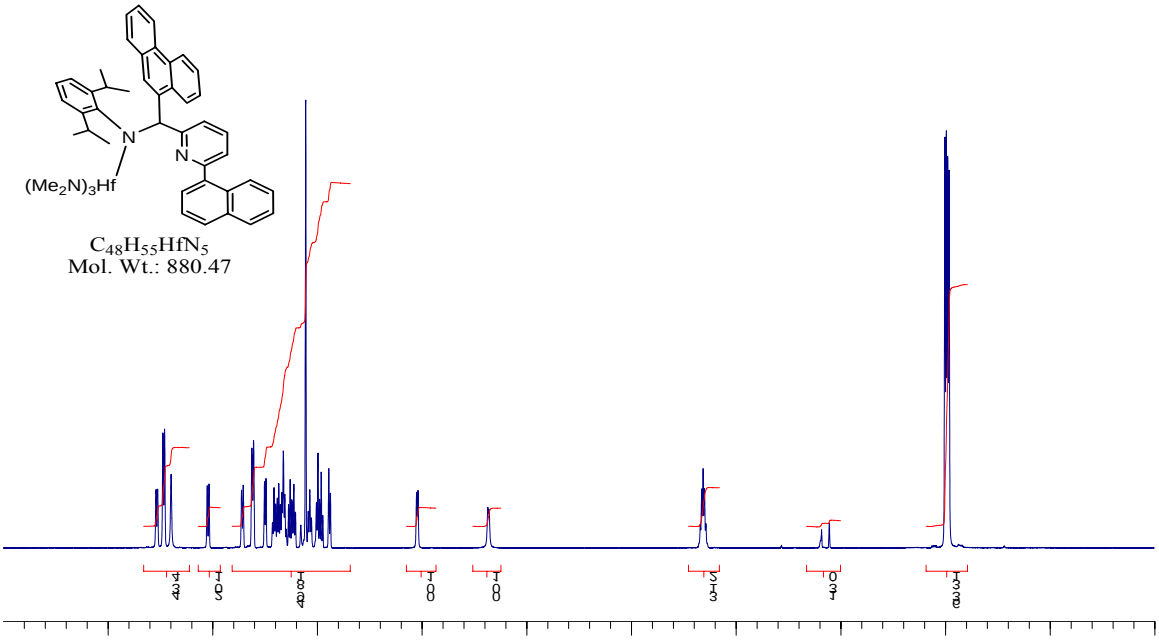

Figure 115. ^{1}H-NMR Spectrum of 4H:

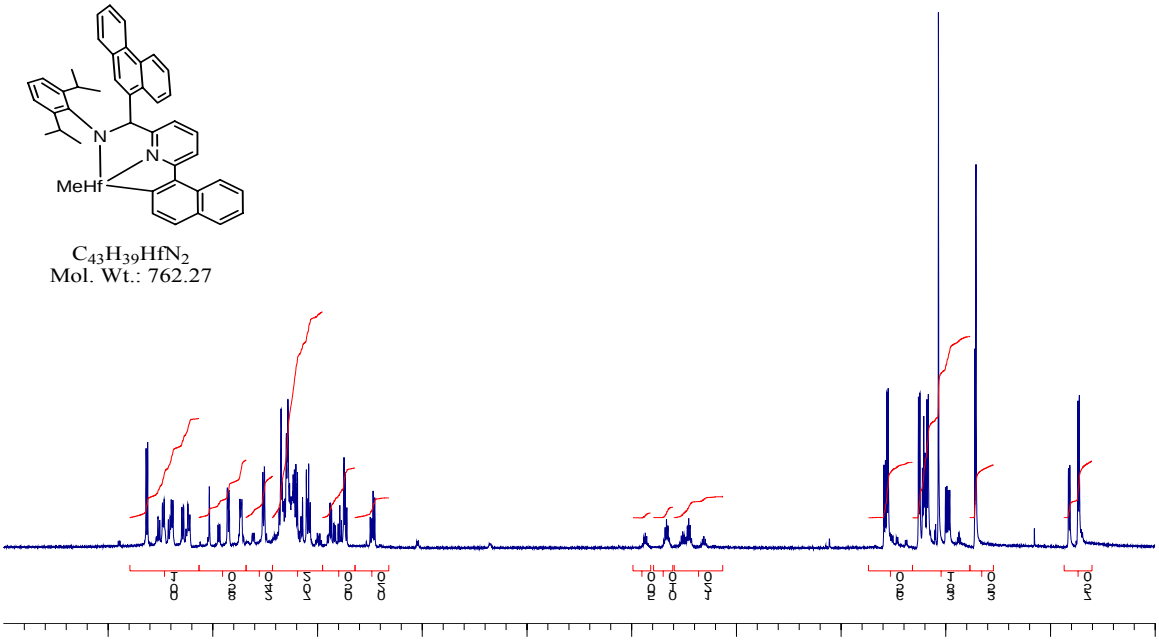

Figure 116. ^{1}H-NMR Spectrum of 5H.

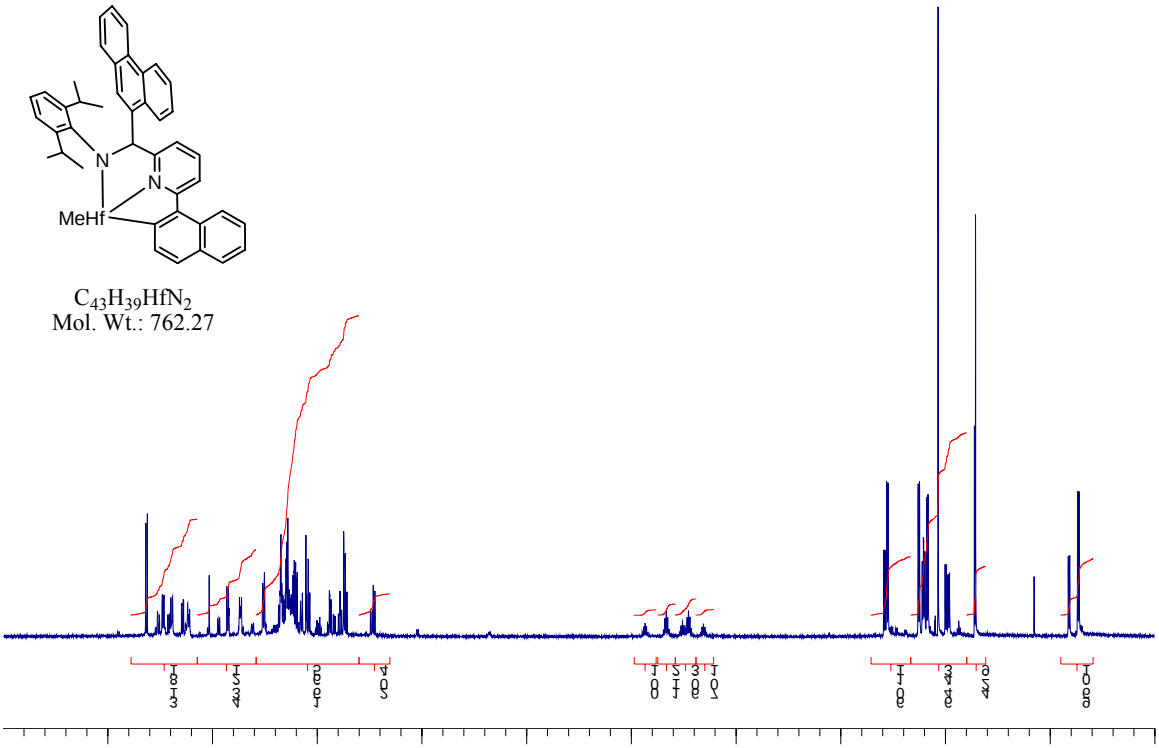

Marriage of the dihydropyrene photoswitch and the pyridyl-amine ligand:

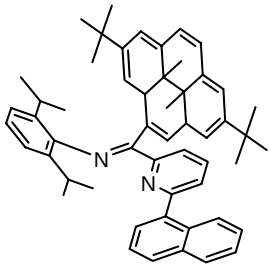

To a pentane slurry containing the Li-DHP complex prepared above was added a solution containing 2.0 g (5.2 mmol) 6-naphtylpyridine-2-(2,6-diisopropylphenyl)imine (see experimental below) dissolved in toluene. The reaction mixture was stirred for 3 days, then poured into water. Organics were collected with a 20% dichloromethane/hexane solution, washed with water, dried over magnesium sulphate, then filtered through silica with 20% dichloromethane/hexane. Solvents were removed in vacuo producing 1.48 g golden brown powder.

Figure 117. ^{1}H-NMR from the crude reaction product from the marriage of the DHP-photoswitch and the pyridyl-imine ligand:

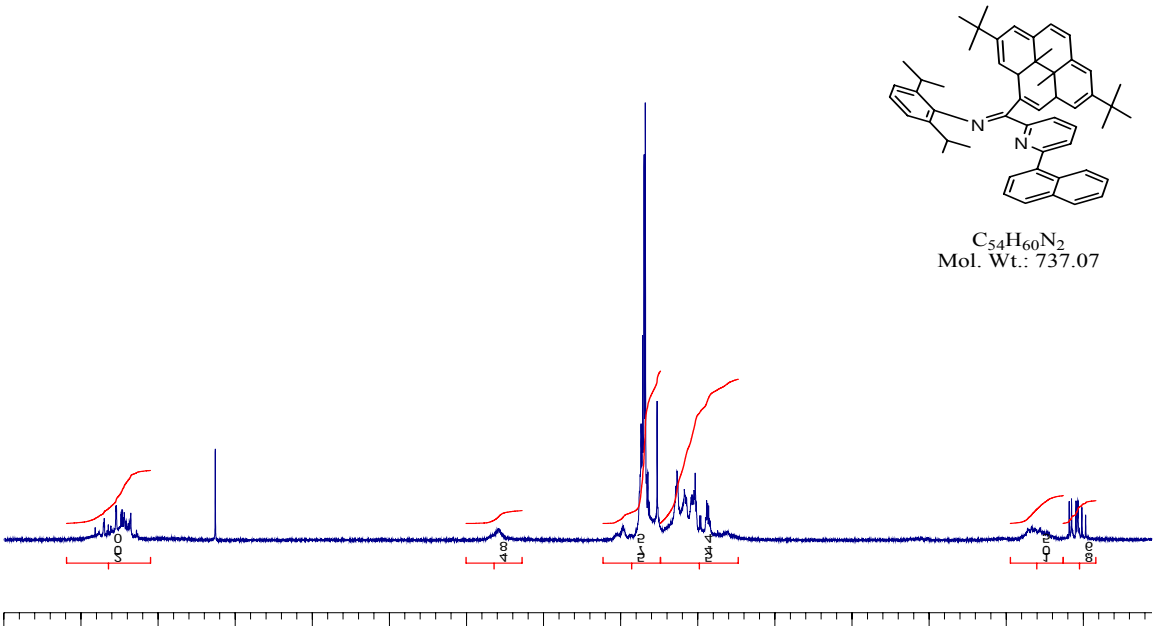

Figure 118. LCMS of the product from the reaction of the DPH Li salt and the pyridyl-imine complex.

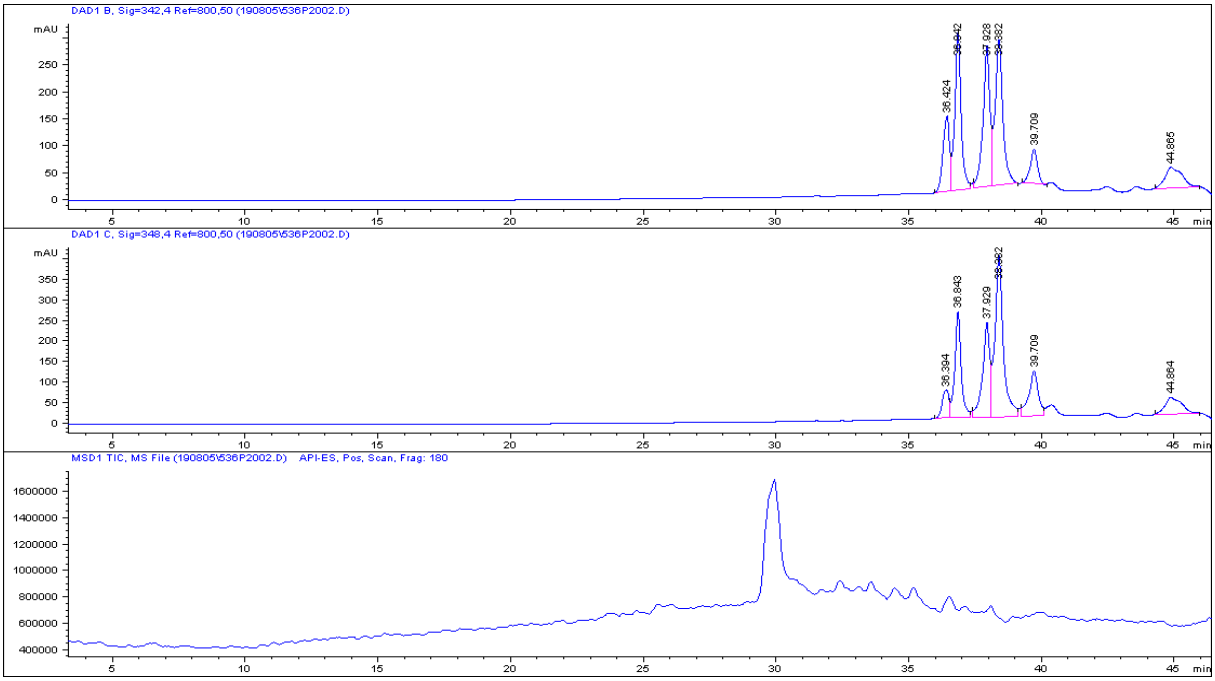

Expansion of the LC from above:

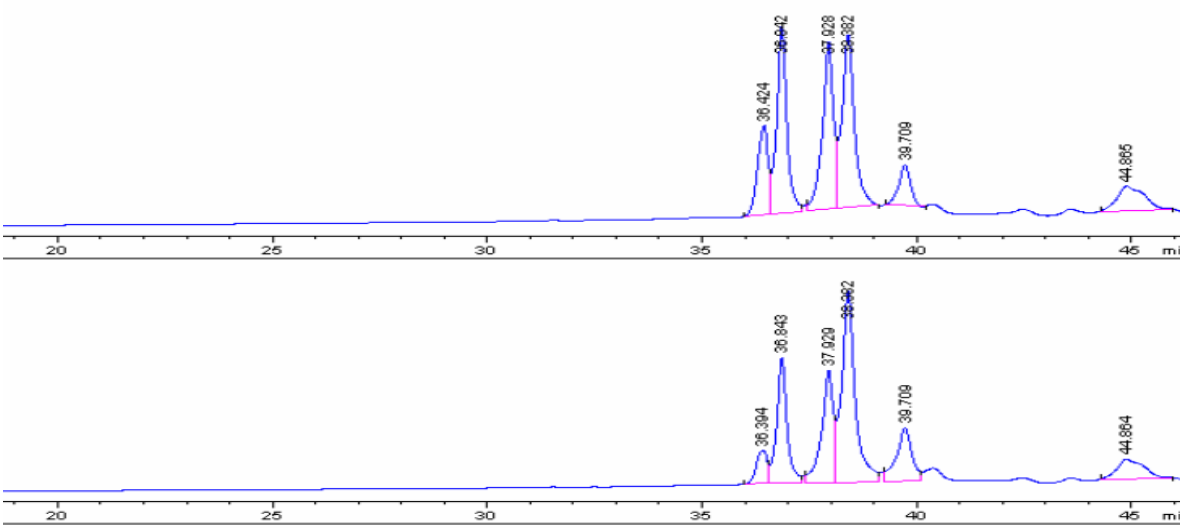

MSD-SPC

time	[M]	
36.489	536.1	
37.032	610.1	
38.118	758.1	target (+Na, 23)
38.612	759.2	isomer? (+Na, 23)
38.896	654.9	
44.993	957.9 - 969.4	

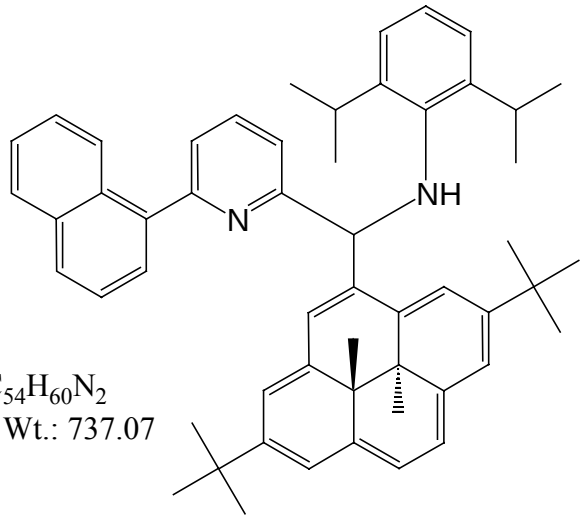 $C_{54}H_{60}N_2$ Mol. Wt.: 737.07		
737 + Na → 759 (found at 38.11 min)		

Figure 119. TLC of reaction products from pyridyl-imine ligand and DHP-Li:

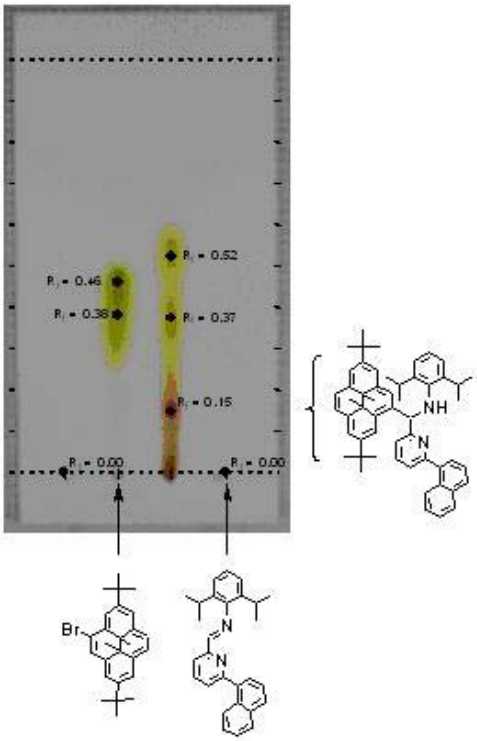

TLC was run using hexane as the mobile phase (Figure 104). Starting materials were spotted on either side of the crude product spot. The appearance of the "red dot" indicated a new product formed. The sample was submitted for LCMS and the results are included in Figure 120.

Figure 120. The TLC Red Spot:

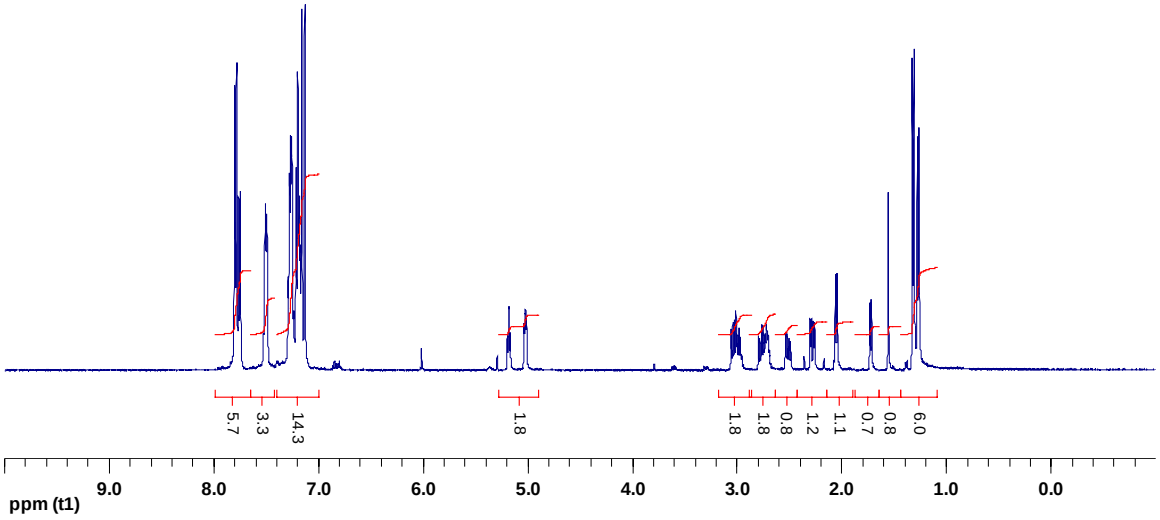

The "red dot: was isolated by preparative HPLC. ^{1}H-NMR of the isolated compound gave a very clean spectrum having high signal to noise ratio however, after integration the required quantity of *tert*-butyl signals that would originate from the DHP substitution were not found and this was not the target.

4.3 Polymerization procedures

4.3.1 Standard Polymerization procedures, Liquid Propylene:

Polymerizations with homogeneous catalysts: Polymerizations were conducted in 1L stainless steel Buchi reactor equipped with circulating oil temperature control bath. The reactor was swept with dry nitrogen at 110°C for 1 h prior to polymerization. At room temperature 2-4 mL of a 1 M toluene solution of $Al(iBu)_3$ was added by syringe as scavenger followed by 250 g of liquid propylene. Stirring was initiated and the reactor was heated to the polymerization temperature. Hydrogen was added (if required). A toluene solution of the zirconocene (0.5 mg/mL solution) was reacted with MAO in toluene for 10 minutes and polymerization was initiated by charging the catalyst solution to the reactor with 50 g of propylene under pressure. At the end of the run stirring was stopped and all residual monomers were vented while cooling the reactor to room temperature. After sweeping the reactor with nitrogen for 10 minutes and injecting 5 mL of methanol, the reactor was opened. The polymer was removed from the reactor by hand or extracted with hot toluene if the polymer was amorphous or the reactor was severely fouled with polymer. If toluene was used the solution was transferred to a separate container and the toluene was evaporated. The polymer was further dried in a vacuum oven at 50°C for 2 h under nitrogen sweep. Reported activities were calculated from polymer and zirconocene weights.

4.3.2 Standard Polymerization procedures, Toluene solution:

In a 30 ml Schlenk tube with Teflon stirring bar was placed 20 ml toluene and a solution containing MAO (2.8 mmol, 0.9 ml, 1.58M in toluene). In a separate vial, the catalyst (1) was weighed and a solution made with 5 ml toluene and an additional amount of MAO (2.8 mmol, 0.9 ml, 1.58M in toluene). The color change was noted and the solutions were combined. Propylene was bubbled through the solution at a rate of about 15 to 25 l/h and the time recorded. The polymerization reaction mixture was poured into an acidic methanol solution; the polymer was precipitated with acetone and collected by filtration. The organic phase was collected, solvents removed in vacuo, and the weight recorded. The polymer was dried and the weights recorded.

4.3.3 Polyethylene polymerizations

Polymerizations were done in a 1L flask equipped with a reflux condenser and mechanical stir. The reactor was charged with toluene, hexene (where required) and the MAO/Catalyst solution. Ethylene was added at a constant flow rate (about 20 l/h) for the duration of the experiment. When the reaction was completed the reactor was sparged with argon, then a solution containing acidic methanol was added to the reactor. The polymer was collected by filtration, washed with methanol, dried in a vacuum oven to constant weight then the weight recorded.

4.4 Analytical Methods

4.4.1 Complexes Analysis:

HPLC

Normal phase liquid chromatographic separations were done on a Waters LC3000 Preparative Scale system (with solvent gradient controller) using an ISCO UV-6 detector. Pre-packed, commercially available columns containing either 330g or 120g SiO_2 or C18 end capped silica were used (Isco). Isocratic separations using hexane at decreasing flow rates with and without recycle onto the column for SiO_2, and acetonitrile and acetonitrile/deionized water mixtures were used to effect the separations.

TLC

Thin Layer Chromatography was done on Silica Gel on Aluminum Plates (Aldrich Z193291) containing fluorescent indicator and typically using 20% dichloromethan/80% hexane as the eluent.

GCMS/FID

Gas chromatographic analysis using both flame ionization (FID) and synchronized electron ionization mass detection (EIMS) of the eluting components was performed on a Agilent 6890 GC (FID)/5973 EIMS. Agilent Ultra-1, 25m, 0.2 mm ID, 0.33 um film thickness (micro-bore), and Agilent HP-5 30 m, 0.53 ID, 0.88um mega-bore) columns were used.

^{1}H-NMR and ^{13}C-NMR of the ligands and organometallic complexes[128]:

Between 10-50 mg of each compound were dissolved in CD_2Cl_2, $CDCl_3$, DMSO-D_6 or C_6D_6 (~0,75 ml, 99,8 atom% D).

A Bruker DMX 500 Avance FT-NMR spectrometer operating at 500 MHz (1H), equipped with a 5mm QNP probe with z-gradient, was used for recording ^{1}H, ^{13}C, DEPT135, ^{1}H-^{13}C-HMQC and ^{1}H-^{13}C-HMC spectra at 300K. Chemical shifts were calibrated against TMS for 0,000 ppm ^{1}H or residual CD_2Cl_2 5,30 ppm) and 53,70 ppm for ^{13}C. For other solvents such as $CDCl_3$, DMSO-D_6 or C_6D_6 the chemical shifts were also calibrated according to their typical solvent resonances at 300K.
1D proton spectra were obtained at 500 MHz with a 30 degree read pulse, a spectral width of 22 kHz and a relaxation delay of 1s. Carbon spectra were obtained at 125 MHz using a 30 degree read pulse, a spectral width of 32 kHz, size 128K and a relaxation delay

[128] Analytical description of method prepared by Dr. Winkelman, Covion Organic Semiconductor GmbH in Frankfurt/Main Germany.

of 2s. The 1D ^{13}C spectra were proton decoupled using Waltz16 decoupling routine. DEPT135 spectra (with decoupling during acquisition) were recorded with a 135 degree read pulse to give XH, XH_3 positive and XH_2 negative resonances.

2D homonuclear shift correlation (**gs-COSY**) using gradient pulses for selection were recorded using a 90 degree read pulse; 1K FID´s were recorded in t1 of size 1K and 1 scan each. The data matrix was symmetrized with a sine window function and zero filled to 2K x 2K matrix, using also for ward linear prediction to generate the final data matrix. 2D ^{1}H-^{13}C correlations were obtained via heteronuclear zero and double quantum coherence (**HMQC**) in the phase sensitive mode using TPPI. Gradient pulses were used for selection. Typically 32 scans per increment were recorded. Zero filling in both directions provided a final matrix of 2K x 1K data points.

2D Long-range ^{1}H-^{13}C correlations (**HMBC**) were obtained with low-pass J-filter to suppress one bond correlations, with no decoupling during acquisition and using gradient pulses for selection. Typically 32 scans per increment were recorded. Zero filling in both directions provided a final matrix of 2K x 1K data points.

NMR experiments were recorded in the NMR-lab of Covion Organic Semiconductor GmbH in Frankfurt/Main Germany.

UV-Vis Spectroscopy

UV/Visible spectroscopy measurements were taken on a Cary UA-3 instrument. Scans were made from 800 nm to 190 nm with UV change-over at 330nm. Scans were smoothed equally (control vs irradiation treatment) using Cary software. Typically, 5 x 10^{-5}M concentration of sampled material was prepared using benzene as a solvent: benzene was used as a blank in the dual spectrophotometer for comparison.

4.4.2 Polymer analyses[129]

Determination of the viscosity number (I.V.):

The viscosity number was determined in decalin at 135°C in an Ubbelohde viscometer PVS 1 with an S 5 measuring head (both from Lauda). For the sample preparation, 20 mg of polymer were dissolved in 20 ml of decalin at 135°C over a period of 2 hours. 15 ml of the solution were placed in the viscometer; the instrument carried out a minimum of three running-out time measurements until a consistent result was obtained. The I.V. is calculated from the running-out times in accordance with I.V. = $(t/t_0-1)*1/c$, where t = mean of the running-out time of the solution, t_0= mean of the running-out time of the solvent, c = concentration of the solution in g/ml.

[129] Descriptions of these standard methods for polymer analysis were adopted from written procedures available from the department of Polymer Characterization and Physics: the methods were modified from Basell Polyolefins internal and external reports containing these published, standard methods.

Gel permeation chromatography:

Gel permeation (GPC) was carried out at 145°C in 1,2,4–trichlorobenzene using a Waters 150C GPC apparatus. The data were evaluated using the software Win-GPC from HS–Entwicklungsgesellschaft für wissenschaftliche Hard– und Software mbH, Ober–Hilbersheim. The columns were calibrated by means of polypropylene standards having molar masses ranging from 100 to 10^7 g/mol. Mass average (M_w) and number average (M_n) molar masses of the polymers were determined. The Q value is the ratio of mass average molar mass (M_w) to number average molar mass (M_n).

Determination of the melting point:

The melting point T_m was determined by DSC measurement in accordance with ISO Standard 3146 in a first heating phase at a heating rate of 20°C per minute to 200°C, a dynamic crystallization at a cooling rate of 20°C per minute down to 25°C and a second heating phase at a heating rate of 20°C per minute back to 200°C. The melting point was then the temperature at which the curve of enthalpy versus temperature measured in the second heating phase displayed a maximum.

^{13}C-NMR of the Polymers[130]

^{13}C-NMR spectra of PP were acquired on a DPX-400 spectrometer operating at 100.61 MHz in the Fourier transform mode at 120 °C. The peak of the *mmmm* pentad carbon were used as internal reference at 21.8 ppm and 29.9 ppm respectively. The samples were dissolved in 1,1,2,2-tetrachloroethane-*d2* at 120 °C with a 8% wt/v concentration in a 5mm tube. Each spectrum was acquired with a 90° pulse, 12 seconds of delay between pulses and CPD (WALTZ 16) to remove ^{1}H-^{13}C coupling. About 2500 transients were stored in 32K data points using a spectral window of 6000 Hz.

The assignments of PP spectra were made according to Resconi *et al*[131].
The *mmmm* content was obtained modelling the experimental pentad distribution with the enantiomorphic site model. The *mmmm* content of PP with high content of 2,1 (E) and 1,3 (H) errors was obtained as:

$[mmmm] = 100\ (\Sigma[CH_3]-5[mrrm]-5[E]-5[H]) / (\Sigma[CH_3])$

where $\Sigma[CH_3]$ is the sum of all CH3 groups

The content of 2,1 and 3,1 errors was obtained as:

$[E] = 100\ (E_9/\Sigma[CH_2])$

$[H] = 100\ (0.5\ H_2/\Sigma[CH_2])$

where E_9 is the peak at 42.14 ppm, H_2 is the peak at 30.82 ppm and $\Sigma[CH_2]$ is the sum of all CH_2 groups

---

[130] The description from the ^{13}C-NMR characterization method was provided by Dr. Isabella Camurati, Basell Polyolefines, Gulio Natta Research Center, Ferrara, Italy.

[131] Selectivity in Propylene Polymerization with Metallocene Catalysts, L. Resconi, L. Cavallo, A. Fait, F. Piemontesi, *Chem. Rev.*, (**2000**) *100*, 1253.

5.0 Acknowledgements

In 1986 when I was out of work and unemployment in Houston was 13%, Dr. John Ewen gave me a job testing catalysts and making polypropylene in a 2L zipperclave: I owe him the lot. In the end, Mike Elder abandoned me and left me without a bass guitar player, so the rock band went the way of the fishes. He is however, one of the best synthetic chemists I have ever met: I learned as much from him as I did from Dr. Ewen.

Dr. Winkelmann did the ^{1}H-NMR analysis of the complexes and put up with a lot of my pontificating about the wonders of science and how all of this would change the world as we know it.

Fatima Cheurfa and DI Martina Mahler did the MALDI-TOF analysis and helped identify what was what. Much thanks and gratitude for their patience and tutoring.

Veseyl Albyrak did most all of the polymerizations included here and this would have been very difficult without him. He was young, and had energy, and kept me going, even though I could never seem to get more than 2 polymerizations a day out of him.

Dr. Patrik Müller made this dream come true. Being my boss during this time, Müller was always interested and kept it all under his belt: he let me do this work for and with Basell. His encouragement and love of science kept this project alive and made it possible.

In my academic experiences I have met many different personalities. Early on, the professors were positive and provided support and encouragement: Dr. H. T. Freebairn at the University of Houston was particularly influential.

It was always difficult to imagine how it would be possible to achieve the Ph.D.academic goal: it was Prof. Sitzmann who made this real. He made this dream come true. Without him, this work would (maybe at best) be lost as a technical report in the world of industrial chemistry, and probably never have seen the light of day. God sent Prof. Dr. Sitzmann as an angel

Prof. Dr. Hubert Wadepohl at the X-Ray Crystallography Laboratory, Anorganisch-Chemisches Institut der Universität, Heidelberg, is acknowledged here for the crystallographic analysis.

There are others: Dr. Carsten Bingel, who patiently worked on the claims and descriptions in the patent and got the brief through IP to Munich: I owe a sincere debt of gratitude. His patience and company in the early mornings before the lab work started, in discussions about how and what I was doing, was invaluable.

I appreciate Dr. S. Mihan for going on vacation for 3 weeks and letting me use his polymerization people and equipment (even though he didn't plan it quite that way), and

Dr. Lars Kölling, with whom I shared an office and also put up with my pontifications and “come ‘ere, you gotta see this”…….

6.0 Appendix:

6.1 Molecular Modelling

A single point energy computation using MOPAC (semi-empirical molecular modelling application) was carried out. After minimizing the energy for the model constructed from (**79**), essentially no difference between the parallel conformations (143.7 kcal/mol vs. 143.8 kcal/mol for the anti-parallel model) was found: the energy differences between the 2 conformers are low.

Figure 121. Molecular modelling of the conformational isomers of (**79**).

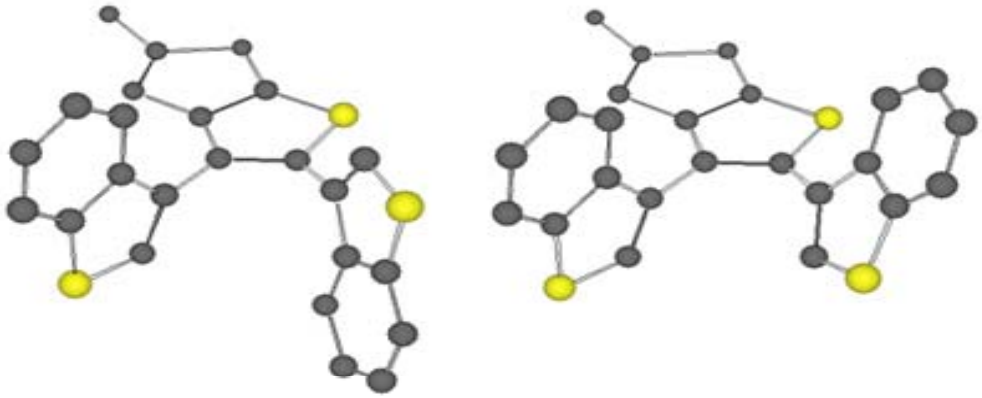

anti-parallel conformation parallel conformation

6.2 Additional References (used but not cited).

For examples of switching catalytic systems making unique structures see: R. Manivannan, G. Sundararajan and W. Kaminsky,"Studies in Switching the Mechanism of Polymerisation by Single-Site Catalysts-from Vinyl Addition to Metathesis", *J. Mol. Catal* (**2000**) *160*, 85-95 (Proceedings of ISOM 13), b) R. Manivannan, G. Sundararajan & W. Kaminsky, "Switching the Mechanism of Polymerization from Vinyl Addition to Metathesis using Single- Site Catalysts", *Macromol. Rapid Comm.* (**2000**) *21*, 968-72.

6.2.1 Bercaw

1. “Isotactic-Hemiisotactic Polypropylene from C1-Symmetric, Ansa-Metallocene Catalysts: A New Strategy for the Synthesis of Elastomeric Polypropylene”’ Stephen A. Miller and John E. Bercaw, *Organometallics* (**2002**) *21*, 934.

6.2.2 Waymouth

2. “2-ArylIndene Metallocenes: Conformationally Dynamic Catalysts to Control the Structure and Properties of Polypropylene,” S. Lin and R.M. Waymouth, Acc. Chem. Res., (**2002**) *35*(9), 765-773.

3. “Coordination Chemistry of Stable Radicals: Homolysis of a Titanium-Oxygen Bond,” K-W. Huang and R.M. Waymouth, *J. Am. Chem. Soc*., (**2002**)*124*, 8200-8201.

4. “Cyclocopolymerization: A Mechanistic Probe for Dual-Site Alternating Copolymerization of Ethylene and a-Olefins,” T.N. Choo and R.M. Waymouth, *J. Am. Chem. Soc.*, (**2002**) *124*, 4188-4189.

5. “Titanium-Mediated Syndiospecific Styrene Polymerizations: Role of Oxidation State,” M. Mahanthappa and R.M. Waymouth, *J. Am. Chem. Soc*., (**2002**) *123*, 12093-12094.

6. “Catalysts Rise to the Challenge,” F.J. Gomez and R.M. Waymouth, *Science*, (**2002**) *295* (25 Jan), 635-636.

7. G.W. Coates, R.M.Waymouth, *Science,* (**1995**) *267*, 217.

8. “Kinetics of Propylene Polymerization Using (2-Phenylindenyl)2ZrCl2 / MAO” S. Lin, R.M. Waymouth, M. Nele, S. Collins, and J.C. Pinto, *J. Am. Chem. Soc*., (**2000**) *122*, 11275-11285.

9. Willy Wiyatno, Zhong-Ren Chen, Yuxiang Liu, Robert M. Waymouth, Val Krukonis, and Kara Brennan, “Heterogeneous Composition and Microstructure of Elastomeric Polypropylene from a Sterically Hindered 2-Arylindenylhafnium Catalyst”, *Macromolecules*, (**2004**) *37* (3), 701 -708.

6.2.3 ePP

10. Wiyatno, W., Fuller, G.G., Pople, J.A., Gast, A.P., Chen, Z.R., Waymouth, R.M. and Myers, C.L. “Component stress-strain behavior and small-angle neutron scattering investigation of stereoblock elastomeric polypropylene” *Macromolecules*, (**2003**) *36*(4), 1178-1187.

11. Wiyatno, W., Pople, J.A., Gast, A.P., Waymouth, R.M. and Fuller, G.G. “Dynamic response of stereoblock elastomeric polypropylene studied by rheooptics and X-ray scattering. 1. Influence of isotacticity” *Macromolecules,* (**2002**) *35*(22), 8488-8497.

12. Wiyatno, W., Pople, J.A., Gast, A.P., Waymouth, R.M. and Fuller, G.G. “Dynamic response of stereoblock elastomeric polypropylene studied by rheooptics and X-ray scattering. 2. Orthogonally oriented crystalline chains” *Macromolecules,* (**2002**) *35* (22), 8498-8508.

6.2.4. Chiral epoxides:

13. Bernhard Rieger, Gerhard Jany, Riad Fawzi, and Manfred Steimann, “Unsymmetric ansa-Zirconocene Complexes with Chiral Ethylene Bridges: Influence of Bridge Conformation and Monomer Concentration on the Stereoselectivity of the Propene Polymerization Reaction” *Organometallics* (**1994**) *13*, 647-653,

6.2.5. Additional Information:

14. Georgiev, G.: Tzoneva, A “ Photozymes- New Light harvesting polymerization catalysts”, *Khimicheski Fakultet* (**2002**) *95*, 89 – 93.

6.3 Reference Spectra:

Figure 122. 2,5-dimethylthiopentalene (isomers):

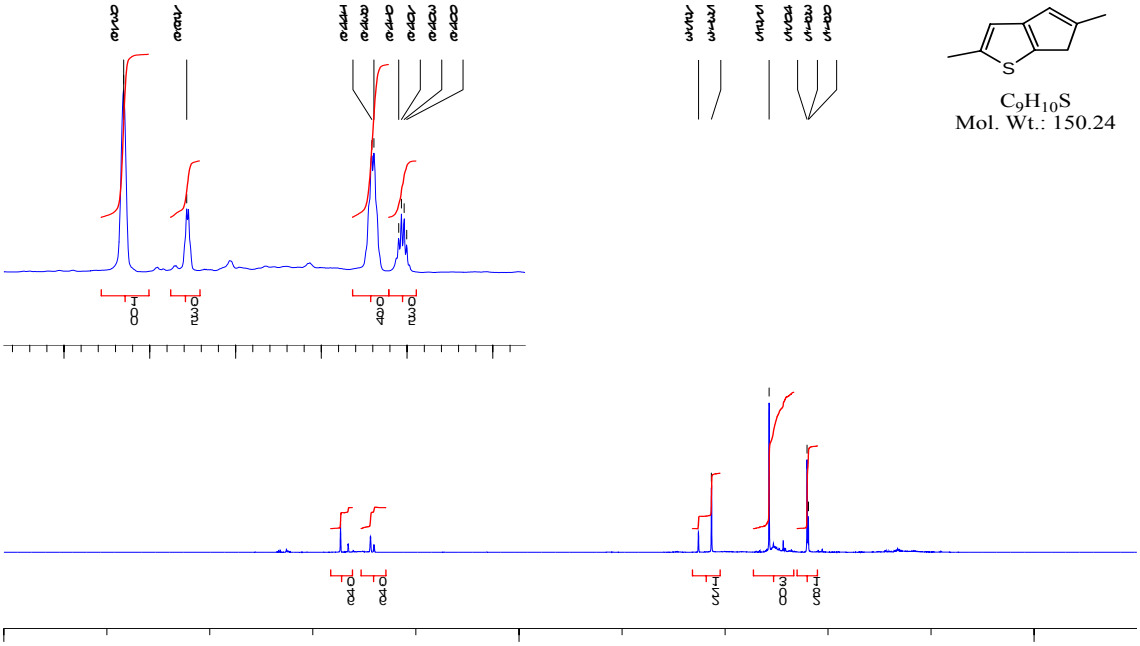

Figure 123. 2-methylcyclopenta[b] Benzo[d]thiophene/ (2-methyl-benzo[b]thiopentalene)

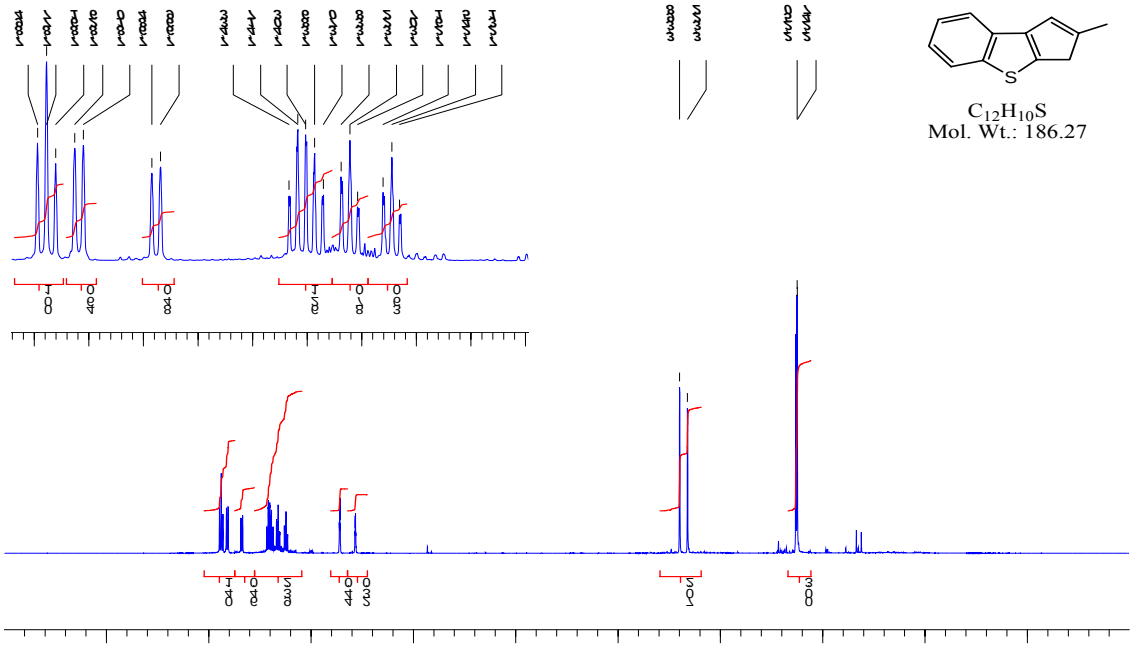

Figure 124. Photograph of apparatus used in irradiation of (**22**), and diaryl-DAE catalysts (**25**), (**26**), and (**27**).

Spectral distribution of UV immersion lamp in glass cooling tube filled with deionized water:

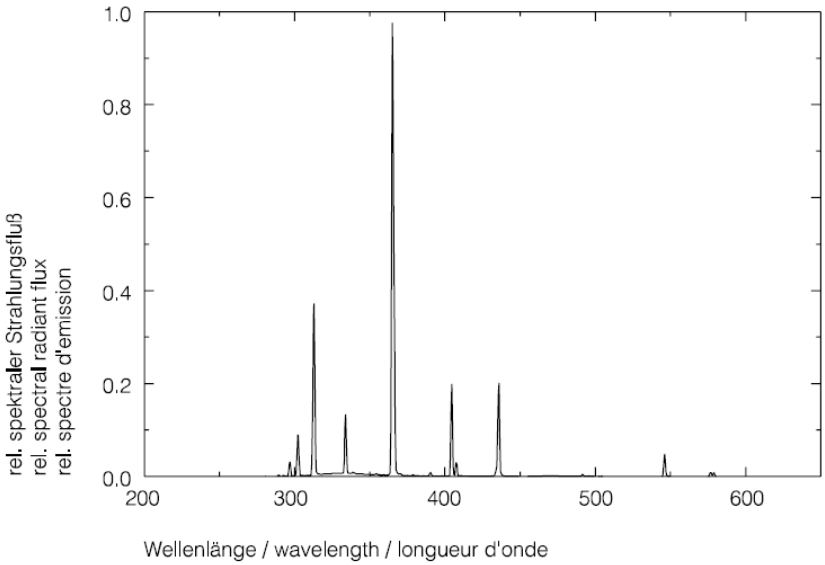

END